CHARGE-SHIFTING POLYCATIONS FOR BIOMATERIAL APPLICATIONS

BY

SAMANTHA ROS, B.Sc.

A THESIS SUBMITTED TO THE SCHOOL OF GRADUATE STUDIES OF
MCMASTER UNIVERSITY IN PARTIAL FULFILMENT OF THE REQUIREMENTS
FOR THE DEGREE OF DOCTOR OF PHILOSOPHY IN CHEMISTRY

Doctor of Philosophy, Chemistry

McMaster University, Hamilton, Ontario, Canada

Title:	Charge-Shifting Polycations for Biomaterial Applications
Author:	Samantha Ros, B.Sc. (McMaster University)
Supervisor:	Professor Harald D. H. Stöver
Number of Pages:	XXVII, 267

Abstract

Polycations are used extensively in a wide range of applications from enhanced oil recovery, wastewater treatment, and to biomaterials for delivery of therapeutics. This thesis focuses on the design, synthesis, and study of polycations towards improving the cyto- and immuno- compatibility in polyelectrolyte-based biomaterial applications. Alginate-based polyelectrolyte encapsulation and DNA delivery were chosen as applications to demonstrate the properties of the polycations developed, as a proof of concept.

The work in this thesis represents significant contributions to the field, in particular, in the study of polymers based on N,N-(dimethylamino)ethyl acrylate (DMAEA) as charge-shifting polycations where it provides an in-depth study of the hydrolysis of PDMAEA that probes the mechanism of its unique reactivity.

The hydrolysis of polymers of DMAEA was found to be highly pH dependent and sensitive to various neighboring groups on its pendent side chain, polymer backbone, and of comonomers. The effects were hypothesized to be due to a combination of interactions including hydrogen-bonding, steric hinderance, as well as ionic, hydrophilic, and hydrophobic interactions. These studies led to the synthesis of polycations with various rates of hydrolysis, with half-lives ranging from years to minutes. As these esters hydrolyze, the polymers have the potential to undergo transitions in net charge from cationic to zwitterionic, followed by anionic, due to the formation of carboxylate groups. Hence, the polymers are known as “charge-shifting” polycations in the field.

As a proof of concept, charge-shifting polycations based on DMAEA were studied in alginate-based polyelectrolyte materials for encapsulation. Copolymers of DMAEA and 3-aminopropyl methacrylamide (APM), called PAD copolymers, were used as coating materials with polyanionic calcium alginate hydrogel capsules. The charge-shifting ability was confirmed as the coatings were shown to degrade over time due to disruption of electrostatic interactions. It was further demonstrated that covalent cross-linking could preserve the structural integrity of the membrane coating. Electrophoretic mobility measurements of PAD coated microspheres confirmed the shift in net surface charge from cationic to anionic with progressive hydrolysis.

The charge-shifting ability of PAD copolymers was then tested for improving cytocompatibility as DNA delivery agents. PAD copolymers were shown to condense 60bp DNA to form polyplexes with very high cellular uptake efficiency in comparison to the gold standard polycation in the field, branched polyethylenimine (PEI). Cells exposed to PAD copolymers with the greatest charge-shifting ability were shown to have improved viabilities relative to non-charge-shifting polycations. This was attributed to the reduction of cytotoxic cationic charge of the polymer with progressive DMAEA hydrolysis.

The results described in this thesis provide fundamental structure–function information to help design and develop new polymers and materials with tunable properties towards biomaterial applications.

Acknowledgements

First and foremost, I would like to thank my supervisor Prof. Harald Stöver for giving me the opportunity of a lifetime to conduct our wonderful research with such patience, guidance, freedom, and trust. I am forever grateful for his endless support and motivation to become a better scientist every day. I have come such a long way from when I first started in his group as an undergrad, growing as a researcher and as a person, all of which would not be possible without him believing in me, even when I didn't. To Dr. Stöver, thank you.

Words cannot begin to describe how grateful I am to Dr. Nick Burke and his impact on our research. Nick has taught me almost everything I know about research and beyond. From teaching me the absolute basics about science, to our countless and fruitful, hours-long discussions about research, I would not be the scientist I am today without him. When life gives you lemons, make lemonade. Thank you, Nick!

I am forever grateful to the past and current Stöver group members for their support over the years, in particular, Dr. Rachelle Kleinberger for being a mentor that I needed at the start of it all. Her knowledge, help, and advice were instrumental to our research and would not have been possible without her. I want to extend this thanks to the group members, in particular, Sheilan Sinjari, Jing Zhao, Alison Stewart, Laurent Goujon, Jessie Wang, Mitchell Johnson, Christal Zhou, Allison Abdilla, Yuqing Zhao, Derrick Hastings, Carl Ellis, and Michael Coulson, all of whom I have conducted research with in one way or another, which helped me in my development as a scientist. I am also very

grateful to my colleagues Stu McNelles and Greg Bahun for their support and the many fruitful discussions that helped me through some of the toughest times in research.

I am grateful for the incredible research opportunity I had in Dr. David Smith's group at the Fraunhofer Institute IZI in Leipzig, Germany. For 3 months, he welcomed me into his research group where I learned invaluable lessons for both research and personal growth. Thanks to his group members Jesse Lorenz, Christin Möser, Robel Belay, and Martin Sajfutdinow for the unforgettable experience.

I am very thankful for my committee members Dr. Jim McNulty and Dr. Todd Hoare for the help and support over the years. Moreover, the help I received from the NMR facility, in particular Dr. Bob Berno, was invaluable to progressing our research. I would like to further thank the Department of Chemistry and Chemical Biology for the most incredible undergraduate and graduate experience over the past decade. I've had the most memorable experience with so many of you (too many to name) through my days on the MCGSS, TAing, the intramural volleyball "ball blockers" team, and as an occasional player on the softball "mother liquors" team – thanks for a great time.

I am truly lucky to have such an incredible supporting cast of friends, to which I owe them for all the laughs and help in maintaining my sanity over the years. To Rachelle Kleinberger, Peter Ho, Blossom Yan, Philip Lim, Sheilan Sinjari, and Greg Bahun, thank you for being there for me.

Finally, I am eternally grateful to my mom (mommy), my sister (Monica Lim) and her husband (Prabh Gidda), for their constant love, encouragement, and support. Thank you for everything you've done for me – I would not have made it here without you guys.

List of Abbreviations

7-AAD	7-Aminoactinomycin D
AA	Acrylic acid
AEA	2-aminoethyl acrylate
AIBN	Azobisisobutyronitrile
APA	Alginate–poly-L-lysine–alginate
APM	3-Aminopropylmethacrylamide
ATCC	American Type Culture Collection
ATR	Attenuated Total Reflection
BDMAPA	1,3-Bis(dimethylamino)propyl acrylate
bp	Base-pair
CHES	N-Cyclohexyl-2-aminoethanesulfonic acid
CLSM	Confocal Laser Scanning Microscopy
CTP	4-Cyano-4-(phenylcarbonothioylthio)pentanoic acid
Cy3	Cynanine-3
DABCO	1,4-Diazabicyclo[2.2.2]octane
DCC	N,N'-Dicyclohexylcarbodiimide
DCl	Deuterium chloride
DCM	Dichloromethane
DEMEA	2-((2-(Dimethylamino)ethyl)(methyl)amino)ethyl acrylate
DHMA	2-(Dimethylamino)ethyl 2-(hydroxymethyl)acrylate
DIPEA	Diisopropylethylamine
DLS	Dynamic light scattering
DMAE	2-(Dimethylamino)ethanol
DMAEA	2-(Dimethylamino)ethyl acrylate
DMAEIB	2-(Dimethylamino)ethyl isobutyrate
DMAEMA	2-(Dimethylamino)ethyl methacrylate
DMAP	3-(Dimethylamino) propanol
DMAP	4-(Dimethylamino)pyridine

DMAPMA	3-(Dimethylamino)propyl methacrylamide
DMEM	Dulbecco's Modified Eagle Medium
DMF	Dimethylformamide
DMPA	2,2-Dimethoxy-2-phenylacetophenone
DNA	Deoxyribonucleic acid
DP	Degree of polymerization
DPBS	Dulbecco's phosphate buffered saline
EDTA	Ethylenediaminetetraacetic acid
FCS	Fetal calf serum
FITC	Fluorescein isothiocyanate
FT-IR	Fourier-transform infrared
GPC	Gel permeation chromatography
HCl	Hydrochloric acid
HEA	2-Hydroxyethyl acrylate
HEPES	4-(2-Hydroxyethyl)-1-piperazineethanesulfonic acid
HMAA	2-(Hydroxymethyl)acrylic acid
HPLC	High performance liquid chromatography
Da	Dalton
LbL	Layer-by-Layer
LPEI	Linear polyethylenimine
MEM	Modified Eagle medium
MeOH	Methanol
MHMA	Methyl 2-(hydroxymethyl)acrylate
M_n	Number average molecular weight
MOM	Methoxymethyl
MOM-HMAA	2-((Methoxymethoxy)methyl)acrylic acid
M_p	Peak molecular weight
MW	Molecular weight
M_w	Weighted molecular weight

N/P	Nitrogen to phosphate ratio
NaOH	Sodium hydroxide
NMR	Nuclear magnetic resonance
nt	nucleotide
PAA	Poly[acrylic acid]
PAD	Poly[3-aminopropylmethacrylamide-*co*-2-(dimethylamino)ethyl acrylate]
PAEA	Poly[2-aminoethyl acrylate]
PBDMAPA	Poly[1,3-bis(dimethylamino)propyl acrylate]
PBS	Phosphate buffered saline
PDA	Poly[2-(dimethylamino)ethyl acrylate-*co*-acrylic acid]
PDEMEA	Poly[2-((2-(dimethylamino)ethyl)(methyl)amino)ethyl acrylate]
PDH	Poly[2-(dimethylamino)ethyl acrylate-*co*-2-hydroxyethyl acrylate]
PDHMA	Poly[2-(dimethylamino)ethyl 2-(hydroxymethyl)acrylate]
PDI	Polydispersity index
PDMAEA	Poly[2-(dimethylamino)ethyl acrylate]
PDMAEMA	Poly[2-(dimethylamino)ethyl methacrylate]
PEC	Polyelectrolyte complex
PEG	Poly[ethylene glycol]
PEI	Poly[ethylenimine]
PLL	Poly[L-lysine]
PMSM	Poly[4-methylstyrene-*alt*-maleic acid]
PTMAEA	Poly[2-(trimethylammonium)ethyl acrylate]
RAFT	Reversible Addition-Fragmentation Chain-Transfer
siRNA	Short interfering ribonucleic acid
TBS	*Tert*-butyldimethylsilyl ether
TEA	Triethylamine
TES	Triethylsilyl ether
THF	Tetrahydrofuran

THPC	Tetrakis(hydroxymethyl)phosphonium chloride
TMAEA	2-(Trimethylammonium)ethyl acrylate
TMS	Trimethylsilyl ether
UV-vis	Ultraviolet-visible
V501	4,4'-Azobis(4-cyanovaleric acid)
VDMA	2-Vinyl-4,4-dimethylazlactone
WST-1	Water-soluble tetrazolium assay

List of Figures

CHAPTER 1

CHAPTER 2

CHAPTER 3

CHAPTER 4

CHAPTER 5

List of Schemes

CHAPTER 1

CHAPTER 2

CHAPTER 3

CHAPTER 4

List of Tables

CHAPTER 2

CHAPTER 3

CHAPTER 4

CHAPTER 5

Statement of Academic Achievement

CHAPTER 2

I designed the experiments with the help of Dr. Burke. I performed all of the experiments described in the chapter, with initial experiments completed as part of my undergraduate senior thesis research project. Those experiments include the synthesis of PAD copolymers by conventional free radical polymerization, reactivity ratio determination, and the initial hydrolysis study of the PAD copolymers at pH 7. All of the following experiments in the chapter were completed during my graduate degree. I wrote the manuscript with edits and guidance from Dr. Stöver and Dr. Burke.

CHAPTER 3

I designed and performed all of the experiments described in the chapter with Dr. Kleinberger having given the initial inspiration for the study. I wrote the manuscript with edits and guidance from Dr. Stöver, Dr. Burke, Dr. Kleinberger, and Dr. Rossi.

CHAPTER 4

I performed all of the experiments described in the chapter with guidance from Dr. Freitag (née Lorenz) on designing the procedures for transfection, WST-1 assay, and apoptosis assay. Dr. Freitag helped with the analysis of flow cytometry data. I wrote the manuscript with edits and guidance from Dr. Freitag, Dr. Stöver, and Dr. Smith.

CHAPTER 5

I supervised and conducted some preliminary experiments with Ms.Wang as part of her undergraduate senior thesis project that led to the work described in this chapter. I designed and performed all of the experiments in this chapter. I wrote the manuscript with edits and guidance from Dr. Burke and Dr. Stöver.

TABLE OF CONTENTS

CHAPTER 1: INTRODUCTION

1.1. Polyelectrolytes

Polyelectrolytes are a class of charged polymers with monomer units comprising ionizable groups – this includes polycations where the charge is positive, and polyanions where the charge is negative. Polycations and polyanions are comprised of ionizable functional groups, and due to their high charge density, they are typically used in aqueous media and organic solvents capable of solubilizing salts. For polycations, the ionizable functional group of the monomer is commonly an amine, as the base can be protonated below its pKa, forming a charged ammonium cation.[1] Ammonium cations make up the majority of commonly used polycations as they are chemically and thermally stable, have good solubility in water, and have infinite variations of substitution at the nitrogen.[1,2] Phosphonium cations[3-6] have also been used in polyelectrolytes due to their chemical and thermal stability, as they are less likely to undergo Hoffman elimination in comparison to ammonium cations,[4] however they are less commonly used mainly due to the synthetic challenges involved with phosphine precursors. Other more exotic cationic moieties include sulfonium[7,8] and boronium[9] cations, however they often suffer from poor chemical stability, as they are susceptible to nucleophilic attack and dealkylation.[10,11] In addition, metallic ferricinium and cobalticenium cationic groups have been used in polyelectrolytes for applications including fuel cells and magnetic nanomaterials.[12,13]

As for polyanions, the three most commonly used groups include carboxylate, phosphonate, and sulfonate groups due to their acidic nature and ionization at the

appropriate pH in aqueous media. Polyelectrolytes are often used in applications that exploit their interactions with oppositely charged material to form polyelectrolyte complexes (PECs).[14] This includes simply mixing a solution of a polycation and a polyanion together. The driving force of polyelectrolyte complexation is not solely due to the electrostatic attraction of opposite charges but more importantly due to the favourable entropic release of counter ions associated with the polyelectrolyte.[15] This phenomenon allows for the spontaneous formation of polyelectrolyte complexes, which has been exploited in a variety of industrial applications ranging from wastewater treatment,[16,17] enhanced oil recovery,[18] gas separation,[19,20] to biomaterial[21] applications. In these fields, much research has been devoted to synthetic polycations in particular to compliment the polyanionic properties of nature and its materials such as DNA and phospholipid membranes in cells. Some of the most commonly used synthetic polycations in the industry include polyallylamine,[22,23] polyethylenimine (PEI),[24,25] poly-L-lysine (PLL),[24] poly[2-(dimethylamino)ethyl methacrylate] (PDMAEMA),[24,26] and polydiallyldimethylammonium chloride (PDADMAC).[27,28] These polymers share an amino group in common, though with varying degrees of substitution and polymer backbone diversity. Polymers containing primary and secondary amines are nucleophilic and their ionization is pH sensitive. Tertiary amines are less nucleophilic than primary amines, and their ionization is also pH sensitive. The pKa of these polymeric ammonium cations can vary greatly, though typically fall in the range of 7.5–9. Quaternary ammonium groups are not nucleophilic and are permanently charged rendering them pH insensitive. The different ammonium forms give rise to very different chemical and

physical properties with varying strengths of interactions with anionic species, hence their versatility in a wide range of applications.

1.2. Polycations for Biomaterial Applications

Polycations have been studied extensively in biomaterial applications such as gene transfection,[24,26,29-32] antimicrobials,[24,33] and other therapeutic delivery applications.[21,24,34-37] In comparison to natural polycations such as chitosan,[38] synthetic polymers allow for the exploration of various structure–property relationships, providing access to highly tunable systems for the desired application. For gene transfection, polycations are a more safe, inexpensive, and readily accessible alternative to viral vectors.[26,29-31] Polycations are used to complex with polyanionic DNA to form polyplexes to protect DNA from nucleases and intracellularly deliver the nucleic acid payload.

Polycations and cationic peptides have also been used as antimicrobials in part as their cationic charge density interacts strongly with the negatively charged membrane of bacterial cells, causing cell lysis[39] or disruption of vital cell membrane processes.[33,40] The rise in popularity of polycations for antimicrobials is in part due to their broad effectiveness and their success against the development of bacterial resistance.[41]

Since the interaction of polycations and polyanions occurs spontaneously, their complexation has been used to form a variety of materials such as layer-by-layer (LbL) thin films and hydrogel capsules.[14,21] These PEC constructs have been developed to encapsulate and release drug molecules and other payloads for extended, stimuli release mechanisms.[21,36] Although research involving commonly used polyelectrolytes has shown

much success in these biomaterial applications, one of the long-standing challenges in the field includes the toxicity of the polycation.

1.3. Cytotoxicity and Immunogenicity of Polycations

It is well known that polycations are typically cytotoxic as they can bind to anionic components of the cell including the phospholipid membrane as well as nucleic acids.[42,43] In addition, polycations may illicit pro-inflammatory and pro-apoptotic pathways as they mimic cationic charge of endogenous compounds associated with those pathways.[42,43] Charged surfaces, in addition to hydrophobic surfaces, of PEC materials may cause biofouling due to protein and cellular adsorption, which may result in failure or reduced performance of material functions i.e. as implants.[44] Although efficient complexation and strong binding of polycations are desirable properties for the production of PEC materials, those very characteristics of polycations seem to be the inherent cause of their cytotoxicity and biofouling of materials.

Efforts to mitigate biofouling in PEC materials formed by the LbL process include depositing a final layer of polyanion to mask residual cationic charge on the surface of the construct.[45-47] In general, this approach has failed in practice due to the inherent heterogeneity of polyelectrolyte complexation as polyelectrolytes may form uncomplexed portions resulting in patchy surface charge.[46] The significance of this issue has been demonstrated in the implantation of such PEC materials *in vivo*. For example, calcium alginate capsules that have been coated with cationic PLL, followed by a final coating of anionic alginate, called APA capsules, were implanted in mice to observe the

compatibility of the PEC material. *Ex vivo*, the capsules showed significant protein and cellular deposition on the surface of the capsules after 6 weeks of implantation.[47] Tam and coworkers tested the biocompatibility of alginate beads, AP and APA capsules, and pinpointed that there was a clear increase in host cell adhesion to capsules that incorporate the polycation and that there was little difference between AP and APA capsules.[46] Thus, APA capsules failed to maintain biocompatibility despite the final coating of alginate in an attempt to mask the cationic charge of PLL. Another attempt at reducing surface charge in PEC materials include masking the polycation with a neutral, hydrophilic polymer such as poly[ethylene glycol] (PEG) with architectures such as PLL-*block*-PEG[48] or PLL-*graft*-PEG.[49,50] Although these polymers were more cytocompatible[49] and showed less protein adhesion[50] due to decreased cationic charge density, this type of polymer architecture encountered issues with steric hinderance of the PEG block as PLL-*g*-PEG showed lower affinity towards polyanions, which further complicates electrostatic complexation.[50] Other attempts to reduce cationic charge density include copolymers of cationic monomers with anionic[51] and neutral/zwitterionic[52-54] comonomers which may indeed reduce cytotoxicity and biofouling of PEC materials, however sacrifice cationic charge density required for strong and efficient electrostatic complexation.

In another example, polycations are studied as a safer and inexpensive alternative to viral vectors for DNA delivery for gene therapy.[26,29-32] Similar to PEC materials, polycations are used to complex with anionic nucleic acids to form “polyplexes” as in PEC nanoparticles. In this case, cationic charge of the polycation is required to condense

and protect the nucleic acids from nucleases, in addition to facilitate cellular uptake of the polyplexes.[26,29-32] It is known that the net charge of the polyplexes needs to be cationic to trigger internalization by endocytosis, however, an excess of cationic charge invariably leads to cell death.[55,56] Research typically relies on balancing transfection efficiency with cytotoxicity by optimizing the ratio of polycation to DNA often referred to as the nitrogen to phosphate (N/P) ratio. The gold standard polycation used for transfection is PEI,[25,30,57,58] in particular branched 25-kDa PEI,[59,60] however, it is still known to have varying cytotoxic effects and transfection efficiency depending on molecular weight[60,61] and polymer architecture.[60,62,63] Researchers have also attempted to reduce cytotoxic cationic charge of PEI by masking with PEG[64] and polyanions,[65] in addition to acetylation of secondary and primary amines to form neutral amides.[66] Similar to the PLL examples mentioned previously, these modified PEI polymers sacrifice cationic charge density required for efficient complexation to condense nucleic acids and cellular uptake. Another more recent concern for PEI, and other polycations, as DNA delivery agents includes the final intracellular fate of the polymer.[63] As the mechanism of polycation-mediated transfection is still not fully understood,[66-68] speculation on the potential for either the accumulation or release of the polycation following internalization both suggest more issues in damaging intracellular components.[63]

1.4. Degradable Synthetic Polycations

For a number of applications, it is clear that there is a need to develop more cytocompatible polycations that maintain strong complexation properties, an idea that

inherently seems contradictory. Further attempts at creating such polycations include incorporating degradable linkages within the polymer backbone[69-75] or pendant side-chains[69,76-79] to reduce cationic charge of the polymer following PEC formation. It should be differentiated at this point that the cytotoxicity of cationic small molecules is not susceptible to the same mechanism of cell death as polymers with cationic charge and do not form polyelectrolyte complexes. These degradable polycations initially have a high cationic charge density that enables strong electrostatic interactions with polyanions for efficient complexation, but then undergo degradation, typically hydrolysis, where the cationic charge of the polymer is reduced. These polymers have been termed "charge-shifting",[77,78,80-82] "charge-reversing",[83-85] "decationized",[86,87] and "self-destroying",[88] cationic polymers by researchers as a result. Although this reduction of cationic charge of the polymer may not be suitable for all applications of polycations, these charge-shifting polycations are appropriate for applications where cationic charge is required temporarily i.e. for initial PEC formation and to facilitate cellular uptake. Charge-shifting of the polycation would reduce the electrostatic interactions with the polyanion and cause dissociation of the PEC. This concept has been exploited as a release mechanism of entrapped molecules, most commonly used for DNA delivery,[69-79,82-88] as well as other therapeutic molecules.[89,90] Alternatively, PECs formed with charge-shifting polycations can be covalently cross-linked to preserve the construct if long-term integrity is required.[80] The use of charge-shifting polycations in this way results in a reduction of net-cationic charge of PECs, which is a desirable feature as described previously, not attainable with standard polyelectrolytes.

David Lynn and Robert Langer were among the first to describe degradable polycations based on β-amino esters.[71] These polymers were synthesized by polycondensation of secondary diamino alkanes and diacrylates via Michael addition reactions. Since these esters are part of the polymer backbone, the hydrolysis results in degradation of the main polymer chain. Though not "charge-shifting" by definition, the interaction of β-amino groups to polymeric esters was studied as polycations capable of forming PEC constructs with polyanions in a layer-by-layer fashion due to their initial high charge density, followed by their degradation to dissociate the PEC. Lynn utilized these degradable polycations to condense and deliver polyanionic DNA as more cytocompatible alternatives to standard polycations such as PLL and polyethylenimine (PEI). With varying alkyl amino spacers as in cyclic piperazine and linear N,N'-dimethylethylenediamine, Lynn showed that these polyesters degraded with half-lifes of less than 5 hours at pH 7.4 and 7–8 hours at pH 5.1 at 37 °C to mimic the conditions of the cytoplasm and endosomal vesicle, respectively.[71]

1.5. Charge-Shifting Polycations

In later reports, Lynn described charge-shifting polycations that further exploit labile aminoalkyl esters. In this system, the secondary amines of linear PEI (LPEI) were reacted with methyl acrylate by Michael-addition (Figure 1.1.).[91]

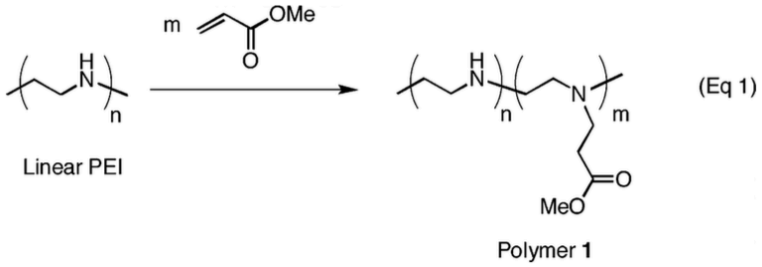

Figure 1.1. Charge-shifting polycations based on linear PEI. Reprinted (adapted) with permission from Liu, X. et al. *Macromolecules* **2005**, *38*(19), 7907-7914. Copyright (2005) American Chemical Society.

These modified PEI polymers contain tertiary amines, as well as unreacted secondary amines and thus retain their initial high cationic charge density. The methyl esters in the pendant side-chain are similarly labile as β-amino esters. Their hydrolysis results in the formation of anionic carboxylate groups and methanol as a by-product at physiological pH, which reduces the net cationic charge of the polymer. Hydrolysis kinetics by ^{1}H NMR spectroscopy of the LPEI functionalized at approximately 100, 60, and 20 mol% in 100 mM HEPES-*d18* buffered D_2O at pH 7.2 at 37 °C revealed half-lifes of approximately 2 days. In addition, the hydrolysis of the polymers was measured indirectly by gel electrophoresis, using the release of complexed DNA as an indication of charge-shifting ester hydrolysis. It was found that LPEI with the greatest degrees of functionalization of 100 and 80 mol% exhibited the fastest release rates of complexed DNA in comparison to lower percent functionalized LPEIs e.g. 40 and 60 mol%. This was attributed to higher percent-functionalized LPEIs having the greatest charge-shifting ability and thus corresponding dissociation ability with DNA.[91]

David Lynn and coworkers later developed another charge-shifting system based on poly[2-vinyl-4,4-dimethylazlactone] (PVDMA). PVDMA was functionalized by ring-opening the pendant azlactone groups with N,N-dimethylamino alkyl alcohols with ethyl and propyl spacer lengths (Scheme 1.1.).[78,79]

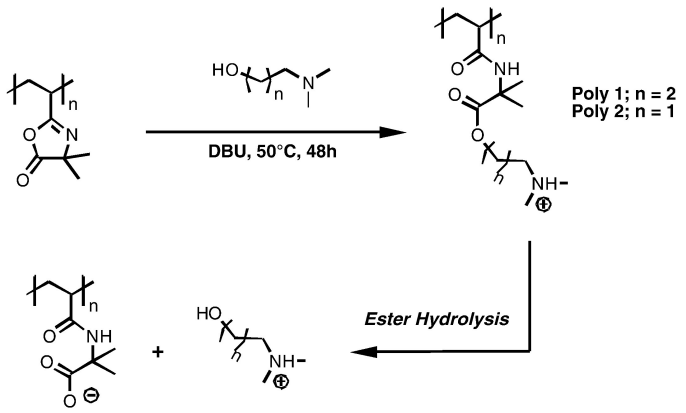

Scheme 1.1. Reprinted from Journal of Controlled Release, Vol. 148, Sun, B. and Lynn, D. M., Release of DNA from polyelectrolyte multilayers fabricated using 'charge-shifting' cationic polymers: Tunable temporal control and sequential, multi-agent release, Pages No. 91-100, Copyright (2010), with permission from Elsevier.

In this system, the pendant side-chains contain a labile ester with a neighboring amine group, similar to previous β-amino ester based charge-shifting polycations. Initially, these polymers are cationic at physiological pH due to the dimethylamino group, and hydrolysis of the esters results in anionic carboxylate groups on the polymer and small molecule N,N-dimethylaminoethanol (DMAE) or N,N-dimethylaminopropanol as small-molecule byproducts. In contrast to the previous systems based on LPEI, this charge-shifting polycation has the ability to switch its net-charge to anionic beyond 50 % hydrolysis of the side-chains. Lynn showed that there was a drastic difference in the hydrolytic stability of the esters given the propyl and ethyl spacers between the tertiary

amine and the ester. Hydrolysis kinetics by ^{1}H NMR spectroscopy in phosphate buffered D_2O at pH 7.4 at 37 °C revealed half-lifes for the propyl and ethyl spacer derivatives as approximately 200 and 6 days, respectively.[79] This stark difference in reactivity was attributed to the possibility of intra-molecular interactions of the tertiary amine with the ester being greater with the shorter ethyl spacer. In addition, the propyl spacer may be more hydrophobic than the ethyl analogue, leading to slower rates of hydrolysis. The differences in the rates of hydrolysis of these 2 polymers was used to form blends with tunable rates of hydrolysis and subsequent release profiles of complexed polyanions such as DNA from approximately 3 days to 1 month at physiological conditions.[79]

1.6. PDMAEA as Charge-Shifting Polycations

Similar to Lynn's PVDMA based charge-shifting polycations, acrylic based monomers with amine groups in the pendent side-chain such as N,N-(dimethylamino)ethyl (meth)acrylate are commercially available and readily (co)polymerizable by either conventional or controlled free-radical polymerization.[26] In fact, one of the first examples of a charge-shifting polycation was poly[N,N-(dimethylamino)ethyl acrylate] (PDMAEA). PDMAEA is much less commonly used and should not be confused with the methacrylate version poly[N,N-(dimethylamino)ethyl methacrylate] (PDMAEMA) which is used much more often. In 1989, McCool and Senogles first described the self-catalyzed hydrolysis of PDMAEA to poly[acrylic acid] (PAA).[92] PDMAEA units hydrolyze via the labile ester linkage, resulting in the formation of anionic acrylic acid units on the polymer and small-molecule by-product N,N-

dimethylaminoethanol (DMAE). The hydrolysis was studied by ^{1}H and ^{13}C NMR in D_2O at the natural pH of the polymer isolated in the free-base form where they state a limiting hydrolysis of ~60 % after approximately 10 days under ambient conditions (Figure 1.2.).[92]

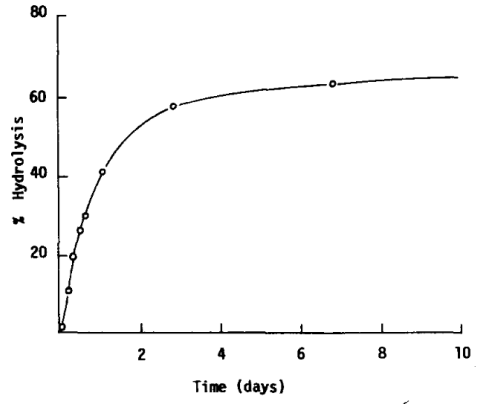

Figure 1.2. Percent hydrolysis of PDMAEA vs. time in D_2O (10 % w/v) at ambient temperature. Reprinted from European Polymer Journal, Vol. 25 No.7/8, McCool, M. B. and Senogles, E., The self-catalysed hydrolysis of poly(N,N-dimethylaminoethyl acrylate, Pages No. 857-860, Copyright (1989), with permission from Elsevier.

This extent of hydrolysis results in a copolymer of DMAEA and AA in a 40:60 mol ratio i.e. a polyampholyte as it contains cationic and anionic charges on separate monomer units. The hydrolysis of PDMAEA was termed "self-catalyzed" due to the possible intra-molecular interactions of the tertiary amine to the ester, similar to Lynn's β-amino ester systems. Interestingly, it should be noted that the methacrylate version, PDMAEMA, does not undergo hydrolysis readily. Hennink and coworkers describe the mechanism of monomeric and polymeric DMAEMA hydrolysis along with related small-molecule structures including DMAEA, N,N-(dimethylamino)ethyl isobutyrate (DMAEIB) and N,N-(dimethylamino)propyl methacrylate (DMAPMA).[93] In Hennink's report, they show

the hydrolysis of the monomers and related small-molecules to be highly pH dependent with differences in rates up to six orders of magnitude (Figure 1.3.).

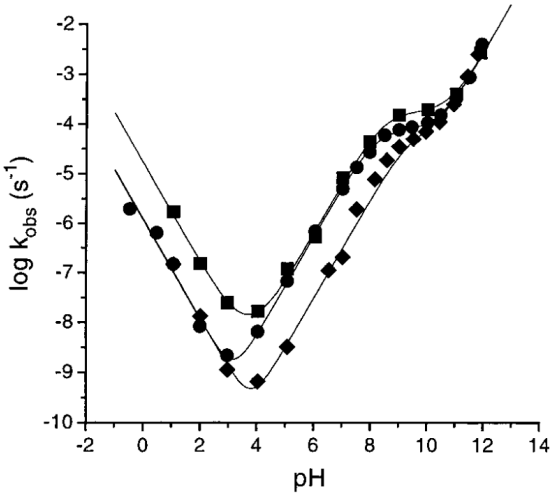

Figure 1.3. Log k_{obs}-pH profile of DMAEMA (circle), DMAEIB (square), and DMAPMA (diamond), measured at 37 °C. Reprinted (adapted) with permission from van de Wetering, P., *et al*. *Macromolecules* **1998**, *31*, 8063−8068. Copyright (1998) American Chemical Society.

In addition, they reported the remarkable stability of polymeric DMAEMA (PDMAEMA), citing increased hydrophobicity and more steric hinderance in the local environment of the ester due to the methacrylate polymer backbone. In contrast, the acrylate polymer backbone in PDMAEA with hydrogen as the α-substituent to the ester instead of a methyl group in PDMAEMA, was cited as more hydrophilic and less sterically hindered relative to the methacrylate.[93] The differences in stability of PDMAEA and PDMAEMA demonstrate the importance of neighboring substituents on the reactivity of the DMAE esters. This further highlights the sensitivity of these β-amino esters and related systems as shown by Lynn and coworkers.

In 2011, the hydrolysis of PDMAEA was studied by Monteiro and coworkers.[94] They showed that the hydrolysis of PDMAEA was independent of molecular weight in the range of 3000 to 8600 g/mol, though most surprisingly, they showed that hydrolysis was independent of pH between pH 5.5 and 10.1 (Figure 1.4.).[94]

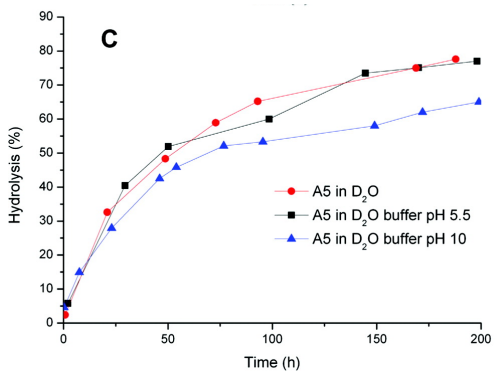

Figure 1.4. Hydrolysis of PDMAEA (8600 g/mol) in D_2O at different pH (5.5, 7.2, 10.1). Reprinted (adapted) with permission from Truong, N. P., et al. *Biomacromolecules* **2011**, *12*, 1876–1882. Copyright (2011) American Chemical Society.

The authors cite that the hydrolysis is due to the self-catalyzed nature of hydrolysis. They also showed that methylating the tertiary amine to produce the permanently charged quaternary ammonium cation results in a stable polymer that does not hydrolyze readily, an outcome previously reported by Hennink et al.[93] In order to understand the stability of the ester, the role of the tertiary amine of PDMAEA in the hydrolysis needs to be probed. It is hypothesized that the tertiary amine interacts with the ester in the following ring conformations under basic (deprotonated) and acidic (protonated) conditions (Figure 1.5.).

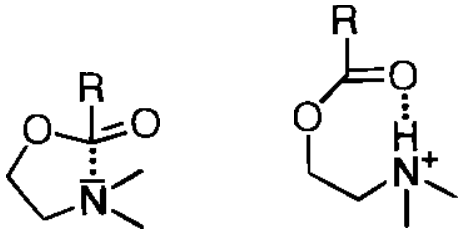

Figure 1.5. Ring conformations of deprotonated (left) and protonated (right) 2-(dimethylamino)ethyl esters. Reprinted (adapted) with permission from van de Wetering, P., *et al*. *Macromolecules* **1998**, *31*, 8063−8068. Copyright (1998) American Chemical Society.

Under basic conditions, the lone pair of the amine interacts with the carbon of the carbonyl in a 5-membered ring conformation. This interaction would lead to a more delocalized lone pair of electrons, which was supported by the authors with a lower pKa for the ammonium conjugate acid relative to typical tertiary ammonium protons.[93] This interaction would also lead to a weakening of the C–O bond of the ester which may explain the unique reactivity of the ester toward degradation. Under acidic conditions, the tertiary ammonium proton may coordinate with the oxygen of the carbonyl in a 7-membered ring conformation, which mimics the protonation mechanism of the typical acid-catalyzed hydrolysis pathway and results in a more electrophilic carbon. Although the 7-membered ring is not as favourable, the intra-molecular interaction may be facilitated by the proximity of the tertiary ammonium group to the ester. Thus, it is clear why the methylated version of PDMAEA to the quaternary ammonium cation results in a more stable ester as the proposed interactions with the lone pair and proton are both eliminated. These proposed intra-molecular interactions are very important and will lay the foundation of much of the work in this thesis.

Although most of the previous findings are consistent with the proposed interactions, the pH independent hydrolysis of PDMAEA reported by Monteiro[94] still stands out, especially given the highly pH dependent hydrolysis of the monomer DMAEA and related small molecules as reported by Hennink in 1998.[93] Despite this inconsistency between polymer and small molecule hydrolysis, there have been numerous reports relying on the pH independent hydrolysis of PDMAEA, citing Monteiro's work in 2011. Upon close inspection of the experimental procedure cited for the pH independent hydrolysis of PDMAEA, we noticed that the final concentration of the buffer solutions prepared for the hydrolysis was not appropriate for the molar concentration of PDMAEA that was used, with ~1.9 mol eq. of polymer repeat unit relative to buffer, meaning that the targeted pH was likely not obtained. It should also be noted that the pH of the buffer solution was measured only prior to the dissolution of the polymer (free base). The article by Haddleton and coworkers in 2018 repeat the hydrolysis experiments as described by Monteiro in 2011, and thus further propagates the error (Figure 1.6.).[95]

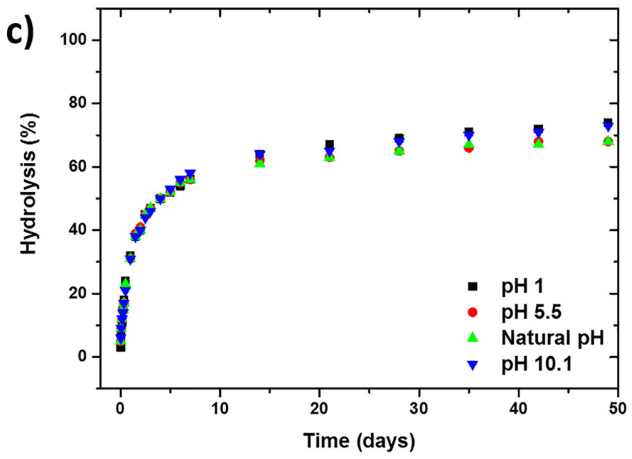

Figure 1.6. Effect of pH on the hydrolysis of star PDMAEA (6200 g/mol). Reprinted (adapted) with permission from (Whitfield, R., *et al*. *ACS Macro Letters* **2018**, *7(8)*, 909-915), ACS AuthorChoice. Copyright (2018) American Chemical Society.

We determined that under these conditions, the pH of a solution of PDMAEA at the stated concentration in its free base form in D_2O is around pH 8.5–9. Thus, the pH of the three solutions were all in the range of pH 8.5–9 instead of the targeted pH (i.e. 5.5, 7, and 10.1) and therefore all showed the same rate of hydrolysis, hence, the seemingly pH "independent" rate of hydrolysis. Therefore, it is of great importance to study the hydrolysis of PDMAEA under proper pH-controlled conditions to understand the mechanism of hydrolysis of these uniquely labile esters, which will give fundamental information to design and tune the properties of new degradable polymers. In addition, it is of great importance to clear up misunderstandings in the field, especially with the growing number of reports that cite, reproduce, or propagate the incorrect pH independent phenomenon.[95-102]

1.7. Thesis Objectives

The focus of this doctoral thesis was to design, synthesize, and study, novel charge-shifting polycations based on poly[N,N-(dimethylamino)ethyl acrylate] towards biomaterial applications. The use of charge-shifting polycations as materials for calcium alginate based cell encapsulation and DNA delivery was conducted as a proof of concept. As materials based on PDMAEA continually receive attention in biological applications, it is of great importance that the mechanism of hydrolysis and the factors that affect the unique reactivity of such esters is well understood. Such knowledge would allow for the

development of degradable polymers with tunable kinetics suitable for the desired application.

In chapter 2 of this thesis, copolymers of N,N-(dimethylamino)ethyl acrylate and 3-aminopropylmethacrylamide, called PAD copolymers, were synthesized and their hydrolysis was studied by ^{1}H NMR spectroscopy at various pH, temperature, and salt concentrations. PAD copolymers of varying compositions were synthesized by RAFT polymerization and the effect of high and low molecular weight polymers were studied as coating materials with anionic calcium alginate beads. The charge-shifting ability of PAD copolymers was demonstrated as part of PEC coatings as the polymer dissociate from the anionic calcium alginate beads due to the decrease in net cationic charge. Covalent crosslinking was employed to retain the PEC coating structure while reducing net-cationic surface charge.

In chapter 3, a novel analogue of DMAEA was synthesized to probe the effect of an added hydroxyl group capable of intramolecular hydrogen-bonding with the ester, as well as increasing the hydrophilicity of the polymer backbone. 2-(Dimethylamino)ethyl 2-(hydroxymethyl)acrylate (DHMA) was synthesized and hydroxyl-protected versions were polymerized. The homopolymer of DHMA (PDHMA) was prepared and the hydrolysis was studied by ^{1}H NMR spectroscopy in comparison to PDMAEA and PDMAEMA with a proton and methyl group in the α-position to the ester, respectively. As the side-chains are identical in these polymers, the effect of polymer backbone on the stability of DMAE esters was probed. The α-hydroxymethyl group of PDHMA appeared to significantly accelerate the rate of hydrolysis of DMAE esters in comparison to

PDMAEA and PDMAEMA, likely due to activation by hydrogen-bonding interaction of the hydroxyl group and the ester, in addition to increased hydrophilicity of the polymer backbone. Copolymers of DHMA and DMAEA were synthesized with varying mol compositions to study the effect of hydroxymethyl groups in the polymer backbone. The degree of hydroxymethylation of the polymer backbone was shown to tune the rate of hydrolysis as copolymers with increasing mol compositions of DHMA increased the rate of hydrolysis.

In chapter 4, charge-shifting PAD copolymers were studied as tunable, synthetic vectors for in vitro DNA delivery. PAD copolymers of varying composition were synthesized by RAFT polymerization as described in chapter 2, and their complexation with 60bp DNA to form polyplexes was studied as function mol ratios i.e. nitrogen to phosphate (N/P) ratios. Cellular uptake and cytotoxicity of PAD–60bp DNA polyplexes after exposure to HeLa human cervical cancer cells was studied as a function of copolymer composition as well as N/P ratios in comparison to PEI, the gold standard polycation for gene transfection.

In chapter 5, the hydrolysis of PDMAEA was studied in controlled pH conditions from pH 0.3 to 13.3. As the extent of PDMAEA hydrolysis is known to reach a limiting extent of 50–60 % at pH 7, the factors that affect hydrolysis of esters in the polymer side-chain were studied by probing the base and acid catalyzed mechanisms of hydrolysis. The effect of anionic, neutral/hydrophilic, and cationic functional groups on neighboring monomers in DMAEA copolymers was explored. Finally, novel analogues of DMAEA with an added amine in the side-chain were synthesized and polymerized to probe the

interaction of the dimethylamino group with the ester. 1,3-Bis(dimethylamino)propyl-2-acrylate (BDMAPA) and 2-((2-(dimethylamino)ethyl)(methyl)amino)ethyl acrylate (DEMEA) have an added amine in varying proximity to the ester in the side-chain in a branched-like and linear structure, respectively.

1.8. References

[1] Jaeger, W.; Bohrisch, J.; Laschewsky, A. Synthetic polymers with quaternary nitrogen atoms—Synthesis and structure of the most used type of cationic polyelectrolytes. *Progress in Polymer Science* **2010**, *35*, 511–577.

[2] Laschewsky, A. Recent trends in the synthesis of polyelectrolytes. *Current Opinion in Colloid & Interface Science* **2012**, *17*, 56–63.

[3] Rose, V. L.; Mastrotto, F.; Mantovani, G. Phosphonium polymers for gene delivery. *Polym. Chem*. **2017**, *8*, 353-360.

[4] Hemp, S. T.; Zhang, M.; Tamami, M.; Long, T. E. Phosphonium ionenes from well-defined step-growth polymerization: thermal and melt rheological properties. *Polym. Chem*. **2013**, *4*, 3582-3590.

[5] Beland, V. A.; Ross, M. A. S.; Coady, M. J.; Guterman, R.; Ragogna, P. J. Patterned Phosphonium-Functionalized Photopolymer Networks as Ceramic Precursors. *Chem. Mater*. **2017**, *29*, 8884-8891.

[6] Cuthbert, T. J.; Jadischke, J. J.; de Bruyn, J. R.; Ragogna, P. J.; Gillies, E. R. Self-Healing Polyphosphonium Ionic Networks. *Macromolecules* **2017**, *50*, 5253−5260.

[7] Herold, M.; Håkanson, M.; Brunner, H., Tovar, G. E. M. Modular surfmers with activated ester function—a colloidal tool for the preparation of bioconjugated nanoparticles. *Prog. Colloid Polym. Sci.* **2006**, *133*, 30–34.

[8] Kim, Y.J.; Kang, H.; Leolukman, M.; Nealey, P.F.; Gopalan, P. Synthesis of photoacid generator-containing patternable diblock copolymers by reversible addition-fragmentation transfer polymerization. *Chem. Mater*. **2009**, *21*, 3030–3032.

[9] Cui, C.; Bonder, E. M.; Jäckle, F. Organoboronium Amphiphilic Block Copolymers. *Journal of Polymer Science: Part A: Polymer Chemistry* **2009**, *47*, 6612–6618.

[10] Shouji, E.; Nishimura, S.; Yamamoto, K.; Tsuchida, E. Synthesis of poly(sulfonium cation) as an alkylating reagent. *Polymers for Advanced Technologies* **2009**, *5*(9), DOI:10.1002/pat.1994.220050907

[11] Haryono, A.; Yamamoto, K.; Shouji, E.; Tsuchida, E. Synthesis and Nucleophilic Dealkylation of Poly[alkyl-(4-(phenylthio)phenyl)sulfonium trifluoromethanesulfonate]s. *Macromolecules* **1998**, *31*, 1202-1207

[12] Dragutan, I.; Dragutan, V.; Filip, P.; Simionescu, B. C.; Demonceau, A. ROMP Synthesis of Iron-Containing Organometallic Polymers. *Molecules* **2016**, *21*, 198.

[13] Gu, H.; Ciganda, R.; Hernández, R.; Castel, P.; Vax, A.; Zhao, P.; Ruiz, J.; Astruc, D. Diblock metallocopolymers containing various iron sandwich complexes: living ROMP synthesis and selective reversible oxidation. *Polym. Chem*. **2016**, *7*, 2358-2371.

[14] Decher, G.; Hong, J. D.; Schmitt, J. Buildup of ultrathin multilayer films by a self-assembly process: III. Consecutively alternating adsorption of anionic and cationic polyelectrolytes on charged surfaces. *Thin Solid Films* **1992**, *210/211*, 831-835.

[15] Ou, Z.; Muthukumar, M. Entropy and enthalpy of polyelectrolyte complexation: Langevin dynamics simulations. *J. Chem. Phys*. **2006**, *124*, 154902.

[16] Bolto, B.; Gregory, J. Organic Polyelectrolytes in Water Treatment. *Water Res*. **2007**, *41*, 2301−2324.

[17] Saveyn, H.; Hendrickx, P. M. S.; Dentel, S. K.; Martins, J. C.; Van der Meeren, P. Quantification of hydrolytic charge loss of DMAEA-Q-based polyelectrolytes by proton

NMR spectroscopy and implications for colloid titration. *Water Res*. **2008**, *42*, 2718−2728.

[18] Wever, D. A. Z.; Picchioni, F.; Broekhuis, A. A. Polymers for enhanced oil recovery: A paradigm for structure−property relation- ship in aqueous solution. *Prog. Polym. Sci.* **2011**, *36*, 1558−1628.

[19] Pramanik, N. B.; Regen, S. L. Hyperthin Membranes for Gas Separations *via* Layer-by-Layer Assembly. C*hem. Rec.* **2019**, *19*, 1–12.

[20] Heo, J.; Choi, M.; Chang, J.; Ji, D.; Kang, S. W.; Hong, J. Highly Permeable Graphene Oxide/Polyelectrolytes Hybrid Thin Films for Enhanced CO_2/N_2 Separation Performance. *Scientific Reports* **2017**, *7*, 456. DOI:10.1038/s41598-017-00433-z

[21] Peyratout, C. S.; Dähne, L. Tailor-Made Polyelectrolyte Microcapsules: From Multilayers to Smart Containers. *Angew. Chem., Int. Ed*. **2004**, *43*, 3762−3783.

[22] Boussif, O.; Delair, T.; Brua, C.; Veron, L.; Pavirani, A.; Kolbe, H. V. J. Synthesis of Polyallylamine Derivatives and Their Use as Gene Transfer Vectors in Vitro. *Bioconjugate Chem*. **1999**, *10*, 877−883.

[23] Janeesh, P. A.; Sami, H.; Dhanya, C. R.; Sivakumar, S.; Abraham, A. Biocompatibility and genotoxicity studies of polyallylamine hydrochloride nanocapsules in rats. *RSC Adv*. **2014**, *4*, 24484-24497.

[24] Samal, S. K.; Dash, M.; Van Vlierberghe, S.; Kaplan, D. L.; Chiellini, E.; van Blitterswijk, C.; Moroni, L.; Dubruel, P. Cationic polymers and their therapeutic potential *Chem. Soc. Rev*. **2012**, *41*, 7147–7194.

[25] Boussif, O.; Lezhoualc'ht, F.; Zanta, M. A.; Mergny, M. D.; Scherman, D.; Demeneix, B.; Behr, J.- P. A versatile vector for gene and oligonucleotide transfer into cells in culture and in vivo: Polyethylenimine. *Proc. Natl. Acad. Sci.* **1995**, *92*, 7297-7301.

[26] Agarwal, S.; Zhang, Y.; Maji, S.; Greiner, A. PDMAEMA based gene delivery materials. *Mater. Today* **2012**, *15*, 388−393.

[27] Wandrey, C.; Hermindez-Barajas, J.; Hunkeler, D. Diallyldimethylammonium Chloride and its Polymers. *Advances in Polymer Science* **1999**, *145*, 123-183.

[28] Olsson, J.; Pham, S. T. H.; Jannasch, P. Poly(N,N-diallylazacycloalkane)s for Anion-Exchange Membranes Functionalized with N-Spirocyclic Quaternary Ammonium Cations. *Macromolecules* **2017**, *50*, 2784−2793.

[29] Thomas, M.; Klibanov, A. M. Non-viral gene therapy: polycation-mediated DNA delivery. *Appl Microbiol. Biotechnol*. **2003**, *62*, 27–34.

[30] Pollard, H.; Remy, J. S.; Loussouarn, G.; Demolombe, S.; Behr, J. P.; Escande, D. Polyethylenimine but Not Cationic Lipids Promotes Transgene Delivery to the Nucleus in Mammalian Cells. *J. Biol. Chem*. **1998**, *273*, 7507–7511.

[31] Kabanov, A. V.; Kabanov, V. A. DNA Complexes with Polycations for the Delivery of Genetic Materials into Cells. *Bioconjugate Chem*. **1995**, *6*, 7-20.

[32] Pack, D. W.; Hoffman, A. S.; Pun, S.; Stayton, P. S. Design and Development of Polymers for Gene Delivery. *Nature Reviews Drug Discovery* **2005**, *4*, 581–593.

[33] Kuroda, K.; Caputo, G. A. Antimicrobial polymers as synthetic mimics of host defense peptides. *WIREs Nanomed. Nanobiotechnol*. **2013**, *5*, 49–66. doi: 10.1002/wnan.1199.

[34] Ghidoni, I; Chlapanidas, T.; Bucco, M.; Crovato, F.; Marazzi, M.; Vigo, D.; Torre, M. L.; Faustini, M. Alginate cell encapsulation: new advances in reproduction and cartilage regenerative medicine. *Cytotechnology* **2008**, *58*, 49–56.

[35] Sakr, O. S.; Borchard, G. Encapsulation of Enzymes in Layer-by-Layer (LbL) Structures: Latest Advances and Applications. *Biomacromolecules* **2013**, *14*, 2117−2135.

[36] Wang, Y.; Hosta-Rigau, L.; Lomas H.; Caruso, F. *Phys. Chem. Chem. Phys*. **2011**, *13*, 4782–4801.

[37] Zhao, L.; Skwarczynski, M.; Toth, I. Polyelectrolyte-Based Platforms for the Delivery of Peptides and Proteins. *ACS Biomater. Sci. Eng*. **2019**, *5*(10), 4937-4950.

[38] Cheung, R. C. F.; Ng, T. B.; Wong J. H.; Chan, W. Y. Chitosan: An Update on Potential Biomedical and Pharmaceutical Applications. *Mar. Drugs* **2015**, *13*, 5156-5186.

[39] Yang, L.; Weiss, T. M.; Lehrer, R. I.; Huang, H. W. Crystallization of antimicrobial pores in membranes: magainin and protegrin. *Biophys. J.* **2000**, *79*, 2002-2009.

[40] Matsuzaki, K. Why and how are peptide±lipid interactions utilized for self-defense? Magainins and tachyplesins as archetypes. *Biochim. Biophys. Acta* **1999**, *1462*, 1-10.

[41] Zasloff, M. Antimicrobial peptides of multicellular organisms. *Nature* **2002**, *415*, 389-395.

[42] Lonez, C.; Vandenbranden, M.; Ruysschaert, J.-M. Cationic lipids activate intracellular signaling pathways. Advanced Drug Delivery Reviews **2012**, *64*, 1749–1758.

[43] Cobourn, R. F. Polyamine Effects on Cell Function: Possible Central Role of Plasma Membrane PI(4,5)P2. *J. Cell. Physiol*. **2009**, *221*, 544–551.

[44] Wei, Q.; Becherer, T.; Angioletti-Uberti, S.; Dzubiella, J.; Wischke, C.; Neffe, A. T.; Lendlein, A.; Ballauff, M.; Haag, R. Protein Interactions with Polymer Coatings and Biomaterials. *Angew. Chem., Int. Ed*. **2014**, *53* (31), 8004−8031.

[45] Thu, B.; Bruheim, P.; Espevik, T.; Smidsrød, O.; Soon-Shiong, P.; Skjak Bræk,G. Alginate polycation microcapsules I. Interactions of Alginate and Polycation. *Biomaterials* **1996**, *17*, 1031−1040.

[46] Tam, S. K.; Bilodeau, S.; Dusseault, J.; Langlois, G.; Hallé, J. -P.; Yahia, L. H. Biocompatibility and physicochemical characteristics of alginate–polycation microcapsules. *Acta Biomaterialia* **2011**, *7*, 1683–1692.

[47] Gardner, C. M.; Potter, M. A.; Stöver, H. D. H. Improving covalent cell encapsulation with temporarily reactive polyelectrolytes. *J. Mater. Sci. Mater. Med*. **2012**, *23*, 181−193.

[48] Wong, S. Y.; Han, L.; Timachova, K.; Veselinovic, J.; Hyder, M. N.; Ortiz, C.; Klibanov, A. M.; Hammond, P. T. Drastically Lowered Protein Adsorption on Microbicidal Hydrophobic/Hydrophilic Polyelectrolyte Multilayers. *Biomacromolecules* **2012**, *13*, 719−726.

[49] Wilson, J. T.; Cui, W.; Kozlovskaya, V.; Kharlampieva, E.; Pan, D.; Qu, Z.; Krishnamurthy, V. R.; Mets, J.; Kumar, V.; Wen, J.; Song, Y.; Tsukruk, V. V.; Chaikof, E. L. Cell Surface Engineering with Polyelectrolyte Multilayer Thin Films. *J. Am. Chem. Soc.* **2011**, *133*, 7054− 7064.

[50] Sawhney, A. S.; Hubbell, J. A. Poly(ethylene oxide)-graft-poly(L-lysine) copolvmers to enhance the biocompatibility of poly(L-lysine)-alginate microcapsule membranes. *Biomaterials* **1992**, *13*, 863−870.

[51] Dubey, A.; Burke, N. A. D.; Stöver, H. D. H. Preparation and Characterization of Narrow Compositional Distribution Polyampholytes as Potential Biomaterials: Copolymers of N-(3-Aminopropyl)methacrylamide Hydrochloride (APM) and Methacrylic Acid (MAA). *J. Polym. Sci., Part A: Polym. Chem*. **2015**, *53*, 353−365.

[52] Kleinberger, R. M.; Burke, N. A. D.; Zhou, C.; Stöver, H. D. H. Synthetic polycations with controlled charge density and molecular weight as building blocks for biomaterials. *J. Biomater. Sci., Polym. Ed*. **2016**, *27*(4), 351–369.

[53] Hastings, D. E.; Stöver, H. D. H. Crosslinked Hydrogel Capsules for Cell Encapsulation Formed Using Amino/Betaine Dual-Functional Semibatch Copolymers. *ACS Appl. Polym. Mater.* **2019**, *1*, 2055−2067.

[54] Pu, Y.; Hou, Z.; Khin, M. M.; Zamudio-Vaźquez, R.; Poon, K. L.; Duan, H.; Chan-Park, M. B. Synthesis and Antibacterial Study of Sulfobetaine/Quaternary Ammonium-Modified Star-Shaped Poly[2-(dimethylamino)ethyl methacrylate]-Based Copolymers with an Inorganic Core. *Biomacromolecules* **2017**, *18*, 44−55.

[55] Hu, Y.; Gong, X.; Zhang, J.; Chen, F.; Fu, C.; Li, P.; Zou, L.; Zhao, G. Activated Charge-Reversal Polymeric Nano-System: The Promising Strategy in Drug Delivery for Cancer Therapy. *Polymers* **2016**, *8*, 99.

[56] Chen, L.; McCrate, J. M.; Lee, J. C.- M.; Li, H. The role of surface charge on the uptake and biocompatibility of hydroxyapatite nanoparticles with osteoblast cells. *Nanotechnology* **2011**, *22*, 105708.

[57] Kircheis, R.; Kichler, A.; Wallner, G.; Kursa, M.; Ogris, M.; Felzmann, T.; M Buchberger, M.; Wagner, E. Coupling of cell- binding ligands to polyethylenimine for targeted gene delivery. *Gene Ther*. **1997**, *4*, 409-418.

[58] Hsu, C. Y. M.; Uludag, H. A simple and rapid nonviral approach to efficiently transfect primary tissue–derived cells using polyethylenimine. *Nature protocols* **2012**, *7*(5), 935-945.

[59] Tiera, M. J. Winnik, F. M.; Fernandes, J. C. Synthetic and Natural Polycations for Gene Therapy: State of the Art and New Perspectives. *Current Gene Therapy* **2006**, 6, 59-71.

[60] Thomas, M.; Ge, Q.; Lu, J. J.; Chen, J.; Klibanov, A. M. Cross-linked Small Polyethylenimines: While Still Nontoxic, Deliver DNA Efficiently to Mammalian Cells *in Vitro* and *in Vivo*. *Pharm. Res*. **2005**, *22*, 373- 380.

[61] Godbey, W. T.; Wu, K. K.; Mikos, A. G. Size matters: Molecular weight affects the efficiency of poly(ethylenimine) as a gene delivery vehicle. *Journal of Biomedical Materials Research* **1999**, *45* (3), 268-275.

[62] Wightman, L.; Kircheis, R.; Rossler, V.; Carotta, S.; Ruzicka, R.; Kursa, M.; Wagner, E. Different behavior of branched and linear polyethylenimine for gene delivery in vitro and in vivo. *J. Gene Med*. **2001**, *3*, 362–372.

[63] Parhamifar, L.; Larsen, A. K.; Hunter, A. C.; Andresen, T. L.; Moghimi, S. M. Polycation cytotoxicity: a delicate matter for nucleic acid therapy—focus on polyethylenimine. *Soft Matter* **2010**, *6*, 4001–4009.

[64] Ogris, M.; Steinlein, P.; Carotta S.; Brunner, S.; Wagner, E. DNA/polyethylenimine transfection particles: Influence of ligands, polymer size, and PEGylation on internalization and gene expression. *AAPS PharmSci.* **2001**, *3*(3), 1-11.

[65] Ito, T.; Iida-Tanaka, N.; Koyama, Y. Efficient *in vivo* gene transfection by stable DNA/PEI complexes coated by hyaluronic acid. *Journal of Drug Targeting* **2008**, *16*(4), 276–281.

[66] Gabrielson, N. P.; Pack, D. W. Acetylation of Polyethylenimine Enhances Gene Delivery via Weakened Polymer/DNA Interactions. *Biomacromolecules* **2006**, *7*, 2427-2435.

[67] Dubruel, P.; Christiaens, B.; Rosseneu, M.; Vandekerckhove, J.; Grooten, J.; Goossens, V.; Schacht, E. Buffering Properties of Cationic Polymethacrylates Are Not the Only Key to Successful Gene Delivery. *Biomacromolecules* **2004**, *5*, 379-388.

[68] Benjaminsen, R. V.; Mattebjerg, M. A.; Henriksen, J. R.; Moghimi, S. M.; Andresen, T. L. The Possible "Proton Sponge" Effect of Polyethylenimine (PEI) Does Not Include Change in Lysosomal pH. *Molecular Therapy* **2013**, *21*(1), 149–157.

[69] Luten, J.; van Nostrum, C. F.; De Smedt, S. C.; Hennink, W. E. Biodegradable polymers as non-viral carriers for plasmid DNA delivery. *J. Controlled Release* **2008**, *126*, 97−110.

[70] Jiang, X.; Lok, M. C.; Hennink, W. E. Degradable-Brushed pHEMA−pDMAEMA Synthesized *via* ATRP and Click Chemistry for Gene Delivery. *Bioconjugate Chem*. **2007**, *18*, 2077−2084.

[71] Lynn, D. M.; Langer, R. Degradable Poly(β-amino esters): Synthesis, Characterization, and Self-Assembly with Plasmid DNA. *J. Am. Chem. Soc*. **2000**, *122*, 10761−10768.

[72] Vazquez, E.; Dewitt, D. M.; Hammond, P. T.; Lynn, D. M. Construction of Hydrolytically-Degradable Thin Films via Layer-by-Layer Deposition of Degradable Polyelectrolytes. *J. Am. Chem. Soc.* **2002**, *124*, 13992−13993.

[73] You, Y. Z.; Manickam, D. S.; Zhou, Q. H.; Oupicky, D. Reducible poly(2-dimethylaminoethyl methacrylate): Synthesis, cytotoxicity, and gene delivery activity. *J. Controlled Release* **2007**, *122*, 217−225.

[74] Dai, F.; Sun, P.; Liu, Y.; Liu, W. Redox-cleavable star cationic PDMAEMA by arm-first approach of ATRP as a nonviral vector for gene delivery. *Biomaterials* **2010**, *31*, 559−569.

[75] Mizutani, M.; Palermo, E. F.; Thoma, L. M.; Satoh, K.; Kamigaito, M.; Kuroda, K. Design and Synthesis of Self-Degradable Antibacterial Polymers by Simultaneous Chain- and Step-Growth Radical Copolymerization. *Biomacromolecules* **2012**, *13*, 1554−1563.

[76] Luten, J.; Akeroyd, N.; Funhoff, A.; Lok, M. C.; Talsma, H.; Hennink, W. E. Methacrylamide Polymers with Hydrolysis-Sensitive Cationic Side Groups as Degradable Gene Carriers. *Bioconjugate Chem.* **2006**, *17*, 1077−1084.

[77] Sinclair, A.; Bai, T.; Carr, L. R.; Ella-Menye, J. R.; Zhang, L.; Jiang, S. Engineering Buffering and Hydrolytic or Photolabile Charge Shifting in a Polycarboxybetaine Ester Gene Delivery Platform. *Biomacromolecules* **2013**, *14*, 1587−1593.

[78] Zhang, J.; Lynn, D. M. Ultrathin Multilayered Films Assembled from "Charge-Shifting" Cationic Polymers: Extended, Long-Term Release of Plasmid DNA from Surfaces. *Adv. Mater*. **2007**, *19*, 4218− 4223.

[79] Sun, B.; Lynn, D. M. Release of DNA from polyelectrolyte multilayers fabricated using 'charge-shifting' cationic polymers: Tunable temporal control and sequential, multi-agent release. *J. Controlled Release* **2010**, *148*, 91−100.

[80] Ros, S; Burke, N. A. D.; Stöver, H. D. H. Synthesis and Properties of Charge-Shifting Polycations: Poly[3-aminopropylmethacrylamide-*co*-2-(dimethylamino)ethyl acrylate] *Macromolecules* **2015**, *48*, 8958−8970.

[81] Ros, S.; Kleinberger, R. M.; Burke, N. A. D.; Rossi, N. A. A.; Stöver, H. D. H. Charge-Shifting Polycations with Tunable Rates of Hydrolysis: Effect of Backbone Substituents on Poly[2-(dimethylamino)ethyl acrylates]. *Macromolecules* **2018**, *51*, 5752−5761.

[82] Ho, H. T.; Bohec, M. L.; Frémaux, J.; Piogé, S.; Casse, N.; Fontaine, L. Pascual, S. Tuning the Molar Composition of "Charge-Shifting" Cationic Copolymers Based on 2-(N,N-Dimethylamino)Ethyl Acrylate and 2-(tert-Boc-Amino)Ethyl Acrylate. *Macromol. Rapid Commun*. **2017**, DOI: 10.1002/marc.201600641

[83] Qiu, N.; Gao, J.; Liu, Q.; Wang, J.; Shen, Y. Enzyme-responsive charge-reversal polymer-mediated effective gene therapy for intraperitoneal tumors, *Biomacromolecules* **2018**, *19*, 2308–2319.

[84] Chen, X.; Liu, L.; Jiang, C. Charge-reversal nanoparticles: novel targeted drug delivery carriers. *Acta Pharmaceutica Sinica B* **2016**, *6*(4), 261–267.

[85] Werfel, T. A.; Swain, C.; Nelson, C. E.; Kilchrist, K. V.; Evans, B. C.; Miteva, M.; Duvall, C. L. Hydrolytic charge-reversal of PEGylated polyplexes enhances intracellular un-packaging and activity of siRNA. *J. Biomed. Mater. Res. Part A* **2016**, *104A*, 917–927.

[86] Novo, L.; Takeda, K. M.; Petteta, T.; Dakwar, G. R.; van den Dikkenberg, J. B.; Remaut, K.; Braeckmans, K.; van Nostrum, C. F.; Mastrobattista, E.; Hennink, W. E. Targeted Decationized Polyplexes for siRNA Delivery. *Mol. Pharmaceutics* **2015**, *12*, 150−161.

[87] Novo, L.; Rizzo, L. Y.; Golombek, S. K.; Dakwar, G. R.; Lou, B.; Remaut, K.; Mastrobattista, E.; van Nostrum, C. F.; Jahnen-Dechent, W.; Kiessling, F.; Braeckmans, K.; Lammers, T.; Hennink, W. E. Decationized polyplexes as stable and safe carrier systems for improved biodistribution in systemic gene therapy. *Journal of Controlled Release* **2014**, *195*, 162–175.

[88] Lim, Y. -B.; Choi, Y. H.; Park, J. -S. A Self-Destroying Polycationic Polymer: Biodegradable Poly(4-hydroxy-L-proline ester). *J. Am. Chem. Soc*. **1999**, *121*, 5633-5639.

[89] Wood, K. C.; Boedicker, J. Q.; Lynn, D. M.; Hammond, P. T. Tunable Drug Release from Hydrolytically Degradable Layer-by-Layer Thin Films. *Langmuir* **2005**, *21*, 1603-1609.

[90] Hong, J.; Kim, B. -S.; Char, K.; Hammond, P. T. Inherent Charge-Shifting Polyelectrolyte Multilayer Blends: A Facile Route for Tunable Protein Release from Surfaces. *Biomacromolecules* **2011**, *12*, 2975–2981.

[91] Liu, X.; Yang, J. W.; Miller, A. D.; Nack, E. A.; Lynn, D. M. Charge-Shifting Cationic Polymers That Promote Self-Assembly and Self-Disassembly with DNA. *Macromolecules* **2005**, *38*, 7907-7914.

[92] McCool, M. B.; Senogles, E.The Self-Catalyzed Hydrolysis of Poly(N,N-dimethylaminoethyl acrylate). *Eur. Polym. J.* **1989**, *25*, 857–860.

[93] van de Wetering, P.; Zuidam, N. J.; van Steenbergen, M. J.; van der Houwen, O. A. G. J.; Underberg, W. J. M.; Hennink, W. E. A Mechanistic Study of the Hydrolytic Stability of Poly(2-(dimethylamino)ethyl methacrylate). *Macromolecules* **1998**, *31*, 8063−8068.

[94] Truong, N. P.; Jia, Z.; Burges, M.; McMillan, N. A. J.; Monteiro, M. J. Self-Catalyzed Degradation of Linear Cationic Poly(2-dimethylaminoethyl acrylate) in Water. *Biomacromolecules* **2011**, *12*, 1876–1882.

[95] Whitfield, R.; Anastasaki, A.; Truong, N. P.; Cook, A. B.; Omedes-Pujol, M.; Rose, V. L.; Nguyen, T. A. H.; Burns, J. A.; Perrier, S.; Davis, T. P.; Haddleton, D. M. Efficient Binding, Protection, and Self-Release of dsRNA in Soil by Linear and Star Cationic Polymers. *ACS Macro Lett*. **2018**, *7*, 909−915.

[96] Truong, N. P.; Jia, Z.; Burgess, M.; Payne, L.; McMillan, N. A. J.; Monteiro, M. J. Self-Catalyzed Degradable Cationic Polymer for Release of DNA. *Biomacromolecules*, **2011**, *12*, 3540-3548.

[97] Cotanda, P.; Wright, D. B.; Tyler, M.; O'Reilly, R. K. A Comparative Study of the Stimuli-Responsive Properties of DMAEA and DMAEMA Containing Polymers. *J. Polym. Sci., Part A: Polym. Chem.* **2013**, *51*, 3333–3338.

[98] Rolph, M. S.; Pitto-Barry, A; O'Reilly, R. K. The hydrolytic behavior of N,N'-(dimethylamino) ethyl acrylate-functionalized polymeric stars. *Polym. Chem*. **2017**, *8*, 5060-5070.

[99] Zhao, W.; Fonsny, P.; FitzGerald, P.; Warr, G. G.; Perrier, S. Unexpected behavior of polydimethylsiloxane/ poly(2-(dimethylamino)ethyl acrylate) (charged) amphiphilic block copolymers in aqueous solution. *Polym. Chem*., **2013**, *4*, 2140–2150.

[100] Cook, A. B.; Peltier, R.; Hartlieb, M.; Whitfield, R.; Moriceau, G.; Burns, J. A.; Haddleton, D. M.; Perrier, S. Cationic and hydrolysable branched polymers by RAFT for complexation and controlled release of dsRNA. *Polym. Chem*., **2018**, *9*, 4025–4035.

[101] Truong, N. P.; Gu, W.; Prasadam, I.; Jia, Z.; Crawford, R.; Xiao, Y.; Monteiro, M. J. An influenza virus-inspired polymer system for the timed release of siRNA. *Nat. Commun.* **2013**, *4*:1902. doi: 10.1038/ncomms2905

[102] Whitfield, R.; Anastasaki, A.; Truong, N. P.; Wilson, P.; Kempe, K.; Burns, J. A.; Davis, T. P.; Haddleton, D. M. Well-Defined PDMAEA Stars via Cu(0)-Mediated Reversible Deactivation Radical Polymerization. *Macromolecules* **2016**, *49*, 8914−8924.

CHAPTER 2: Synthesis and Properties of Charge-Shifting Polycations: Poly[3-Aminopropylmethacrylamide-*co*-2-(Dimethylamino)ethyl acrylate]

Samantha Ros, Nicholas A. D. Burke, Harald D. H. Stöver*

Department of Chemistry and Chemical Biology, McMaster University, Hamilton, ON, Canada L8S 4M1

Reprinted (adapted) with permission from Ros, S. *et al.*, *Macromolecules* **2015**, *48* (24), 8958-8970.

2.1. Abstract

Charge-shifting copolymers of N-(3-aminopropyl)methacrylamide (APM) and 2-(dimethylamino)ethyl acrylate (DMAEA) were prepared and investigated as potential replacements for conventional polycations like poly(L-lysine) (PLL) in biomaterial applications. ^{1}H-NMR was used to determine the reactivity ratios of APM and DMAEA to be 0.89 and 0.37, respectively, at pH 3-4 where both monomers were protonated and DMAEA was hydrolytically stable. Conventional free radical and reversible addition-fragmentation chain transfer (RAFT) copolymerization were used to prepare a series of P(APM-*co*-DMAEA) (PAD) copolymers with different MWs and compositions. Charge-shifting from cationic towards neutral and anionic net charges by hydrolysis of DMAEA units was determined by ^{1}H NMR to depend both an composition and pH, (pH 9 > 7 > 5). PAD copolymers bound strongly to anionic polymer particles and calcium alginate beads. For calcium alginate, the amount of PAD bound and the shell thickness depended on copolymer composition and MW. The PAD coating underwent hydrolysis and was released from the anionic surfaces as shown by microscopy and electrophoretic mobility

measurements. PAD coatings that were crosslinked with tetrakis(hydroxymethyl) phosphonium (THPC) remained on the capsule surface after hydrolysis, to form amphiphilic or anionic crosslinked surfaces.

2.2. Introduction

Polyelectrolytes have been used extensively in material applications as the electrostatic interaction of oppositely charged polymers allows for their self-assembly into various polyelectrolyte complexes.[1,2] We are interested in using synthetic polyelectrolytes for the encapsulation and immuno-isolation of mammalian cells as an approach to cell-based therapies for enzyme and hormone deficiency disorders. The standard alginate-poly(L-lysine)-alginate (APA) capsules used for such purposes, composed of calcium alginate cores coated with poly(L-lysine) and a final alginate layer, have shown issues with mechanical stability and biocompatibility.[3,4] As the APA capsule is held together solely by electrostatic interactions (Ca-alginate and alginate-PLL), its long-term stability in *vivo* can be compromised by processes such as exchange of calcium for sodium in the serum.[5] Although the high-charge density of poly(L-lysine) (PLL) allows for strong electrostatic complexation with alginate, it is can still be desirable to covalently crosslink the polyelectrolyte complex to ensure long-term stability of the capsule shell.[6-8] In applications such as cell encapsulation for long-term therapies, it can be advantageous to hide the PLL on the capsule surface to avoid adverse immune responses including cellular overgrowth triggered by cationic patches and hydrophobic complexes.[9,10]

One approach to reduce the detrimental effects of such high-charge density polycations is to reduce or mask the cationic charge by combining cationic monomers with neutral, polar[11] or anionic[12] comonomers, or by grafting with poly(ethylene glycol) chains.[13,14] Many of these charge-reduced polycations suffer from relatively weak electrostatic binding to the calcium alginate cores. Thus, a polymer with a high cationic charge density, able to form strong polyelectrolyte complexes with alginate, is desirable for initial deposition, though a mechanism of cationic charge reduction may be desirable for compatibility of the final hydrogel for certain applications.

We recently described temporarily reactive polyanions that can a) form a 1:1 charge complex with PLL coated onto calcium alginate, b) spontaneously crosslink with amines on the polycation and c) undergo hydrolysis of residual electrophilic units to give an overall anionic charge to the complex.[10,15]

There has been recent interest in polyelectrolytes able to reduce or switch the charge on cationic polymer chain by hydrolysis, generating carboxylates. These polymers, often called "charge-shifting", "charge-reversing" or "charge-conversion" polymers, are of particular interest where the high initial cationic charge allows formation of polyelectrolyte complexes which then disassemble upon hydrolysis of the cationic groups.[16-18] McCool and Senogles first reported the self-catalyzed hydrolysis of poly(2-(dimethyl)aminoethyl acrylate), pDMAEA, to form acrylic acid units (AA) and 2-dimethylaminoethanol (DMAE).[19] More recently, Monteiro et al. explored the preparation and hydrolysis (charge-shifting) of various DMAEA-containing polymers with potential applications as DNA or siRNA delivery devices.[20-22]

In the present work, copolymers of DMAEA and N-(3-aminopropyl) methacrylamide (APM) were prepared and studied as a potential replacement for high charge density polycations such as PLL or poly(APM) in applications involving a temporary need for strong electrostatic complexation with polyanions. It was anticipated (Scheme 2.1.) that the highly cationic p(APM-co-DMAEA) (PAD) copolymers would a) form strong polyelectrolyte complexes with polyanions such as alginate, b) be covalently crosslinked by reacting the primary amino group of APM with small-molecule[23] or polymeric[10,15] electrophilic crosslinker, and c) undergo hydrolysis of DMAEA units to reduce or even invert the cationic charge density, thereby creating a charge-shifted or zwitterionic polymer network at the surface of the capsule. The extent of crosslinking and charge reduction should be controlled by varying the APM/DMAEA ratio with copolymers with higher APM content crosslinking more efficiently but showing lower charge reduction due to their lower DMAEA content.

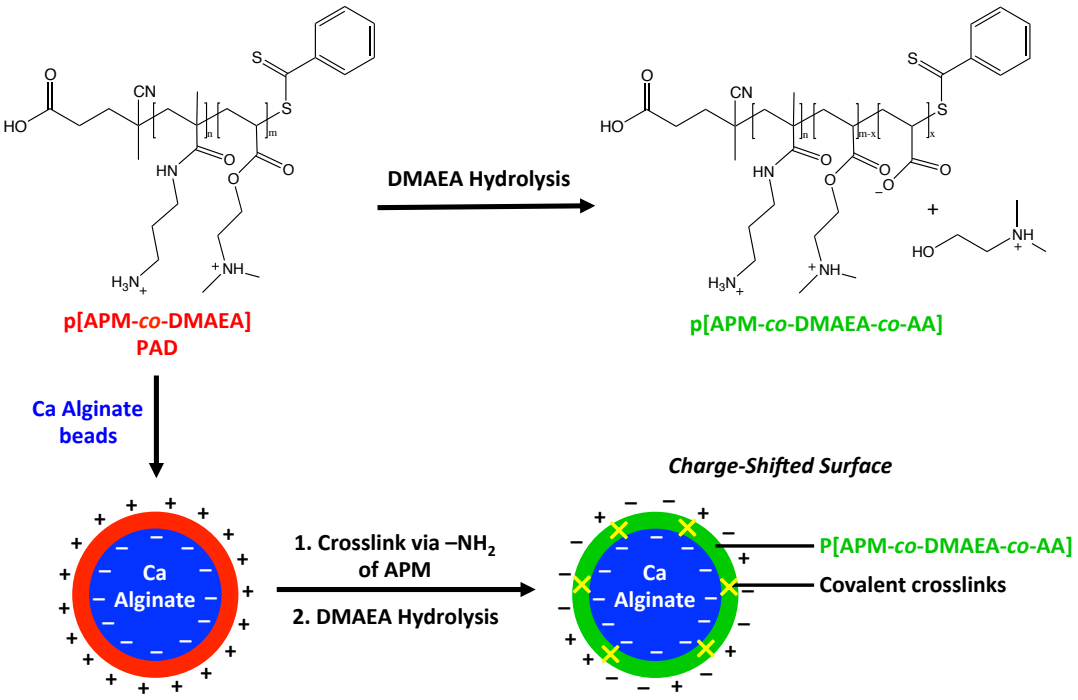

Scheme 2.1. Complexation, crosslinking, and hydrolytic charge-shifting of P[APM-*co*-DMAEA], PAD, to form capsules with decreased cationic charge densities.

Conventional free radical and reversible addition-fragmentation chain transfer (RAFT)[24,25] polymerization were used to prepare polymers with different molecular weight (MW), as polycation MW can affect the structure and stability of alginate-based capsules.[4,26] Hydrolysis of the DMAEA units of PAD was examined as a function of copolymer composition, pH, and temperature. PAD-coated calcium alginate capsules and crosslinked poly(4-methylstyrene-*alt*-maleic anhydride) microspheres were investigated to determine the effect of copolymer composition, MW, and hydrolysis on the nature of the capsule membrane. Finally, tetrakis(hydroxymethyl)phosphonium chloride (THPC), a small molecule crosslinker,[23] was used to demonstrate the ability to covalently crosslink the alginate–PAD (A–PAD) capsule membrane to enhance their mechanical stability.

2.3. Experimental

2.3.1. Materials

N-(3-Aminopropyl)methacrylamide hydrochloride was purchased from PolySciences and was used as received. 2-(Dimethylamino)ethyl acrylate (98%), 2,2'-azobis(2-methylpropionamidine) dihydrochloride (Vazo-56), 4-cyano-4-(phenylcarbonothioylthio) pentanoic acid (≥98%), 4,4-azobis(4-cyanovaleric acid) (>97%), tetrakis(hydroxymethyl) phosphonium chloride (80 wt.% in water), fluorescein isothiocyanate isomer I (FITC, ≥90%), deuterium chloride (DCl, 35% in D_2O, 99% D), N,N-dimethylformamide (≥98%) and tetrakis(hydroxymethyl)phosphonium chloride (THPC) were purchased from Sigma-Aldrich and used as received unless otherwise stated. DMSO-D6 (99.9% D), MeOD-D_4 (99.8% D), and D_2O (99.9% D) from Cambridge Isotope Laboratories Inc., 1,4-Dioxane (≥99 %) from Caledon Laboratories, basic alumina (activity I) from Fisher Scientific and sodium alginate (Pronova UP MVG, 69% G, BP-1105-06) from Nova Matrix were used as received.

2.3.2. Reactivity Ratio Determination of APM and DMAEA

Copolymerizations of APM and DMAEA were conducted within a 500 MHz Bruker Avance spectrometer and followed by ^{1}H NMR spectroscopy. Solutions of APM and DMAEA at 10% w/v total monomer loading with 1 mol% Vazo-56 in D_2O, with initial feed ratios of 20:80, 25:75, 50:50, 60:40, 75:25, and 90:10 mol% were prepared. The pH of the polymerization solutions was adjusted to 3-4 with 1 M DCl in D_2O to ensure that APM and DMAEA were protonated and to prevent premature hydrolysis of the DMAEA units. The solutions were transferred to 5 mm NMR tubes and placed in the

NMR instrument. The reaction mixtures were rapidly heated to 55 °C, following which spectra were collected every minute. The vinyl signals of APM and DMAEA monomers were integrated with respect to the signal at 3.94 ppm, which represents the methylene protons adjacent to the amine of DMAEA in both monomer and polymer and remains constant throughout the polymerization. The amount of each monomer consumed in small conversion steps (5–10 %) throughout copolymerization was calculated from the ^{1}H NMR data. The reactivity ratios were calculated both by the Fineman-Ross method,[27] and by fitting the (Mayo-Lewis) instantaneous copolymer composition equation to the incremental comonomer conversion data using the least squares method with the Solver tool in Microsoft Excel.

2.3.3. Preparative Conventional Radical Copolymerization of APM and DMAEA

Copolymers of APM and DMAEA were synthesized in H_2O at pH 3-4 with 10% w/v total monomer loading using 1 mol% Vazo-56 initiator. The molar feed ratios of APM:DMAEA were 0:100, 10:90, 15:85, 50:50, and 75:25 targeting PAD_{100}, PAD_{85}, PAD_{75}, PAD_{50}, and PAD_{25}, respectively, where the subscript denotes the DMAEA content. The preparation of PAD_{50} is provided as an example. APM (0.555 g, 3.11 mmol) and Vazo-56 (16.9 mg, 0.062 mmol) were dissolved in a mixture of 6.9 mL deionized water and 3.1 mL of 1 M HCl (3.1 mmol) before DMAEA (0.445 g, 3.11 mmol) was added. The pH was adjusted to 3.45 using 1 M NaOH. The reaction mixture, in a 20 mL vial equipped with a septum, was heated in a water bath at 55°C for 90 min. The polymerization was followed by ^{1}H NMR spectroscopy by taking 0.3 mL aliquots at 30 min intervals with a syringe purged with nitrogen, and then diluting the aliquot with D_2O

prior to analysis. The polymerizations typically reached about 70% overall conversion after 90 min of heating.

The polymer was purified by dialysis in cellulose tubing (Spectrum Laboratories; 3.5 kDa MW cutoff) with water at pH 3 with 1 M HCl replaced twice per day until the dialysate showed no absorbance due to monomers or other small molecules with UV-vis spectroscopy, typically after three days. The dialyzed polymer solution was freeze-dried, resulting in PAD_{50} in the hydrochloride form as a white solid. Polymers were analyzed by ^{1}H NMR spectroscopy using a Bruker AV 600 spectrometer to determine copolymer composition. Gel permeation chromatography (GPC) was performed with a Waters GPC consisting of a 717plus auto sampler, 515 HPLC pump, Ultrahydrogel (120, 250, 500) columns (30 cm x 7.8 mm (i.d.); 6 μm particles), and a 2414 refractive index detector, using a 1 M acetate buffer (pH 4.8) with flow rate of 0.8 mL/min at 30°C as the mobile phase. The GPC system was calibrated with poly(ethylene glycol) (PEG) standards (Waters Inc.) ranging in molecular weight from 106 Da to 584 kDa.

2.3.4. Reversible Addition-Fragmentation Chain Transfer (RAFT) Polymerization of APM and DMAEA

RAFT copolymerization of APM and DMAEA was conducted using a 5:1 mol ratio of RAFT agent (4-cyano-4-(phenylcarbonothioylthio) pentanoic acid) (CTP) to initiator 4,4-azobis(4-cyanovaleric acid) (V501) as shown in Figure 2.1.

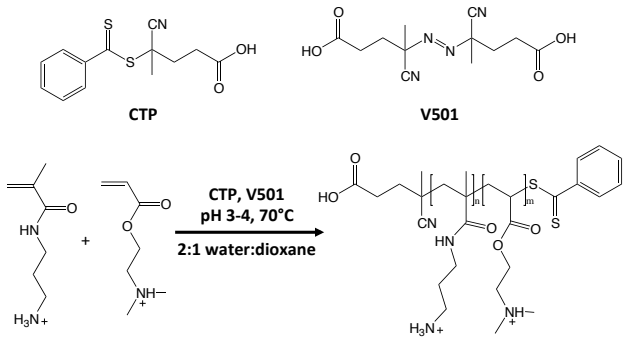

Figure 2.1. RAFT copolymerization of APM and DMAEA using CTP as chain transfer agent and V501 as initiator.

DMAEA was passed neat through a basic alumina (activity I) plug to remove the inhibitor and was used immediately after purification. The reactions were carried out with 30 % w/v total monomer loading in a 2:1 water:1,4-dioxane solvent mixture with one equivalent of HCl to protonate DMAEA and prevent hydrolysis during copolymerization. The reaction mixture was placed in an ice-water bath before DMAEA addition to limit heating due to neutralization. Exploratory reactions were conducted with 0.9 g total monomer in 3 mL of solvent and aliquots (~200 μL) were taken from the polymerization mixture at various intervals with a N_2-purged syringe. A fraction of each aliquot was diluted with D_2O and then analyzed with ^1H NMR spectroscopy (600 MHz) to determine conversion. The remainder of each aliquot was diluted with GPC mobile phase (1 M acetate buffer) and analyzed by GPC as described above to estimate M_n and polydispersity. Preparative copolymerizations employed 1.8 g of total monomer in 6 mL of solvent and aliquots were taken less frequently to ensure a targeted conversion of about 80 %. The preparative RAFT copolymerization targeting PAD_{50} with MW of 8 kDa is given as an example.

In a 20 mL glass vial, APM (0.910 g, 5.09 mmol), CTP (54.6 mg; 0.196 mmol), V501 (11.0 mg; 0.0391 mmol) were dissolved in 6 mL of solvent consisting of 2.00 mL 1,4-dioxane, 2.96 mL water and 1.04 mL of 6 M HCl (6.22 mmol). The solution was cooled in an ice bath as DMAEA (0.891 g; 6.22 mmol) was added. The vial containing the transparent pink reaction mixture was fitted with a septum and the solution was purged for 45 min with N_2 gas while stirring at room temperature. The vial was placed in a 70°C oil bath with the reaction mixture kept under positive N_2 pressure while being stirred. When the conversion had reached about 80%, the solution was cooled in an ice bath and exposed to air to halt polymerization. The polymerization mixture was dialyzed and then freeze-dried as described above resulting in PAD_{50} (HCl form) as a pink solid. Preparative reactions targeting PAD_{25}, PAD_{50}, and PAD_{75} with MWs of 8 and 30 kDa were conducted by RAFT polymerization in a similar fashion.

Measured M_n values were compared to theoretical values ($M_{n,th}$) obtained from eq. **(1)**, where $[m]_i$ and $[CTP]_i$ are the initial concentrations of the monomer and chain-transfer agent, M_{m^*} is the average monomer MW and M_{CTP} is the MW of the chain-transfer agent.

$$M_{n,th} = conversion \times \left(\frac{[m]_i}{[CTP]}\right) \times M_{m^*} + M_{CTP} \quad (\mathbf{1})$$

2.3.5. Rate of Hydrolysis of PAD by ^{1}H NMR Spectroscopy

The rate of hydrolysis of DMAEA units within PAD_{100}, PAD_{88}, PAD_{74}, PAD_{43}, and PAD_{24} was monitored by ^{1}H NMR spectroscopy (600 MHz). The polymers were dissolved at a concentration of 0.5 or 1 % w/v in D_2O buffered with 50 or 100 mM

acetate (pH 5), phosphate (pH 7) or borate (pH 9) buffers. In most cases, the solution pH was measured and adjusted if necessary. The solutions were transferred to NMR tubes, which were maintained at room temperature or 37 °C. At various time intervals, ^{1}H NMR spectra were obtained and the solution pH was measured. The percent hydrolysis of DMAEA was determined by comparing the area of the peaks at 3.9 and 4.5 ppm corresponding to the CH_2O methylene protons in DMAE (hydrolysis by-product) and DMAEA units, respectively.

2.3.6. Fluorescent Labeling of PAD

PAD polymers were fluorescently labeled using FITC with a targeted degree of labeling of 1 mol% (relative to total monomer units). The labeling of PAD_{50} is provided as an example. A solution of PAD_{50} (100 mg or 0.622 mmol monomer units) in 10 mL water was adjusted to pH 7.5 before the addition of 240 μL of a 1% w/v solution of FITC in DMF (2.4 mg; 6.2 μmol). The mixture was stirred at room temperature for 1 h before the pH was adjusted to pH 3 with 1 M HCl. The sample was purified by dialysis as described above except that dialysis was carried out for only 1 day. The polymer was isolated by freeze-drying as a yellow solid and stored in the dark. UV-vis analysis showed that the labeling degree was about 1 % for all PAD-*f* samples.

2.3.7. Preparation of Calcium Alginate Beads

Calcium alginate beads were prepared as reported previously.[28] Briefly, 5 mL of 1 % w/v sodium alginate in saline was syringe filtered (0.2 μm) and then extruded through a 27-gauge needle at 0.5 mL/min using a syringe pump into 60 mL of a 100 mM $CaCl_2$, 77 mM NaCl gelling bath solution. The needle passed through an orifice (~1.2 mm dia.)

and the droplet size, and hence bead size, was controlled using an annular airflow of 3.6 L/min, providing an airspeed near the needle tip of about 60 m/s. The calcium alginate beads were isolated from the gelling bath 15 min after bead formation was complete and were stored in a 3.3-fold volume of saline (e.g., 3 mL beads to 10 mL saline). The average diameter of the resulting calcium alginate beads was 500 ± 23 μm (n = 88) measured using optical microscopy.

2.3.8. Coating Calcium Alginate Beads with PAD

Calcium alginate beads were coated with PAD-*f* in a procedure similar to those previously reported for other polycations.[28] Settled calcium alginate beads (0.3 mL) were coated with PAD by adding 1 mL of 0.1% w/v PAD in 35 mM 4-(2-hydroxyethyl)-1-piperazineethanesulfonic acid (HEPES)-buffered saline at pH 7.8 and occasionally agitating for 6 min. The supernatant was removed and the resulting coated beads (A–PAD_x) were washed once with 1 mL of 100 mM $CaCl_2$, 77 mM NaCl gelling bath solution, followed by 1 mL of saline with each wash taking 2 min. The capsules were then stored in 1 mL of 35 mM HEPES-buffered saline at pH 7.8 in the absence of light at 22°C.

2.3.9. PAD coated Poly(4-methylstyrene-alt-maleic acid) particles

Anionic poly(4-methylstyrene-*alt*-maleic acid) (PMSM) particles, provided by Yuqing Zhao and Marta Skreta in our group, were obtained by hydrolysis of lightly crosslinked poly(4-methylstyrene-*alt*-maleic anhydride) particles that had been prepared as described by Frank et al.[29] A suspension of PMSM particles (0.1 mL, 6 % w/v, dia. = 7.92 ± 0.74 μm, n = 200) was added to 4.5 mL of a 0.1 % w/v solution of PAD in 35 mM

HEPES buffered saline. The particles were exposed to the polycation solution for 10 min with occasional mixing. The suspension was centrifuged at 3500 rpm for 5 min. The supernatant was removed and the particles were re-suspended in 2 mL of HEPES-buffered saline. This process was performed twice to remove excess polycation. The particles were stored in 2 mL of pH 7.2 HEPES-buffered saline at 22°C.

Electrophoretic mobility of uncoated and PAD-coated PMSM particles was measured using a Malvern ZEN3600 Zetasizer Nano ZS. Measurements were performed 10 times for each sample (n = 10) at room temperature with approximately 0.7 mL of the particle suspension using a Malvern Zeta-Dip Cell. Electrophoretic mobility was measured in units of $10^{-8}m^2/(sV)$, which describes the velocity of a particle (m/s) in a given electric field strength (Vm^{-1}).

2.3.10. Crosslinking of A–PAD$_{75}$-30kf-coated Capsules with THPC

A dense suspension of calcium alginate beads (0.3 mL) that had been coated with PAD$_{75}$-30k*f* were exposed to 1 mL of 0.1 % THPC in 35 mM HEPES-buffered saline for 2 min, then washed once with 1 mL of saline for 2 min. The capsules were stored in 1 mL of the HEPES-buffered saline (pH 7.8) at 22°C in the dark.

2.3.11. Microscopy of Calcium Alginate Beads and Capsules

Calcium alginate beads, uncoated and PAD-*f*-coated, were examined by conventional and fluorescence microscopy with a Nikon Eclipse LV100ND optical microscope equipped with an Andor Zyla sCMOS camera and Nikon Elements software, as well as by Confocal Laser Scanning Microscopy (CLSM) using a Nikon A1 Confocal

Eclipse T*i* microscope with Nikon Elements software. Images of the capsules on Day 0 were taken immediately after coating. Line profiles of the fluorescence intensity of cross-sectional images of the capsules were obtained using Nikon Elements software and the thickness of the capsule membranes was determined by the full-width at half-height.

2.3.12. Sodium Citrate and Sodium Hydroxide Test for A–PAD-f Complex Integrity

A droplet of HEPES-buffered saline containing A–PAD-*f* capsules was placed on a glass slide and a few drops of 50 mM sodium citrate was added to the capsules and gently agitated for about one minute. The supernatant was removed from the capsules on the glass slide and a few drops of 0.1 M sodium hydroxide was added. The capsules were monitored during this process by conventional fluorescence microscopy.

2.4. Results and Discussion

2.4.1. Copolymerization of APM and DMAEA

Since DMAEA is susceptible to hydrolysis or nucleophilic attack, it was important to find polymerization conditions under which both the monomer and polymer were stable. DMAEA has been (co)polymerized in organic solvents such as dioxane,[20,30] acetonitrile[31] or isopropanol[32] in which it is stable. However, APM, which must be used as the hydrochloride salt to avoid reaction with DMAEA, is not soluble in these solvents and is typically polymerized in aqueous solvents or methanol (MeOH).

^{1}H NMR spectroscopy confirmed rapid trans-esterification between DMAEA and MeOH, likely facilitated by the presence of free amine (Figure 2A.1). This was seen previously by McCool and Senogles for both DMAEA and its homopolymer, and had led

the suggestion that aqueous and alcoholic solvents be avoided.[19] We found that DMAEA and APM were stable in their protonated form in water at pH 3 (Figure 2.2.) at 22°C, and hence carried out the copolymerizations under these conditions (pH 3-4).

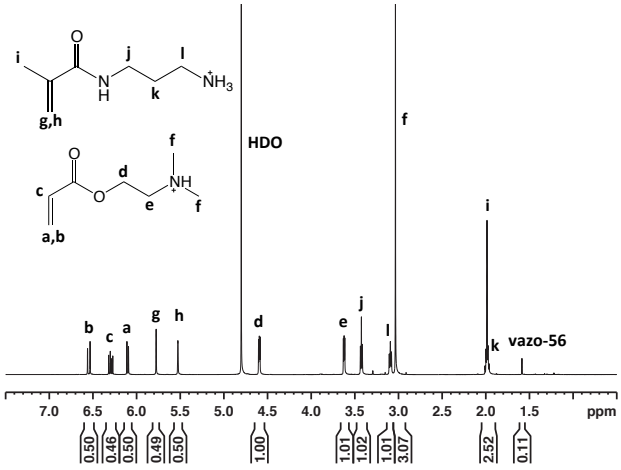

Figure 2.2. ^{1}H NMR spectrum of a 50:50 mixture of DMAE and APM with Vazo-56 initiator at pH 3-4in D_2O, showing no hydrolysis at 22 °C.

2.4.2. Reactivity Ratios

The reactivity ratios for the APM/DMAEA system were determined by following a series of copolymerizations by ^{1}H NMR spectroscopy, similar to experiments described by Aguilar et al.[33] The amounts of each monomer consumed in small, consecutive steps in monomer conversion (5-10%) were determined, with the residual monomers present at the end of one step serving as the starting monomer mix for the next small step in conversion. In this way, it was possible to get a set of data points (monomer feed ratio, copolymer composition) from each copolymerization.

The composition of the residual monomer vs. conversion for various feed ratios of APM and DMAEA is shown in Figure 2.3. There is a slight preference for APM incorporation except for monomer mixtures with high APM content, where the comonomers are incorporated in the feed ratio. The data obtained from these copolymerizations is summarized in Table 2A.1. Reactivity ratios for APM and DMAEA were determined using the Fineman-Ross method (0.86 and 0.38) as shown in Figure 2A.2 and by a least-squares fitting of the copolymer equation **(2)** to the data shown in Figure 2.3, with the resulting fit shown in Figure 2.4 (r_1,r_2 = 0.89, 0.37). The values are near identical, consistent with those measured for another methacrylamide–acrylate copolymer system: N-[3-(dimethylamino)propyl]methacrylamide/methyl acrylate (0.63/0.48).[34] The reactivity ratios obtained from fitting equation (**2**) were used to select the comonomer feed ratios required to produce copolymers of the desired compositions. The joint confidence region at 95 % confidence level for the reactivity ratios obtained by the non-linear least squares fitting is provided in the Supporting Information (Figure 1A.3).

$$F_1 = \frac{r_1 f_1^2 + f_1 f_2}{r_1 f_1^2 + 2 f_1 f_2 + r_2 f_2^2} \qquad (\mathbf{2})$$

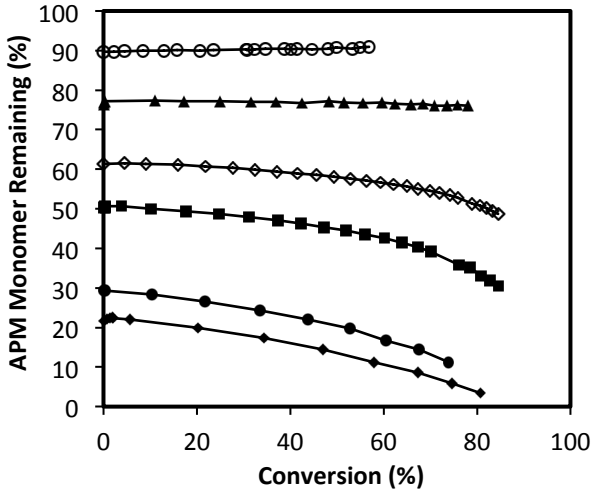

Figure 2.3. Fraction of APM remaining in the monomer mixture as a function of conversion for various feed ratios of APM and DMAEA.

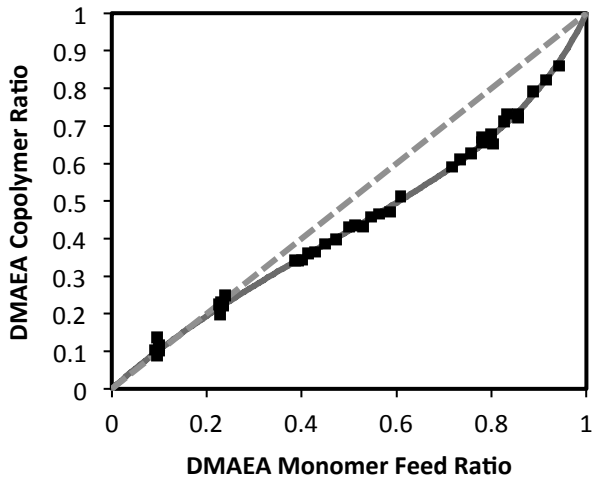

Figure 2.4. Composition of PAD copolymer formed from various APM/DMAEA feed ratios. The solid line shows the best-fit of the copolymer equation to the data with reactivity ratios of 0.89 and 0.37 for APM and DMAEA, respectively.

2.4.3. Conventional Radical Polymerization of APM and DMAEA

A series of PAD copolymers of varying compositions were prepared by conventional radical copolymerizations of APM and DMAEA in water at pH 3 (Table

2.1.). Monomer feeds enriched with DMAEA were used when targeting PAD_{85} and PAD_{75} such that they would give the desired average copolymer compositions at 70 % conversion. The polymers were purified by dialysis at pH 3 to avoid DMAEA hydrolysis, and then isolated by freeze-drying. The copolymers were analyzed by ^1H NMR spectroscopy in D_2O and representative spectra are provided in the Supporting Information (Figures 2A.4–2A.6). Copolymer compositions were determined using the areas of the DMAEA peak at 4.5 ppm (2H) and the backbone proton signals at 0.5-2.8 ppm (3H from DMAEA; 7H from APM). The measured compositions were close to the targeted compositions as shown in Table 2.1, with the offset from comonomer feed ratios being in accord with the reactivity ratios. The DMAEA content of PAD_{43} formed from a 50:50 feed ratio was lower than expected on the basis of the reactivity ratios (46% DMAEA at 70% conversion), perhaps due to uncertainty in the NMR analysis. In later experiments, PAD with 50 mol% DMAEA was obtained by employing a 45:55 feed ratio. For each PAD copolymer, the area of the backbone signals was consistent with the area of the DMAEA and APM signals at 3-4.5 ppm indicating that the polymers did not contain significant amounts of AA, and, hence, little or no hydrolysis occurred during the copolymerization and purification process. In addition, NMR analysis of solid PAD samples stored for several months at room temperature revealed that PAD in the hydrochloride form was stable to hydrolysis and trans-amidation (Figure 2A.7). Additional experiments to support monomer and polymer stability to trans-amidation are provided in the Supporting Information (Figures 2A.8 and 2A.9). Hence, the use of an

acidic pH during copolymerization and purification was successful in preventing premature hydrolysis of DMAEA.

Table 2.1. Properties of PAD copolymers.

Polymer (target)	Feed Ratio (APM:DMAEA)	Polymer Composition[a]	Mp[b] (kDa)
PAD_{100}	0:100	0:100	197
PAD_{88} (85)	10:90	12:88	204
PAD_{74} (75)	15:85	26:74	211
PAD_{43} (50)	50:50	57:43	239
PAD_{24} (25)	75:25	76:24	270

[a] From ^{1}H NMR analysis. [b] Peak MW values estimated by GPC using PEG calibration.

GPC analysis of PAD_{100}, PAD_{88}, PAD_{74}, PAD_{43}, and PAD_{24} indicated that the polymers had high MWs and polydispersities (Figure 2A.10). Only M_p values (MW at the peak maximum) are reported in Table 2.1 because these polymers contained high MW fractions that exceeded both the exclusion limits (~300 kDa) of the GPC columns, and the MW of the highest calibration standard used (584 kDa).

2.4.4. MW Control

An initial attempt to control MW using cysteamine (2-aminoethanethiol) as a chain transfer agent was found to be complicated by Michael addition of the cysteamine to the DMAEA monomer units even though the pH was well below 7. As shown in Figures 2A.11 and 2A.12, the Michael addition is fairly rapid, and leads to significant fractions of the cysteamine, and in some cases DMAEA, being consumed within minutes after solution preparation. Although the Michael product should be easily removed by dialysis, this side reaction would cause an undesirable drift in both comonomer ratio and

MW during copolymerization. Thus, RAFT polymerization was investigated as an alternative method to control MW and polydispersity.

2.4.5. RAFT Polymerization

RAFT copolymerization of APM and DMAEA has not been reported in the literature, though RAFT polymerizations of each of these monomers in other (co)polymer systems have been studied.[20,30,31,35-37] CTP has previously been used for RAFT (co)polymerizations involving APM and DMAEA and, thus, was chosen as the RAFT agent for the APM-DMAEA copolymerization. The stability and solubility of RAFT agents in aqueous solvents has been an issue, especially at extremes of pH, ionic strength, and temperature.[38-41] In the case of CTP, organic cosolvents have been used to improve solubility and CTP has been shown to be hydrolytically stable at pH 3-4,[42] which was also ideal for minimizing DMAEA hydrolysis. Thus, RAFT copolymerization of APM and DMAEA was carried out at 70°C in a 2:1 (v:v) water:1,4-dioxane solvent mixture at pH 3-4 using CTP and V501 as the RAFT agent and initiator (Figure 2.1). The high monomer concentration (30% w/v) also helped to solubilize the RAFT agent and initiator, as they had limited solubility in water at pH 3-4. The CTP:V501 ratio was always 1:0.2 as it allowed for control of the RAFT polymerization, while the monomer:CTP ratio was varied to obtain the PAD copolymers of 8 or 30 kDa. These MWs were selected to demonstrate the effect of MW on in-diffusion of the polycations into calcium alginate beads.

Exploratory RAFT copolymerizations targeting PAD_{25}, PAD_{50}, and PAD_{75} copolymers with MWs of 8 and 30 kDa were conducted and the progress of the

copolymerizations was followed by ^{1}H NMR and GPC analysis of aliquots sampled during the course of the reactions. Results for PAD_{75}-30k are shown below (Figure 2.5) and results for the other copolymerizations are shown in the Supporting Information (Figures 2A.13-2A.16). The copolymerization went to high conversion, reaching 95% conversion after 3.5 h at 70°C, showed linear 1st order kinetics (Figure 2.5C), linear growth of MW with conversion and low polydispersity (Figure 2.5B/2.5D), characteristic features of a controlled radical polymerization. Similar results were obtained for PAD_{75}-8k, PAD_{50} (8 and 30k), PAD_{25} (8 and 30k) (Figures 2A.15-2A.16), indicating that the RAFT polymerization system was suitable for this copolymerization.

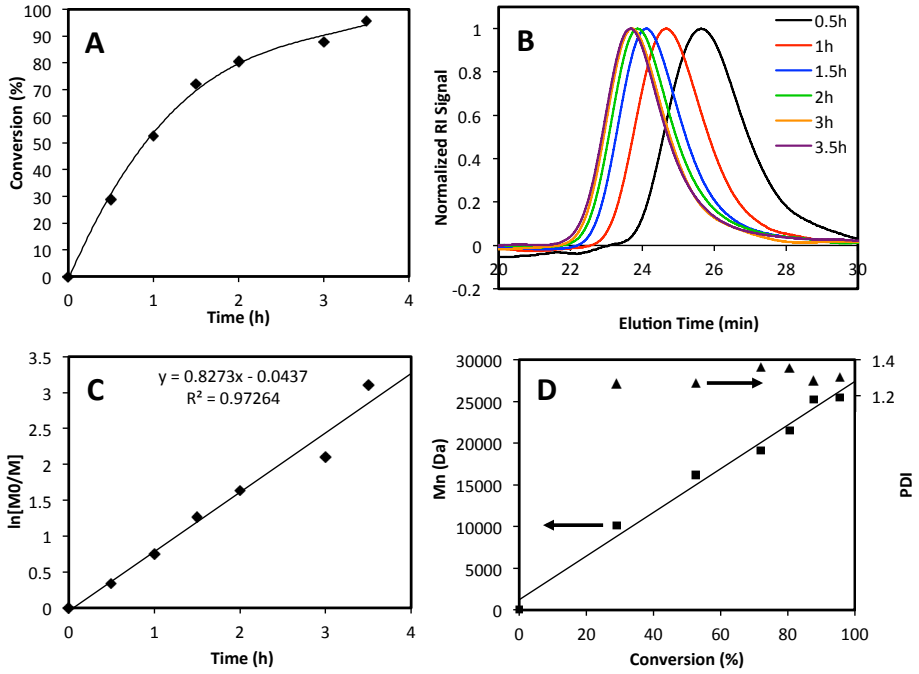

Figure 2.5. Representative results for the RAFT copolymerization to form PAD_{75}-30k. Conversion vs. time (**A**). GPC chromatograms of aliquots sampled from the copolymerization mixture (**B**). First-order kinetic plot (**C**). MW and PDI vs. conversion (**D**).

Larger-scale preparations of PAD_{25}, PAD_{50}, and PAD_{75} with MWs of 8 and 30 kDa were performed by using monomer:CTP ratios of about 60:1 and 220:1, respectively, and stopping the polymerizations at about 80-85% conversion. Some details of the copolymerizations and the resulting copolymers are given in Table 2.2.

Table 2.2. GPC, ^{1}H NMR, and UV-vis data for PAD Synthesized by RAFT Polymerization.

Polymer	[M]:[CTP]:[V501][a]	%Conv.[b]	$M_{n,th}$[c]	$M_{n,NMR}$[b]	$M_{n,UV}$[d]	$M_{n,GPC}$ (PDI)[e]	APM:DMAEA[b]
PAD_{75}-8k	58:1:0.20	78	8.1	7.2	9.1	4.5 (1.31)	25:75
PAD_{42}-8k	54:1:0.19	92	9.0	9.8	15.4	9.1 (1.36)	58:42
PAD_{21}-8k	58:1:0.20	82	8.4	8.8	10.4	7.3 (1.39)	79:21
PAD_{75}-30k	218:1:0.20	74	28.7	20.1	29.0	15.4 (1.19)	25:75
PAD_{45}-30k	212:1:0.20	84	31.8	25.3	37.0	21.1 (1.28)	55:45
PAD_{25}-30k	211:1:0.20	74	28.0	20.3	30.4	17.6 (1.35)	75:25

[a] Monomer mixtures containing 85, 47-48 and 23-24 mol% DMAEA were used in experiments targeting PAD_{75}, PAD_{50}, and PAD_{25}, respectively. [b] From ^{1}H NMR analysis. [c] Theoretical M_n (kg/mol) calculated using equation (**1**). [d] M_n from dithiobenzoate end group analysis by UV-vis spectroscopy in MeOH. [e] M_n (kg/mol) and PDI values estimated by GPC analysis with 1 M acetate buffer (pH 4.8) and PEG calibration.

The monomer feed ratios were not intentionally adjusted for differing reactivities except for PAD_{75} where a 15:85 APM:DMAEA feed was used. The compositions of the copolymers determined by ^{1}H NMR spectroscopy were fairly close to the targeted compositions and, in accord with the reactivity ratios, showed a slight enrichment in APM compared to the feed. In living polymerizations, the differing reactivities of APM and DMAEA lead to compositional drifts within each copolymer chain, i.e., to gradient copolymers.

The MWs of these PAD copolymers as measured by GPC were lower than expected, which is likely due to a poor match between the high charge density PAD polycations and the PEG standards used for calibration. Determination of M_n by analysis of the dithiobenzoate end group by ^{1}H NMR (Figures 2A.17-2A.22) and UV-vis spectroscopy resulted in values close to targeted MWs. The PAD copolymers made by RAFT and conventional polymerization were used in the hydrolysis and capsule coating studies described below.

2.4.6. Hydrolysis of PAD

The hydrolysis of DMAEA-containing polymers leading to a change in polymer charge and, hence, solubility or complexation ability, has sparked an interest in using the polymers in various applications, principally controlled delivery.[20-22] This interest extends to polymers containing the closely related monomers with primary amino (AEA)[43] or trimethylammonium (TMAEA)[44,45] groups in place of the dimethylamino group. Hydrolysis of polymers containing DMAEA, TMAEA or AEA units has been investigated in a number of studies and a range of sometimes contradictory kinetic behavior has been reported, under a number of different conditions.[19,20,30,43-47]

pDMAEA in water is often reported to show rapid initial hydrolysis that slows and approaches a plateau at about 50-70% hydrolysis, with 2-3 days at room temperature needed to reach 50% hydrolysis.[19,20,30,46] On the other hand, more rapid and nearly complete hydrolysis has been reported after 2 h at 60 °C in water.[30] In contrast, Hennink and coworkers saw much slower hydrolysis with about 12 days at 80 °C in a pH 7 buffer needed for 50% hydrolysis.[47]

Some studies have found polymers containing TMAEA and AEA groups to be much more hydrolytically stable than pDMAEA. For example, pTMAEA has been reported to be largely unchanged after a week or longer in water at room temperature,[20,46] while pAEA underwent only 5.7% hydrolysis after 8 weeks at pH 7 and 37 °C.[43] However, extensive hydrolysis (30-50%) within a day at 20-30 °C and pH 7 has been seen for TMAEA groups in acrylamide-TMAEA copolymers.[44,45]

There are also contradictory reports on the effect of pH on hydrolysis in these systems. Dimethylamino-substituted small molecule esters closely related to DMAEA show pH-dependent hydrolysis, with a minimum rate at pH 3-4. Hydrolysis was about 10^4-fold faster at pH 9 than pH 4 and the small molecules had half-lives of about one day at pH 7 and 37 °C.[47] Similarly, the TMAEA units in acrylamide-TMAEA copolymers were found to be fairly stable at pH 3.5-5 but hydrolysis became progressively faster as pH was raised with half-lives of less than 1 h seen at pH 8.5.[44,45] In distinct contrast, a recent study of pDMAEA reported that hydrolysis was pH-independent between pH 5.5 and pH 10.[20]

The inconsistency in these reported kinetic results may be attributed to difficulties in establishing and maintaining consistent pH throughout the hydrolyses. For example, the more rapid hydrolysis seen for pDMAEA in water compared to pAEA or pTMAEA is likely because the initial solution pH is much higher, about 9 to 9.5 for the free-amine form of pDMAEA dissolved in water.[19,30] It would be <7 for the fully protonated pAEA trifluoroacetate salt,[43] and ≤7 for pTMAEA.

As DMAEA, TMAEA or AEA units hydrolyze to form acrylic acid units, the solution pH may drop and, in many cases, it would be necessary to adjust the pH or use a buffer to keep the solution near the initial pH. The pH change would be slow for pDMAEA in its free-amine form, as the polymer can act as a buffer, while TMAEA polymers would see a more rapid drop. Saveyn et al. identified this as the reason for the seemingly different stability of TMAEA polymers in dilute and concentrated solutions.[44] In concentrated solutions, hydrolysis of a small fraction of the TMAEA groups can decrease the pH to a point where hydrolysis of the remaining TMAEA groups becomes very slow (pH ≤5). In dilute solutions, such as those used during charge titrations,[44,45] a much larger fraction of the TMAEA units must be hydrolyzed to cause the same pH decrease. The much greater apparent stability reported for pTMAEA in water compared to pDMAEA[20,46] is thus likely because the pH of pTMAEA solutions rapidly falls to pH ≤5 where hydrolysis is very slow.

In the small-molecule hydrolysis experiments, buffer concentrations well in excess of the substrate concentration were used such that there would have been little change in solution pH upon substrate dissolution or hydrolysis.[47] However, the buffers used in the experiments where pH-independent hydrolysis of pDMAEA was reported appear to have been too dilute (0-150 mM) to respond to the pH change caused upon dissolution of the polymer in the free-amine form (280 mM) such that all the solutions likely had similar initial pH values.[20]

In the current work, buffers with concentrations equal to or greater than that of the monomer repeat units were used to minimize the pH drift (i.e., 50-100 mM buffer and 25-

50 mM monomer units) and the pH of the solutions were monitored during the hydrolysis experiments. PAD in the protonated form was dissolved in D_2O containing acetate, phosphate, or borate buffer, and then the pH was adjusted to the desired pH before the first NMR spectrum was measured.

Initial experiments explored the hydrolysis of 1% solutions of the high MW samples of PAD_{88}, PAD_{74}, PAD_{43}, and PAD_{24} at pH 7 in 50 mM phosphate-buffered D_2O at 37°C. NMR spectra measured during hydrolysis of PAD_{88} are shown in Figure 2.6. The disappearance of the DMAEA side-chain peaks at 3.5 and 4.5 ppm and the appearance of sharp peaks due to the small molecule by-product DMAE at 3.3 and 3.9 ppm are used to track the hydrolysis. Some of the polymer signals broaden as hydrolysis proceeds, attributed to the increasing number of chemical environments and possibly to the onset of chain collapse as the net charge decreases. Such peak broadening is not uncommon and can make determining the degree of hydrolysis challenging.[30,44]

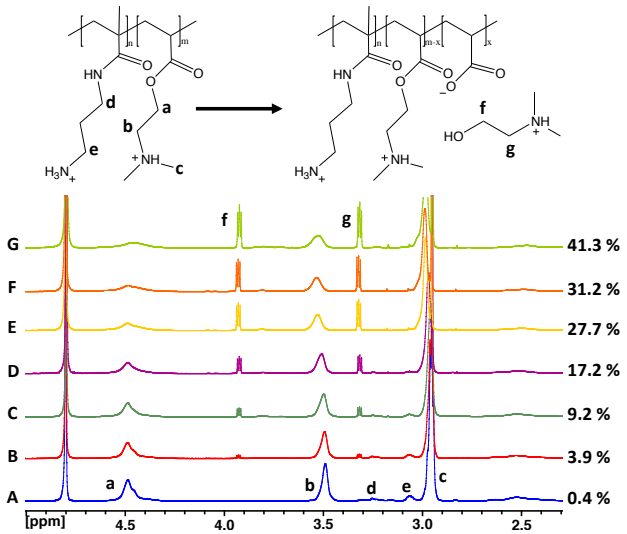

Figure 2.6. ^{1}H NMR spectra of a 1% solution of PAD_{88} in 50 mM phosphate-buffered D_2O (pH 7) at 37°C for (**A**) 0 h, (**B**) 2 h, (**C**) 4 h, (**D**) 9 h, (**E**) 23 h, (**F**) 34 h, and (**G**) 96 h, with the corresponding percent hydrolysis of DMAEA units.

All four copolymers showed rapid initial hydrolysis that slowed after 2 or 3 days and each plot approached a distinct plateau that depended on the copolymer composition (Figure 2.7A). The solutions had initial pH values of 6.8–6.9, which decreased during hydrolysis due to the production of AA groups. After 38 days, the PAD_{88} solution had exhibited the largest pH drift, falling from pH 6.80 to 6.03 with smaller decreases observed for PAD_{74} (6.84 to 6.30), PAD_{43} (6.90 to 6.60) and PAD_{24} (6.85 to 6.60).

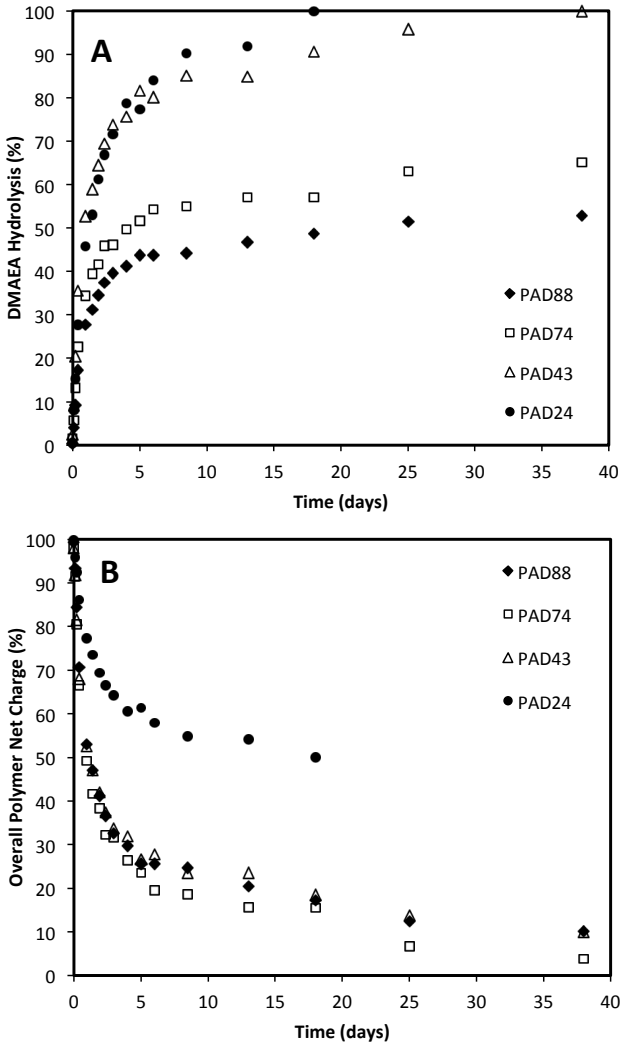

Figure 2.7. Hydrolysis of PAD_{88}, PAD_{74}, PAD_{43} and PAD_{24} at pH 7 and 37 °C shown as the percent of DMAEA hydrolyzed (**A**) and the overall net charge (**B**).

The drop in pH does not seem significant enough to have caused the dramatic slowing of hydrolysis seen after a few days or the very different plateaus observed for the different PAD copolymers in Figure 2.7A. In the case of PAD_{24} with only 24 mol% DMAEA, hydrolysis goes to completion while PAD_{88} plateaus near 50% hydrolysis. As hydrolysis progresses, the cationic charge on the polymer chain is reduced and a polyampholyte (polymer-bound cationic and anionic groups) is formed. This may result

in reduced local hydroxide counter anion levels, a change (collapse) in chain conformation, possibly creating a more hydrophobic local environment, and perhaps a reduced driving force for hydrolysis (fewer cation-cation interactions). It has also been suggested previously that ester units located between two hydrolyzed units (an AA-DMAEA-AA triad) might be stable to hydrolysis.[19] With PAD_{24}, the polymer still has a significant net cationic charge when hydrolysis is complete because of the 76% APM content. In contrast, the PAD_{88} chains are approaching zero net charge when about 55% of the DMAEA units are hydrolyzed.

The hydrolysis data from Figure 7A is replotted in terms of net polymer charge in Figure 2.7B. Net charge, or %excess of cationic groups, was calculated from the fractions of cationic (APM + DMAEA) and anionic (AA) units. Figure 2.7B shows that hydrolysis slows dramatically as the polymer chains approach zero net charge, which in the case of PAD_{43} also corresponds to complete hydrolysis of the DMAEA units. It is interesting that even after nearly 6 weeks at 37 °C none of the systems in this particular experiment had crossed over the zero net charge line to produce chains with a net negative charge.

If electrostatic interactions play an important role in hydrolysis, increasing the ionic strength may affect the rate and extent of hydrolysis. As shown in Figure 2A.23, ionic strength did not have a pronounced effect on the rate or extent of hydrolysis of PAD_{88}. The initial rate of hydrolysis appeared to be slowest in the presence of 500 mM NaCl, consistent with a reduction of cation-cation repulsion or cation-hydroxide attraction, however, the effect was small and all of the systems showed a similar plateau. After about 10 days, the systems with added NaCl showed slightly higher extents of

hydrolysis, perhaps because the electrostatic interactions leading to chain collapse were lessened, but the added salt could not prevent the dramatic slowing of hydrolysis as PAD_{88} approached zero net charge (57% hydrolysis). Polyampholytes can precipitate when near zero net charge, but 500 mM NaCl is sufficient to prevent phase separation for p(APM-AA),[48] suggesting that phase separation is not the major reason for the leveling off of the rate of hydrolysis. As seen in the earlier experiment, the pH fell from 6.9 to about 6.1 for all the samples.

2.4.7. Effect of pH on PAD Hydrolysis

The effect of pH on PAD hydrolysis was examined. To minimize pH drift during hydrolysis, buffer concentrations were increased to 100 mM with acetate, phosphate and borate buffers used for pH 5, 7, and 9, respectively, and the concentration of PAD_{88} was decreased to 0.5 % w/v (cf. 1% in previous experiments) such that the initial concentration of DMAEA units was about 25 mM. The pH remained fairly stable during hydrolysis: initial pH values were 4.99, 6.94, and 9.20, and after 40-45 days, when 40-85% hydrolysis had occurred, the pH values were 4.94, 6.88, and 9.35, respectively.

Hydrolysis of the DMAEA units of PAD is pH-dependent as shown in Figure 2.8. After 3 days at 37 °C in the pH 5, 7 and 9 buffers, 15, 47 and 71% hydrolysis had occurred, respectively. At each pH, hydrolysis was more rapid initially and then slowed and approached a plateau but with higher plateaus at higher pH. The experiments at pH 7 and 9 were repeated and directly monitored by ^{1}H NMR allowing data points to be collected over the first hour of hydrolysis. The data from the early stages of PAD_{88} hydrolysis gave reasonably linear first-order kinetic plots (Figure 2A.24), with half-lives

at pH 7 and 9 (~8 and 2.5 h) that were similar to those observed for the small-molecule analogs studied by Hennink.[47]

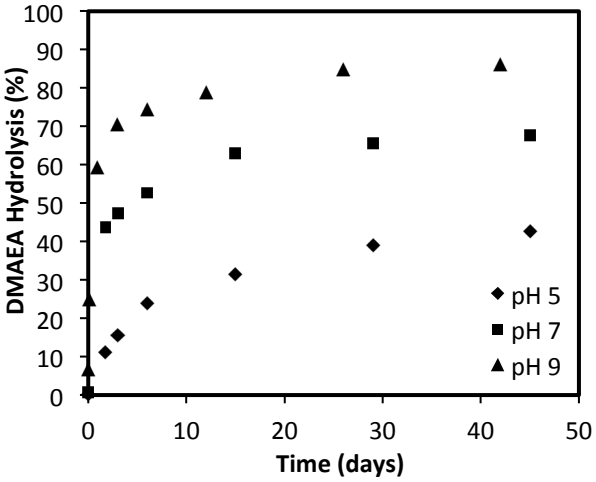

Figure 2.8. Hydrolysis of PAD_{88} in 100 mM buffer solutions at pH 5, 7, and 9, at 37°C.

Ester groups in polymers such as poly(2-(dimethylamino)ethyl methacrylate)[47] or poly(2-aminoethyl methacrylate)[49] are typically more stable than the monomers or other small-molecule analogs because of steric hindrance and a hydrophobic local environment that hinder hydrolysis. This suggests that the environment around the ester units in DMAEA polymers is, at least initially, less hindered and less hydrophobic than in the polymethacrylates. However, as hydrolysis progresses, the DMAEA units in the polymer hydrolyze much more slowly than the small-molecule analogs indicating that there is a dramatic change in the local environment (e.g., reduced cation-cation repulsion, reduced local hydroxide concentration, increased hydrophobicity). The hydrolysis of the polymer-bound DMAEA units is clearly more complicated than with the small-molecules.

The PAD_{88} hydrolysis at pH 7 presented in Figure 2.8 was faster, and reached a higher plateau than seen in Figure 2.7A, because the pH did not drift downwards. Hydrolysis continued past the point of zero net charge to give a polymer with a net anionic charge. After 45 days at pH 7, when 67.7% of the initial DMAEA units had been hydrolyzed (Figure 2.8), the polymer consisted of about 60% anionic AA units and 40% cationic units (APM + DMAEA). The PAD_{88} solution turned slightly cloudy as it reached zero net charge, typical behavior for a polyampholyte near its isoelectric point, and then cleared again as hydrolysis continued and the polymer gained a net anionic charge.[12,50]

To allow a better comparison with literature data, hydrolysis of the DMAEA homopolymer (pDMAEA or PAD_{100}) was examined at room temperature in the pH 5, 7 and 9 buffers (Figure 2.9). The pH of the solutions was stable throughout the experiment: 5.05, 7.02, and 9.32 initially, and 5.09, 6.94, and 9.35, respectively, after 21 days of hydrolysis. Not surprisingly, hydrolysis was slower at room temperature (22 °C) than had been seen for PAD_{88} at 37 °C. pDMAEA hydrolysis showed a marked pH dependence with nearly 50% hydrolysis after 4 days at pH 9 but only 22 and 2% at pH 7 and 5, respectively. The curve obtained for pDMAEA in pH 9 buffer is similar to that obtained in other studies of pDMAEA (free-base form) dissolved in water.[19,20,30] Thus, as observed for small-molecule analogs, PAD and TMAEA-containing copolymers, the rate of pDMAEA hydrolysis decreases significantly as the pH is decreased, which might have implications for some applications such as gene transfection.

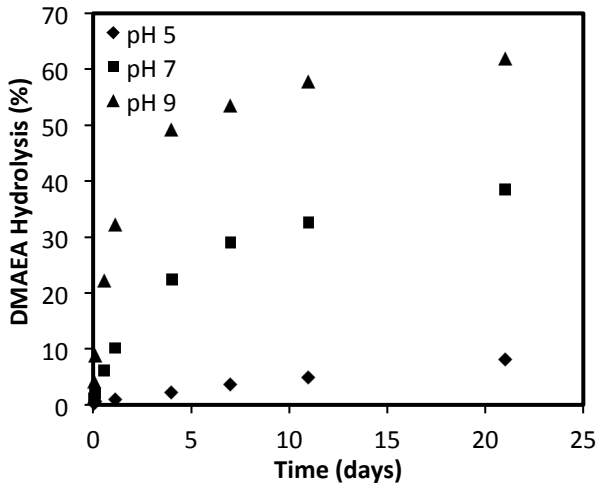

Figure 2.9. Hydrolysis kinetics of pDMAEA in 100 mM buffer solutions at pH 5, 7, and 9, at room temperature (22 °C).

In summary, the PAD copolymers showed complex hydrolytic behavior with rapid initial hydrolysis that slowed dramatically as the net charge on the polymer chains decreased. The composition of the PAD copolymers had a pronounced effect on the rate and/or extent of DMAEA hydrolysis observed with more rapid and complete hydrolysis seen for APM-rich copolymers because the chains had net positive charge throughout the hydrolysis. The rate of PAD and pDMAEA hydrolysis depends on pH, consistent with some but not all literature reports.

2.4.8. PAD-Coated Alginate Capsules

The PAD polycations have high charge density initially allowing them to form polyelectrolyte complexes, e.g., in coating anionic calcium alginate beads. Subsequent hydrolysis of DMAEA units would cause a reduction of cationic charge, and perhaps even a shift to net anionic charge, and as such, the polyelectrolyte complex would be

expected to dissociate, unless it were covalently crosslinked. Thus, calcium alginate beads were coated with PAD copolymers (8 and 30 kDa), and then maintained at pH 7 where, if PAD hydrolysis occurred, the capsule shells could disassemble in the absence of crosslinking.

The capsules were examined by conventional bright field and fluorescence microscopy just after coating with 8 and 30 kDa PAD-*f* copolymers (Figures 2A.25 and 2A.26). The high charge density polycations bound to the anionic calcium alginate hydrogel, but the capsule surface became wrinkled for PAD_{25}, and to a lesser extent PAD_{50}. Surface wrinkling has been seen for polycation-coated hydrogels,[51,52] including calcium alginate,[7,53] and indicates strong binding to the surface to give a coating that is unable to restructure itself when the core of the hydrogel shrinks due to changes in osmotic pressure. The results with the PAD copolymers suggest that higher APM content leads to stronger binding to alginate. In contrast, the fluorescence images of the capsules coated with PAD_{75} were brighter than those coated with PAD_{50} or PAD_{25} indicating that greater amounts of the DMAEA-rich PAD_{75} copolymers had been bound.

CLSM images of the calcium alginate capsules just after coating with 8 and 30 kDa PAD-*f* copolymers are shown in Figures 2.10 and 2.11, respectively. As seen by conventional microscopy, there were distinct differences in the nature of the shell formed depending on the copolymer composition. The APM-rich PAD_{21}-8k and PAD_{25}-30k copolymers were restricted to the surface of the beads (Figures 2.10A and 2.11A) giving very thin shells for both MWs (5.2 ± 2.5 and 8.5 ± 3.0 μm). The higher MW PAD_{45}-30k was restricted to the surface (Figure 2.11B; 3.8 ± 0.8 μm) but the lower MW PAD_{42}-8k

was able to diffuse more deeply into the hydrogel bead (Figure 2.10B) and form a thicker membrane (11.6 ± 1.3 μm). The DMAEA-rich PAD_{75}-8k and PAD_{75}-30k copolymers diffused furthest into the calcium alginate hydrogel, which led to a greater amount of these copolymers being bound to the beads as indicated by the area under the line profiles. A significant fraction of the smaller PAD_{75}-8k reached the core of the bead (Figure 2.10C) while the larger PAD_{75}-30k was more limited to the surface region of the bead but gave a thicker membrane (21.5 ± 2.9 μm) than seen with the other copolymers. The more limited diffusion of the larger 30 kDa copolymer into the hydrogel was expected but the effect of composition was not. The differing degrees of in-diffusion with copolymer composition may be due to different strengths of electrostatic binding of primary and tertiary ammonium ions with the carboxylate groups of alginate. This will be explored in future studies using isothermal titration calorimetry. The smaller size of the primary ammonium ion of APM may allow closer approach to the anion, and with three H-atoms, hydrogen-bonding to the carboxylate may be more efficient than with the more sterically hindered tertiary ammonium ions of DMAEA. Strong binding of the APM-rich copolymers to the anionic alginate prevents these chains from diffusing further into the gel and prevents restructuring (or annealing) of the shell when the capsule core shrinks, which leads to surface wrinkling.

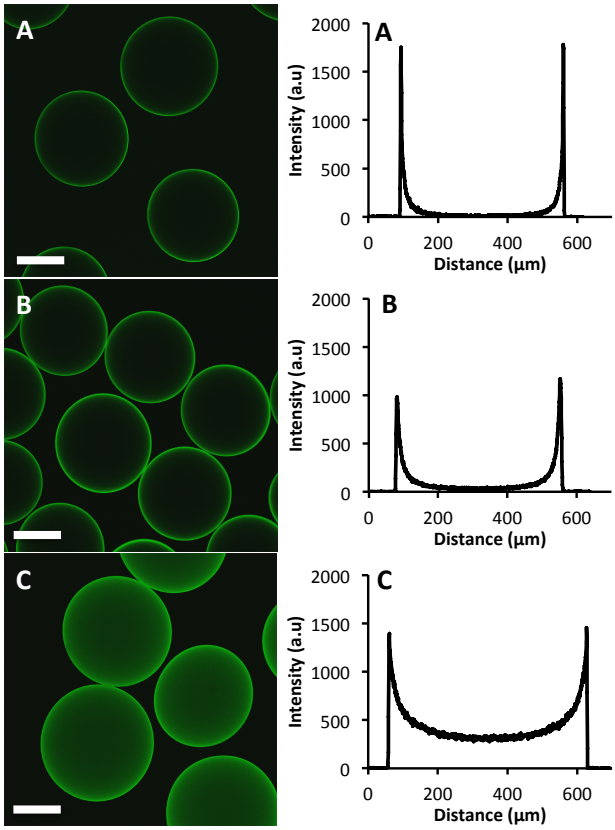

Figure 2.10. CLSM images of PAD_{21}-8k*f* (**A**), PAD_{42}-8k*f* (**B**), and PAD_{75}-8k*f* (**C**) coated calcium alginate capsules with the corresponding representative line profiles. Capsules were imaged with the same microscope settings. Scale bars are 250µm.

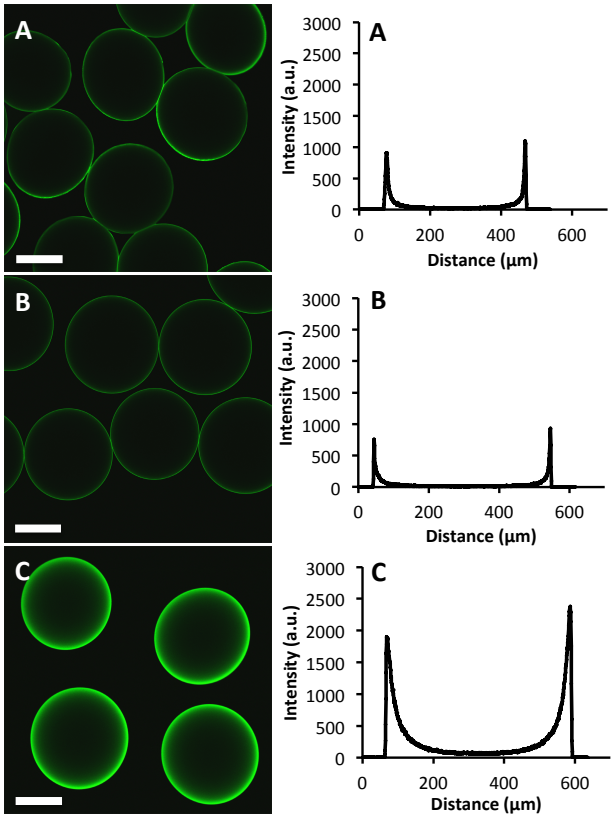

Figure 2.11. CLSM images of PAD_{25}-30k*f* (**A**), PAD_{45}-30k*f* (**B**), and PAD_{75}-30k*f* (**C**) coated calcium alginate capsules with the corresponding representative line. Capsules were imaged with the same microscope settings. Scale bars are 250 µm.

These results demonstrate that it possible to control characteristics of the capsule shell such as thickness, and, likely, stiffness and permeability, through the MW and composition of the PAD copolymers. For strength and cytocompatibility reasons, it is probably best to have the polycation concentrated near the capsule surface without getting a shell that is too thin and weak to resist mechanical and osmotic stresses.[7,26] PAD copolymers rich in DMAEA were of interest as they have the most potential for charge-shifting of the capsule surface. As the lower MW PAD_{75}-8k diffused throughout the

hydrogel, calcium alginate beads coated with higher MW PAD_{75}-30k were the focus of further experiments.

2.4.9. Hydrolysis of the PAD Coating

It was expected that hydrolysis of PAD would cause it to dissociate from the capsule as the electrostatic interactions were weakened. Figure 2.12 shows CLSM images of PAD_{75}-30k coated calcium alginate beads as formed (Fig. 2.12A) and after 9 days in a pH 7.8 buffer at room temperature in the dark (Fig. 2.12B and C). The capsule coating is no longer clearly visible when imaged at the same detector gain (Figure 2.12B) and when imaged at higher gain, fluorescence is seen throughout the supernatant with slightly higher intensity at the capsule surface. This indicates that most of the PAD-*f* has dissociated from the surface, consistent with PAD hydrolysis leading to a loss of electrostatic binding. After 9 days, about 30-40% of the DMAEA groups would have been hydrolyzed if hydrolysis occurred at a similar rate in the polyelectrolyte complex as for the free polymer in solution. This would result in a polymer that was still cationic with about 20-30% of the monomer units converted to AA.

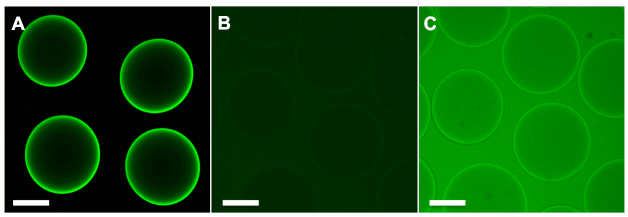

Figure 2.12. CLSM images of PAD_{75}-30k*f*-coated capsules as formed (**A**), and after 9 days at pH 7.8 and room temperature taken with the same microscope settings (**B**), and with increased detector gain (**C**). Scale bars are 250 μm.

2.4.10. Electrophoretic Mobility of PAD-coated Polyanionic Microspheres

To model the charge reduction occurring for the alginate–PAD complex, PAD was coated onto anionic PMSM microspheres (7.92 ± 0.74 μm dia.). The electrophoretic mobility of the PMSM microspheres was measured before and after coating with PAD_{75}-30k*f* and PAD_{25}-30k*f*, and after the coated particles were stored at pH 7.2 (Figure 2A.27). As expected, the anionic PMSM particles had a negative mobility (-1.0 ± 0.2 $10^{-8}m^2/Vs$) that remained relatively unchanged after 11 days in 35 mM HEPES-buffered saline (pH 7.2). The particles became positive after they were coated with PAD_{75}-30k*f* and PAD_{25}-30k*f* with values of 1.18 ± 0.07 and 1.78 ± 0.08 $10^{-8}m^2/Vs$, respectively. The difference between the two PAD coatings is attributed to hydrolysis occurring before the first measurement, and possibly differences in the amount of polycation bound. After a week at pH 7.2 and 22°C, the mobility of both PAD-coated particles had fallen and the PAD_{75}-30k*f* coated particles had a mobility near zero (-0.03 ± 0.03 $10^{-8}m^2/Vs$) due to hydrolysis of the DMAEA-rich copolymer. After 12 days, the mobility of PAD_{25}-30k*f* coated particles remained positive at 0.98 ± 0.06 $10^{-8}m^2/Vs$, whereas PAD_{75}-30k*f* coated particles had a negative mobility at -0.68 ± 0.06 $10^{-8}m^2/Vs$. The pH of the particle suspensions remained fairly constant over the course of the experiment. The charge reversal of PAD_{75}-30k*f* coated particles is likely due to both hydrolysis of the DMAEA-rich copolymer and loss of the hydrolyzed polymer, which would expose anionic groups of the underlying PMSM particle. These results are consistent with those seen for the analogous alginate-PAD capsules.

2.4.11. Covalent Crosslinking of PAD-Coated Capsules with THPC

The charge shifting that occurs upon PAD hydrolysis weakens the electrostatic interactions holding PAD in polyelectrolyte complexes such as the coating on calcium alginate capsules. Hence, in some cases it would be desirable to introduce covalent crosslinks into the complex once formed to enhance the mechanical strength and stability of the complex. The primary amines provided by the APM units in PAD are good sites for crosslinking by reaction with electrophilic polymers or small molecules. In this work, the crosslinking agent selected was THPC, which was shown by Chung et al. to be a crosslinking agent in hydrogels made from elastin-like proteins.[23]

As a proof of concept, calcium alginate beads coated with PAD_{75}-30k*f* were exposed briefly to a 0.1% THPC solution. If all of the PAD_{75} had been bound to the capsules in the coating step, this would be a 3-fold molar excess of THPC and an even greater excess of potential reaction sites since each THPC molecule can react with up to four amines. It was assumed that only a fraction of the THPC molecules would become bound to PAD during the brief exposure and that these groups would continue to react after the excess THPC was removed. To demonstrate crosslinking, the capsules were treated with citrate to remove calcium and liquefy the capsule core, and then 0.1 M NaOH to neutralize the ammonium ions of PAD and disrupt the electrostatic interaction holding the shell together. As shown in Figure 2.13, the THPC-treated capsules swelled when exposed to citrate (Figure 2.13B) and, while a few capsules tore open from mechanical agitation or osmotic stress, most remained intact. After addition of NaOH and 10 min of gentle agitation, the capsule shell survived either as part of a whole capsule or as shell

fragments (Figure 2.13C). In contrast, capsules that had not been crosslinked with THPC swelled when treated with citrate and then dissolved when NaOH was added.

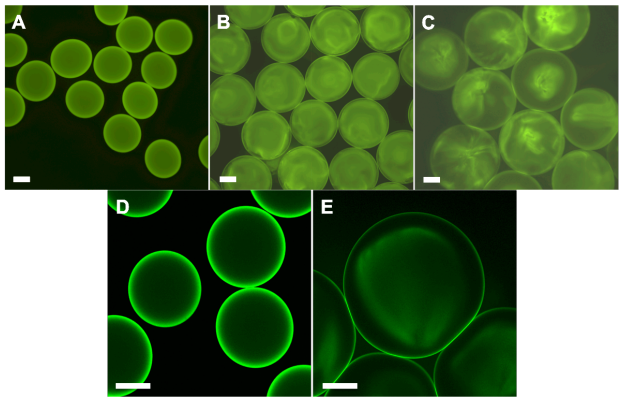

Figure 2.13. Fluorescence microscopy images of PAD_{75}-30k*f*-coated capsules after crosslinking with THPC: as formed (**A**), after 10 min in 50 mM citrate (**B**), and after 10 min in 0.1 M NaOH (**C**). CLSM images of capsules as formed (**D**) and after treatment with citrate and NaOH (**E**). Scale bars are 250 μm.

CLSM images taken of the capsules just after crosslinking (Figure 2.13D) revealed that THPC treatment had not affected the polymer distribution as it was similar to that seen in capsules formed without crosslinking (Figure 2.12A). After being treated with citrate and NaOH, the capsules displayed a thin outer-shell that appeared to have pulled away from a more diffuse inner region (Figure 2.13E). The inner region, which was also visible in the conventional fluorescence microscopy image (Figure 2.13C), may be a very lightly crosslinked gel or viscous liquid formed from PAD_{75} that diffused further into the calcium alginate bead. The lower PAD concentration below the capsule surface (see Figure 2.11C, line profile) would make crosslinking less efficient. These results demonstrate that it was possible to crosslink the PAD coating on the capsules with

THPC, which would increase the long-term mechanical strength of the capsule by preventing loss of PAD when hydrolysis generates a lower charge density surface.

Future work will explore cell compatibility of analogous hydrogel films and capsules, as a function of MW, composition, and degree of DMAEA hydrolysis.

2.5. Conclusions

The novel charge-shifting PAD polycations have promise as material building blocks. The high cationic charge allows ready formation of polyelectrolyte complexes with anionic polymers or surfaces, the primary amino groups of the APM units allow easy crosslinking and functionalization, and subsequent hydrolysis of the DMAEA units reduces cationic charge following assembly. Hydrolysis of DMAEA groups within PAD copolymers showed complicated kinetics as it depended on the net charge on the polymer chains (copolymer composition, degree of hydrolysis) and the solution pH. The studies offered insight into the variable results found in the literature for hydrolysis of polymers containing DMAEA or related monomers. The nature of the PAD-coating (amount bound, thickness) on calcium alginate beads depended on the composition and MW with high APM content and/or MW favoring thin shells. Hydrolysis also occurred for PAD that was part of a polyelectrolyte complex, either bound to calcium alginate capsules or anionic polymer particles, leading to loss of non-crosslinked PAD coatings. The PAD coating on the capsules could be crosslinked with THPC demonstrating that it would be possible to generate a strong capsule shell with low charge density.

Supporting Information Available

^{1}H NMR spectrum showing reaction of MeOH with DMAEA; Data for reactivity ratio calculations; Fineman-Ross plot; ^{1}H NMR spectra of PAD_{88}, PAD_{43} and PAD_{24} in D_2O; GPC traces of PAD copolymers; ^{1}H NMR spectra from attempted trans-amidation experiments; ^{1}H NMR spectrum showing reaction of cysteamine with DMAEA; Conversion vs. time and 1st-order kinetic plots for RAFT copolymerizations; ^{1}H NMR spectra of PAD copolymers made by RAFT polymerization in D_2O; Additional kinetic plots for PAD hydrolysis; Microscopic images of PAD-coated calcium alginate capsules; electrophoretic mobility data of PAD-coated PMSM particles. This material is available at free of charge via the Internet at http://pubs.acs.org

Author Information

Corresponding Author

E-mail: stoverh@mcmaster.ca, Ph.: 1-905-525-9140 ext. 24983.

Notes:

The authors declare no competing financial interest.

2.6. Acknowledgements

The authors are grateful for funding support from the Canada Foundation for Innovation and the Natural Sciences and Engineering Research Council of Canada (Discovery Grant (RGPIN89661-11) and CREATE (CREATE398058-11) programs). The authors wish to thank Rachelle Kleinberger for valuable insight regarding RAFT

polymerization and capsule work, and Yuqing Zhao and Marta Skreta for supplying the PMSM particles.

2.7. References

1. Decher, G.; Hong, J.D.; Schmitt, J. *Thin Solid Films* **1992**, *210/211*, 831-835.

2. Peyratout, C.S.; Dähne, L. *Angew. Chem. Int. Ed*. **2004**, *43*, 3762–3783.

3. Lim, F.; Sun, A.M. *Science* **1980**, *210*, 908–909.

4. Thu, B.; P. Bruheim, P.; T. Espevik, T.; O. Smidsrød, O.; P. Soon-Shiong, P.; G. Skjåk-Bræk, G. *Biomaterials* **1996**, *17*, 1031–1040.

5. Rokstad, A.M.; Donati, I.; Borgognac, M.; Oberholzer, J.; Strand, B.L.; Espevik, T.; Skjåk-Bræk, G. *Biomaterials* **2006**, *27*, 4726–4737.

6. Wang, Y.J. *Mater. Sci. Eng. C* **2000**, *13*, 59–63.

7. Mazumder, M.A.J.; Shen, F.; Burke, N.A.D.; Potter, M.A.; Stöver, H.D.H. *Biomacromolecules* **2008**, *9*, 2292-2300.

8. Dusseault, J.; Leblond, F.A.; Robitaille, R.; Jourdan, G.; Tessier, J.; Ménard, M.; Henley, N.; Hallé, J.-P. *Biomaterials* **2005**, *26*, 1515-1522.

9. Tam, S.K.; Bilodeau, S.; Dusseault, J.; Langlois, G.; Hallé, J.P.; Yahia, J.H. *Acta Biomater*. **2011**, *7*, 1683–1692.

10. Gardner, C.M.; Potter, M.A.; Stöver, H.D.H. J. *Mater. Sci. Mater. Med*. **2012**, *23*, 181-193.

11. Kleinberger, R.M.; Burke, N.A.D.; Zhou, C.; Stöver, H.D.H. *Submitted to J. Biomater. Sci. Polym. Ed.*

12. Dubey, A.; Burke, N.A.D.; Stöver, H.D.H. *J. Polym. Sci. A: Polym. Chem*. **2015**, *53*, 353-365.

13. Wilson, J.T.; Cui, W.; Kozlovskaya, V.; Kharlampieva, E.; Pan, D.; Qu, Z.; Krishnamurthy, V.R.; Mets, J.; Kumar, V.; Wen, J.; Song, Y.; Tsukruk, V.V.; Chaikof, E.L. *J. Am. Chem. Soc*. **2011**, *133*, 7054-7064.

14. Sawhney, A.S.; Hubbell, J.A. *Biomaterials* **1992**, *13*, 863-870.

15. Gardner, C.M.; Stöver, H.D.H. *Macromolecules* **2011**, *44*, 7115-7123.

16. Liu, X.; Yang, J.W.; Miller, A.D.; Nack, E.A.; Lynn, D.M. *Macromolecules* **2005**, *38*, 7907-7914.

17. Zhang, J.; Lynn, D.M. *Adv. Mater*. **2007**, *19*, 4218–4223.

18. Sinclair, A.; Bai, T.; Carr, L.R.; Ella-Menye, J.R.; Zhang, L.; Jiang, S. *Biomacromolecules* **2013**, *14*, 1587−1593.

19. McCool, M.B.; Senogles, E. *Eur. Polym. J*. **1989**, *25*, 857-860.

20. Truong, N.P.; Jia, Z.; Burges, M.; McMillan, N.A.J.; Monteiro, M.J. *Biomacromolecules* **2011**, *12*, 1876–1882.

21. Tran, N.T.D.; Truong, N.P.; Gu, W.; Jia, Z.; Cooper, M.A.; Monteiro, M.J. *Biomacromolecules* **2013**, *14*, 495–502.

22. Tran, N.T.D.; Jia, Z.; Truong, N.P.; Cooper, M.A.; Monteiro, M.J. *Biomacromolecules* **2013**, *14*, 3463–3471.

23. Chung, C.; Lampe, K.J.; Heilshorn, S.C. *Biomacromolecules* **2012**, *13*, 3912-3916.

24. Chiefari, J.; Chong, Y.K.; Ercole, F.; Krstina, J.; Jeffery, J.; Le, T.P.T.; Mayadunne, R.T.A.; Meijs, G.F.; Moad, C.L.; Moad, G.; Rizzardo, E.; Thang, S.H. *Macromolecules* **1998**, *31*, 5559-5562.

25. Moad, G.; Rizzardo, E.; Thang, S.H. *Aust. J. Chem*. **2005**, *58*, 379–410.

26. Ma, X.; Vacek, I.; Sun, A.M. *Artif. Cells, Blood Substitutes, Immobilization Biotechnol*. **1994**, *22*, 43-69.

27. Fineman, M.; Ross, S.D. *J. Polym. Sci*. **1950**, *5*, 259–262.

28. Kleinberger, R.M.; Burke, N.A.D.; Dalnoki-Veress, K.; Stöver, H.D.H. *Mater. Sci. Eng. C* **2013**, *33*, 4295–4304.

29. Frank, R.S.; Downey, J.S.; Yu, K.; Stöver, H.D.H. *Macromolecules* **2002**, *35*, 2728-2735.

30. Cotanda, P.; Wright, D.B.; Tyler, M.; O' Reilly, R.K. *J. Polym. Sci. A: Polym. Chem*. **2013**, *51*, 3333-3338.

31. Boyer, C.; Whittaker, M.R.; Chuah, K.; Liu, J.; Davis, T.P. *Langmuir* **2010**, *26*, 2721–2730.

32. Truong, N.P.; Gu, W.; Prasadam, I.; Jia, Z.; Crawford, R.; Xiao, Y.; Monteiro, M.J. *Nat. Commun*. **2013**, 4:1902 doi: 10.1038/ncomms2905.

33. Aguilar, M.R.; Gallardo, A.; Fernandez, M.D.; Roman, J.S. *Macromolecules* **2002**, *35*, 2036-2041.

34. Si, K.; Qiu, K.Y. J. *Macromol. Sci*. **1995**, *A32*, 1139-1148.

35. Deng, Z.; Bouchékif, H.; Babooram, K.; Housni, A.; Choytun, N.; Narain, R. J. *Polym. Sci. A: Polym. Chem*. **2009**, *46*, 4984-4996.

36. York, A.W.; Zhang, Y; Holley, A.C.; Guo, Y.; Huang, F.; McCormick, C.L. *Biomacromolecules* **2009**, *10*, 936–943.

37. Mendonça, P.V.; Serra, A.C.; Popov, A.V.; Guliashvili, T.; Coelho, J.F.J. *React. Funct. Polym.* **2014**, *81*, 1-7.

38. Thomas, D.B.; Convertine, A.J.; Hester, R.D.; Lowe, A.B.; McCormick, C.L. *Macromolecules* **2004**, *37*, 1735-1741.

39. Lowe, A.B.; McCormick, C.L. *Acc. Chem. Res*. **2004**, *37*, 312-325.

40. Mertoglu, M.; Laschewsky, A.; Skrabania, K.; Wieland, C. *Macromolecules* **2005**, *38*, 3601-3614.

41. Albertin, L.; Stenzel, M.H.; Barner-Kowollik, C.; Davis, T.P. *Polymer* **2006**, *47*, 1011-1019.

42. Liu, G.; Shi, H.; Cui, Y.; Tong, J.; Zhao, Y.; Wang, D.; Cai, Y. *Polym. Chem*. **2013**, *4*, 1176-1182.

43. Ho, H.T.; Pascual, S.; Montembault, V.; Casse, N.; Fontaine, L. *Polym. Chem*. **2014**, *5*, 5542-5545.

44. Saveyn, H.; Hendrickx, P.M.S.; Dentel, S.K.; Martins, J.C.; Van der Meeren, P. *Water Res*. **2008**, *42*, 2718 – 2728.

45. Aksberg, R.; Wågberg, L. J. Appl. *Polym. Sci*. **1989**, *38*, 297-304.

46. Zhao, W.; Fonsny, P.; FitzGerald, P.; Warr, G.G.; Perrier, S. *Polym. Chem*. **2013**, *4*, 2140-2150.

47. van de Wetering, P.; Zuidam, N.J.; van Steenbergen, M.J.; van der Houwen, O.A.G.J.; Underberg, W.J.M.; Hennink, W.E. *Macromolecules* **1998**, *31*, 8063-8068.

48. Zhao, J.; Burke, N.A.D.; Stöver, H.D.H. *unpublished results*.

49. Thompson, K.L.; Read, E.S.; Armes, S.P. *Polym. Degrad. Stab*. **2008**, *93*, 1460-1466.

50. Lowe, A.B; McCormick, C.L. *Chem Rev*. **2001**, *102*, 4177-4189.

51. Bysell, H.; Malmsten, M. *Langmuir* **2006**, *22*, 5476-5484.

52. Bysell, H.; Hansson, P.; Malmsten, M. J. *Colloid Interface Sci*. **2008**, *323*, 60-69.

53. Strand, B.L.; Mørch, Y.A., Espevik, T.; Skjåk-Bræk, G. *Biotechnol. Bioeng*. **2003**, *82*, 386-394.

2.8. Appendix

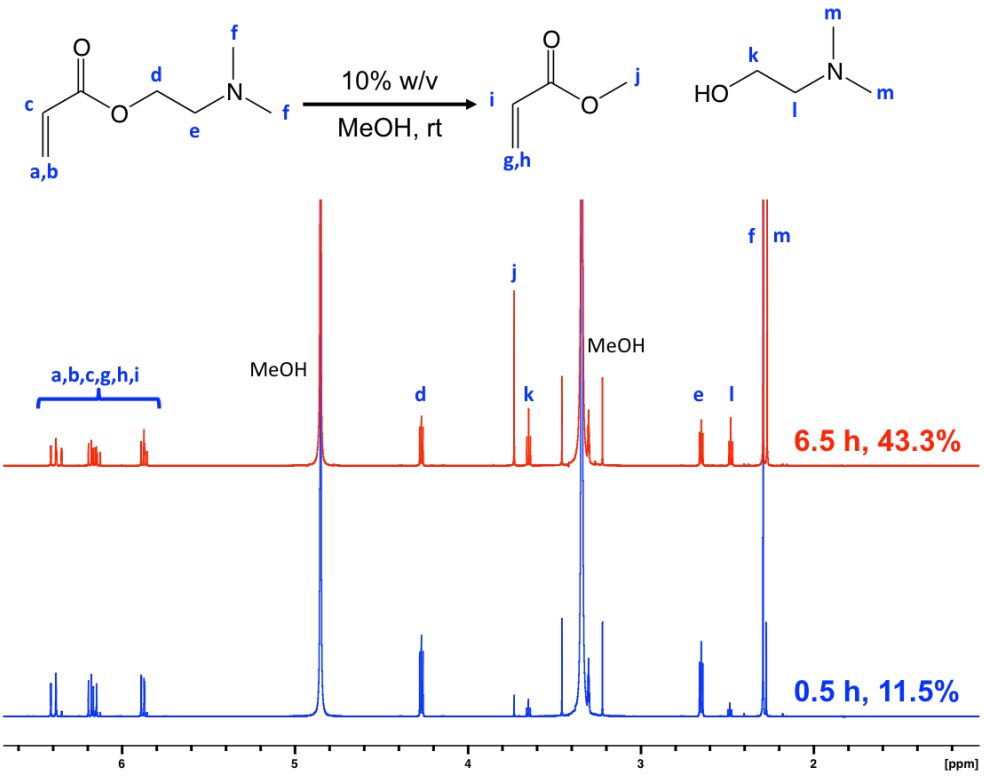

Figure 2A.1. ^{1}H NMR spectrum of 10% w/v DMAEA in MeOH at room temperature (22°C), after dilution with MeOH-D4 for analysis, showing about 11.5% and 43.3% trans-esterification at 0.5 h and 6.5 h, respectively, as evidenced by the decrease of the DMAEA methylene signal **d**, and increase of the corresponding methylene signal **k** in 2-(N,N-dimethylamino)ethanol.

Table 2A.1. Monomer feed ratios (f1) and polymer composition (F1) values obtained from monitoring APM and DMAEA copolymerizations *in situ* by ^{1}H NMR spectroscopy. (DMAEA monomer 1, APM monomer 2).

f1 (monomer feed)	F1 (polymer composition)	F1 calculated	f1 (monomer feed) (continued)	F1 (polymer composition) (continued)	F1 calculated (continued)
0.780	0.669	0.651	0.401	0.344	0.350
0.800	0.677	0.672	0.415	0.360	0.360
0.827	0.711	0.702	0.428	0.365	0.370
0.855	0.732	0.736	0.450	0.386	0.385
0.887	0.793	0.781	0.472	0.399	0.401
0.914	0.823	0.822	0.0999	0.101	0.104
0.941	0.860	0.869	0.0997	0.110	0.104
0.500	0.430	0.421	0.0982	0.117	0.102
0.513	0.436	0.431	0.0958	0.0889	0.0998
0.528	0.432	0.442	0.0965	0.138	0.100
0.547	0.459	0.455	0.0922	0.103	0.0964
0.564	0.466	0.468	0.716	0.591	0.590
0.585	0.471	0.484	0.734	0.612	0.606
0.609	0.512	0.502	0.756	0.627	0.627
0.227	0.224	0.216	0.780	0.656	0.650
0.228	0.221	0.217	0.803	0.651	0.675
0.229	0.231	0.218	0.833	0.731	0.709
0.229	0.199	0.218	0.855	0.721	0.736
0.234	0.226	0.222			
0.235	0.221	0.223			
0.239	0.248	0.226			
0.386	0.343	0.339			
0.393	0.341	0.344			

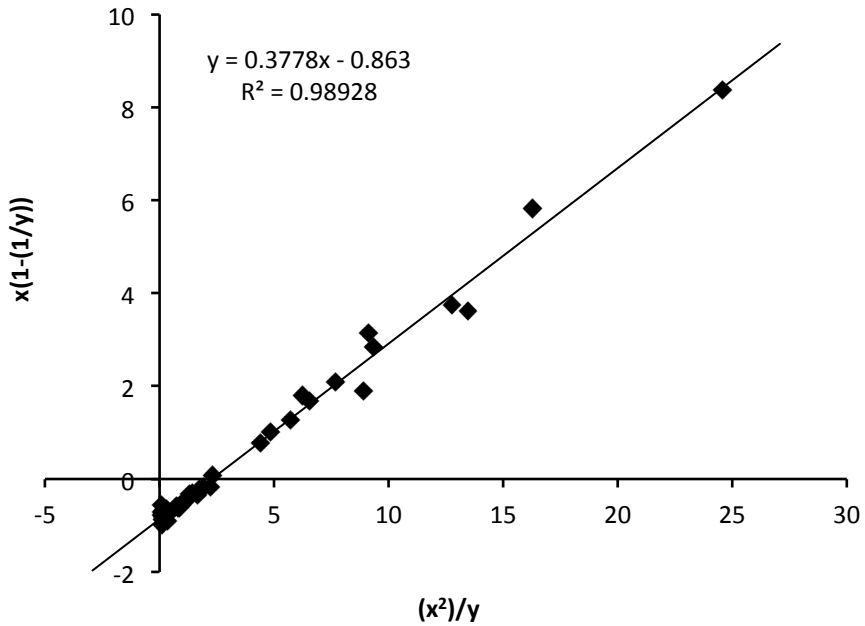

Figure 2A.2. Fineman-Ross plot for the copolymerization of APM and DMAEA, where x is the monomer feed ratio ([DMAEA]/[APM]) at the beginning of a particular step and y is the ratio of the monomers incorporated into copolymer in that step (d[DMAEA]/d[APM]). Reactivity ratios of APM and DMAEA were calculated to be 0.86 and 0.38, respectively.

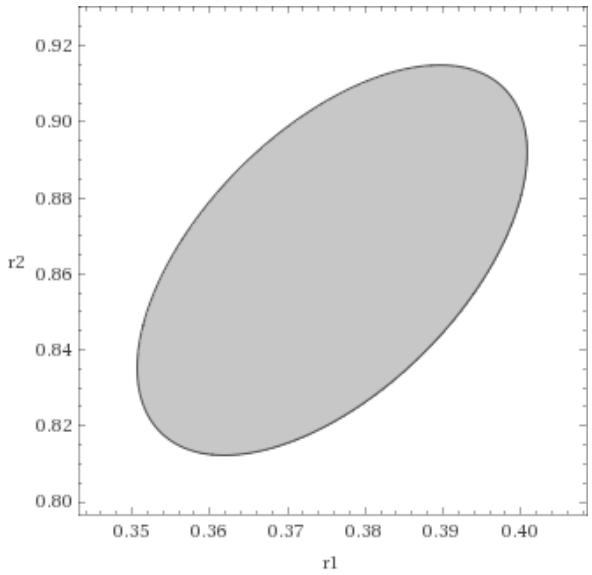

Figure 2A.3. Joint confidence region at 95 % confidence for reactivity ratios $r_1 = 0.38$ (DMAEA) and $r_2 = 0.86$ (APM) by a method described by Kitanidis et al.[1]

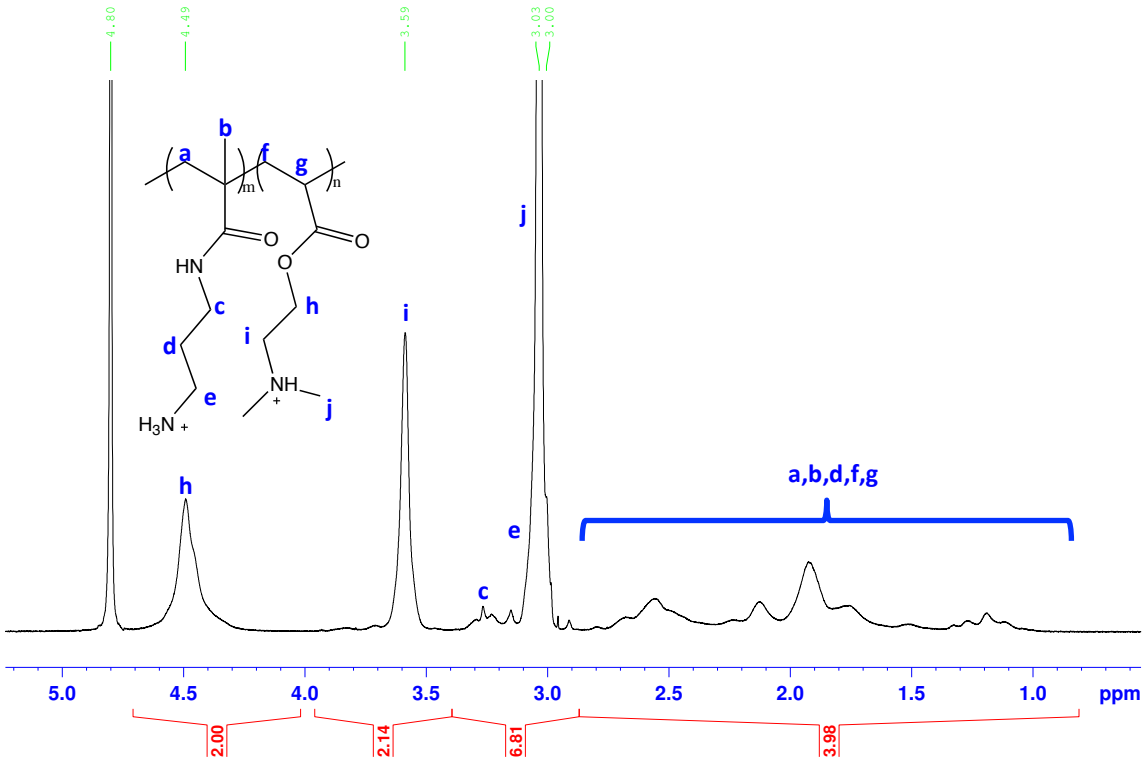

Figure 2A.4. ^{1}H NMR spectrum of PAD_{88} in D_2O at pH 3-4.

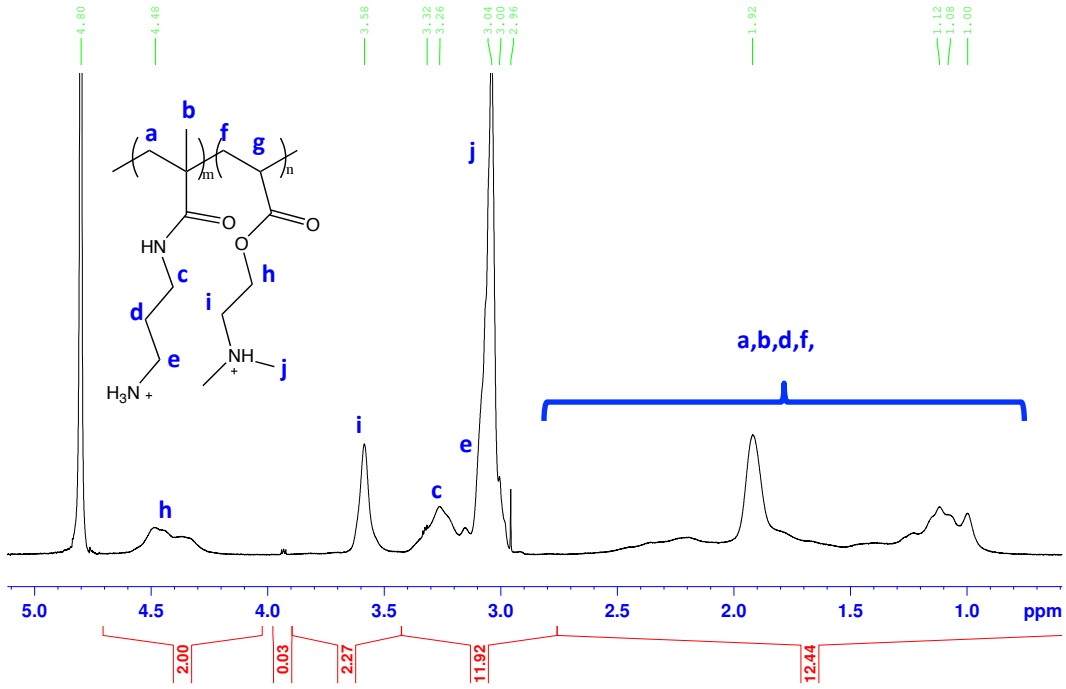

Figure 2A.5. ^{1}H NMR spectrum of PAD_{43} in D_2O at pH 3-4.

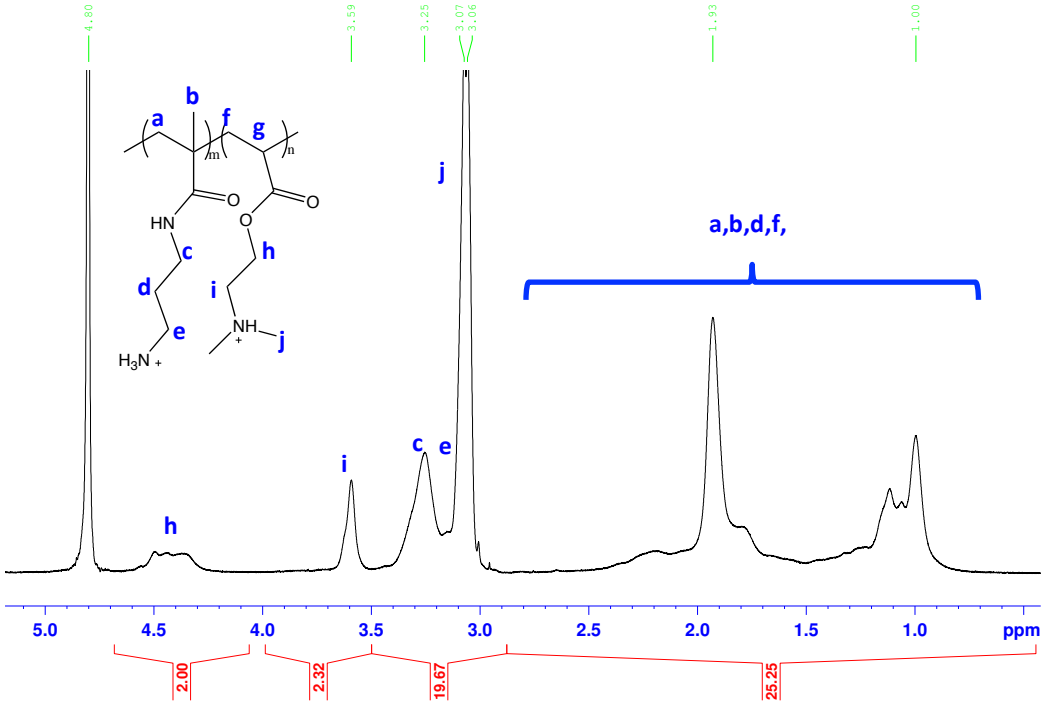

Figure 2A.6. ^{1}H NMR spectrum of PAD_{24} in D_2O at pH 3-4.

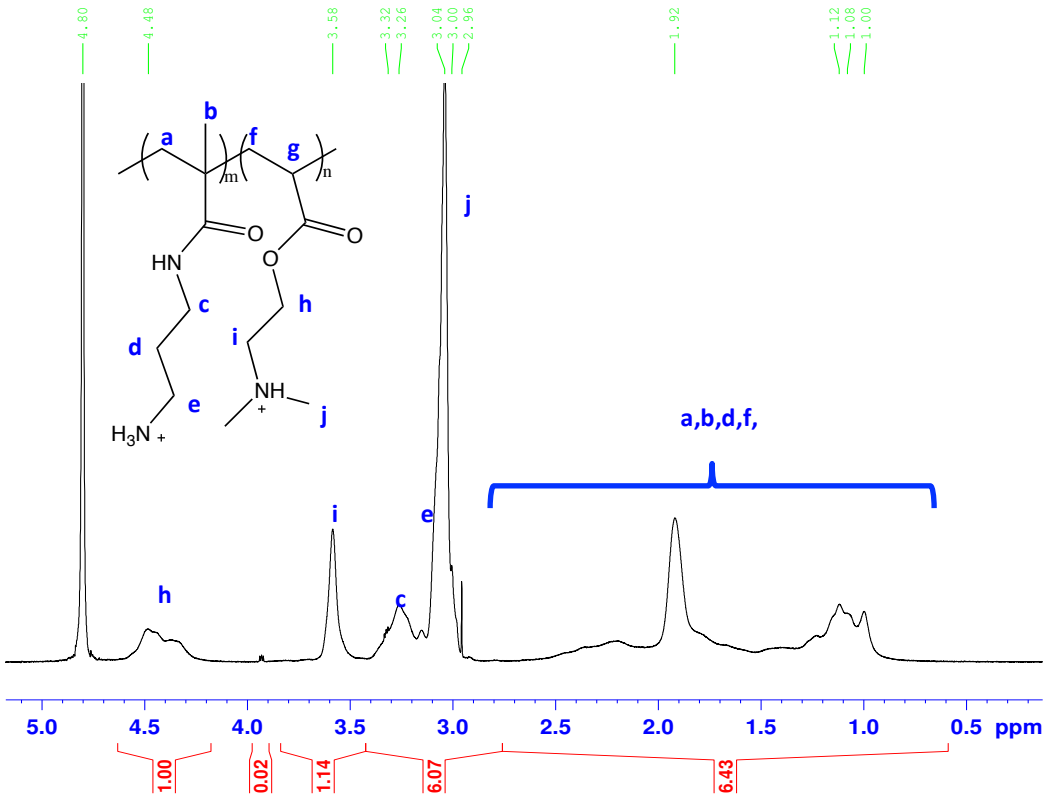

Figure 2A.7. ^{1}H NMR spectrum of PAD_{43} in D_2O after 45 days storage of the solid, protonated form.

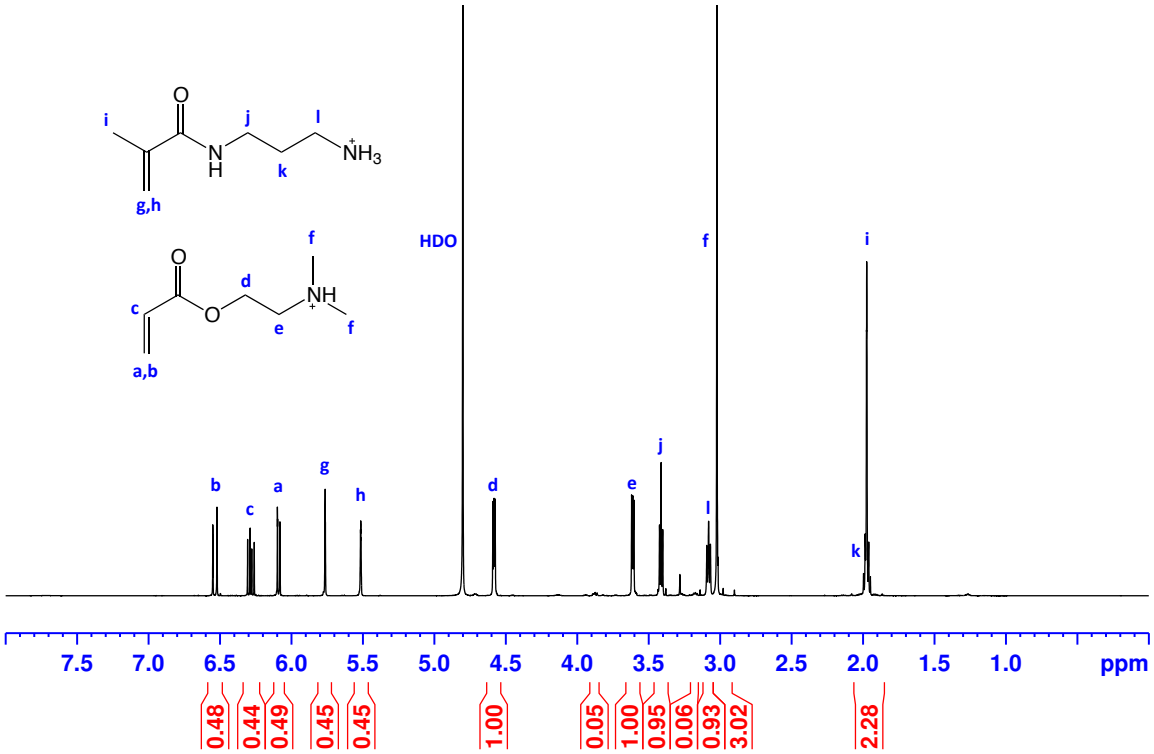

Figure 2A.8. Monomer mixture of 1:1 APM:DMAEA (10 wt.%) in D_2O with no initiator at pH 4 was heated at 55°C for 2h, and subsequently heated at 70°C for an additional 2h to mimic conditions of polymerizations. ^1H NMR spectrum of the sample showed that the monomers were stable, showing less than 5 % hydrolysis.

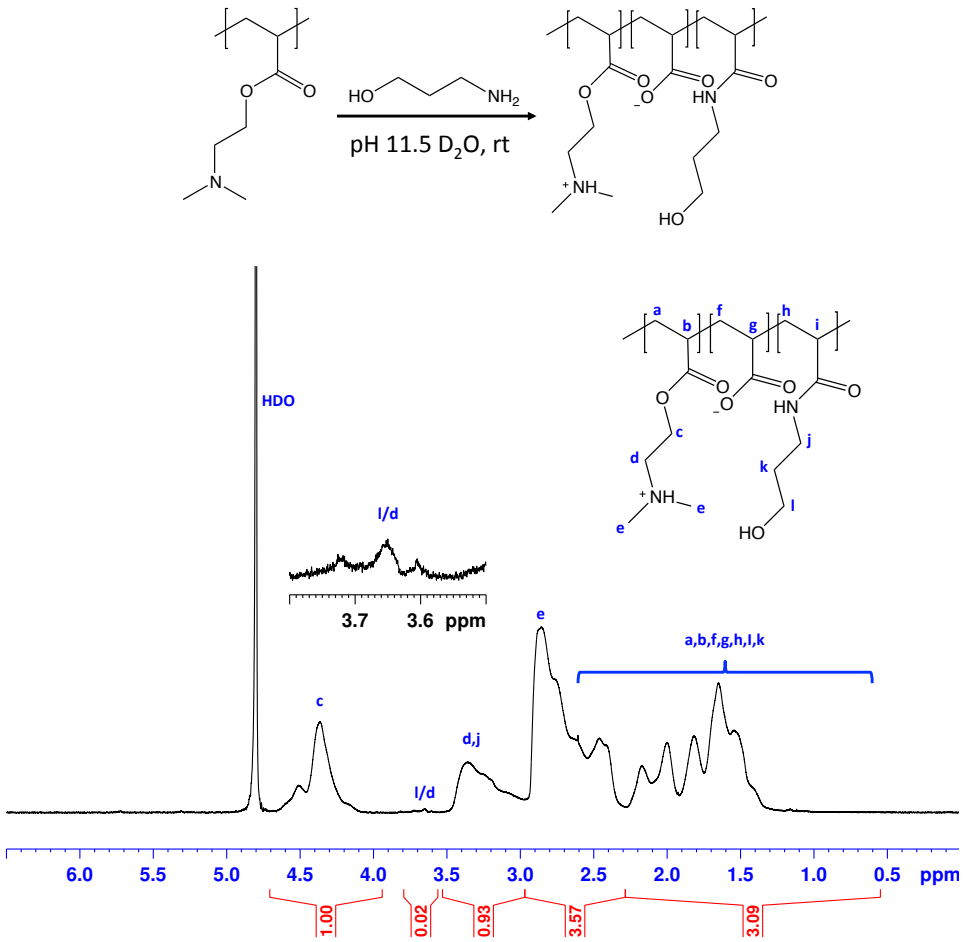

Figure 2A.9. A model trans-amidation experiment was carried out using PDMAEA and small molecule 3-amino-1-propanol (1 mol eq.) to mimic the primary amino group of APM units in the PAD copolymer. The reaction mixture was left for 4 days at room temperature, and then dialyzed for 1 day in pH 10-11 water to remove small molecules, followed by freeze-drying. The polymer was re-dissolved in D_2O and analyzed by ^1H NMR spectroscopy. The reaction was conducted at high pH, in which trans-amidation would be most efficient by allowing the primary amine to be in the nucleophilic, free base form. It is important to note that at this pH, ester hydrolysis is a significant, competing reaction. If trans-amidation occurs, it would lead to formation of 3-hydroxypropyl acrylamide monomer units within the polymer. The small, broad signal labeled l/d may be from the -C$\underline{H_2}$OH methylene protons as a result of trans-amidation and/or from the increased broadening of the methylene protons adjacent to the dimethylamino group C$\underline{H_2}$N(CH$_3$)$_2$ due to hydrolysis of the polymer varying the chemical environment of remaining side chains. This suggests that while trans-amidation may be possible under basic conditions, it does not occur to a significant extent – less than 2 % relative to the remaining DMAEA units.

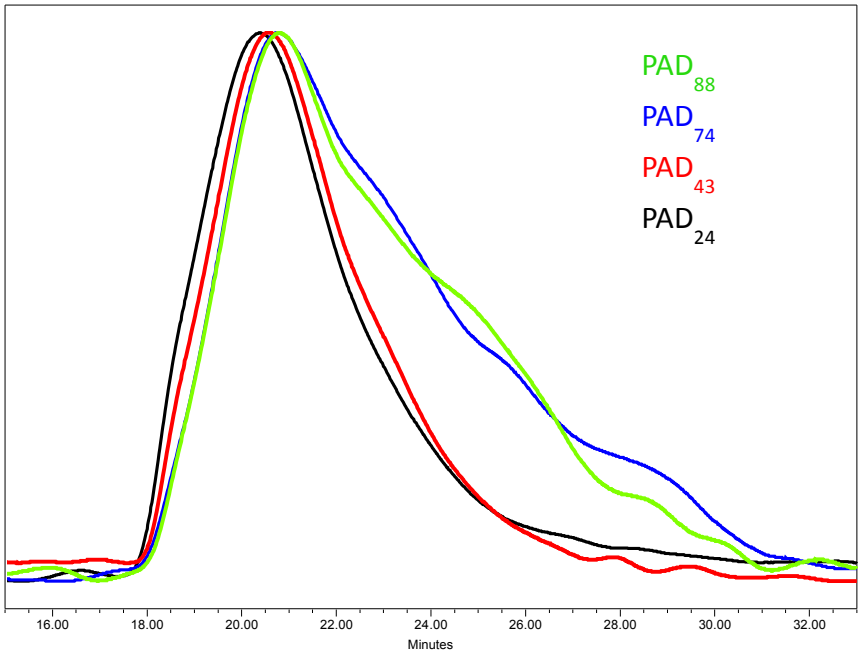

Figure 2A.10. GPC traces for PAD_{88}, PAD_{74}, PAD_{43}, and PAD_{24} prepared by conventional free radical polymerization. GPC traces are normalized.

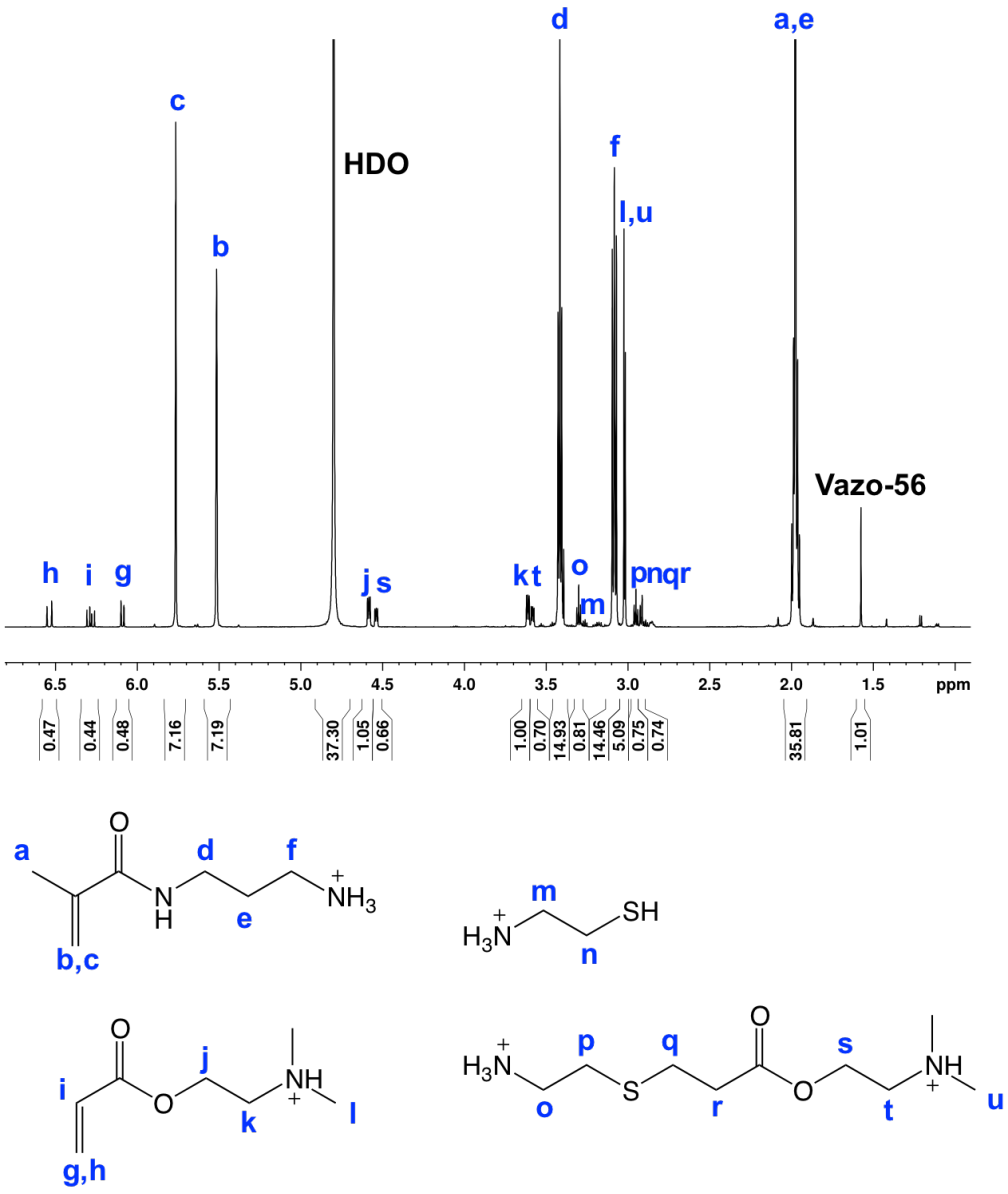

Figure 2A.11. ^{1}H NMR spectrum showing evidence of Michael addition of cysteamine to DMAEA in a 90:10 APM:DMAEA monomer mixture at pH 3-4 and room temperature. The initial concentration of cysteamine was 5 mol% relative to total monomers (50% relative to DMAEA) and the spectrum reveals that about 40% of the DMAEA had been consumed by the Michael reaction after approximately 20 min.

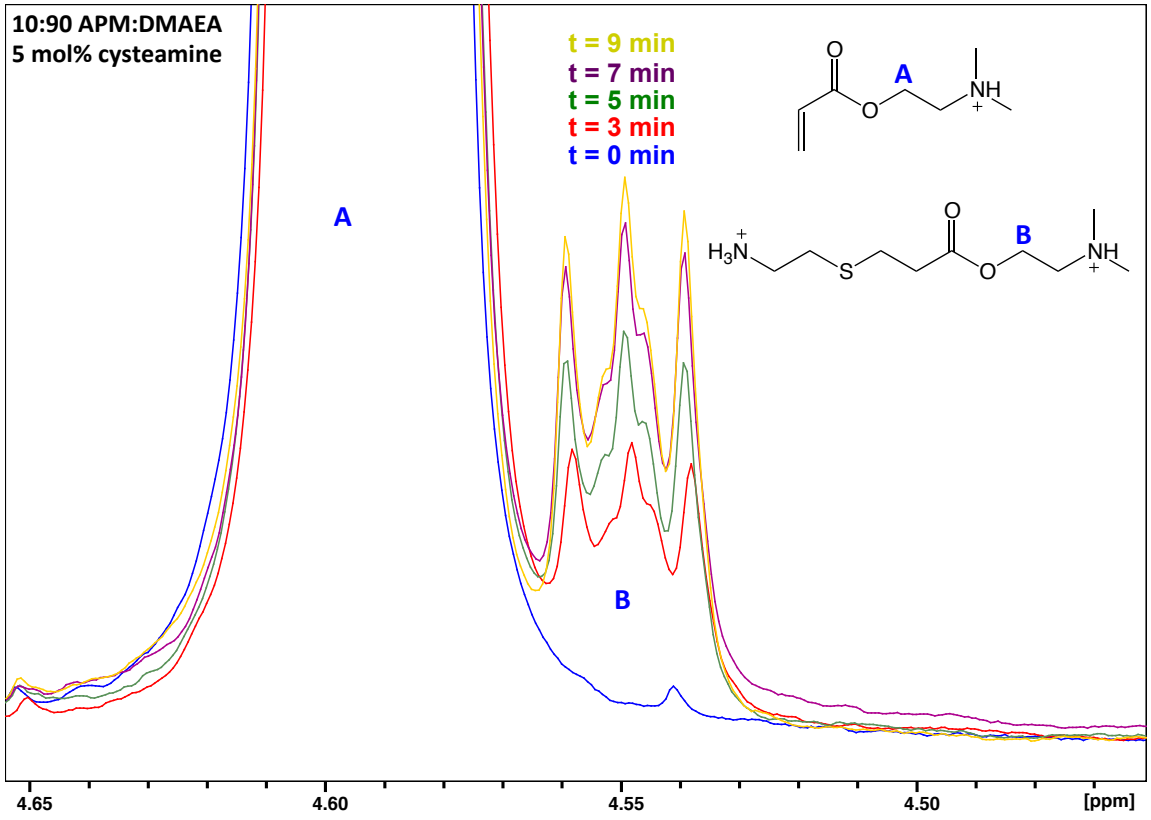

Figure 2A.12. ^{1}H NMR (500 MHz; D_2O) spectra revealing the Michael addition of cysteamine to DMAEA in a 10:90 APM:DMAEA mixture at pH 3-4 and 25 °C. The solution contained 10 wt% monomer and 5 mol% of cysteamine relative to the total monomer (DMAEA:cysteamine = 90:5). After 9 min, approximately 6 % DMAEA and 55% cysteamine had been consumed.

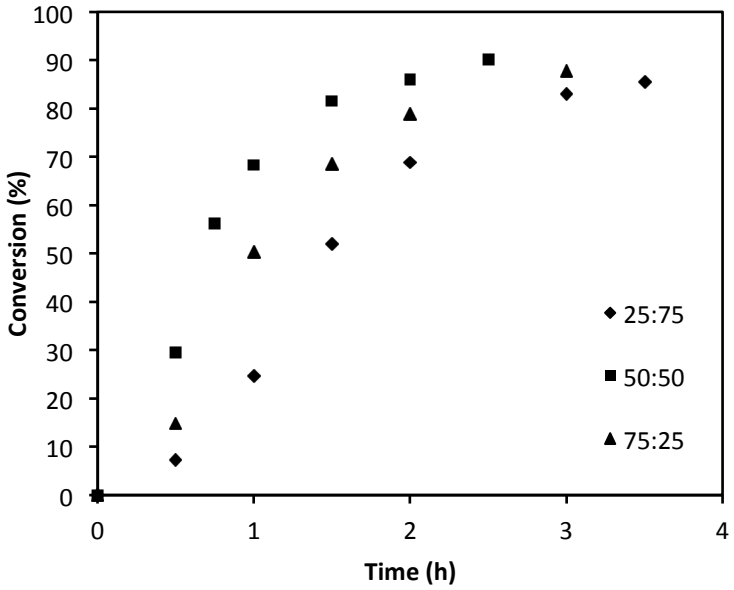

Figure 2A.13. Conversion *vs*. time plots for the RAFT copolymerizations of 25:75, 50:50 and 75:25 APM:DMAEA monomer mixtures targeting a MW of 8 kDa.

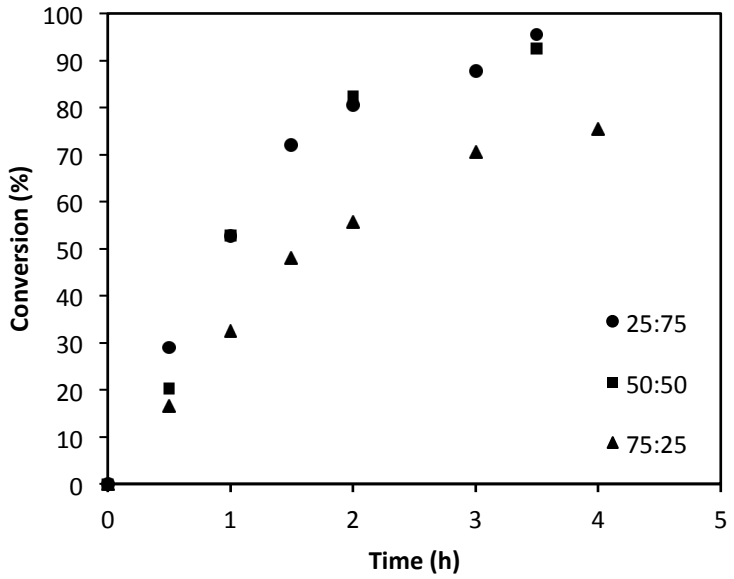

Figure 2A.14. Conversion *vs*. time plots for the RAFT copolymerizations of 25:75, 50:50 and 75:25 APM:DMAEA monomer mixtures targeting a MW of 30 kDa.

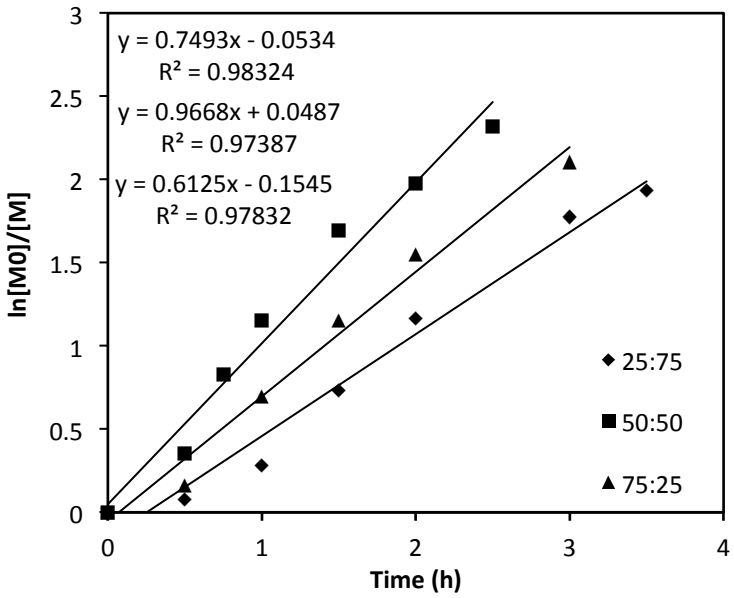

Figure 2A.15. First-order kinetic plot of the RAFT copolymerization of 25:75, 50:50 and 75:25 APM:DMAEA monomer mixtures targeting a MW of 8 kDa.

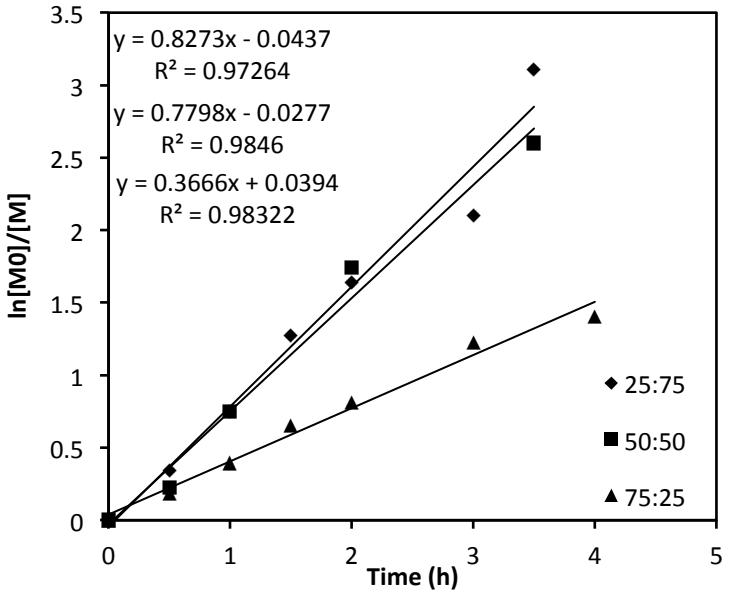

Figure 2A.16. First-order kinetic plot of the RAFT copolymerizations of 25:75, 50:50 and 75:25 APM:DMAEA monomer mixtures targeting a MW of 30 kDa.

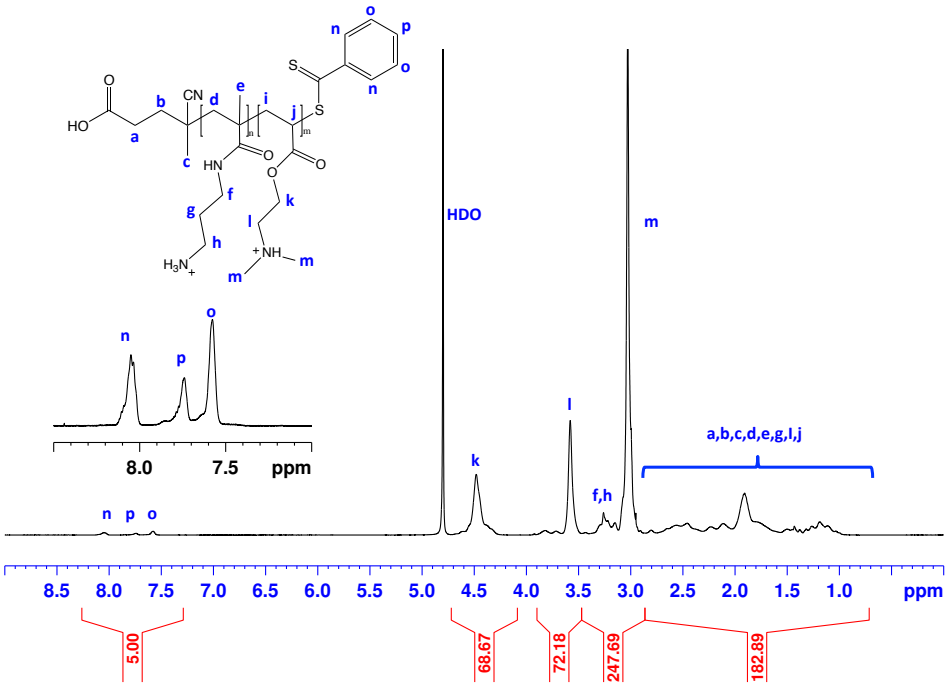

Figure 2A.17. ^{1}H NMR of PAD_{75}-8k in D_2O on an AV600 MHz spectrometer with 1024 scans for end-group analysis.

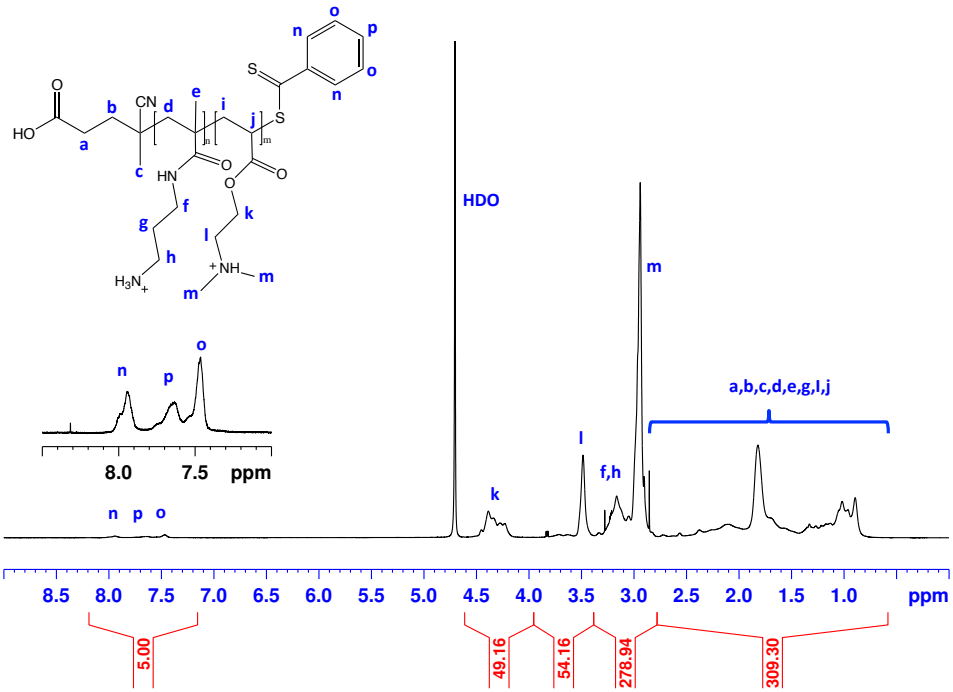

Figure 2A.18. ^{1}H NMR of PAD_{50}-8k in D_2O on an AV600 MHz spectrometer with 1024 scans for end-group analysis.

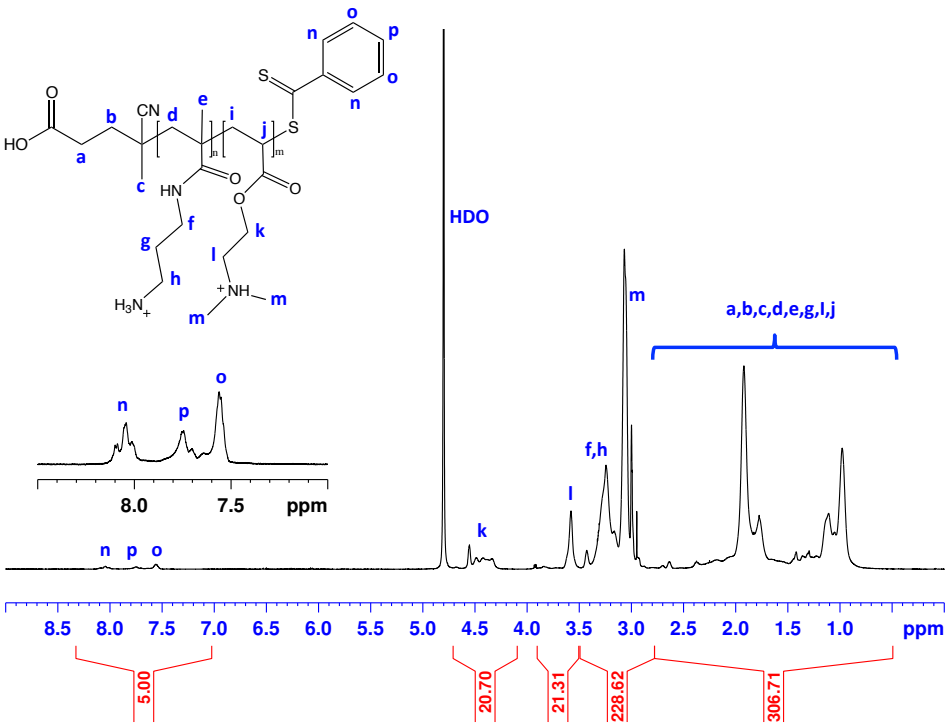

Figure 2A.19. ^{1}H NMR of PAD_{25}-8k in D_2O on an AV600 MHz spectrometer with 1024 scans for end-group analysis.

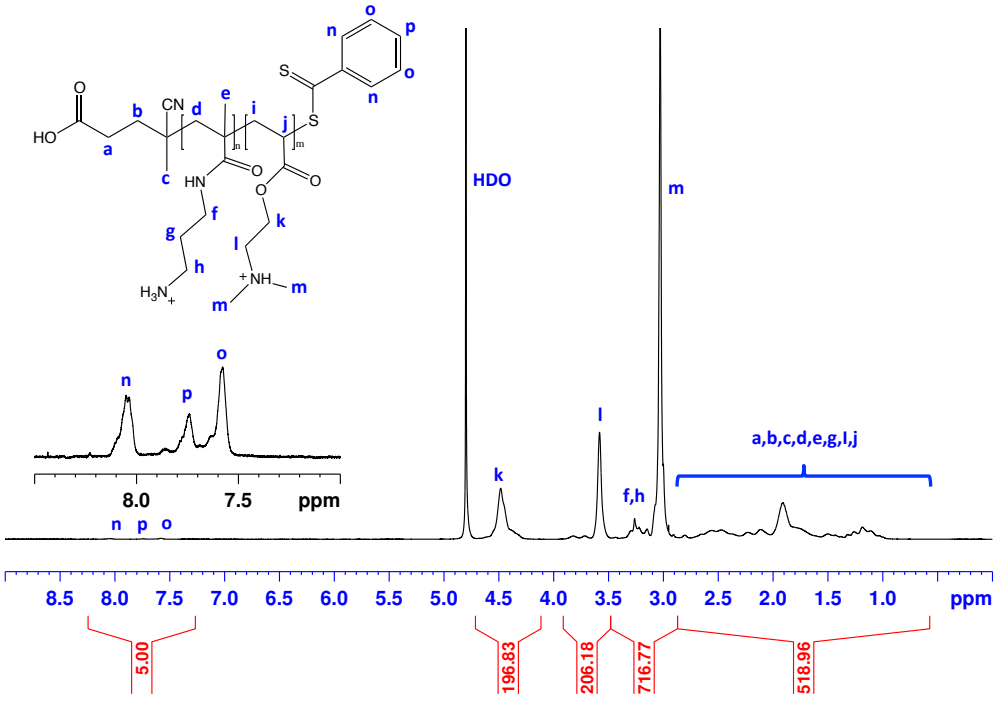

Figure 2A.20. ^{1}H NMR of PAD_{75}-30k in D_2O on an AV600 MHz spectrometer with 1024 scans for end-group analysis.

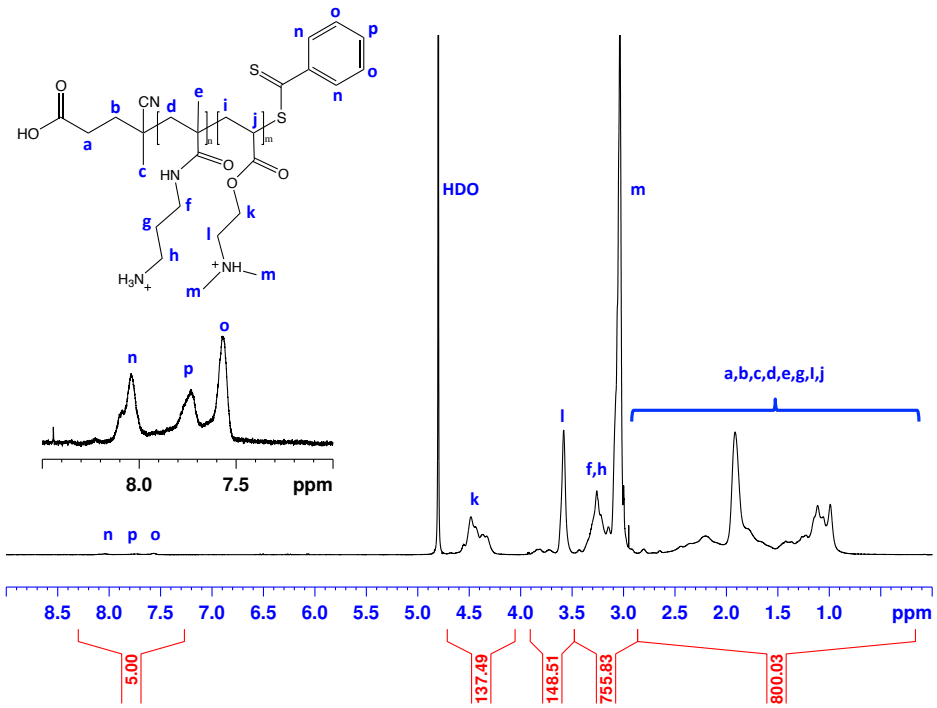

Figure 2A.21. ^{1}H NMR of PAD_{50}-30k in D_2O on an AV600 MHz spectrometer with 1024 scans for end-group analysis.

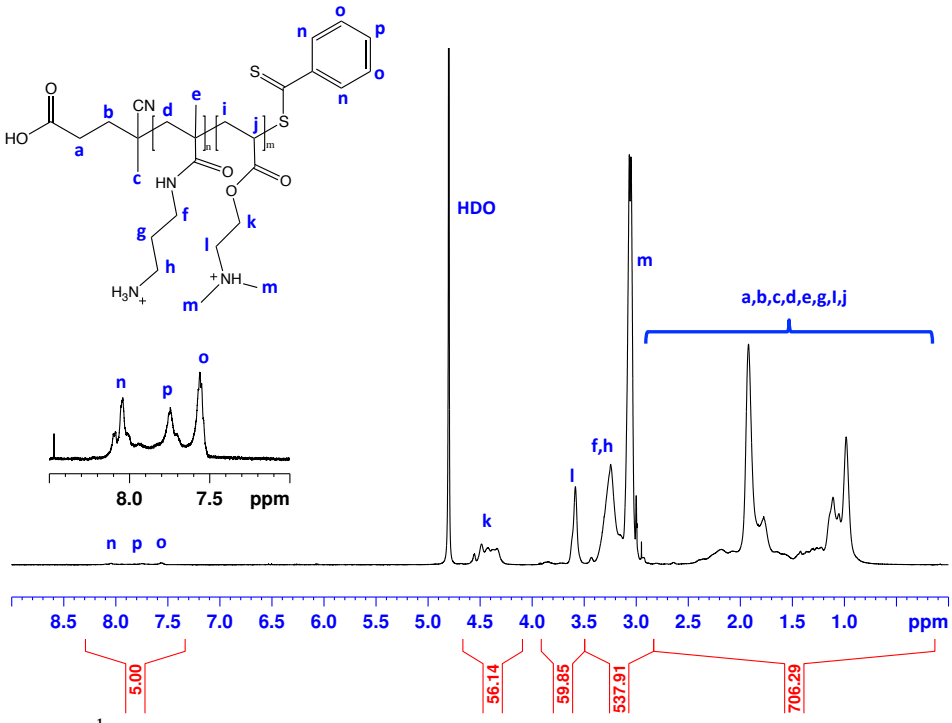

Figure 2A.22. ^{1}H NMR of PAD_{25}-30k in D_2O on an AV600MHz spectrometer with 1024 scans for end-group analysis.

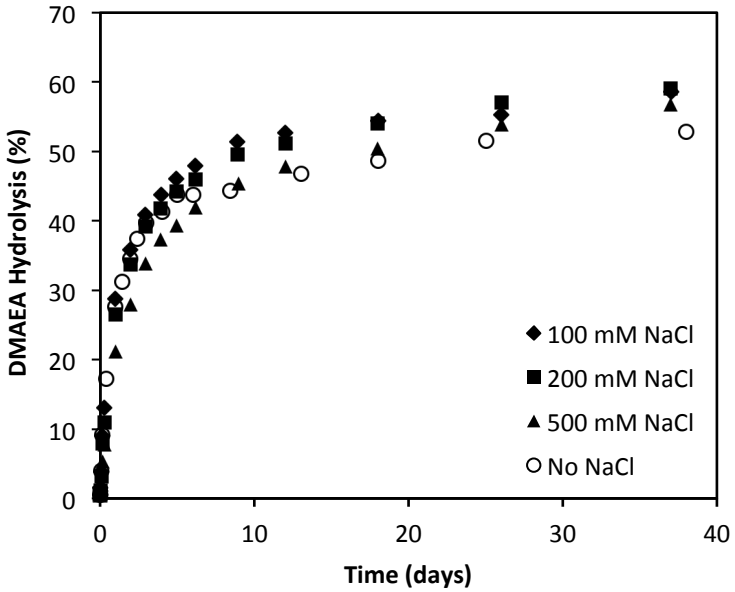

Figure 2A.23. Hydrolysis kinetics of 1% PAD_{88} in the presence of 0, 100, 200, and 500 mM sodium chloride in 50 mM phosphate buffer at pH 7 and 37°C in D_2O.

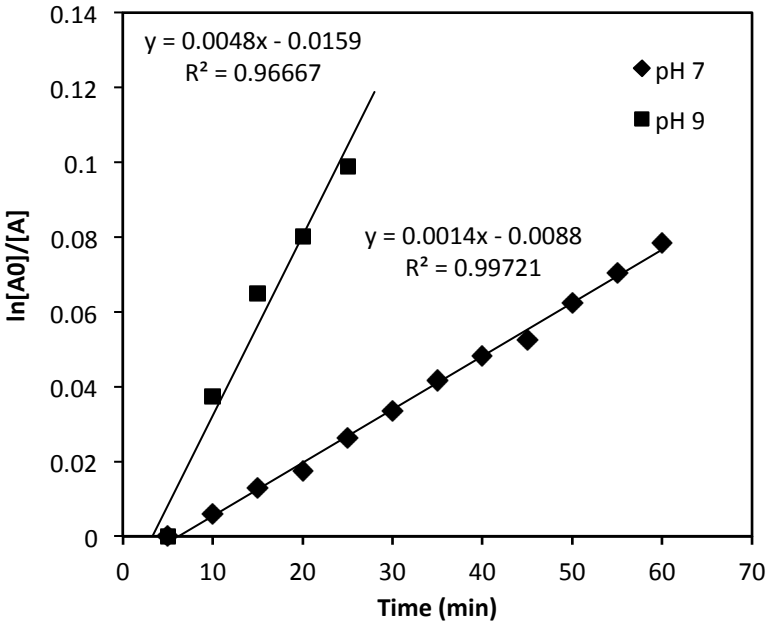

Figure 2A.24. First order kinetic plots for initial stage of PAD_{88} hydrolysis in pH 7 and pH 9 buffers at 37°C.

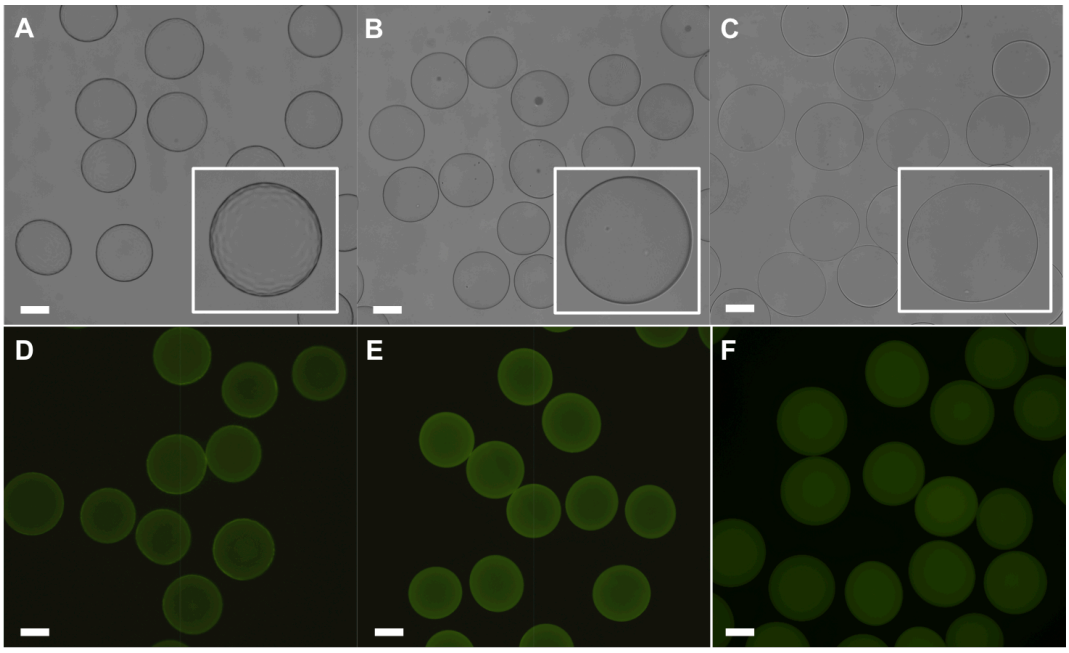

Figure 2A.25. Bright field optical microscopy images of capsules coated with PAD_{20}-8k-*f* (**A**), PAD_{42}-8k-*f* (**B**), and PAD_{75}-8k-*f* (**C**) with the corresponding fluorescence images **D**, **E**, and **F**, respectively. The contrast of **D** was increased by 50 % relative to the original image. Scale bars are 250 μm.

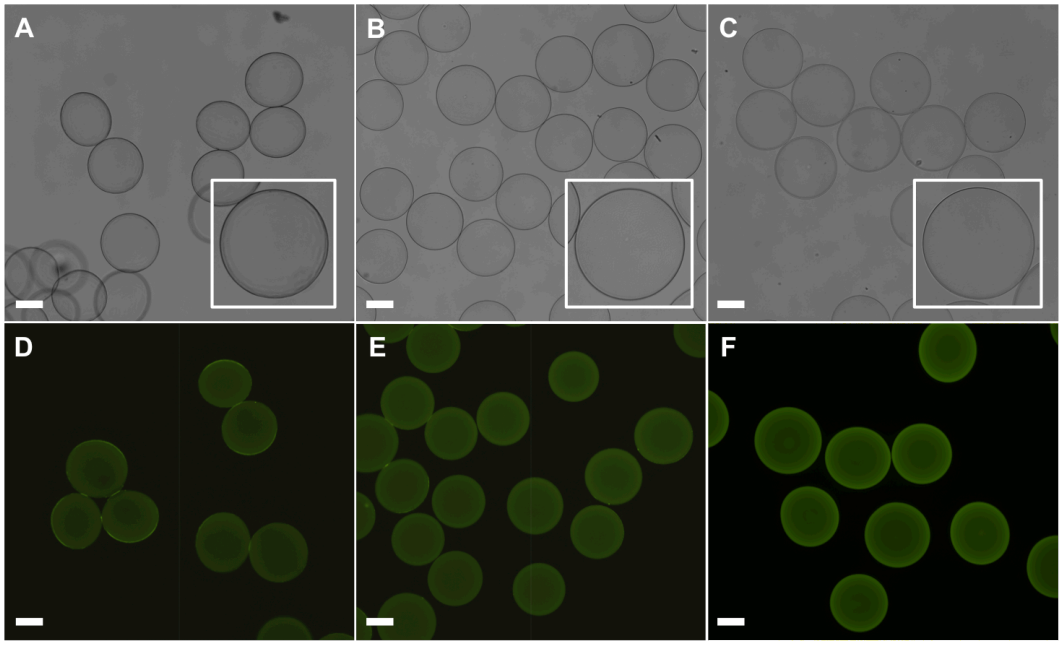

Figure 2A.26. Bright field images of capsules coated with PAD_{24}-30k-*f* (**A**), PAD_{45}-30k-*f* (**B**), and PAD_{76}-30k-*f* (**C**), and their corresponding fluorescence images **D**, **E**, and **F**, respectively. The contrast of **D** was increased by 50 % relative to the original image. Scale bars are 250 μm.

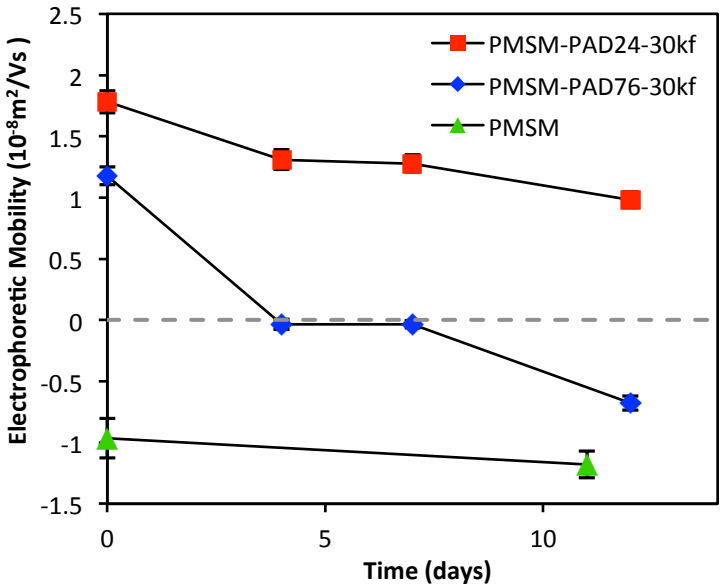

Figure 2A.27. Electrophoretic mobility of PMSM particles uncoated and coated with PAD_{76}-30k-*f* and PAD_{24}-30k-*f* at various time intervals in HEPES-buffered saline.

References

[1] Smith, L. H.; McCarty, P. L., Kitanidis, P. K. Spreadsheet Method for Evaluation of Biochemical Reaction Rate Coefficients and Their Uncertainties by Weighted Nonlinear Least-Squares Analysis of the Integrated Monod Equation. *Applied and Environmental Microbiology* **1998**, *64(6)*, 2044–2050.

CHAPTER 3: Charge-Shifting Polycations with Tunable Rates of Hydrolysis: Effect of Backbone Substituents on Poly[2-(Dimethylamino)ethyl acrylates]

Samantha Ros[1], Rachelle M. Kleinberger[1], Nicholas A. D. Burke[1], Nicholas A. A. Rossi[2], Harald D. H. Stöver[1*]

[1]McMaster University, Hamilton, ON, L8S 4M1, Canada

[2]Mirus Bio LLC, Madison, WI, 53711, USA

Reprinted (adapted) with permission from Ros, S. *et al.*, *Macromolecules* **2018**, *51* (15), 5752-5761. Copyright (2018) American Chemical Society.

For Table of Contents Only

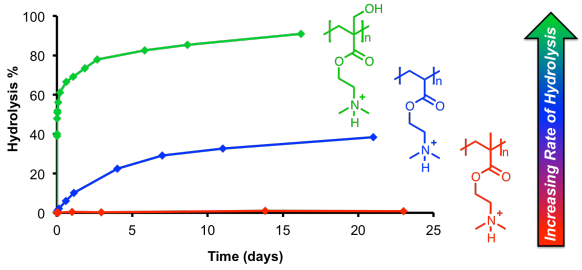

3.1. Abstract

While polycations based on 2-(dimethylamino)ethyl methacrylate and 2-(dimethylamino)ethyl acrylate are used in applications ranging from biomaterials to wastewater treatment, few studies have considered the remarkable differences in the hydrolytic stabilities of the respective ester groups. Here, we describe how the nature of

non-methyl α-substituents affect the rates of ester hydrolysis of such polymers, with an emphasis on the resulting shift of net polymer charge from cationic towards anionic. We introduce 2-(dimethylamino)ethyl 2-hydroxymethyl acrylate (DHMA) as a new, very hydrolytically labile, cationic monomer that can be used to form homopolymers as well as a means to tune copolymer hydrolysis. DHMA synthesis and free radical polymerization are described, including reactivity ratios for hydroxyl-protected derivatives of DHMA and 2-(dimethylamino)ethyl acrylate (DMAEA). Hydrolyses of PDHMA, P[DHMA-*co*-DMAEA], PDMAEA, and PDMAEMA in pH 5 and 7 buffer are reported. The presence of the hydroxymethyl α-substituent in PDHMA led to rates of hydrolysis two to three orders of magnitude faster than the already rapid hydrolysis of PDMAEA. Furthermore, hydrolysis rates of P[DHMA-*co*-DMAEA] copolymers were shown to increase as the DHMA mol fraction increased. As a result, a new route to adjusting the charge-shifting rates of such polycations in aqueous media is described.

3.2. Introduction

Polycations are used extensively for applications including wastewater treatment,[1,2] oil recovery,[3] and biomaterials.[4] While poly[2-(dimethylamino)ethyl methacrylate], PDMAEMA, stands out among these due to its low cost and relative ease of polymerization,[5] there have been only a few studies on the hydrolytic stability of this polymer. The nature of the ester linkage is key to the polymer's biomaterial applications, as the net charge of the polymer moves from cationic towards anionic, as hydrolysis occurs under physiological conditions.

Hennink et al. reported that PDMAEMA hydrolyzed >2000 times more slowly than its monomer under physiological conditions, which was attributed to its hydrophobic and crowded methacrylate backbone.[6] We recently found the hydrolysis of the acrylic analogue, poly[2-(dimethylamino)ethyl acrylate] (PDMAEA), initially proceeded at rates comparable to that of 2-(dimethylamino)ethyl isobutyrate, the small-molecule model compound of the polymer reported by Hennink. This was attributed to the less hydrophobic and more accessible acrylate backbone of PDMAEA.[6,7]

There is currently great interest in developing additional degradable analogues of PDMAE(M)A for DNA delivery, cell encapsulation, and towards other biomaterial applications.[7-23] Most reports focus on changing side-chain functionality[9,11,12,14,16] and comonomer composition,[7,18,19,21,22] or incorporating labile linkages in the polymer backbone[10,13,15,20,23] to tune degradation. To our knowledge, this is the first report studying the effect of functional groups in the α-position of DMAE(M)A on the hydrolytic stability of the associated polymers.

The common routes to new (meth)acrylic monomers involve reacting (meth)acryloyl chloride or (meth)acrylic anhydride with suitable nucleophiles, or using carbodiimide coupling chemistry of (meth)acrylic acid with suitable alcohols or amines. While efficient, the resulting polymers are limited to acrylate or methacrylate backbones. Mathias et al. in 1987 pioneered the synthesis and polymerization of methyl-α-hydroxymethyl acrylate (MHMA),[24] and later studied the polymerization behaviour of various ester[25-27] and ether[28,29] derivatives of MHMA, as well as of higher alkyl α-hydroxymethyl acrylate analogues.[30] Recent studies by Joy et al. further explored

analogous hydroxymethylation of acrylic monomers in the α-position to increase polymer backbone diversity. Hydrophobic acrylates carrying α-hydroxymethyl groups were used in RAFT polymerization and as bi-functional monomers to form polyesters and poly(ester urethanes),[31] as well as in self-emulsion polymer lattices.[32] These α-substituted acrylates were formed using the Baylis-Hillman reaction (also known as Morita-Baylis-Hillman reaction[33]), which can introduce functional groups to an alkene conjugated to an electron-withdrawing group, as in an acrylate, involving initial reaction of the alkene with a tertiary amine or phosphine catalyst.[33-35]

We report here the introduction of an α-hydroxymethyl group into DMAEA to study its effect on the rate and mechanism of acrylate ester hydrolysis on the corresponding homo- and copolymers. We hypothesized that the hydroxymethyl group in 2-(dimethylamino)ethyl 2-hydroxymethylacrylate (DHMA) would activate the acrylic ester towards hydrolysis by a general increase of hydrophilicity of the backbone, as well as through two specific mechanisms shown in Figure 3.1: either by increasing the electrophilicity of the acrylic ester by 6-membered ring hydrogen-bonding with α-hydroxymethyl groups (Figure 3.1**A)**, or *via* activation of acrylic esters on neighbouring monomer units through an intermediate δ-lactonization pathway (Figure 3.1**B**).

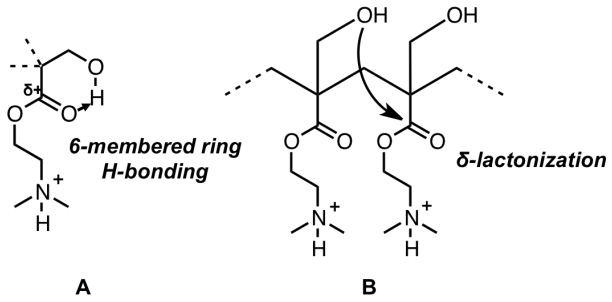

Figure 3.1. Possible mechanisms of hydroxymethyl activation of ester hydrolysis in DHMA polymers. Activation of the ester via 6-membered ring hydrogen-bonding to the carbonyl oxygen (**A**), and by attack of hydroxymethyl groups on neighbouring monomer units, forming 6-membered ring lactones (**B**).

The expected increase in the rate of ester hydrolysis means the rate of "charge-shifting" of DMAE(M)A-type polymers could be tuned for biomaterial applications.[7,17-19,21,22] This paper focuses on the synthesis of DHMA and protected versions of DHMA, homo and copolymerization of some of the monomers, and comparison of the effect of the hydrogen, methyl and hydroxymethyl α-substituents (Figure 3.2) on ester hydrolysis and charge shifting of a series of polycations.

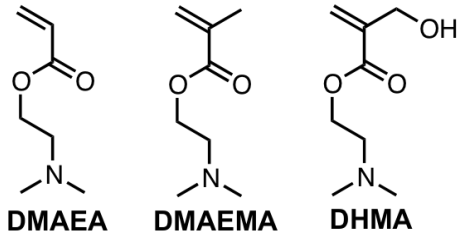

Figure 3.2. Structures of DMAEA, DMAEMA, and DHMA with hydrogen, methyl, or hydroxymethyl in the α-position, respectively.

3.3. Experimental

3.3.1. Materials

2-(Dimethylamino)ethyl acrylate (DMAEA, 98 %), 2-(dimethylamino)ethyl methacrylate (DMAEMA, 98 %), methyl acrylate (99 %), 37 wt.% formaldehyde solution in H_2O with 10-15% methanol, 35 wt.% deuterium chloride in D_2O (≥99 atom % D), 1,4-diazabicyclo[2.2.2]octane (DABCO, ≥99 %), N,N-diisopropylethylamine (DIPEA, ≥99 %), N,N-dimethylaminopyridine (DMAP, ≥99 %), triethylamine (TEA, ≥99 %), N,N'-Dicyclohexylcarbodiimide (DCC, 99 %), 2-(dimethylamino)ethanol (DMAE, ≥99.5 %), tert-butyldimethylsilyl chloride (TBSCl, 97 %), chlorotriethylsilane (TESCl, 99 %), chlorotrimethylsilane purified by redistillation (TMSCl, ≥99 %), bromotrimethylsilane (TMSBr, 97 %), chloromethyl methyl ether (MOM chloride) (technical grade), 2,2-dimethoxy-2-phenyl-acetophenone (DMPA, 99 %), and 4 M HCl in 1,4-dioxane were purchased from Sigma-Aldrich and used as received. Dichloromethane (DCM) (reagent grade), chloroform ($CHCl_3$) (reagent grade), methanol (MeOH) (reagent grade), 1,4 dioxane (reagent grade), dimethylsulfoxide (DMSO) (reagent grade), acetone (reagent grade), acetonitrile (HPLC grade), and potassium hydroxide (KOH) (reagent grade) were purchased from Caledon Laboratories Ltd. and used as received unless stated otherwise. Benzene (ACS reagent grade) was purchased from Fisher Scientific and used as received. 2,2'-Azobis(2-methylpropionitrile) (AIBN) was purchased from DuPont and used as received. D_2O (99.9% D), $CDCl_3$ (99.9 % D), toluene-*d8* (99.9 % D) and DMSO-*d6* (99.9 % D) were purchased from Cambridge Isotope Laboratories Inc. and used as received.

3.3.2. Synthesis of 2-(Dimethylamino)ethyl 2-(Hydroxymethyl)-Acrylate (DHMA)

DMAEA (4 g, 28.0 mmol) was added to a 20 mL vial equipped with a magnetic stir-bar. Formaldehyde solution (37 wt.% aq., 2.27 mL, 28.0 mmol) was added to the stirring reaction mixture, followed by DABCO (1.57 g, 14.0 mmol). DABCO slowly dissolved after 5 min of stirring as the mixture became transparent. The yellow, viscous reaction mixture was stirred at room temperature (22 °C) for 5 hours. The crude mixture was passed through a silica plug using chloroform, and the resulting solution concentrated *in vacuo* by rotary evaporation resulting in a transparent, colourless liquid. The product was further purified by column chromatography with silica gel as the stationary phase and acetone with 2 % v/v triethylamine as the mobile phase. DHMA was obtained as a clear, colourless liquid in 21% yield, and was analyzed by ^{1}H NMR in $CDCl_3$. However, it should be noted that percent conversion of DMAEA starting material to DHMA and higher oligo[oxymethylene] substituted monomer was high at >90 %. DHMA ^{1}H NMR (600 MHz, $CDCl_3$) δ 6.22 (1H, d), 5.75 (1H, d), 4.33 (2H, t), 4.31 (2H, s), 2.63 (2H, t), 2.30 (6H, s).

3.3.3. Polymerization of DMAEA and DMAEMA

DMAEA (1.00 g, 6.98 mmol) and AIBN (12.0 mg, 0.07 mmol) were dissolved in 10.0 mL 1,4-dioxane in a 20 mL vial fitted with a septum and the reaction mixture was purged with nitrogen. The mixture was heated for 11 hours at 70 °C to reach >80 % conversion, followed by purification using precipitation into 40-fold excess hexanes. The polymer was re-dissolved in 1,4-dioxane, followed by re-precipitation into hexanes. This

precipitation cycle was repeated 4 times to yield PDMAEA as a yellow, viscous liquid that was dried *in vacuo*. Polymerization and isolation of PDMAEMA followed the same general procedure as PDMAEA. ^{1}H NMR spectra of PDMAEA and PDMAEMA in $CDCl_3$ are shown in Figure 3A.1 and 3A.2, respectively.

3.3.4. Polymerization of DHMA

DHMA (0.100 g, 0.577 mmol) and AIBN (1.90 mg, 0.015 mmol) were dissolved in 1.0 mL of 1,4-dioxane, DMSO, or acetonitrile in a 4 mL vial sealed with a septum and the reaction mixture was purged with nitrogen to reduce oxygen levels. The reaction mixture was heated at 70 °C in a water bath.

Alternatively, DHMA was polymerized by photo-initiated radical polymerization at lower temperatures (rt and 0 °C). DHMA (0.200 g, 1.15 mmol) and DMPA (6.0 mg, 0.023 mmol) were dissolved in 1.0 mL of DMSO, 1,4-dioxane, chloroform, acetonitrile, toluene, or benzene in a 4 mL vial sealed with a septum, and was purged with nitrogen. The reaction mixture was irradiated with four F8T5-BL 350 nm lamps at either room temperature or in an ice-water bath.

Aliquots of the reaction mixture were removed at intervals, diluted in $CDCl_3$ and monitored by ^{1}H NMR to measure conversion. The polymerization mixtures required typically 24 h of heating or 10 h of irradiation to reach >50 % conversion.

3.3.5. Synthesis of Silylether-Protected DHMA

DHMA (1.00 g, 5.78 mmol) as a crude mixture following a silica plug as described above was dissolved in 30 mL DCM in a round bottom flask equipped with a stir bar, maintained at 0 °C using an ice-water bath. TBSCl, TESCl, or TMSCl (5.78 mmol) and imidazole (0.390 g, 5.78 mmol) were added to the reaction vessel. White precipitate (imidazolium chloride salt) was formed within 5 min, after which the reaction mixture was allowed to warm up to room temperature and stirred for an additional hour. The reaction mixture was filtered and passed through a silica plug using DCM as eluent. The product was concentrated and dried *in vacuo*, resulting in slightly yellow, transparent oils that were further purified by column chromatography using silica gel as the stationary phase and 10:90 v/v hexanes:acetone as the mobile phase. ^{1}H NMR spectra for TBS-, TES-, and TMS-DHMA can be found in the Supporting Information (Figure 3A.3, 3A.4, and 3A.5, respectively). TBS-DHMA ^{1}H NMR (600 MHz, $CDCl_3$) δ 6.27 (1H, d), 5.92 (1H, d), 4.36 (2H, t), 4.30 (2H, t), 2.68 (2H, t), 2.34 (6H, s), 0.92 (9H, s), 0.08 (6H, s). TES-DHMA ^{1}H NMR (600 MHz, $CDCl_3$) δ 6.27 (1H, d), 5.95 (1H, d), 4.37 (2H, t), 4.31 (2H, t), 2.70 (2H, t), 2.36 (6H, s), 0.96 (9H, t), 0.63 (6H, q). TMS-DHMA ^{1}H NMR (600 MHz, $CDCl_3$) δ 6.27 (1H, d), 5.90 (1H, d), 4.34 (2H, t) 4.28 (2H, t), 2.65 (2H, t), 2.32 (6H, s), 0.14 (9H, s).

3.3.6. Synthesis of PDHMA using TES-DHMA

TES-DHMA (0.200 g, 0.696 mmol) and DMPA (3.6 mg, 0.014 mmol) were dissolved in 1 mL of $CDCl_3$ in a Pyrex 5 mm NMR tube. The reaction mixture was

irradiated with four F8T5-BL 350 nm lamps at room temperature, or in an ice-water bath using ^{1}H NMR to monitor conversion at intervals. Polymerization mixtures were typically irradiated for 8 hours to achieve about 70 % conversion. The polymer was simultaneously precipitated and deprotected by dropwise addition into 40-fold excess acetone containing 2 mol equivalents of anhydrous HCl in 1,4-dioxane, resulting in a yellow precipitate. The mixture was centrifuged at 4000 rpm for 10 min, and the supernatant decanted. The precipitate was re-dissolved in DMSO, re-precipitated into 40-fold excess acetone, and subsequently centrifuged. This DMSO/acetone precipitation process was repeated 3 times to remove residual monomer, initiator, and other small molecules. PDHMA was obtained as a yellow, viscous oil that was dried *in vacuo* to form a waxy solid, and characterized by ^{1}H NMR. GPC analysis of the polymer in 1.0 M acetic acid/sodium acetate pH 4.8 buffer gave Mn = 870 g/mol, Mw = 1000 g/mol, Mp = 924 g/mol, and PDI of 1.15.

3.3.7. Synthesis of MHMA

Methyl acrylate (10.0 g, 0.116 mol) and DABCO (6.51 g, 0.058 mol) were dissolved in 80 mL of a 1:1 v/v water:1,4-dioxane in a round bottom flask equipped with a magnetic stir-bar. Aqueous formaldehyde solution (9.41 mL, 0.116 mol) was added to the stirring reaction mixture at room temperature and the reaction was left to stir overnight. The reaction mixture was partitioned with the addition of 50 mL ethyl acetate and 50 mL of brine. MHMA was extracted with 4 fractions of ethyl acetate (50 mL). The combined ethyl acetate fractions were dried over anhydrous sodium sulfate, filtered, and concentrated and dried *in vacuo* by rotary evaporation, resulting in a clear, colourless

liquid. The product was further purified by column chromatography using silica gel as the stationary phase, and 60:40 v/v hexanes:ethyl acetate as the mobile phase. MHMA was obtained as a clear, colourless liquid in 40 % yield. MHMA ^{1}H NMR (600 MHz, $CDCl_3$) δ 6.23 (1H, d), 5.82 (1H, d), 4.30 (2H, d), 3.79 (3H, s), 2.78 (1H, broad).

3.3.8. Synthesis of MOM-ether protected MHMA

MHMA (2.00 g, 17.22 mmol) and DIPEA (2.23 g, 17.22 mmol) were dissolved in 40 mL of DCM in a round bottom flask equipped with a magnetic stir-bar, and cooled to 0 °C in an ice-water bath. MOM chloride (1.39 g, 17.22 mmol) was added drop-wise to the stirring reaction mixture, forming a white vapour upon addition. The yellow, transparent reaction mixture was left to stir at 0 °C for 4 hours, followed by overnight stirring at room temperature. Sodium bicarbonate and ice were added to the reaction mixture to quench any remaining MOM chloride under vigorous stirring for 2 hours. The reaction mixture was washed with 3 fractions of 5 % sodium bicarbonate solution (40 mL), following a wash with brine (40 mL). The DCM layer was dried over anhydrous sodium sulfate, filtered, and concentrated and dried *in vacuo* by rotary evaporation. MOM-ether protected MHMA, MOM-MHMA, was obtained as a yellow, transparent oil in 85 % yield. MOM-MHMA ^{1}H NMR (600 MHz, $CDCl_3$) δ 6.31 (1H, d), 5.88 (1H, d) 4.67 (1H, s), 3.77 (3H, s), 3.38 (3H, s).

3.3.9. Synthesis of MOM- ether protected α-hydroxymethyl acrylic acid (MOM-HMAA)

MOM-MHMA (2.00 g, 12.5 mmol) was dissolved in a 2:1 v/v THF:water mixture (40 mL) in a round bottom flask equipped with a magnetic stir-bar. KOH pellets (2.10 g, 37.5 mmol) were added to the stirring reaction mixture at room temperature and the mixture was left to stir overnight. The reaction mixture was carefully acidified to ~pH 2 using ammonium chloride, following by extraction with 4 fractions of ethyl acetate (40 mL). The fractions were combined, dried over anhydrous sodium sulfate, filtered, and concentrated and dried *in vacuo* by rotary evaporation. MOM-HMAA was obtained as a clear, colourless liquid in quantitative yield. MOM-HMAA ^{1}H NMR (600 MHz, $CDCl_3$) δ 11.59 (1H, broad), 6.46 (1H, d), 6.01 (1H, d), 4.69 (2H, s), 4.29 (2H, s), 3.39 (3H, s).

3.3.10. Synthesis of MOM-ether protected DHMA (MOM-DHMA)

MOM-HMAA (2.60 g, 17.8 mmol) was dissolved in 35 mL DCM in a round bottom flask equipped with a magnetic stir-bar, maintained at 0 °C using an ice-water bath. DCC (3.67 g, 17.8 mmol) was added to the reaction flask and was allowed to stir for 15 min before adding 20 mol% of DMAP (0.435 g, 3.56 mmol), followed by 2-(dimethylamino)ethanol (DMAE) (1.58 g, 17.8 mmol). The reaction was stirred under nitrogen at 0 °C for 4 hours, followed by 2 days at room temperature. The reaction mixture was filtered to remove N,N'-dicyclohexylurea (DCU) precipitate, and the filtrate was further concentrated by rotary evaporation. The resulting mixture was suspended in 20 mL of acetonitrile and maintained at -18 °C overnight to further precipitate remaining DCU. The mixture was filtered, and the filtrate was concentrated by rotary evaporation.

The product was purified by column chromatography using silica gel as the stationary phase and acetone with 1 % v/v of triethylamine as the mobile phase. MOM-DHMA was obtained as a slightly yellow, transparent liquid in 88 % yield. MOM-DHMA ^{1}H NMR (600 MHz, $CDCl_3$) δ 6.31 (1H, d), 5.88 (1H, d), 4.67 (2H, s), 4.27 (2H, s), 4.26 (2H, t), 3.37 (3H, s), 2.61 (2H, t), 2.28 (6H, s).

3.3.11. Synthesis of PDHMA using MOM-DHMA

MOM-DHMA (2.00 g, 9.21 mmol) and DMPA (24.0 mg, 0.092 mmol) were dissolved in 10 mL of benzene in a 20 mL vial fitted with a septum and the solution was purged with nitrogen. The reaction vessel was placed in an ice-water bath, and the mixture was irradiated with four F8T5-BL 350 nm lamps for typically 8 hours to achieve >90 % conversion. The polymerization mixture was concentrated to remove benzene, and the resulting viscous liquid was re-suspended in distilled water adjusted to pH 3 with 1M HCl. The solution was purged with nitrogen until transparent, and the mixture was filtered using 0.2 μm filters to remove residual DMPA precipitate, which is insoluble in water. The polymer solution was dialyzed using 3.5 kDa molecular weight cutoff cellulose acetate dialysis tubing in pH 3 distilled water. Dialysis water baths were changed twice daily for 2-3 days and monitored by UV-vis spectroscopy to confirm the diffusion of residual monomers from the polymer solution was complete. The polymer solution was freeze-dried to remove water, resulting in PMOM-DHMA in the ammonium chloride form as a white solid. ^{1}H NMR spectrum of PMOM-DHMA in D_2O is shown in

Figure 3A.6, and GPC analysis of the polymer in 1 M acetic acid/sodium acetate buffer at pH 4.8 gave Mn = 6,830 g/mol, Mw = 12,030 g/mol, Mp = 12,110 g/mol, and PDI = 1.76.

Deprotection of PMOM-DHMA was carried out using a procedure modified from that described by Dufresne et al.[36] First, PMOM-DHMA in the chloride form (0.100 g, 0.394 mmol) was dissolved in 5 mL of DCM with 4 molar equivalents of triethylamine to give a transparent, colourless solution. Hexanes (5 mL) was added to the mixture to precipitate triethylammonium chloride, which was removed by filtration. The filtrate was concentrated *in vacuo* by rotary evaporation and resulted in PMOM-DHMA in the free base form as a transparent, slightly yellow liquid. PMOM-DHMA was re-dissolved in 5 mL DCM in a round bottom flask equipped with a magnetic stir-bar and cooled at 0 °C in an ice-water bath. TMSBr (0.241 g, 1.58 mmol) was added under stirring, and the reaction mixture was left to stir at 0 °C for 2 hours, followed by overnight stirring at room temperature. The resulting precipitate was washed with chloroform or DCM. ^{1}H NMR analysis of the chloroform/DCM washes show no evidence for any DMAE liberated during the reaction, and the ^{1}H NMR spectrum of the polymer in DMSO-*d6* (Figure 3A.7) similarly showed no evidence of ester hydrolysis. ^{1}H NMR analysis of PDHMA in D_2O did confirm near quantitative disappearance of MOM-ether peaks (Figure 3A.8). GPC analysis of hydrolyzed PDHMA at pH 10 (Mn = 2,400 g/mol , Mw = 3,330, Mp = 3,100, and PDI = 1.39) confirmed the decrease in molecular weight of the polymer following deprotection of MOM-ether groups and hydrolysis of DMAE side-groups in alkaline buffer, while degree of polymerization (DP) values remained the same with approximately 25-30 repeat units.

3.3.12. Reactivity Ratios

Solutions containing TES-DHMA and DMAEA at molar monomer feed ratios of 18:82, 27:73, 57:46, and 75:25 at 10 % w/v total monomer loading and containing 2 mol% DMPA in $CDCl_3$ were prepared. The copolymerization solutions were irradiated for multiple ca. 30 min time intervals designed to achieve 10-15 % conversion steps as measured by ^1H NMR. The monomer conversion for each monomer within each conversion step was obtained from the decrease in integrated monomer signals, and used to estimate reactivity ratios and study compositional drift in the copolymerization. Instantaneous comonomer feed ratios and the corresponding instantaneous copolymer compositions for each conversion step were plotted, and reactivity ratios were determined by fitting the terminal model of the differential copolymer composition equation (eq. **1**) using the least squares method with the Solver tool in Microsoft Excel, as previously described,[7]

$$F_1 = \frac{r_1 f_1^2 + f_1 f_2}{r_1 f_1^2 + 2 f_1 f_2 + r_2 f_2^2} \qquad (\mathbf{1})$$

Where f_1 and f_2, and r_1 and r_2, are the instantaneous mole fractions and reactivity ratios, respectively, for monomers 1 and 2, and F_1 is the instantaneous mol fraction of monomer 1 (TES-DHMA) in the copolymer being formed.

3.3.13. Copolymerizations

Preparative copolymerizations of TES-DHMA with DMAEA were carried out using the following procedure. Various initial molar monomer feed ratios were prepared at 10 % w/v total monomer concentration in $CDCl_3$ with 2 mol% DMPA initiator relative to total monomer. The samples were irradiated with four F8T5-BL 350 nm lamps at room temperature for approx. 8 hours to reach >60 % conversion, as analyzed by ^{1}H NMR. The polymers were precipitated into 40-fold excess acetone containing 2 mol equivalents of anhydrous HCl. The mixture was centrifuged, and the supernatant was removed. The polymers were re-dissolved in DMSO and re-precipitated into 40-fold excess acetone. The precipitation cycle was repeated 3 times. The polymers were dried *in vacuo* and characterized by ^{1}H NMR in DMSO-d_6 (Figures 3A.9-3A.12). Cumulative compositions of P[DHMA-*co*-DMAEA] copolymers were determined by comparing the consumption of each monomer after polymerization from the decrease in their ^{1}H NMR vinyl signals of the reaction mixture after UV irradiation, as analysis of the copolymer by ^{1}H NMR was not possible since the side-chains are identical for each monomer and the methylene protons of the hydroxymethyl group overlap with the side-chain peaks.

3.3.14. Hydrolysis Experiments

The hydrolysis experiments for the (co)polymers were carried out using 0.5 wt.% polymer samples in 100 mM acetate and phosphate buffer solutions in D_2O adjusted to pH 5 and 7, respectively. The samples were transferred to NMR tubes and maintained at room temperature. ^{1}H NMR spectra were recorded at different time intervals on Bruker

AV500, AV600, or AV700 spectrometers, and the degree of hydrolysis determined by comparing the integrated sharp signals for free small-molecule DMAE relative to those of the dimethylamino protons on the polymer and small molecule as the integration internal standard. Figure 3A.13 shows a representative ^{1}H NMR spectrum with sample calculations for % DMAE appearance.

3.3.15. Gel Permeation Chromatography

Gel permeation chromatography (GPC) of the polymers was conducted using a Waters GPC consisting of a 717plus autosampler, 515 HPLC pump, 2414 refractive index detector, Ultrahydrogel (120, 250, and 500) columns (30 cm × 7.8 mm (inner diameter); 6 μm particles) using poly[ethylene glycol] standards ranging from 106 Da to 881 kDa (Waters Inc.) for calibration. The mobile phase was either 1 M acetic acid-sodium acetate buffer at pH 4.8, or 0.5 M $NaNO_3$ buffered with 25 mM 2-(cyclohexylamino)ethanesulfonic acid (CHES) at pH 10.03 with 10 ppm NaN_3 as a preservative.

3.3.16. Infrared Spectroscopy

Polymer and monomer samples were analyzed by attenuated total reflection infrared (ATR) FT-IR spectroscopy using a Thermo Scientific Nicolet 6700 FT-IR with Smart iTX optical base. PDHMA was measured as formed, as a waxy solid. PDHMA samples after degradation at pH 5 and 7 from ^{1}H NMR kinetic studies were measured by placing a droplet of the 0.5 wt.% aq. solutions on the ATR crystal and drying the sample

using a stream of nitrogen gas prior to measurements. Monomer samples were analyzed neat.

3.4. Results and Discussion

3.4.1. Synthesis of DHMA via the Baylis-Hillman Reaction

DHMA was synthesized by reacting DMAEA with 37 % aq. formaldehyde in presence of DABCO acting as the tertiary amine catalyst, as shown in Scheme 1. Mathias and subsequent researchers commonly used catalytic amounts of DABCO, though in our hands stoichiometric amounts were required in order to obtain significant yields of DHMA. This was particularly surprising, given that the starting material, DMAEA, is itself a tertiary amine, and is used in base form.

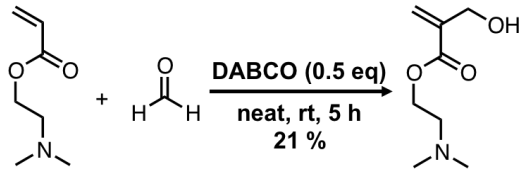

Scheme 3.1. Synthesis of DHMA by Baylis-Hillman reaction of DMAEA with formaldehyde using DABCO as catalyst.

The DHMA yield was fairly low at 21 %, in part due to significant side-reaction. By ^{1}H NMR analysis, it was discovered that the hydroxymethyl substituent underwent oligomerization to produce oligo[oxymethylene] chains (Figure 3A.14). Singlet peaks between 4.5 – 5.0 ppm that were distinct from the methylene protons of poly[oxymethylene] indicated that the oligomers varied in chain length between one and

ten oxymethylene units, with on average 4 repeat units. The oligomerization is due to the reactive nature of formaldehyde and has been noted by previous researchers during the Baylis-Hillman reaction.[37] Attempts at converting the oligomeric side-chain back to hydroxymethyl groups of the oligomer impurity, included placing the crude mixture under reduced pressure, refluxing in 1,4-dioxane, and bubbling N_2 gas to drive off formaldehyde gas, were unsuccessful. Thus, purification of the desired DHMA monomer required the use of column chromatography. The ^{1}H NMR spectrum of DHMA is shown in Figure 3.3.

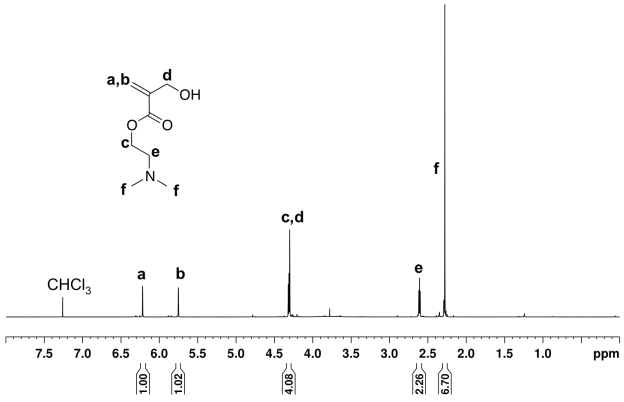

Figure 3.3. ^{1}H NMR spectrum of DHMA in $CDCl_3$ recorded at 600 MHz.

3.4.2. Polymerization of DHMA

Polymerization of DHMA was initially attempted with a thermally-initiated conventional free radical process using AIBN in DMSO-*d6*. It was discovered that although the monomer was stable in DMSO during heating in the absence of initiator, it appeared that the polymer formed underwent a side-reaction that likely involved the lactonization as shown in Figure 3.1**B,** with the hydroxymethyl substituent attacking

neighbouring ester groups to form a δ-lactone. Lactonization would explain the appearance of free DMAE in this non-aqueous, organic solvent, where hydrolysis can be ruled out. Inter-chain trans-esterification was not likely since no crosslinking was observed in the polymer solution. Low temperature polymerization of DHMA at room temperature and 0 °C using photo-initiated free radical polymerization was attempted in various organic solvents to inhibit lactonization. However, significant (>50 %) amounts of DMAE were still detected by ^{1}H NMR analysis of the polymerization mixture. Thus, it was decided to protect the hydroxyl group of DHMA prior to polymerization.

DHMA was protected as *tert*-butyldimethylsilyl (TBS), triethylsilyl (TES), and trimethylsilyl (TMS) ethers. Protection with TBS was successful and subsequent thermally-initiated polymerization proceeded without liberation of DMAE, as determined by ^{1}H NMR. However, deprotection of the resulting PTBS-DHMA proved challenging as complete removal of the bulky *tert*-butyldimethylsilyl group with HCl also led to some acid-catalyzed ester cleavage. TMS-DHMA was not stable during radical polymerization. TES-protected DHMA proved to be more promising as the TES groups were stable during radical polymerization yet also offered facile deprotection with HCl under mild conditions without significant ester cleavage. However, polymerization of TES-DHMA incorporating the bulky TES-groups required long reaction times and led to relatively low molecular weight polymer. Free radical polymerization of similarly bulky methyl α-benzylacrylate was reported to have a ceiling temperature of 67 ± 2 °C.[38,39] As high temperatures typically do not favour the polymerization of sterically hindered monomers

due to lower ceiling temperatures,[40] the polymerization of TES-DHMA was conducted in an ice-water bath using DMPA as photo-initiator.

The simultaneous isolation and deprotection of PTES-DHMA was carried out by precipitating the polymer solution into a 40-fold excess of acetone containing 2 mol equivalents anhydrous HCl. It should be noted that acetone should not be dried prior to use, as stoichiomtric amounts of water are required to hydrolyze the silyl ether groups. The acetone used was not dried prior to use, and was found to contain approximately 3 mol% of water, about equimolar compared to the silyl ether groups present. Since water was not present in excess, hydrolysis of the esters was not significant. ^{1}H NMR analysis of the isolated PDHMA-HCl in DMSO-*d6* and showed quantitative removal of the TES groups and complete retention of the ester groups (Figure 3.4). This suggests that protonation of the tertiary amine in PDHMA prevents lactonization. Further experiments regarding lactonization will be discussed in the degradation studies.

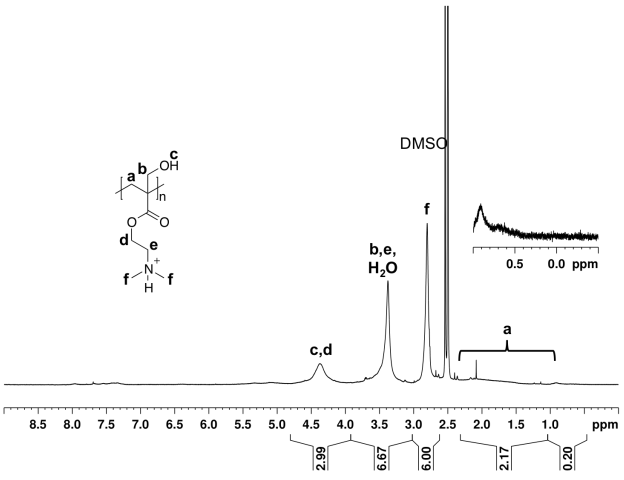

Figure 3.4. ^{1}H NMR of PDHMA in DMSO-*d6* recorded at 600 MHz.

3.4.3. Synthesis and Polymerization of MOM-DHMA

As the polymerization of TES-DHMA was limited to low molecular weight polymers, MOM-ether protected DHMA was synthesized as a less bulky alternative. Treatment of DHMA directly with MOM chloride was not successful as the tertiary amine in the side-chain of DHMA is reactive with such alkyl halides. Thus, an alternate synthetic route was developed to synthesize MOM-DHMA in an overall yield of 30 %, as shown in Scheme 3.2.

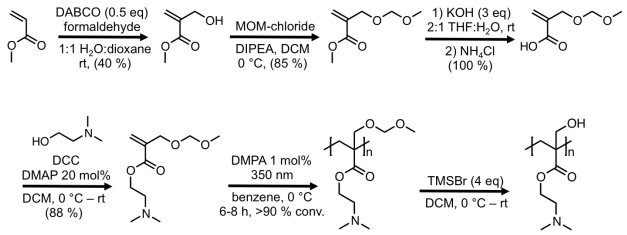

Scheme 3.2. Synthetic route to higher molecular weight PDHMA using MOM-ether protected DHMA.

MOM-DHMA was photo-polymerized at 0 °C to favor polymerization. The resulting polymer, PMOM-DHMA, was soluble in water, and ^{1}H NMR analysis showed that it was stable at pH 3-4 with no appearance of small molecule DMAE after several days in solution (Figure 3A.15). GPC analysis of PMOM-DHMA confirmed formation of higher MW polymers with Mn of 6,800 g/mol, corresponding to DP of approx. 30 repeat units, with a PDI of 1.76.

Deprotection of PMOM-DHMA was achieved by treatment with TMSBr was quantitative by ^{1}H NMR analysis, while leaving the ester groups intact, as previously

reported.[36,41] The higher molecular weight PDHMA obtained through MOM-ether protection allowed for the study of the effect of molecular weight on degradation of polymers derived from α-hydroxymethyl acrylates.

3.4.4. Copolymerization of TES-DHMA and DMAEA

Since the copolymerization of silyl ether protected α-hydroxymethyl substituted acrylates have not yet been studied, the reactivity ratios of TES-DHMA and DMAEA were investigated. TES-DHMA and DMAEA at different initial monomer feed ratios were copolymerized at room temperature using photo-initiation. ^{1}H NMR was used to track monomer conversion over multiple small conversion steps. Reactivity ratios were then estimated by plotting the instantaneous copolymer compositions against the corresponding instantaneous comonomer feed ratios for each conversion step. The instantaneous copolymer equation was fitted to the above experimental data by changing r_1 and r_2 values using the least squares method with the Solver tool in Microsoft Excel. The reactivity ratios obtained were 0.37 and 0.68 for TES-DHMA (r_1) and DMAEA (r_2), respectively. The instantaneous copolymer composition graph is shown in Figure 3.5, and a table of the experimental F_1/f_1 values obtained is given in Table 3A.1. The joint confidence region at 95 % confidence level is for the reactivity ratios obtained is provided in the Supporting Information (Figure 3A.16).

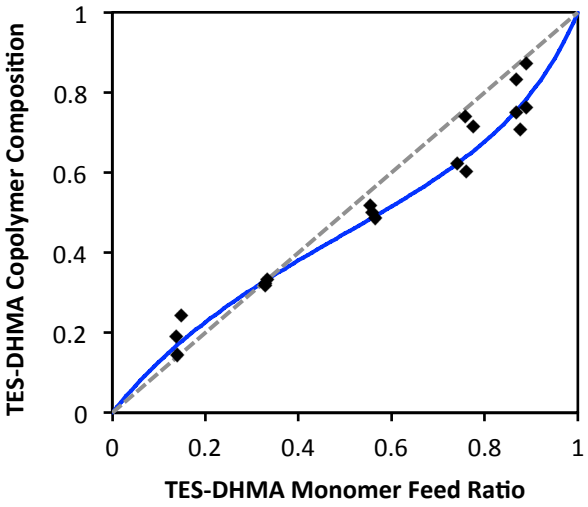

Figure 3.5. The instantaneous copolymer composition graph for copolymerization of TES-DHMA and DMAEA. The best-fit line with $r_1 = 0.37$ and $r_2 = 0.68$ is shown.

Reactivity ratios of 0.37 and 0.68 for TES-DHMA and DMAEA, respectively, reflect a small tendency towards alternation together with small preference for incorporating DMAEA onto the growing polymer chain. This is likely due to the steric effect of the bulky TES groups that favour cross-propagation with less sterically hindered DMAEA monomer units over homo-propagation. P[DHMA-*co*-DMAEA] copolymers of various compositions were prepared for hydrolysis experiments and their properties are summarized in Table 3.1.

Table 3.1. Properties of PDHMA, P[DHMA-*co*-DMAEA], PDMAEA, and PDMAEMA.

Polymer Name	Monomer Feed[a] TES-DHMA: DMAEA	Polymer Composition[b] DHMA:DMAEA	Conv.[a] %	Mn[c] (g/mol)	Mp[c] (g/mol)	Mw[c] (g/mol)	*Đ*[c]
PDHMA	100:0	100:0	52	870	1000	920	1.12
$PDHMA_{78}$	75:25	78:22	64	930	1100	940	1.18

$PDHMA_{50}$	57:46	50:50	88	1220	1760	1320	1.44
$PDHMA_{37}$	27:73	37:63	86	2500	4370	3780	1.75
$PDHMA_{19}$	18:82	19:81	88	2010	3010	2680	1.49
PDMAEA	0:100	0:100	86	11910	24530	22410	2.06
PDMAEMA	N/A	N/A	97	17620	49740	37650	2.82

[a] Calculated by ^{1}H NMR analysis. [b] Calculated from monomer consumption as determined by ^{1}H NMR. [c] GPC analysis using PEG standards for calibration with a 1 M acetic acid-acetate buffer (pH 4.8) as mobile phase; Mn, Mp, and Mw values rounded to the nearest 10.

3.4.5. Degradation of PDHMA, PDMAEA, and PDMAEMA

The hydrolysis of PDHMA was monitored to study the effect of the α-hydroxymethyl substituents relative to the α-H and α-methyl groups in the corresponding acrylate (PDMAEA) and methacrylate (PDMAEMA) backbones. The hydrolysis of PDHMA was expected to be higher due to the increased hydrophilicity of the backbone near the ester. In addition, hydrogen-bonding of the hydroxymethyl to the ester carbonyl oxygen through a six-membered ring (Figure 3.1**A**) could increase the electrophilicity of ester carbonyl and hence hydrolysis. PDHMA, PDMAEA and PDMAEMA hydrolysis was monitored at pH 7 and 5 at room temperature (22 °C) through the appearance of small molecule dimethylaminoethanol (DMAE) by ^{1}H NMR spectroscopy, and the results shown in Figure 3.6 and 3.7, respectively.

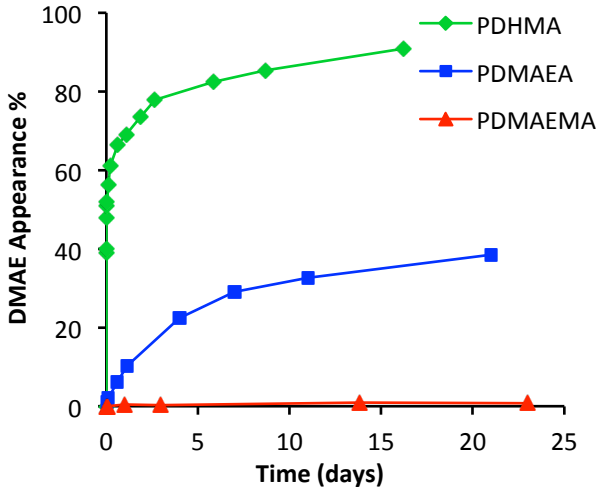

Figure 3.6. Hydrolysis of PDHMA, PDMAEA, and PDMAEMA in 100 mM phosphate buffer at pH 7, room temperature (22 °C).

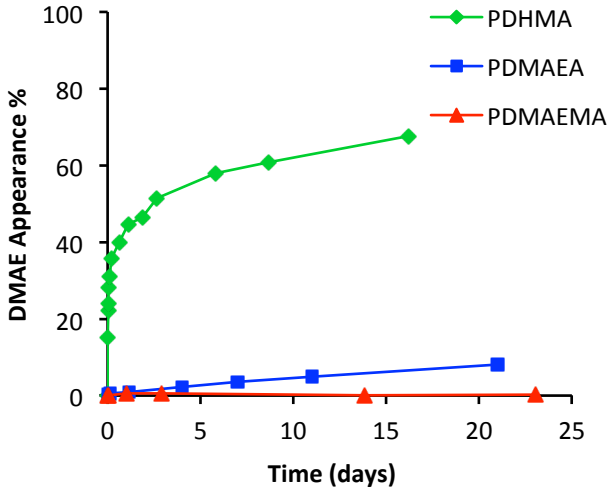

Figure 3.7. Hydrolysis of PDHMA, PDMAEA, and PDMAEMA in 100 mM acetate buffer at pH 5, room temperature (22 °C).

The hydrolysis of PDHMA was significantly faster at pH 7 than at pH 5, showing reasonably linear first-order kinetics within the first 80 minutes with half-lives of approximately 0.8 and 5 hours at pH 7 and 5, respectively (Figure 3A.17), about 350 and 770 times shorter than corresponding values for PDMAEA (Figure 3A.18). It should be noted that first-order analysis of PDHMA hydrolysis at pH 7 is conducted at a later stage

of degradation, relative to the analysis of PDMAEA, due to the rapid nature of its degradation. This high reactivity of PDHMA ester groups at pH of 5 suggests that the electrophilicity has increased significantly due to the presence of the α-hydroxymethyl group, increasing the efficiency of water molecules acting as nucleophiles. It is not clear at this point if this involves simply increased polarity around the ester due to the hydroxymethyl groups, or indeed specific activation of the carbonyl via a 6-membered ring hydrogen-bonding (Figure 3.1**A**). FT-IR analysis of neat DHMA indeed supported hydrogen-bonding interactions of the ester with the hydroxymethyl group as the C=O stretch was observed at a lower wavenumber at 1711 cm^{-1} relative to methyl acrylate control at 1725 cm^{-1} (Figure 3A.19). The C=O stretch of MHMA, a simplified hydroxymethyl acrylate monomer, also appeared at a lower wavenumber at 1712 cm^{-1} (Figure 3A.19), further suggesting hydrogen-bonding interactions.

In agreement with prior results, hydrolysis of PDMAEMA was much slower at pH 5 and 7 relative to PDHMA and PDMAEA, which can be attributed to the crowded and hydrophobic methacrylate backbone.[6] The hydrolysis of PDMAEMA was monitored 1 year later and still showed little to no hydrolysis (<3 %), highlighting the stability of the methacrylate backbone.

These results clearly indicate that the presence of the α-hydroxymethyl substituent on the polymer backbone dramatically increases the rate of 2-(dimethylamino)ethyl ester degradation. Obtaining data points between 0 and 40 % degradation at pH 7 was difficult as the time required for dissolving the sample in the D_2O buffer solution and preparing the NMR sample became limiting factors. ^1H NMR spectra of the polymers obtained in

DMSO-*d6* showed no appearance of small-molecule DMAE, confirming that PDHMA in the ammonium chloride form was stable in non-protic solvents at room temperature (Figure 3.4).

DMAE appearance in solutions of PDHMA in the free base form may also arise from lactonization (Figure 3.1**B**), as was seen during attempts to polymerize non-protected DHMA in DMSO-*d6*. FT-IR spectroscopy of as-formed PDHMA, and of PDHMA after hydrolyses at pH 5 and 7 for about 16 days, was used to test for the distinct C=O stretch of δ-lactones at about 1768 cm^{-1} (Figure 3A.20).[42] Similarly, cyclic esters such as L-lactide have shown C=O stretches in the range of 1758-1767 cm^{-1}.[43] The absence of a lactone C=O stretch beyond the acyclic esters at 1720 cm^{-1} in all as-formed and hydrolyzed PDHMA suggests that degradation in aqueous solution likely occurs by hydrolysis, and not lactonization (Figure 3.1**B**).

3.4.6. Degradation of P[DHMA-co-DMAEA] Copolymers

P[DHMA-*co*-DMAEA] copolymers containing 19, 37, 50, and 78 mol% DHMA were prepared and the hydrolyses at pH 7 and room temperature (22 °C) were monitored by ^{1}H NMR and compared to those of the homopolymers PDHMA and PDMAEA (Figure 3.8).

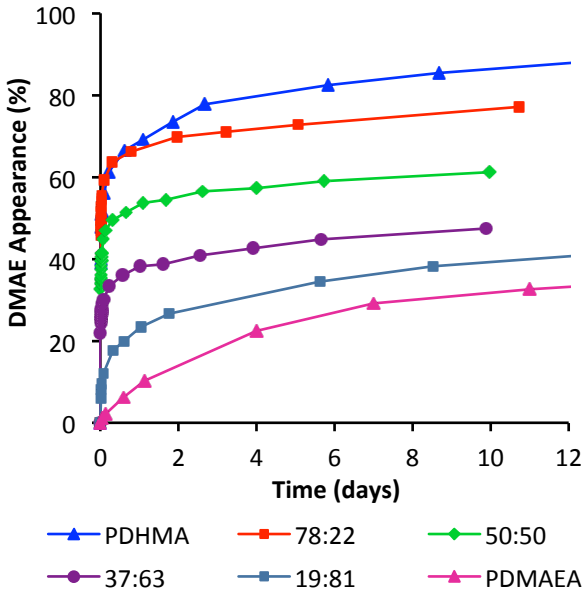

Figure 3.8. Hydrolysis of P[DHMA-*co*-DMAEA] copolymers, PDHMA, and PDMAEA in pH 7 phosphate buffered D_2O at room temperature (22 °C).

The hydrolyses of P[DHMA-*co*-DMAEA] again follow a common trend with a rapid initial rate, followed by a much slower second stage. Similar two-stage rates of hydrolysis have been observed by our group[7] and numerous other researchers[2,6,44-47] for PDMAEA and related polymers. The decrease in rate of hydrolysis of PDMAEA following the initial rapid rate coincides with the formation of anionic acrylate units which may 1) cause a collapse in polymer conformation due to ion-pair formation (isoelectric point), and 2) repel anionic hydroxide ions from attacking remaining DMAE ester groups.[6,7,45,48] In agreement with a recent report, O'Reilly et al. noted that hydrolysis of PDMAEA may only reach a maximum of 60 % based on theoretical calculations by Higuchi et al. that indicate the electrostatic repulsion of anionic acrylic acid units of the polymer and hydroxide increases the activation energy of further ester hydrolysis.[45,48] Saveyn et al.

also noted that the charge density of quaternized PDMAEA, as well as solution pH, influenced the hydrolysis kinetics.[2] The increased rate of hydrolysis of PDHMA, and of P[DHMA-*co*-DMAEA] with increasing DHMA mole fraction, is proposed to be due to the following: Since a collapse in polymer conformation due to ion-pair formation creates a hydrophobic environment for remaining ester groups, hydrolysis of PDMAEA is slowed (Figure 3.9**A**). However, as the hydroxymethyl substituents of DHMA units increase the hydrophilicity of the polymer backbone, the polymer may remain partially swollen with water, which allows for hydroxide to attack remaining ester groups (Figure 3.9**B**).

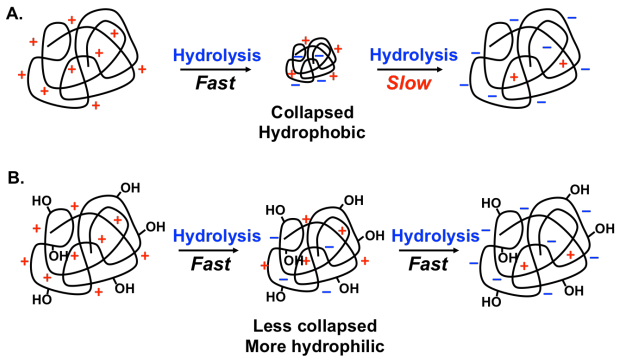

Figure 3.9. Illustration of PDMAEA (**A**) and PDHMA (**B**) representative polymer conformations throughout the hydrolysis at pH 7.

Furthermore, the hydroxymethyl substituent of DHMA units may activate the ester groups *via* a 6-membered ring hydrogen-bonding interaction, which would allow weaker nucleophiles such as water to attack DMAE esters as suggested above in the results obtained for PDHMA hydrolysis at pH 5. Thus, the rate of hydrolysis of DMAE ester groups in PDHMA and in P[DHMA-*co*-DMAEA] copolymers increased with increasing DHMA mole fraction. The effect of the hydroxymethyl substituent and the marked

increase in the rate of hydrolysis is further highlighted as DMAE ester groups of the methacrylate polymer, PDMAEMA, are much more stable (less than 3 % hydrolysis after 2 weeks) with a more hydrophobic and sterically hindering methyl group as the α-substituent on the polymer backbone. These results indicate that the rate of hydrolysis of DMAE esters can be tuned by varying the amount of hydroxymethyl substituents on the polymer backbone, by simply changing the monomer feed ratios to target the desired polymer composition.

3.4.7. Effect of MOM-ether Protecting Group and Molecular Weight on Degradation

During the synthesis of PMOM-DHMA, it was noticed that the polymer was indeed water soluble and stable in aqueous solution at pH 3-4. The degradation of PMOM-DHMA was also attempted in 100 mM acetate buffer at pH 5, and ^{1}H NMR analysis showed that even after 4.5 months, less than 6 % of small molecule DMAE was observed (Figure 3A.21). The stability of PMOM-DHMA is in stark contrast relative to PDHMA, and is a further indication that the free hydroxymethyl substituent is indeed responsible for the very reactive nature of PDHMA.

Deprotection of PMOM-DHMA yielded PDHMA of higher MW at about 6,000 g/mol. The degradation of PDHMA-6k at pH 5 and 7 was monitored by ^{1}H NMR under the same conditions as PDHMA-1k, and the results are shown in Figure 3.10.

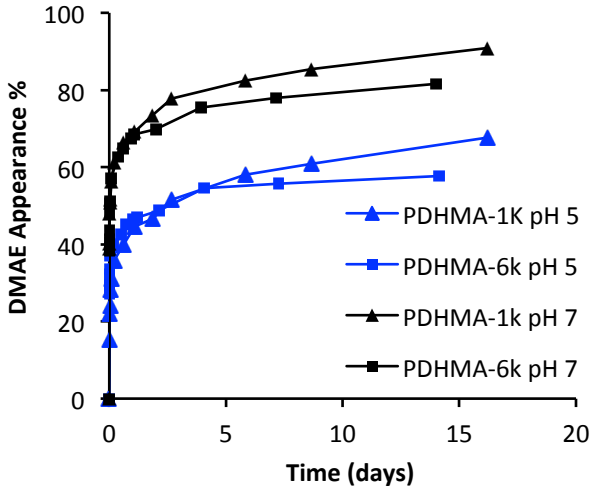

Figure 3.10. Effect of molecular weight on the degradation of PDHMA in 100 mM acetate buffer at pH 5 and 100 mM phosphate buffer at pH 7, room temperature.

The degradation rates of PDHMA-6k and PDHMA-1k at pH 7 and pH 5 appeared to be quite similar, following the same trend of rapid initial rate, followed by a slower second stage as mentioned above. At both pH, degradation of PDHMA-6k after the initial rapid rate appeared slightly slower than the lower molecular weight polymer, however the differences are not significant at less than 10 %. These results are in agreement with previous research that found the hydrolysis of analogous PDMAEA to be independent of molecular weight in the range of 3,000 to 8,600 g/mol.[49]

MOM-ether protected DHMA allowed for the synthesis of higher MW PDHMA homopolymer, and may certainly be used in copolymerizations to synthesize multifunctional and degradable polymers for biomaterial applications.

3.5. Conclusions

The synthesis of DHMA, a novel analogue of DMAEA and DMAEMA, was successfully synthesized by the Baylis-Hillman reaction and protected to form a stable monomer. TES-DHMA was homo- and copolymerized by photo-initiated conventional free radical polymerization. Reactivity ratios of TES-DHMA and DMAEA were determined to be 0.37 and 0.68, respectively, indicating a preferential incorporation of DMAEA. The hydrolysis of PDHMA revealed that the hydroxymethyl substituent played an instrumental role in increasing the rate of DMAE ester hydrolysis, possibly by 6-membered ring hydrogen-bonding of the ester carbonyl, as well as increasing the general hydrophilicity of the polymer backbone. MOM-DHMA was synthesized as a less bulky analogue to form higher MW polymer and the hydrolysis of PDHMA appeared to be independent of molecular weight between 1,000 and 6,000 g/mol. The results obtained for the hydrolysis of PDHMA, PDMAEA, and PDMAEMA, suggests that the hydration of the polymer backbone is key in the reactivity of DMAE esters. The hydrolyses of PDHMA and PDMAEA were much faster than those of PDMAEMA, due to the hydrophobic nature of a methacrylate polymer backbone that protects the ester linkages. The hydrolysis of PDHMA was much faster than PDMAEA due to the α-hydroxymethyl substituents on the polymer backbone, which provided a more hydrophilic environment, as well as possibly activation of the ester carbonyl *via* 6-membered ring hydrogen-bonding, resulting in a more labile and reactive ester.

Supporting Information

^{1}H NMR spectra of PDMAEA, PDMAEMA, TBS-DHMA, TES-DHMA, TMS-DHMA, PMOM-DHMA, P[DHMA-*co*-DMAEA] copolymers, PDHMA hydrolysis with sample calculation, DHMA Baylis-Hillman reaction mixture, and PMOM-DHMA hydrolysis; Experimentally obtained F_1/f_1 values; First-order kinetic plots for PDHMA and PDMAEA at pH 5 and 7; FT-IR spectra of DHMA, MHMA, methyl acrylate, PDHMA, and PDHMA after degradation.

Author Information

Corresponding Author

*E-mail: stoverh@mcmaster.ca, Ph.: 1-905-525-9140 ext. 24983.

Notes:

The authors declare no competing financial interest.

3.6. Acknowledgements

The authors are grateful for funding support from the Canada Foundation for Innovation and the Natural Sciences and Engineering Research Council of Canada Discovery Grant (RGPIN89661-11) and CREATE program (CREATE398058-11). S. R. thanks the late Gregory Bahun for useful discussions on protecting group chemistry.

3.7. References

[1] Bolto, B.; Gregory, J. Organic Polyelectrolytes in Water Treatment. *Water Res*. **2007**, *41*, 2301-2324.

[2] Saveyn, H.; Hendrickx, P. M. S.; Dentel, S. K.; Martins, J. C.; Van der Meeren, P. Quantification of hydrolytic charge loss of DMAEA-Q-based polyelectrolytes by proton NMR spectroscopy and implications for colloid titration. *Water Res*. **2008**, *42*, 2718 – 2728.

[3] Wever, D. A. Z.; Picchioni, F.; Broekhuis, A. A. Polymers for enhanced oil recovery: A paradigm for structure–property relationship in aqueous solution. *Prog. Polym. Sci.* **2011**, *36*, 1558-1628.

[4] Peyratout, C. S.; Dähne, L. Tailor-Made Polyelectrolyte Microcapsules: From Multilayers to Smart Containers. *Angew. Chem. Int. Ed*. **2004**, *43*, 3762–3783.

[5] Agarwal, S.; Zhang, Y.; Maji, S.; Greiner, A. PDMAEMA based gene delivery materials. *MaterialsToday* **2012**, *15*, 388-393.

[6] van de Wetering, P.; Zuidam, N. J.; van Steenbergen, M. J.; van der Houwen, O. A. G. J.; Underberg, W. J. M.; Hennink, W. E. A Mechanistic Study of the Hydrolytic Stability of Poly(2-(dimethylamino)ethyl methacrylate). *Macromolecules* **1998**, *31*, 8063-8068.

[7] Ros, S.; Burke, N. A. D.; Stöver, H. D. H. Synthesis and Properties of Charge-Shifting Polycations: Poly[3-aminopropylmethacrylamide-*co*-2-(dimethylamino)ethyl acrylate]. *Macromolecules* **2015**, *48*, 8958−8970.

[8] Luten, J.; van Nostrum, C. F.; De Smedt, S. C.; Hennink, W. E. Biodegradable polymers as non-viral carriers for plasmid DNA delivery. *J. Controlled Release* **2008**, *126*, 97–110.

[9] Luten, J.; Akeroyd, N.; Funhoff, A.; Lok, M. C.; Talsma, H.; Hennink, W. E. Methacrylamide Polymers with Hydrolysis-Sensitive Cationic Side Groups as Degradable Gene Carriers. *Bioconjugate Chem.* **2006**, *17*, 1077−1084.

[10] Jiang, X.; Lok, M. C.; Hennink, W. E. Degradable-Brushed pHEMA–pDMAEMA Synthesized via ATRP and Click Chemistry for Gene Delivery. *Bioconjugate Chem.* **2007**, *18*, 2077–2084.

[11] Sinclair, A.; Bai, T.; Carr, L. R.; Ella-Menye, J. R.; Zhang, L.; Jiang, S. Engineering Buffering and Hydrolytic or Photolabile Charge Shifting in a Polycarboxybetaine Ester Gene Delivery Platform. *Biomacromolecules* **2013**, *14*, 1587-1593.

[12] Hu, X.; Feeney, M. J.; McIntosh, E.; Mullahoo, J.; Jia, F.; Xu, Q. Thomas III, S. W. Triggered Release of Encapsulated Cargo from Photoresponsive Polyelectrolyte Nanocomplexes. *ACS Appl. Mater. Interfaces* **2016**, *8*, 23517−23522.

[13] Lynn, D. M.; Langer, R. Degradable Poly(β-amino esters): Synthesis, Characterization, and Self-Assembly with Plasmid DNA. *J. Am. Chem. Soc*. **2000**, *122*, 10761-10768.

[14] Zhang, J.; Lynn, D. M. Ultrathin Multilayered Films Assembled from "Charge-Shifting" Cationic Polymers: Extended, Long-Term Release of Plasmid DNA from Surfaces. *Adv. Mater*. **2007**, *19*, 4218-4223.

[15] Vazquez, E.; Dewitt, D. M.; Hammond, P. T.; Lynn, D. M. Construction of Hydrolytically-Degradable Thin Films via Layer-by-Layer Deposition of Degradable Polyelectrolytes. *J. Am. Chem. Soc.* **2002**, *124*, 13992-13993.

[16] Sun, B.; Lynn, D. M. Release of DNA from polyelectrolyte multilayers fabricated using 'charge-shifting' cationic polymers: Tunable temporal control and sequential, multi-agent release. *J. Controlled Release* **2010**, *148*, 91-100.

[17] Truong, N. P.; Jia, Z.; Burges, M.; Payne, L.; McMillan, N. A. J.; Monteiro, M. J. Self-Catalyzed Degradable Cationic Polymer for Release of DNA. *Biomacromolecules*, **2011**, *12*, 3540-3548.

[18] Truong, N. P.; Gu, W.; Prasadam, I.; Jia, Z.; Crawford, R.; Xiao, Y.; Monteiro, M. J. An influenza virus-inspired polymer system for the timed release of siRNA. *Nat. Commun.* **2013**, 4:1902. Doi: 10.1038/ncomms2905

[19] Tran, N. T. D.; Jia, Z.; Truong, N. P.; Matthew A. Cooper, M. A.; Monteiro, M. J. Fine Tuning the Disassembly Time of Thermoresponsive Polymer Nanoparticles. *Biomacromolecules* **2013**, *14*, 3463−3471.

[20] You, Y.Z.; Manickam, D. S.; Zhou, Q. H.; Oupický, D. Reducible poly(2-dimethylaminoethyl methacrylate): Synthesis, cytotoxicity, and gene delivery activity. *J. Controlled Release* **2007**, *122*, 217-225.

[21] Ho, H. T.; Pascual, S. P.; Montembault, V.; Casse, N.; Fontaine, L. Innovative well-defined primary amine-based polyacrylates for plasmid DNA complexation. *Polym. Chem.* **2014**, *5*, 5542-5545.

[22] Ho, H. T.; Le Bohec, M.; Frémaux, J.; Piogé, S.; Casse, N.; Fontaine, L.; Pascual, S. Tuning the Molar Composition of "Charge-Shifting" Cationic Copolymers Based on 2-(N,N-Dimethylamino)Ethyl Acrylate and 2-(tert-Boc-Amino)Ethyl Acrylate. *Macromol. Rapid Commun*. **2017**, DOI: 10.1002/marc.201600641

[23] Dai, F.; Sun, P.; Liu, Y.; Liu, W. Redox-cleavable star cationic PDMAEMA by arm-first approach of ATRP as a nonviral vector for gene delivery. *Biomaterials* **2010**, *31*, 559–569.

[24] Mathias, L. J.; Kusefoglu, S. H.; Kress, A. O. Functional Methacrylate Monomers. Simple Synthesis of Alkyl α-(Hydroxymethyl)acrylate. *Macromolecules* **1987**, *20*, 2326-2328.

[25] Avci, D.; Kusefoglu, S. H.; Thompson, R. D.; Mathias, L. J. Ester Derivatives of α-Hydroxymethylacrylates: ltaconate Isomers Giving High Molecular Weight Polymers. *J. Polym. Sci. Part A: Polym. Chem.* **1994**, *32*, 2937-2945.

[26] Mathias, L. J.; Thigpen, K.; Avci, D. Superfast Methacrylate Photomonomers: Ester Derivatives of Ethyl α-Hydroxymethacrylates. *Macromolecules* **1995**, *28*, 8872-8874.

[27] Avci, D.; Mathias, L. J.; Thigpen, K. Photopolymerization Studies of Alkyl and Aryl Ester Derivatives of Ethyl α-Hydroxymethylacrylate. *J. Polym. Sci. Part A: Polym. Chem.* **1996**, *34*, 3191-3201.

[28] Thompson, R. D.; Barclay, T. B.; Basu, K. R.; Mathias, L. J. Facile Synthesis and Polymerization of Ether Substituted Methacrylates. *Polym. J.* **1995**, *27*(4), 325-338.

[29] Mathias, L. J.; Thompson, R. D.; Michalovic, M. A new polymer with a lower critical solution temperature: poly(α-methoxymethyl acrylic acid). *Polymer* **1998**, *39*(12), 2693-2695.

[30] Avci, D.; Mathias, L. J. Examples of new synthetic routes to pendant ester-ether derivatives of α-hydroxymethylacrylate polymers. *Polymer Bulletin* **1996**, *36*, 133-140.

[31] Peng, C.; Joy, A. Baylis−Hillman Reaction as a Versatile Platform for the Synthesis of Diverse Functionalized Polymers by Chain and Step Polymerization. *Macromolecules* **2014**, *47*, 1258−1268.

[32] Peng, C.; Joy, A. Self-Emulsion Polymerization of Baylis–Hillman-Derived α-Hydroxymethyl- Substituted Acrylates. *J. Polym. Sci. Part A: Polym. Chem.* **2015**, *53*, 1743–1747.

[33] Morita, K.; Suzuki, Z.; Hirose, H. A Tertiary Phosphine-catalyzed Reaction of Acrylic Compounds with Aldehydes. *Bull. Chem. Soc. Jpn*. **1968**, *41*, 2815-2816.

[34] Baylis, A. B.; Hillman, M. E. D. German Patent 2155113, **1972**.

[35] Basavaiah, D.; Rao, A. J.; Satyanarayana, T. Recent Advances in the Baylis−Hillman Reaction and Applications. *Chem. Rev*. **2003**, *103*, 811-891.

[36] Hanessian, S.; Delorme, D.; Dufresne, Y. Mild Cleavage of Methoxymethyl (MOM) Ethers with Trimethylsilyl Bromide. *Tetrahedron Letters* **1984**, *25*(24), 2515-2518.

[37] Turki, T.; Villiéras, J.; Amri, H. An efficient synthesis of alkyl α-(hydroxymethyl)acrylates induced by DABCO in an aqueous medium. *Tetrahedron Letters* **2005**, *46*, 3071-3072.

[38] Roman, J. S.; Madruga, E. L.; Lavia, M. A. Stereochemical Configuration of Poly(methy1 α-benzylacrylate) Synthesized by Radical Polymerization. *Macromolecules* **1984**, *17*, 1762-1764.

[39] Madruga, E. L.; Roman, J. S.; Lavia, M. A.; Monreal, M. C. F. Synthesis and Free Radical Polymerization of Methyl α-Benzylacrylate. *Macromolecules* **1984**, *17*, 989-992.

[40] Stevens, M. P. In *Polymer Chemistry, 3rd ed.*; Oxford University Press, New York, 1999; p 193-194.

[41] Hermann, C.; Pais, G. C. G.; Geyer,A.; Kuhnerta, S. M.; Maier, M. E. Total Synthesis of Hapalosin and Two Ring Expanded Analogs. *Tetrahedron* **2000**, *56*, 8461-8471.

[42] Tucker-Schwartz, A. K.; Garrell, R. L. Simple Preparation and Application of TEMPO-Coated Fe_3O_4 Superparamagnetic Nanoparticles for Selective Oxidation of Alcohols. *Chem. Eur. J.* **2010**, *16*, 12718–12726.

[43] Meaurio, E.; Lopez-Rodriguez, N.; Sarasua, J. R. Infrared Spectrum of Poly(L-lactide): Application to Crystallinity Studies. *Macromolecules* **2006**, *39*, 9291-9301.

[44] Cotanda, P.; Wright, D. B.; Tyler, M.; O'Reilly, R. K. A Comparative Study of the Stimuli-Responsive Properties of DMAEA and DMAEMA Containing Polymers. *J. Polym. Sci., Part A: Polym. Chem.* **2013**, *51*, 3333–3338.

[45] Rolph, M. S.; Pitto-Barry, A.; O'Reilly, R. K. The hydrolytic behavior of N,N'-(dimethylamino) ethyl acrylate-functionalized polymeric stars. *Polym. Chem*. **2017**, *8*, 5060-5070.

[46] McCool, M. B.; Senogles, E.The Self-Catalyzed Hydrolysis of Poly(N,N-dimethylaminoethyl acrylate). *Eur. Polym. J*. **1989**, *25*, 857–860.

[47] Aksberg, R.; Wågberg, L. Hydrolysis of Cationic Polyacrylamides. *J. App. Polym. Sci.* **1989**, *38*, 297-304.

[48] Huguchi, M.; Senju, R. Kinetic Aspects of Alkaline Hydrolysis of Poly(acrylamide). *Polymer J*. **1972**, *3*, 370-377.

[49] Truong, N. P.; Jia, Z.; Burges, M.; McMillan, N. A. J.; Monteiro, M. J. Self-Catalyzed Degradation of Linear Cationic Poly(2-dimethylaminoethyl acrylate) in Water. *Biomacromolecules* **2011**, *12*, 1876–1882.

3.8. Appendix

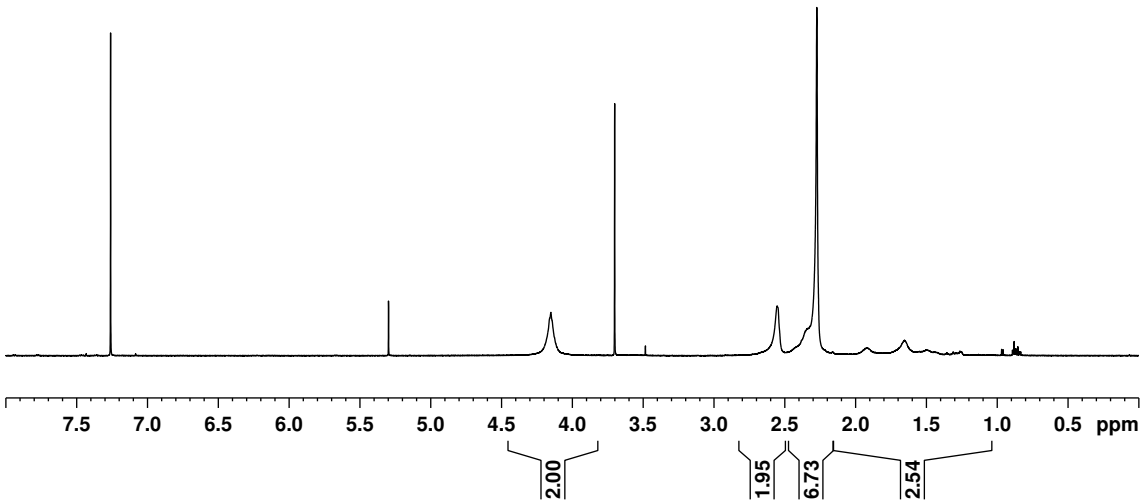

Figure 3A.1. ^{1}H NMR spectrum of PDMAEA in $CDCl_3$ recorded at 600 MHz.

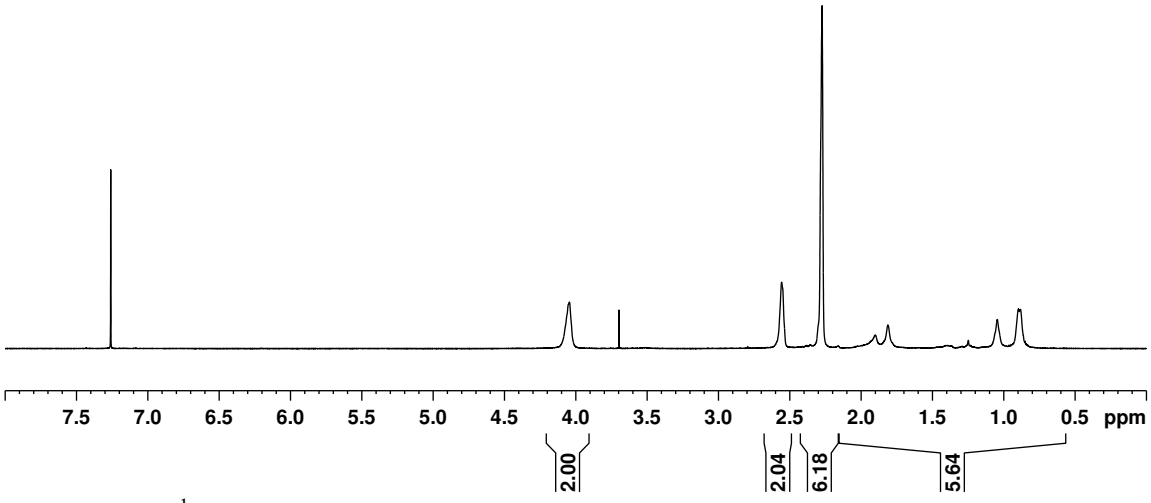

Figure 3A.2. ^{1}H NMR spectrum of PDMAEMA in $CDCl_3$ recorded at 600 MHz.

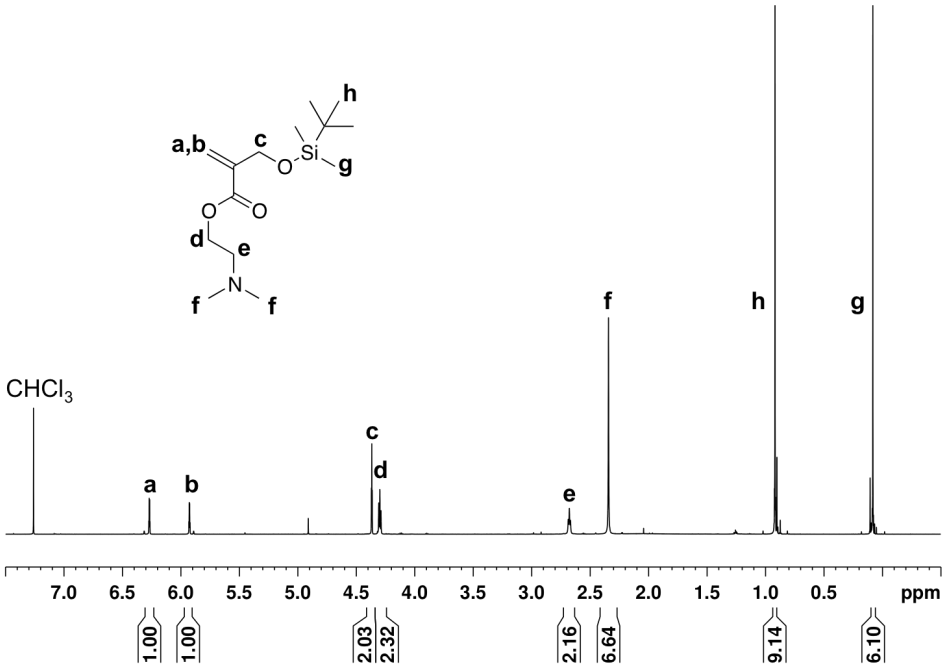

Figure 3A.3. ^{1}H NMR spectrum of TBS-DHMA in $CDCl_3$ recorded at 600 MHz.

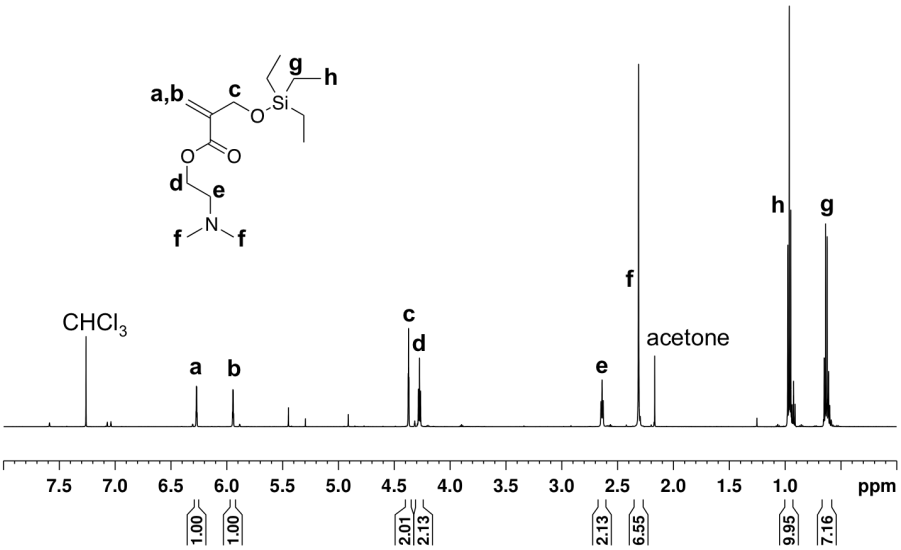

Figure 3A.4. ^{1}H NMR spectrum of TES-DHMA in $CDCl_3$ recorded at 600 MHz.

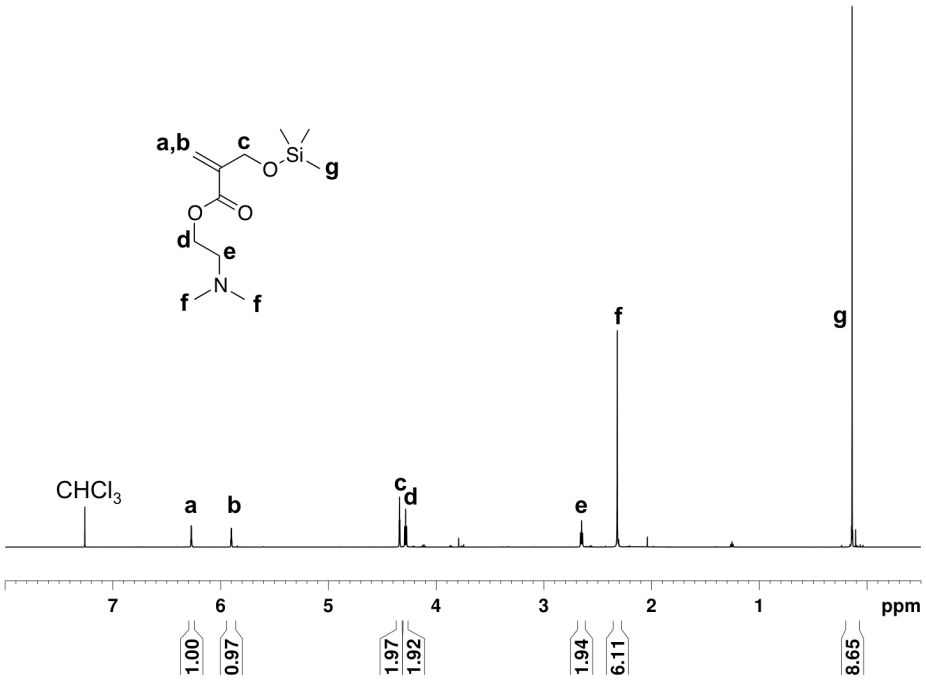

Figure 3A.5. ^{1}H NMR spectrum of TMS-DHMA in $CDCl_3$ recorded at 600 MHz.

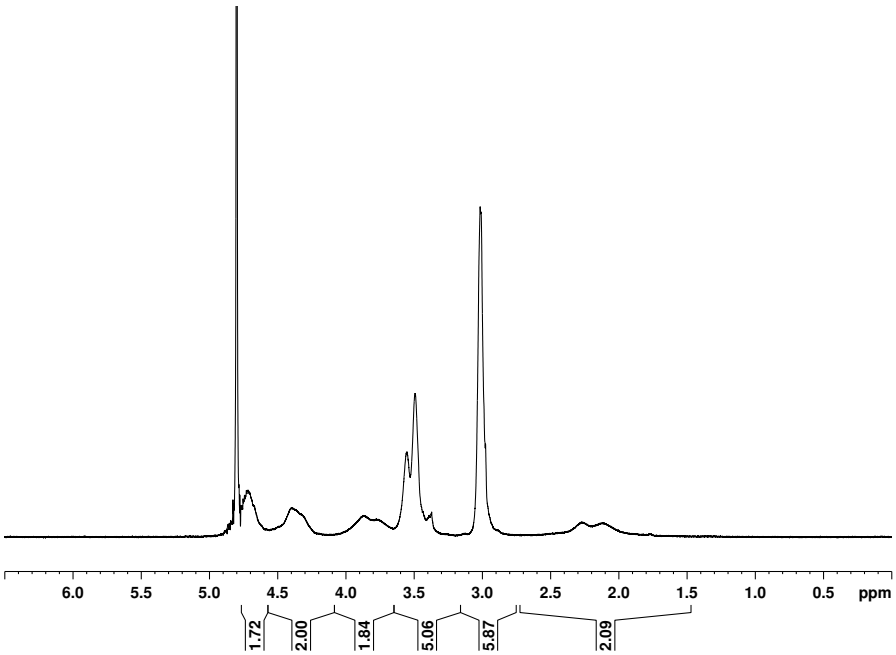

Figure 3A.6. ^{1}H NMR spectrum on PMOM-DHMA in D_2O on a 600 MHz spectrometer

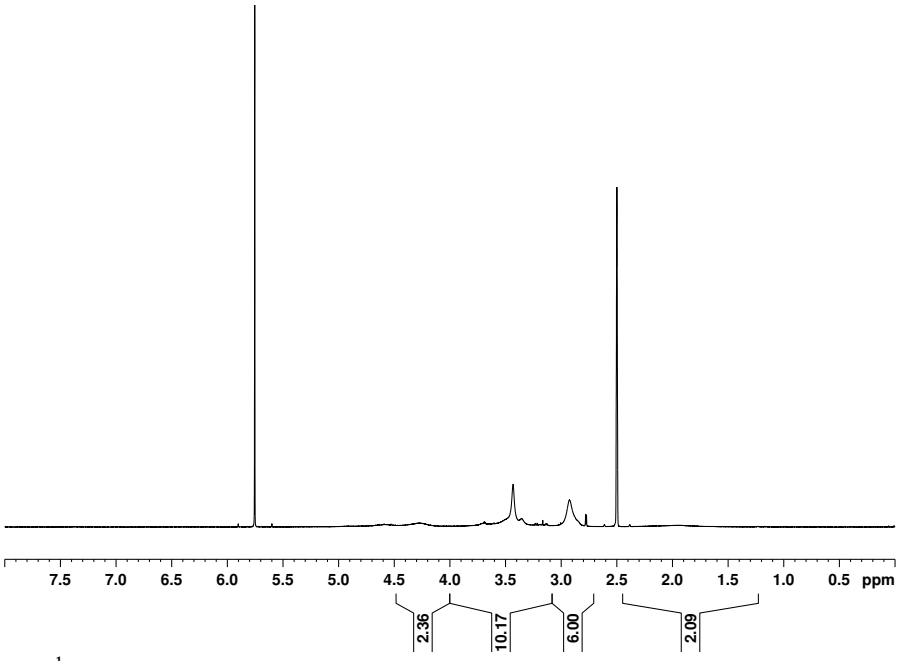

Figure 3A.7. ^{1}H NMR spectrum of PDHMA post MOM-ether deprotection in DMSO-*d6* on a 600 MHz spectrometer.

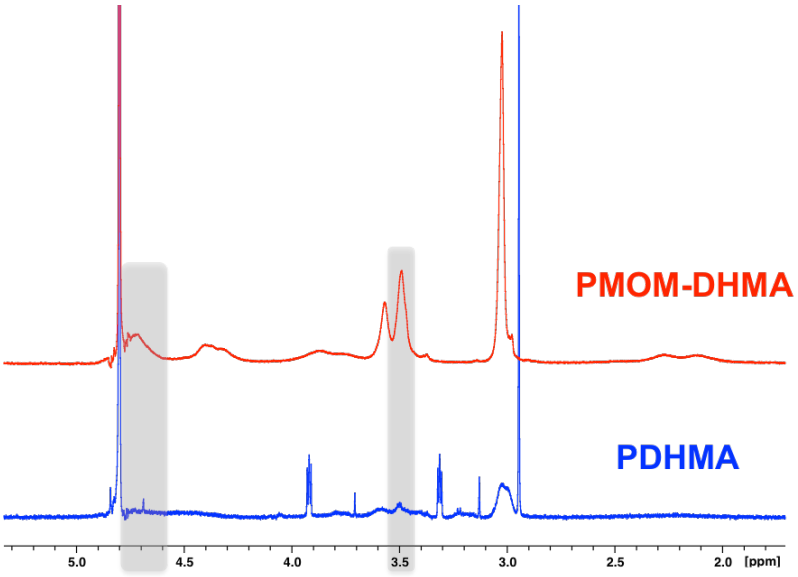

Figure 3A.8. ^{1}H NMR overlay in D_2O of PMOM-DHMA and PDHMA derived from MOM-ether deprotection with TMSBr. PDHMA spectrum showed a disappearance of distinct MOM-ether peaks confirming deprotection. Hydrolysis of the ester was seen by appearance of small molecule DMAE, as expected in D_2O, which does not interfere with the appearance of MOM-ether signals.

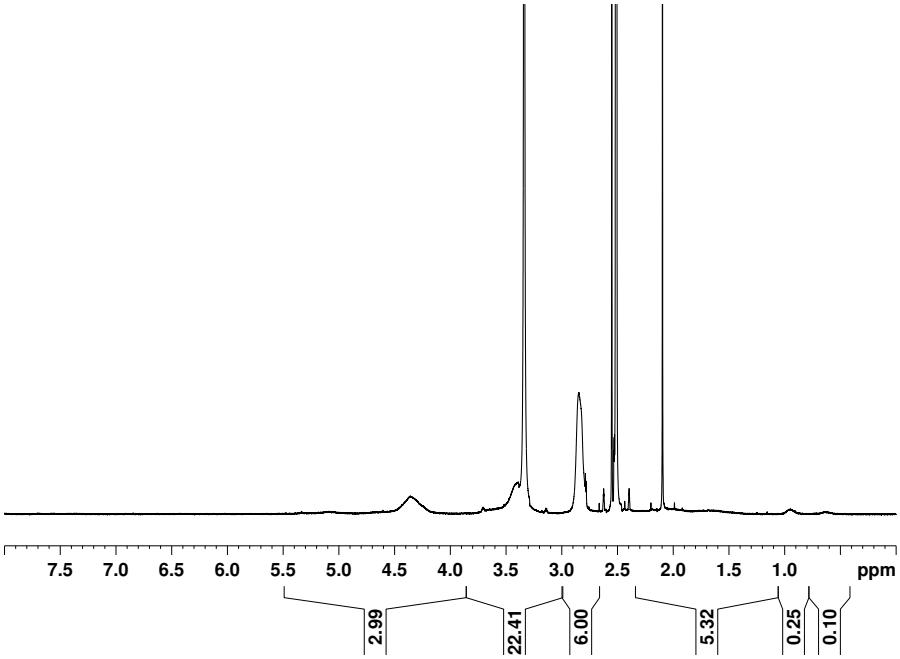

Figure 3A.9. ^{1}H NMR spectrum of 78:22 P[DHMA-*co*-DMAEA] in DMSO-*d6* on a 600 MHz spectrometer.

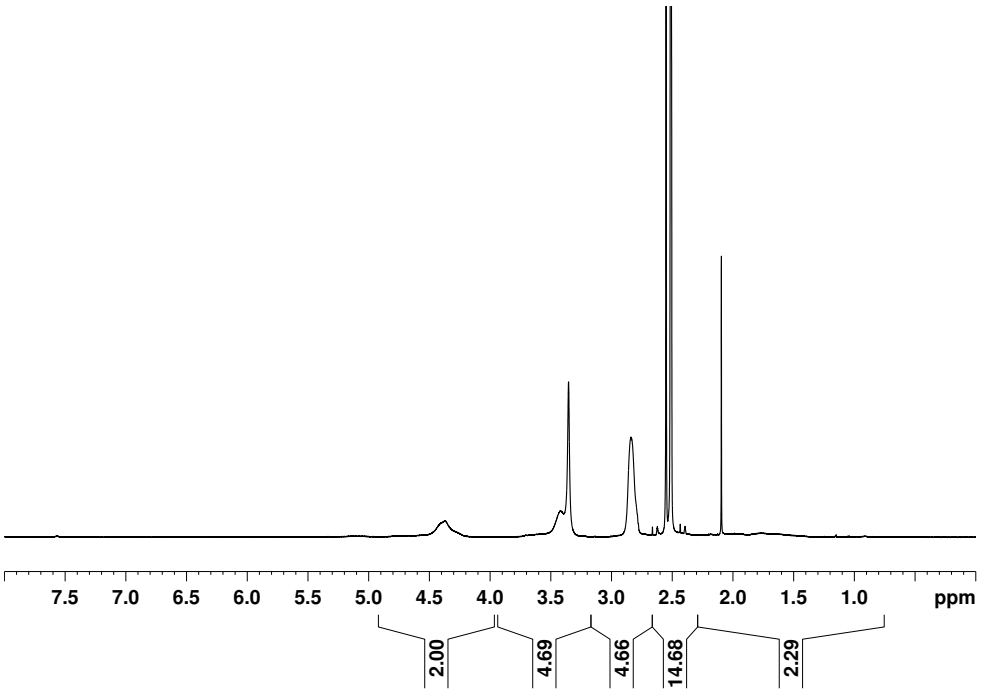

Figure 3A.10. ^{1}H NMR spectrum of 50:50 P[DHMA-*co*-DMAEA] in DMSO-*d6* on a 600 MHz spectrometer.

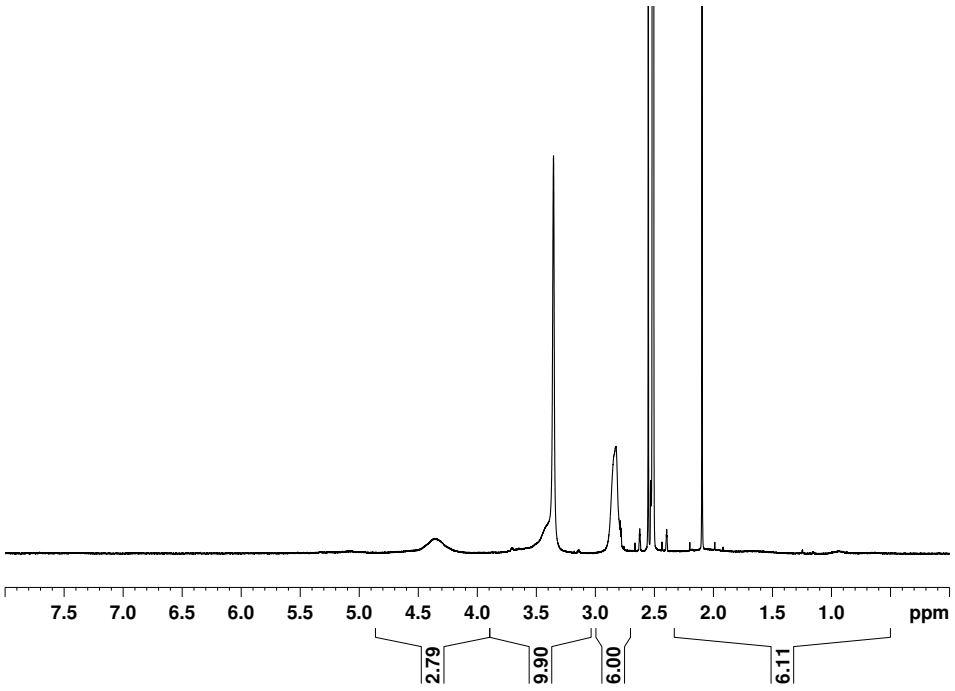

Figure 3A.11. ^{1}H NMR spectrum of 37:63 P[DHMA-*co*-DMAEA] in DMSO-*d6* on a 600 MHz spectrometer.

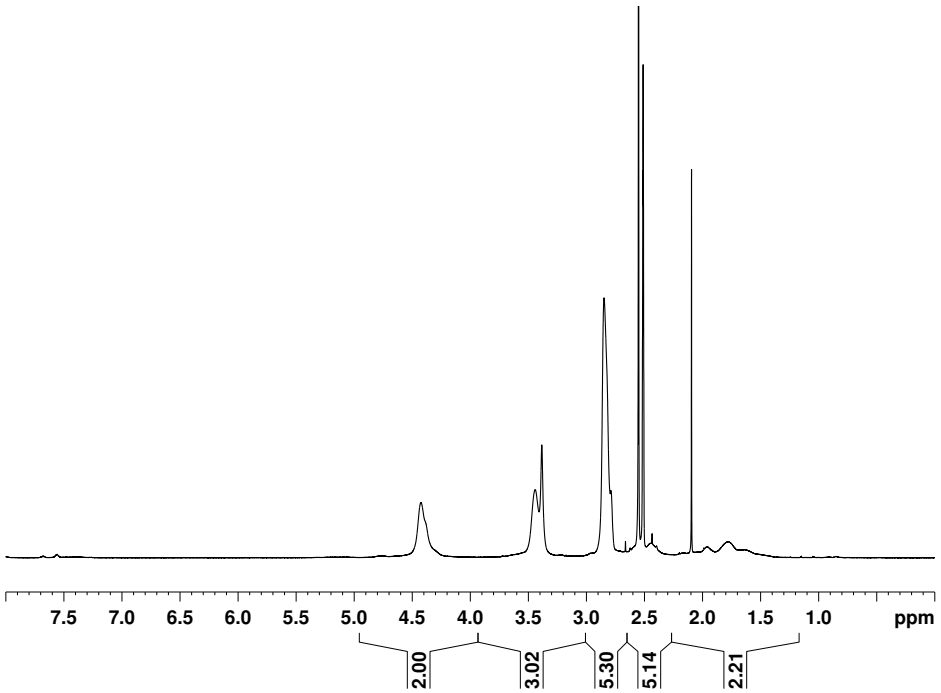

Figure 3A.12. ^{1}H NMR spectrum of 19:81 P[DHMA-*co*-DMAEA] in DMSO-*d6* on a 600 MHz spectrometer.

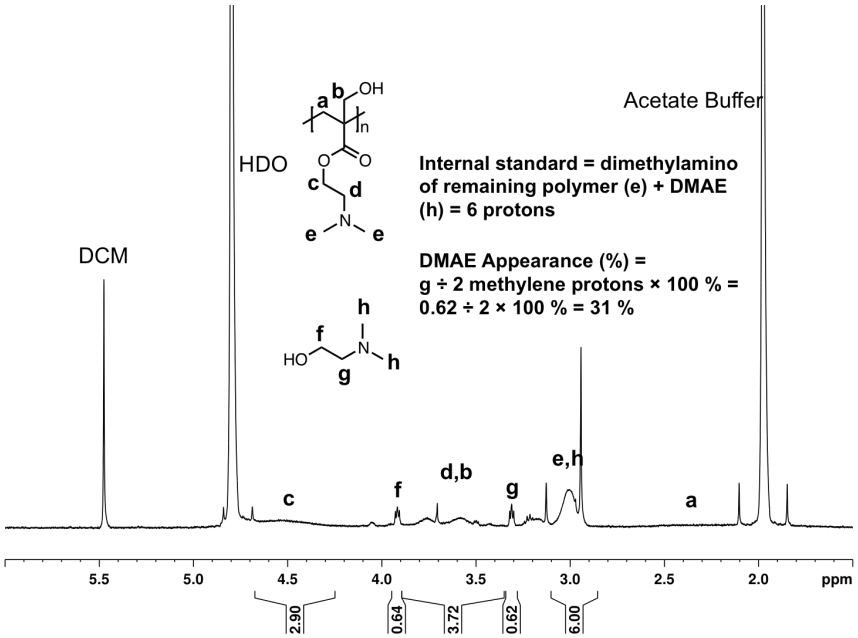

Figure 3A.13. Representative ^{1}H NMR spectrum of PDHMA degradation study in 100 mM acetate buffer in D_2O at pH 5 with sample calculation of DMAE appearance %.

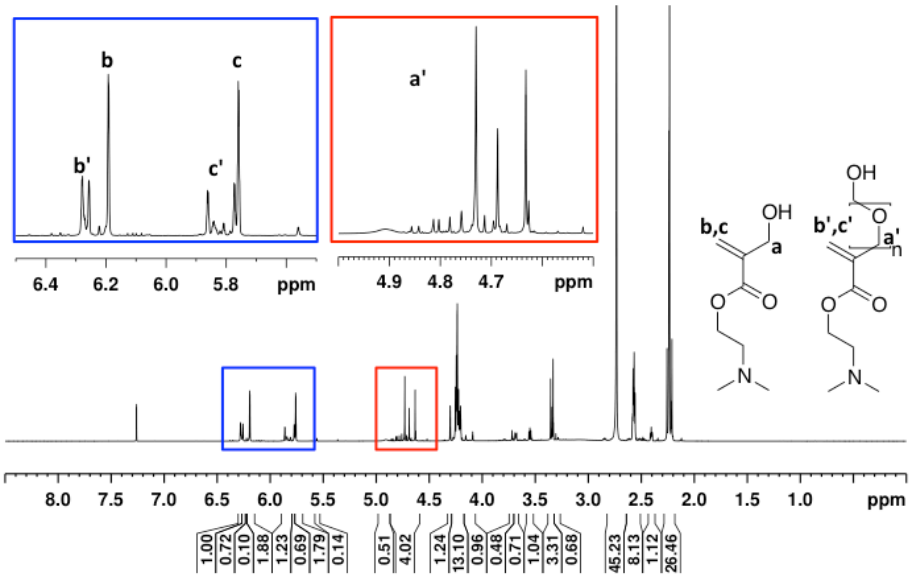

Figure 3A.14. ^{1}H NMR spectrum in $CDCl_3$ of crude reaction mixture of Baylis-Hillman reaction of DHMA after 5 hours at room temperature. Significant oligomerization of formaldehyde was observed, forming poly[oxymethylene] chains. Roughly about 50 % of the product appeared to undergo oligomerization side-reaction.

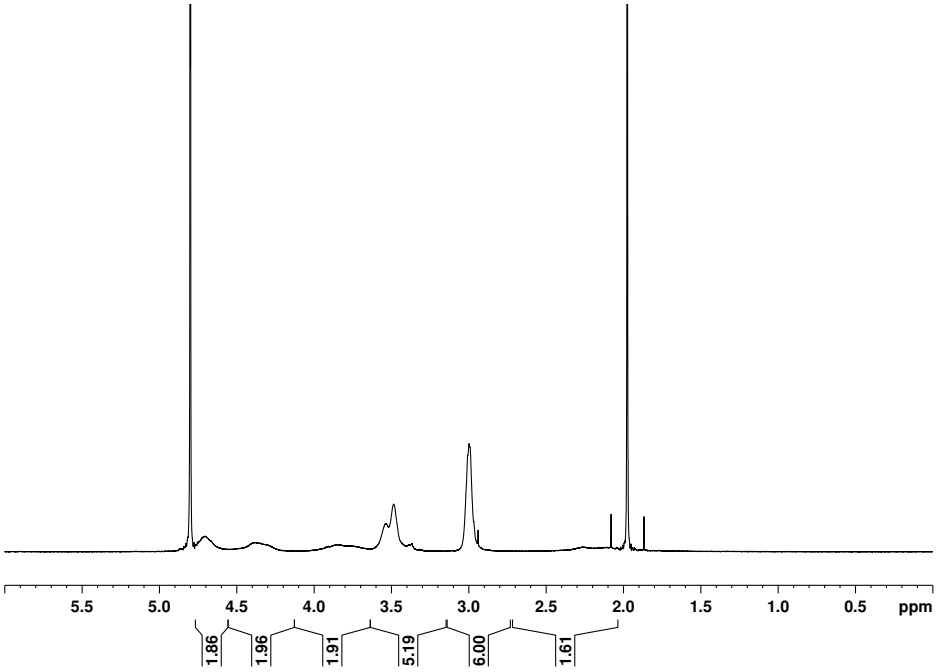

Figure 3A.15. ^{1}H NMR spectrum of PMOM-DHMA after 4 days in D_2O at room temperature on a 600 MHz spectrometer showing little to no DMAE formation.

Table 3A.1. Experimentally obtained F1 and f1 values.

F1, monomer feed	F1, copolymer composition
0.866	0.833
0.868	0.750
0.553	0.519
0.147	0.243
0.877	0.708
0.557	0.500
0.140	0.145
0.889	0.871
0.564	0.486
0.139	0.191
0.334	0.333
0.740	0.621
0.758	0.739
0.891	0.763
0.760	0.602
0.328	0.322
0.775	0.714
0.329	0.317

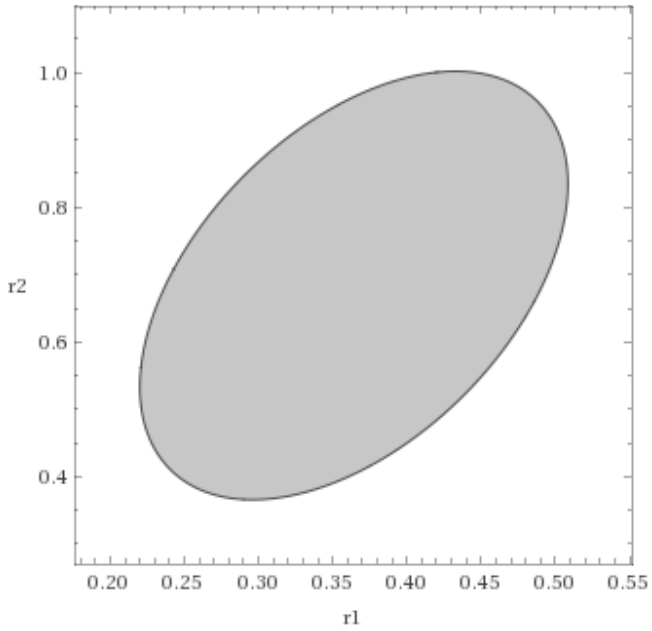

Figure 3A.16. Joint confidence region at 95 % confidence level for reactivity ratios r_1 (TES-DHMA) and r_2 (DMAEA) obtained by a method described by Kitanidis et al.[1]

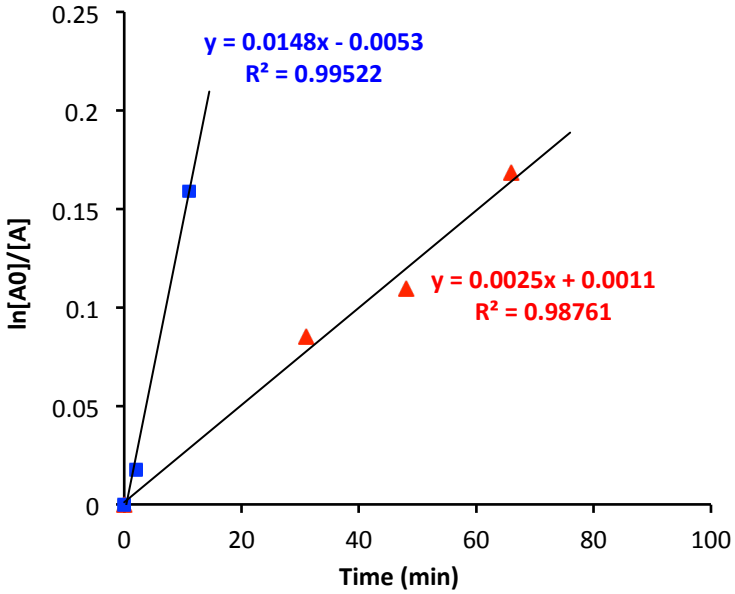

Figure 3A.17. Linear first-order kinetic plots of the initial stages of PDHMA hydrolysis in buffered D_2O solutions at pH 5 (red triangles) and 7 (blue squares), room temperature (22 °C). Analysis for pH 7 covers 39 to 48 % hydrolysis (2^{nd},3^{rd}, and 4^{th} data points in Figure 3.6). Analysis for pH 5 covers 15 to 28 % hydrolysis (2^{nd} to 5^{th} data points in Figure 3.6).

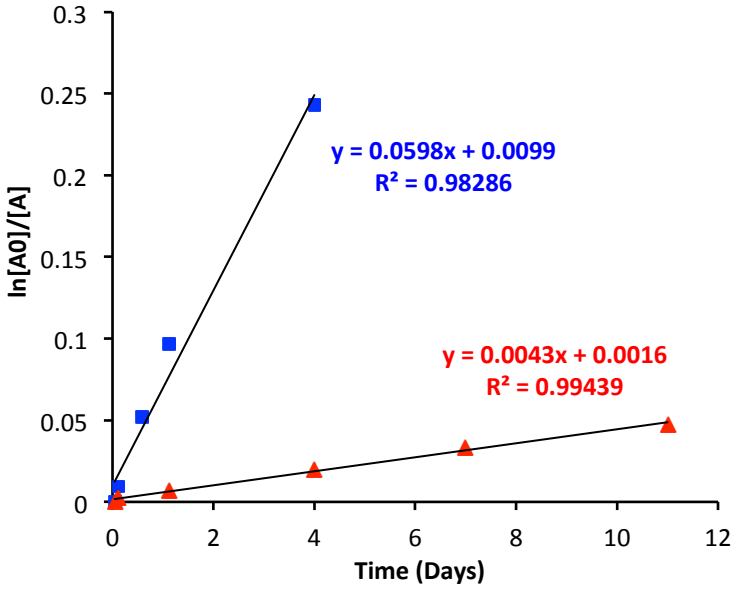

Figure 3A.18. Linear first-order kinetic plots of PDMAEA in buffered D_2O solutions at pH 5 (red triangles) and pH 7 (blue squares), at room temperature (22 °C).

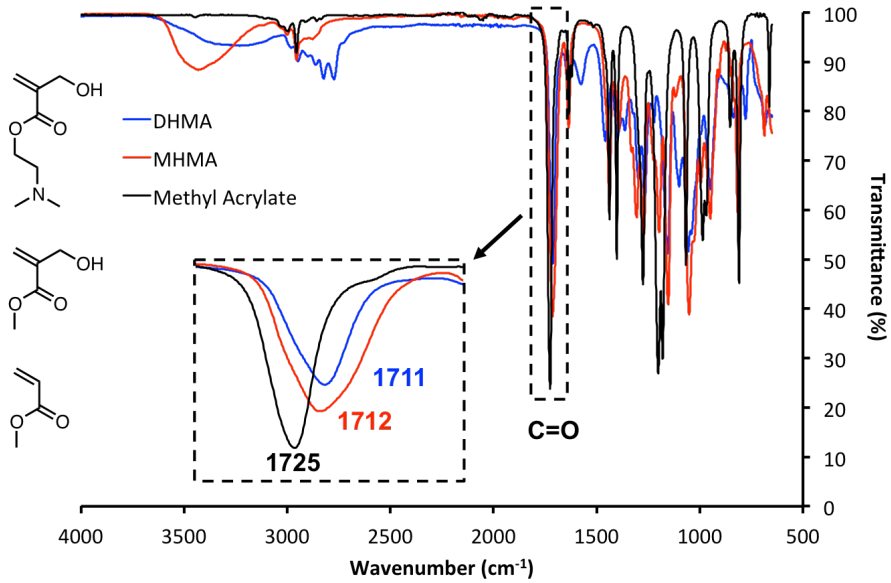

Figure 3A.19. FT-IR spectra of DHMA, MHMA, and methyl acrylate with an inset showing expanded C=O region. C=O stretch of α-hydroxymethyl substituted DHMA and MHMA monomers appeared at a lower wavenumber relative to methyl acrylate due to hydrogen-bonding interaction.

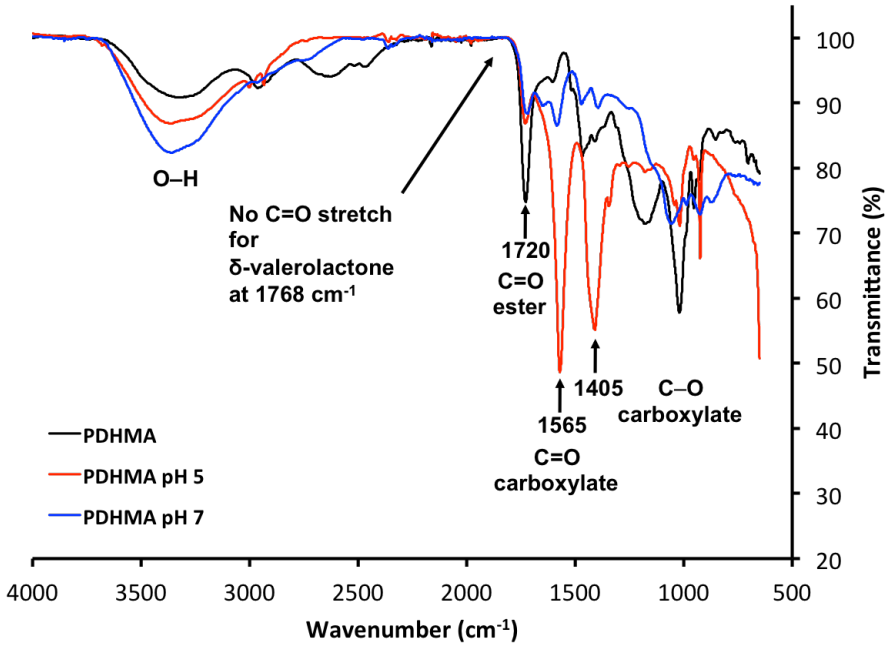

Figure 3A.20. ATR-IR spectra of PDHMA as formed, and after degradation at pH 5 and 7. Lack of C=O stretch of a δ-valerolactone suggests that degradation of PDHMA polymers may not occur by lactonization. IR spectra show carbonyl stretch of DMAE ester groups at 1720 cm^{-1} of PDHMA polymer as formed decrease after hydrolysis at pH 5 and 7.

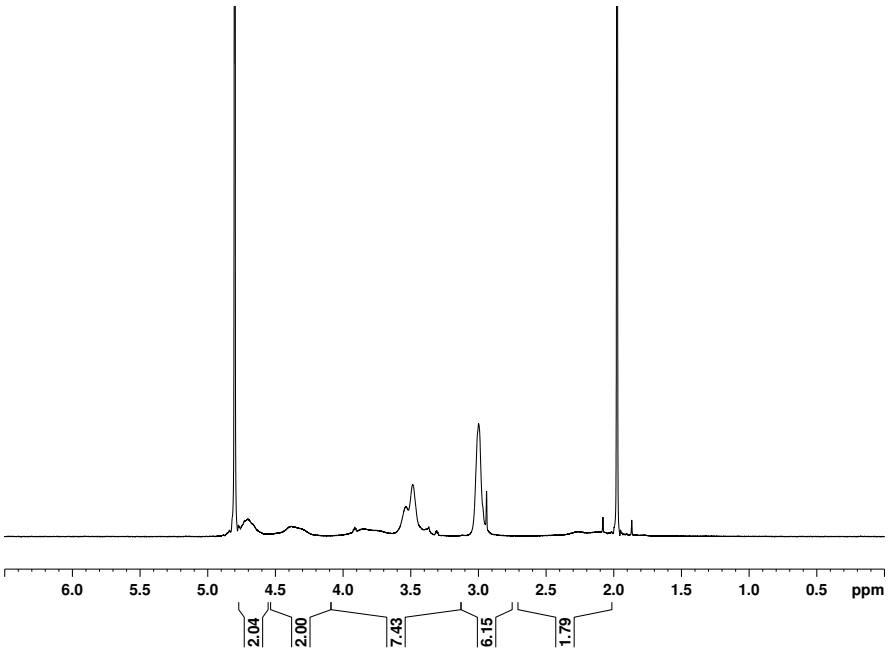

Figure 3A.21. ^{1}H NMR of PMOM-DHMA in 100 mM acetate buffer in D_2O at pH 5, room temperature (22 °C) after 4.5 months.

References

[1] Smith, L. H.; McCarty, P. L., Kitanidis, P. K. Spreadsheet Method for Evaluation of Biochemical Reaction Rate Coefficients and Their Uncertainties by Weighted Nonlinear Least-Squares Analysis of the Integrated Monod Equation. *Applied and Environmental Microbiology* **1998**, *64(6)*, 2044–2050.

CHAPTER 4: Charge-Shifting Polycations based on N,N-(Dimethylamino)ethyl Acrylate for Improving Cytocompatibility During DNA Delivery

Samantha Ros,[a] Jessica S. Freitag,[b] David M. Smith,[b] and Harald D. H. Stöver*,[a]

[a] McMaster University, Hamilton, Ontario, Canada L8S 4L8, Department of Chemistry and Chemical Biology

[b] Fraunhofer Institute for Cell Therapy and Immunology IZI, 04103 Leipzig, Saxony, Germany

For Table of Contents Only

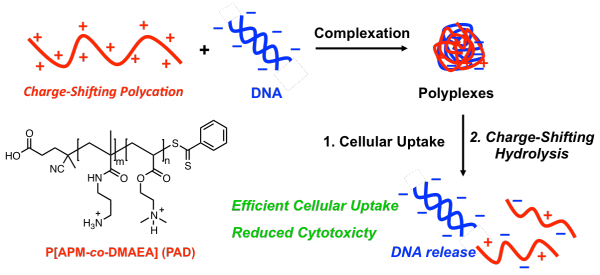

4.1. Abstract

Synthetic polycations are studied extensively as DNA delivery agents due to their ease of production, good chemical stability, and low cost relative to viral vectors. This report describes the synthesis of charge-shifting polycations based on N,N-(dimethylamino)ethyl acrylate (DMAEA) and 3-aminopropylmethacryamide (APM), called PAD copolymers, and their use for *in vitro* DNA delivery into HeLa cells. PAD copolymers of varying composition were prepared by RAFT polymerization to yield

polymers of controlled molecular weights with low dispersities. Model hydrolysis studies were carried out to assess the rate of charge-shifting of the polycations by loss of the cationic dimethylaminoethanol side chains. They showed a reduction in net cationic charge by about 10 to 50 % depending on composition after 2 days at pH 7, forming polyampholytes comprising permanent cationic groups, residual DMAEA, as well as anionic acrylic acid groups. HeLa cells exposed for 4 hours to PAD copolymers with the greatest charge-shifting ability showed comparable or higher viability at high concentrations, relative to the non-charge shifting polycations PAPM and polyethyleneimine (PEI) 2 days post-exposure. Cell uptake efficiency of PAD/60bp-Cy3 DNA polyplexes at 2.5:1 N/P ratio was very high (>95 %) for all compositions, exceeding the uptake efficiency of PEI polyplexes of equivalent composition. These results suggest that these PAD copolymers, and in particular PAD_{80} containing 80 mol% DMAEA, have suitable rates of charge-shifting hydrolysis for DNA delivery, as PAD_{80} showed reduced cytotoxicity at high concentrations, while still retaining high uptake efficiencies. In addition, the polyampholytes formed during DMAEA hydrolysis in PAD copolymers can offer enhanced long-term cytocompatibility.

Keywords: Polycation; Charge-shifting; Hydrolysis; DNA delivery; Polyampholyte

4.2. Introduction

Polycations are used extensively in DNA delivery as non-viral vectors due to their ease of production, stability, and low cost, relative to lipid-based vectors.[1-4] Although

recent research has shown much promise in their ability to deliver nucleic acid payloads, there has been growing interest to develop polycations with further increased transfection efficiency and lower toxicity. Many studies involve probing the effect of various derivatives,[5-7] molecular weight,[8-12] polymer architecture,[8,12-16] and polyplex morphology.[17] Charge-shifting polycations have emerged as a class of polymers attracting significant interest as transfection agents.[18-31] These polymers have high cationic charge densities but undergo a charge-shifting process making the polymer less cationic. The initial high cationic charge density enables efficient binding and protection of anionic nucleic acids from nucleases, forming polyplexes. Following cellular uptake, the polyplexes can dissociate due to the charge-shift of the polycation, releasing the genetic payload for intracellular delivery. Both charge-shifting and reducible polycations based on N,N-(dimethylamino)ethyl (meth)acrylate (DMAE(M)A) have shown promising DNA release capabilities and improved transfection efficiency.[22,23,27,30-32] Further, the cytotoxicity of charge-shifting polycations was lower than that of standard synthetic polycations. This was attributed to the degradation of polymeric cationic charge and the release of byproducts such as dimethylaminoethanol (DMAE) that are non-toxic even at high concentrations.[22,30] The cytotoxicity of polycations has been attributed to their interactions with critical anionic components of the cell including the phospholipid cell membrane and RNA/DNA, as well as their ability to trigger pro-apoptotic and pro-inflammatory signaling.[33,34] Thus, charge-shifting polycations may be a desirable alternative to standard polycations as they can mitigate the accumulation of cytotoxic cationic charges.[22,30,32] Recent findings have demonstrated that polyampholytes showed

similar antifouling properties to zwitterionic polybetaines[35] due their surface hydration[35,36] and have shown promising properties for transfection as the mixed surface charge are reminiscent of certain viruses.[37] Thus, charge-shifting polycations that reduce their cationic charge to polyampholytes may be more cyto-compatible than highly anionic polymers. The extent of cationic charge reduction can be controlled by copolymerization with another cationic monomer that does not undergo hydrolysis. Copolymerization has been used to control charge-shifting hydrolysis in previous studies,[28,30,38,39] providing a useful handle to target such amphoteric materials.

While cellular uptake by different types of endocytosis is reasonably understood, the mechanism of endosomal escape of polyplexes or their DNA payload is still a topic of debate. One of the main theories rests on the "proton-sponge" effect of polycations,[40,41] whereby polyplexes taken up by cells and contained within endosomes are acidified by fusion of endosomes with lysosomes. While the proton-sponge effect is commonly used to explain the mechanism of release in many polycation-mediated transfection systems, this hypothesis has been questioned[42-44] and there is research indicating that endosomal escape of DNA may instead involve diffusion through defects in the endosomal membrane caused by interactions with the polycation.[42,43] The lack of understanding of endosomal escape, including the role of the polycation, further demonstrates a need for new charge-shifting polycations to probe these processes, however these studies will not be included in the current report. The work of this report will focus on the development and study of polycations based on DMAEA and will probe their potential in improving compatibility with cells while maintaining high uptake efficiencies. As for DMAEA

homopolymers previously reported,[22,23] these should degrade into non-toxic byproducts, while retaining high uptake efficiencies.

The effect of charge-shifting hydrolysis on the cytotoxicity in polycation-mediated *in vitro* DNA delivery will be the focus of this study. In this report, we explore charge-shifting polycations based on DMAEA hydrolysis as potential DNA delivery agents with HeLa cells as a model cell line for which toxicity and delivery studies are commonly reported. In particular, poly[3-aminopropylmethacrylamide-*co*-N,N-(dimethylamino)ethyl acrylate] (PAD) copolymers[38] with different mol% of DMAEA were used to study the effect of changing the charge-shifting potential of a series of polycations with constant initial charge density, on cytotoxicity and cellular uptake efficiency (Scheme 1).

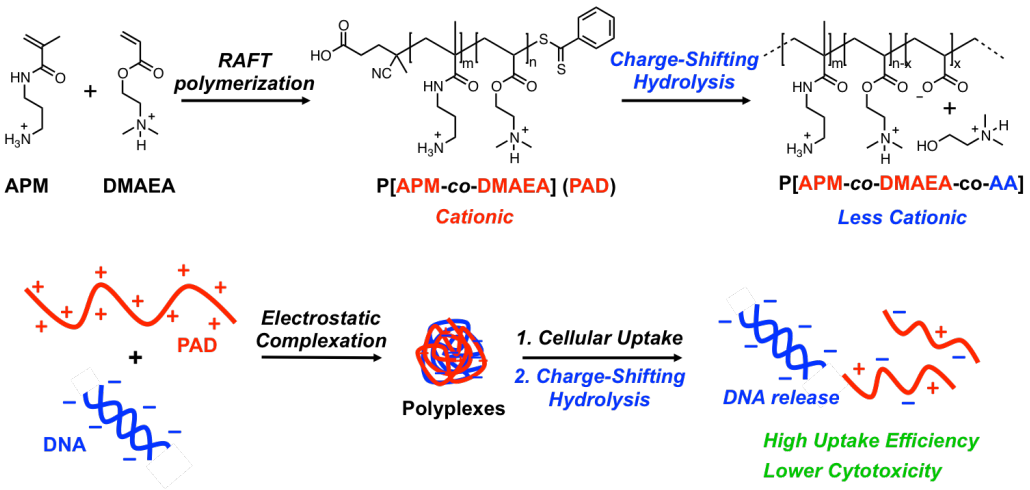

Scheme 4.1. RAFT polymerization of APM and DMAEA to obtain charge-shifting PAD copolymers that undergo hydrolysis with the formation of anionic acrylic acid (AA) units. PAD copolymers, initially highly cationic, complex anionic DNA to form polyplexes. Charge-shifting of PAD copolymers may facilitate intracellular DNA release due to weakening electrostatic interactions. The reduction in net cationic charge may also reduce cytotoxicity.

4.3. Experimental

4.3.1. Materials

N,N-(Dimethylamino)ethyl acrylate (DMAEA, 98 %), 4-cyano-4-(phenylcarbonothioylthio)pentanoic acid (CTP, ≥98 %), 4,4-azobis(4-cyanovaleric acid) (V-501, >97 %), deuterium chloride (DCl, 35 % in D_2O, 99 % D), and WST-1 (Roche) were purchased from Sigma Aldrich and used as received unless otherwise stated. Polyethyleneimine (PEI, branched, 25 kDa) was also purchased from Sigma Aldrich and was fractionated to obtain a lower molecular weight fraction (4–10 kDa) according to a previous report[45] and kindly provided by Susanne Przybylski at Fraunhofer IZI, Leipzig. (3-Aminopropyl)methacrylamide hydrochloride was purchased from PolySciences and was used as received. 1,4-Dioxane (≥99 %) and 12 M HCl aq. solution was purchased from Caledon Laboratories, basic alumina (activity I) from Fisher Scientific, and D_2O (99.9 % D) from Cambridge Isotope Laboratories Inc., and all were used as received. 60nt DNA forward and reverse strands were purchased from Biomers.net GmbH, Germany. Dulbecco's modified eagle medium (DMEM) (4.5 g/L glucose, no sodium pyruvate), Opti-MEM (HEPES, L-glutamine), fetal calf serum (South American origin), and 1x Dulbecco's PBS (DPBS) were purchased from Thermo Fisher Scientific. PE-Annexin V Apoptosis Detection Kit I (BD Pharmingen) was purchased from BD Biosciences.

4.3.2. Synthesis of PAD Copolymers

PAD copolymers of 80, 49, 23 and 0 (PAPM) relative mol% of DMAEA was prepared as described previously.[38] Briefly, reversible addition-fragmentation chain-transfer (RAFT) polymerization of APM and DMAEA was conducted using CTP as the

RAFT agent and V-501 as the initiator, targeting a molecular weight of 30,000 g/mol. In 20 mL screw cap vials, APM and DMAEA feeds of 15:85, 45:55, 75:25, and 100:0 mol ratios (1.8 g total monomer loading) were sequentially dissolved in 6 mL of a 2:1 water:1,4-dioxane solvent mixture with 1.1 mol eq of HCl using a 6 M stock solution added relative to DMAEA. The dissolution of the monomers was carried out in an ice-water bath to remove the heat of neutralization of the monomers and to minimize premature hydrolysis of DMAEA. The reaction mixture was adjusted to pH 3-4 by addition of further HCl prior to the addition of CTP and V-501. Small magnetic stirring bars were added, and the vials capped with septa. The reaction mixture was purged with N_2 gas for 45 min at room temperature with stirring, and then placed in an 80 °C oil bath. The polymerization proceeded until a targeted total monomer conversion of approximately 80 % was reached as confirmed by ^{1}H NMR, which required 1.5 – 2 hours of heating depending on composition. The polymer solutions were dialyzed for 4-5 days against pH 3–4 distilled water using cellulose acetate tubing with a molecular weight cut-off of 3500 g/mol. Purified polymer solutions were freeze-dried, resulting in the polymers as their hydrochloride salt. Typical isolated yields were approximately 70-80 %. ^{1}H NMR spectra of PAD_{80}, PAD_{49}, PAD_{23}, and PAPM in D_2O are shown in Figures 4A.1, 4A.2, 4A.3, and 4A.4, respectively.

4.3.3. NMR Spectroscopy

^{1}H NMR spectra were recorded on a Bruker AV600 or AV500 in D_2O using the residual HDO/H_2O signal at 4.80 ppm as the chemical shift reference.

4.3.4. Gel Permeation Chromatography

Gel permeation chromatography (GPC) of PAD copolymers was conducted using a Waters GPC consisting of a 717plus autosampler, 515 HPLC pump, 2414 refractive index detector, Ultrahydrogel (120, 250, and 500) columns (30 cm × 7.8 mm (inner diameter); 6 μm particles) using poly[ethylene glycol] standards ranging from 106 Da to 881 kDa (Waters Inc.) for a 15-point, third-order polynomial calibration. The mobile phase was a 1 M acetic acid-sodium acetate buffer at pH 4.8.

4.3.5. Model Hydrolysis Studies

PAD copolymers were dissolved in 100 mM phosphate or acetate buffered solutions at pH 7 and 5, respectively, at a concentration of 0.5 wt.%. Samples were maintained at room temperature (22 °C) and ^{1}H NMR spectra were recorded at various time intervals. The pH of the PAD_{80}, PAD_{49}, PAD_{23}, and PAPM of the phosphate buffered solutions just after dissolution were adjusted to pH 7.11, 7.06, 7.14, and 7.15, respectively, prior to analysis. The pH of the PAD_{80}, PAD_{49}, PAD_{23}, and PAPM of the acetate buffered solutions just after dissolution were adjusted to pH 5.03, 5.01, 4.99, and 5.00, respectively, prior to analysis. The pH did not drift significantly (less than 0.09 pH units) after hydrolysis. Hydrolysis percentages were calculated by comparing the integrations of the peaks at 3.9 and 4.5 ppm corresponding to the CH_2O methylene protons of small molecule byproduct DMAE and remaining ester side-chain of the

polymer, respectively. A representative ^{1}H NMR spectrum showing the integration and calculation of percent hydrolysis is shown in Figure 4A.5.

4.3.6. Hybridization of DNA

60nt DNA forward and reverse strands (60nt-fw: 5′-NH2-GCTTTCTTCTCTAAATACATCTTCACGTCGATATCACCATAACTCAGGTAAGG AGGTCAA-3′; 60nt-fw-Cy3: 5′-Cy3-GCTTTCTTCTCTAAATACATCTTCACGTCGATATCACCATAACTCAGGTAAGG AGGTCAA-3′; 60nt-rv: 5′-TTGACCTCCTTACCTGAGTTATGGTGATATCGACGTGAAGATGTATTTAGAGA AGAAAGC-3′) were purchased from Biomers.net GmbH, Germany. Freeze-dried oligonucleotides were dissolved in Millipore water and concentrations were measured by UV/vis spectroscopy using a NanoDrop ND-1000 Spectrophotometer from Peqlab Biotechnologie GmbH, Germany. Complimentary 60nt forward and reverse strands were combined in an equimolar ratio (relative to each strand) in 1x PBS. The oligonucleotides were hybridized using the following thermocycler program: 95 °C for 2 min, 71.6 °C for 15 min, following a drop to 4 °C. 60bp DNA labelled with Cy3 was prepared in the same procedure using a 60nt forward strand end-modified with a Cy3. 60bp and 60bp-Cy3 DNA solutions were stored at -20 °C and defrosted to room temperature prior to use.

4.3.7. Preparation PAD–DNA Polyplexes

Polyplex solutions were prepared at 1:1, 2:1, 5:1, 10:1 and 20:1 mol ratios of polycation to DNA repeat units, resulting in ammonium cation nitrogen to phosphate

anion (N/P) ratios of 0.5:1, 1:1, 2.5:1, 5:1, and 10:1, respectively. DNA solutions were prepared in Opti-MEM for a targeted final concentration of 300 nM according to DNA strand. Polycation solutions were dissolved in DPBS and sterile filtered through a 0.2 μm syringe filter prior to further dilutions, targeting the desired mol stoichiometry relative to DNA for equi-volume mixing. For a typical transfection experiment in a 96-well plate, 50 μL of the DNA solution was added to each polycation solution (50 μL) and pipetted up and down vigorously 10 times using Greiner Bio-One filtered pipette tips. Polycation and polyplex solutions were prepared freshly prior to all transfection experiments.

4.3.8. Dynamic Light Scattering

Freshly prepared polyplex solutions (100 μL) were added to ZEN0400 microcuvettes for dynamic light scattering (DLS) measurements (n = 10) at room temperature with a Malvern Zetasizer Nano ZSP using a 173° backscatter angle.

4.3.9. Cell Culture

HeLa cells, purchased from the American Type Culture Collection (ATCC), USA were cultured in DMEM (4.5 g/L glucose, without sodium pyruvate) containing 10 % fetal calf serum (FCS). Cells were cultured as a monolayer at 37 °C in a humidified atmosphere with 5 % CO_2.

4.3.10. Transfection

HeLa cells were seeded into a tissue cultured 96-well plate at a density of 10,000 cells per well. Plated cells were incubated for 2 days at 37 °C with 5 % CO_2 and reached approximately 70-80 % confluency prior to transfection. Cells were washed with 100 µL 1x DPBS and 100 µL of freshly prepared polyplex solution was added to each well. Each sample was prepared in triplicates. Following the addition of the polyplex solution, the plate was incubated at 37 °C with 5 % CO_2 for 4 hours. The supernatant was removed and the cells were washed with 100 µL of 1x DPBS to remove residual polyplexes, and 150 µL of FCS-containing DMEM were added to each well.

4.3.11. Cell Viability

Viability of transfected HeLa cells was measured after 1 and 2 days following transfection using the WST-1 cell proliferation assay. The assay was performed according to the supplier's (Roche) protocol with minor modifications. Absorbance was measured after 1 hour incubation at 37 °C using a Tecan Infinite M1000 plate reader at 450 nm, using 690 nm as the reference wavelength. Cells were incubated with 7 % (v/v) DMSO in full medium as a positive control.

4.3.12. Cellular Uptake Efficiency

Cellular uptake of PAD–DNA (60bp-Cy3) polyplexes was measured by flow cytometry using an IntelliCyt iQue Screener. After 4 hours of incubation, cells were washed with 1x DPBS to remove residual polyplexes, followed by the addition of 50 µL

of 0.05 % trypsin-EDTA solution and incubation at 37 °C for 3-5 min for cell detachment. FCS-containing DMEM (200 μL) was added to each well. The cell suspensions were transferred into 1.5 mL tubes and centrifuged at 1150 rpm for 5 min. The supernatant was discarded and the cell pellet was re-suspended in 100 μL of DMEM and then transferred into a 96-well v-bottom plate for analysis by flow cytometry. A minimum of 10,000 event counts was recorded for each sample. Measurements were analyzed using IntelliCyt ForeCyt software. Fluorescence of the populations was measured with the FL2 channel (585/40 nm). As cells uptake fluorescent polyplexes, there is an increase in fluorescence intensity relative to the auto-fluorescence of untreated cells. Auto-fluorescence gates were the same for all samples. Cellular uptake efficiency was represented as the percentage of cells showing Cy3 fluorescence relative to the auto-fluorescence of untreated HeLa cells.

4.3.13. Apoptosis Assay

The Annexin V Apoptosis Detection Kit I (BD Pharmingen) was used to identify cell populations as non-, early-, and late-stage apoptotic. During early-stage apoptosis, phosphatidylserine (PS) groups translocate from the inner leaflet to the outer leaflet of the plasma cell membrane. PE-Annexin V selectively binds to PS groups exposed on the outer leaflet of the cell membrane, indicating early-apoptosis. 7-Amino-actinomycin (7-AAD) is a counter stain that binds to double-stranded DNA in late-stage apoptotic cells that have compromised cell membranes. Thus, non-apoptotic cells do not stain positive for either PE-Annexin V or 7-AAD, early-apoptotic cells stain positive for only PE-

Annexin V, and late-apoptotic cells stain positive for both PE-Annexin V and 7-AAD. A preliminary test was conducted on HeLa cells 1 day after exposure to 60bp DNA polyplexes with PAD copolymers and PEI at 1:1 and 10:1 N/P ratios. Cells were seeded in a 24-well plate at a density of 150,000 cells per well. Preparation of polyplexes and transfection of cells was performed as described for transfection in a 96-well plate. After 24 hours, the supernatant of each well was collected into 1.5 mL microcentrifuge tubes prior to washing to retain dead cells for analysis that may be in suspension. Transfected cells were then washed with 1x DPBS and detached with 100 μL of 0.05 % trypsin-EDTA after incubation at 37 °C for 3-5 min. FCS-containing DMEM (200 μL) was added to each well. The cell suspensions were transferred into microcentrifuge tubes containing the corresponding supernatant and centrifuged at 1150 rpm for 2.5 min. The cells were washed twice with ice-cold DPBS (100 μL) and re-suspended in 100 μL of 1x Annexin binding buffer. The concentration of each cell suspension was determined using a Luna-II automated cell counter with Erythosin B as the cell stain and 100,000 cells of each sample were transferred to a 96-well v-bottom plate (total volume 50 μL per well). PE-Annexin V (5 μL) and 7-AAD (5 μL) were added to each well and incubated at room temperature for 20 min in the absence of light. Following incubation, the samples were measured by flow cytometry using an IntelliCyt iQue Screener. PE-Annexin V was detected using the FL2 channel (585/40 nm) and 7-AAD was detected using the FL3 channel (>670 nm) with 25 % compensation to adjust for overlapping emission characteristics. Measurements were analyzed using IntelliCyt ForeCyt software. Gates for the apoptosis Annexin V and 7-AAD fluorescence were the same for all samples.

4.3.14. Statistical Analysis

Sample means were compared using a one-way ANOVA analysis with Bonferroni post hoc test for multiple comparisons. Differences for which $p < 0.05$ were considered statistically significant.

4.4. Results and Discussion

4.4.1. Synthesis of PAD Copolymers

PAD_{80}, PAD_{49}, PAD_{23}, and PAD_0 with 80, 49, 23, and 0 mol% DMAEA, respectively, were synthesized using methods described previously.[38] Herein, PAD_0 will be referred to as PAPM, and was synthesized as a control polycation that does not undergo charge-shifting hydrolysis. It was hypothesized that polyplexes made with charge-shifting polycations would be less toxic to HeLa cells relative to standard polycations such as PAPM and PEI, the latter currently the gold standard polycation transfection agent. In particular, branched PEI of 25 kDa from Sigma Aldrich was fractionated to obtain a lower molecular weight fraction (4–10 kDa) of PEI, which has shown higher transfection efficiency and lower toxicity in several cancer cell lines.[45] Thus, the relative order of cytotoxicity was anticipated to be as follows: PAPM > PEI > PAD_{23} > PAD_{49} > PAD_{80}. In addition, the polyampholytes with cationic/anionic charge-ratios approaching 80/20, 49/51, and 23/77 formed by hydrolysis may be even more cell compatible than the corresponding polyacrylic acids formed during hydrolysis of DMAEA homopolymers described by Monteiro.[22,23]

RAFT polymerization to form the PAD copolymers resulted in reasonably low dispersities, (Table 4.1) as well as controlled molecular weights as shown by their GPC traces in Figure 4.1. Properties of the PAD copolymers are summarized in Table 4.1, and their ^{1}H NMR spectra shown in Figures 4A.1, 4A.2, 4A.3 and 4A.4.

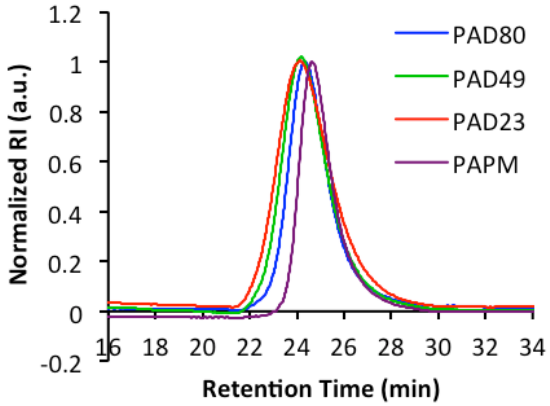

Figure 4.1. GPC traces of PAD_{80}, PAD_{49}, PAD_{23}, and PAPM with a 1 M acetic acid/sodium acetate buffer at pH 4.8.

Table 4.1. Properties of PAD Copolymers.

Polymer	[M]:[CTP]:[V-501]	Conv. (%)[a]	$M_{n,\,NMR}$[a] (g/mol)	$M_{n,\,GPC}$[b] (g/mol)	$Đ$[b]	APM : DMAEA[a]
PAD_{80}	209:1:0.22	90	40,100	26,600	1.26	20:80
PAD_{49}	204:1:0.17	92	32,200	27,200	1.38	51:49
PAD_{23}	206:1:0.17	81	29,700	28,100	1.39	77:23
PAPM	209:1:0.26	63	22,100	23,300	1.17	100:0

[a] Data obtained from 1H NMR analysis in D_2O with 1024 scans. [b] Data obtained from GPC analysis with 1 M acetic acid/sodium acetate buffer at pH 4.8 as the mobile phase, using PEG standards for molecular weight calibration.

The Mn calculated by NMR end group analysis for PAD_{80} was higher than those for the other copolymers, which may be due to degradation of the end group during polymer

purification. In this case, results obtained by GPC analysis would provide more accurate molecular weight information for polymer comparisons. In this study, polymer end groups were not removed since the toxicity of the cationic polymer typically outweighs the effect of the end group. However, it should be noted that end group removal might provide marginal improvements in cytocompatibility.[46]

4.4.2. Hydrolysis of PAD Copolymers

The hydrolysis of DMAEA groups in PAD_{80}, PAD_{49}, PAD_{23}, and PAPM were monitored at pH 7 and room temperature (22 °C) by ^{1}H NMR spectroscopy, and the results are shown in Figure 4.2 in terms of % hydrolysis of their respective initial DMAEA units. These conditions are approximations as in true transfection experiments, DMAEA hydrolysis will be affected by presence of lipases, being part of a polyplex, and by the local pH ranging from pH 7 in media and cytosol to as low as pH 5 within lysosomes. In addition, an increase in temperature to 37 °C will also increase the rate of hydrolysis as shown previously for PAD copolymers and related DMAEA polymers.[31,38]

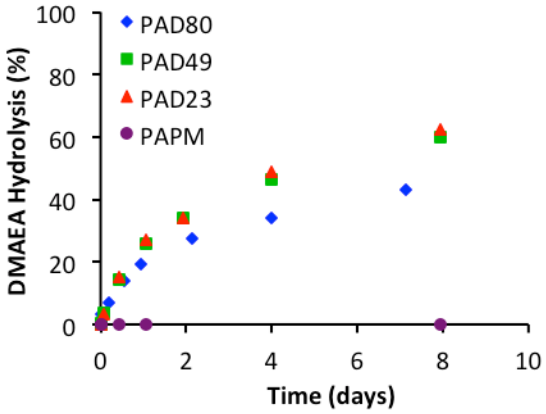

Figure 4.2. Hydrolysis of PAD_{80}, PAD_{49}, PAD_{23}, and PAPM at pH 7, room temperature (22 °C).

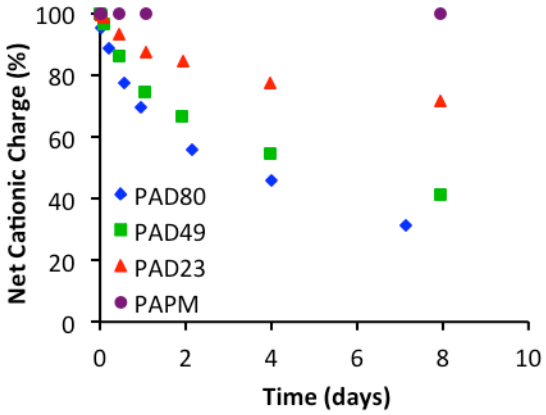

Figure 4.3. Net cationic charge with hydrolysis of PAD_{80}, PAD_{49}, PAD_{23}, and PAPM at pH 7, room temperature (22 °C).

The hydrolysis of PAD copolymers at pH 7 is rapid initially, with all compositions showing first-order kinetics over the first day corresponding to half-life times of 2-3 days (Figure 4A.6). After about one day, however, the rates of hydrolysis slow down for all compositions. This slower, second stage of hydrolysis was noted previously, and was attributed to charge repulsion of hydroxide anions from anionic acrylic acid units formed after each DMAEA unit hydrolyses (Donnan exclusion).[6,38,39,47,48]

The data is re-plotted in terms of polymer net cationic charge % in Figure 4.3. Net cationic charge is defined here as mol % cationic monomer – mol % anionic monomer, or % APM + % DMAEA - % AA. For example, after approximately 2 days, all 3 polymers showed around 30 % hydrolysis of their respective DMAEA groups (Figure 4.2), which corresponds to net cationic charges of about 55 %, 67 %, and 84 % for PAD_{80}, PAD_{49}, and PAD_{23}, respectively. After one week, the net cationic charges dropped to 31 %, 45 % and 72 % (Figure 4.3), respectively. As expected, PAPM did not show any hydrolysis even after 20 days (data not shown), as methacrylamides are much more hydrolytically stable than acrylates.

The hydrolysis of PAD copolymers should be slow enough to allow for prior complexation with DNA to form polyplexes, followed by cellular uptake by interaction of the cationic polyplex with the anionic cellular membrane. The latter would require the polymer to remain net cationic for at least 4 hours, which is in line with the results obtained in Figures 4.2 and 4.3 that show less than 5 % hydrolysis. During incubation after uptake of the polyplexes, the endosomes become more acidic (pH 4 - 5) by uptake of HCl and fusion with lysosomes. Under these conditions, DNA should ideally remain condensed in polyplexes for protection from lysosomal nucleases.[21,23,30,31] This would make DMAEA hydrolysis ideal since we recently showed that DMAEA ester hydrolysis is slowed in the range of pH 3-5.[38,39] The rate of hydrolysis of PAD copolymers at pH 5 was markedly slower than at pH 7, with all compositions showing approximately 16 % hydrolysis after nearly 10 days (Figure 4A.7). PAD copolymers may thus retain enough amino groups, both from APM as well as from DMAEA groups, for pH buffering as well

as for disruption of the endosomal membrane to enable escape by out-diffusion.[24] Once the polyplexes have escaped from the endosomes, the environment of the cytosol with a pH of 7 should allow for accelerated hydrolysis of DMAEA units within PAD copolymers. We recently showed that in presence of adequate amounts of buffer, the rates of hydrolysis of DMAEA units in such copolymers increase significantly with pH.[38,39] The release of DNA from the polyplexes may then occur in the cytosol, during transport to the nucleus, or in the nucleus itself. In addition to providing a potential release mechanism for DNA, charge-shifting hydrolysis may reduce the long-term cytotoxicity of the polymer by decreasing polymeric cationic charge. In the present work, the size and cellular uptake efficiencies of DNA polyplexes incorporating a range of charge-shifting PAD copolymers were assessed, and the viability of cells after exposure to charge-shifting PAD copolymers determined using standard polycations as controls. The hydrolysis experiment serves as a model to better understand the effect of pH in the complex intracellular environment and provides useful insight towards polymer stability for further mechanistic studies.

4.4.3. Size Determination of Polyplexes

Dynamic light scattering (DLS) was used to measure the size of polyplexes made from PAD copolymers and 60bp DNA. Polyplex solutions were prepared using the same procedure as a transfection experiment with no further dilutions. Polyplexes made with PAD copolymers and PEI all showed broad size distributions as shown in a representative

graph for the 2.5:1 N/P ratio (Figure 4.4). The results for the range of concentrations are summarized in Figure 4.5.

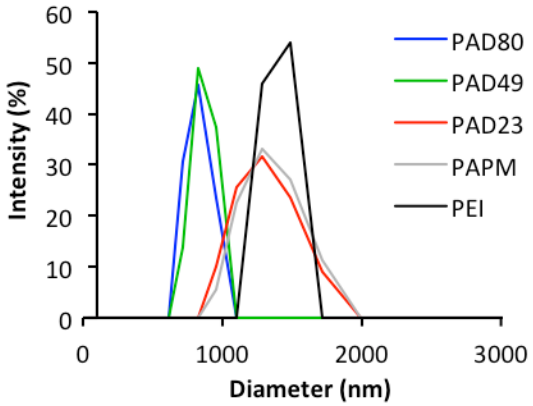

Figure 4.4. Size distribution for polyplexes of PAD copolymers, PAPM and PEI with 60bp DNA at a 5:1 mol ratio, from dynamic light scattering.

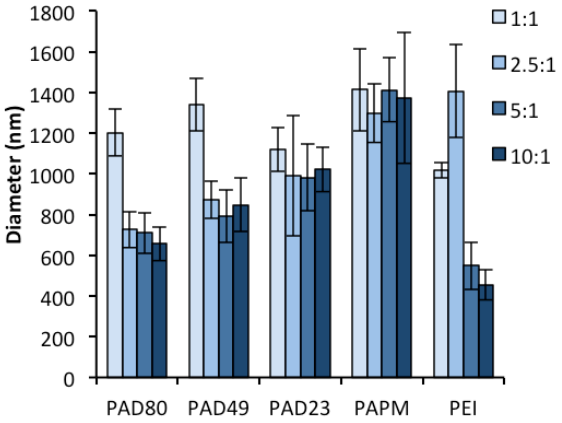

Figure 4.5. Diameters of Polyplexes of PAD copolymers, PAPM, and PEI with 60bp DNA at 1:1, 2.5:1, 5:1, and 10:1 N/P ratios, determined using dynamic light scattering. Error bars represent the standard deviation from 2 polyplex batches with 10 measurements each.

The average diameters of the polyplexes ranged from 400 – 1400 nm. At the 1:1 N/P ratio, the polyplexes were similar between all of the polymers around 1100 nm. However,

at higher polymer loadings, polyplexes with DMAEA-rich PAD copolymers (i.e. PAD_{80}) resulted in smaller particles (~700 nm) than those with DMAEA-poor PAD copolymers and PAPM (~1400 nm). This trend may be due to the different interactions of tertiary and primary ammonium cations of the polymers with phosphate anions of DNA. The relatively large size of polyplexes obtained may also be due to the overall concentration used during complexation, and can be changed to obtain smaller particles. Although the size of polyplexes is known to affect cellular uptake, many other variables can affect cellular uptake that go beyond the scope of this report.[49] Thus, the effects of polyplex diameters on cell uptake and viability were not further explored in this study.

4.4.4. Cell Viability

Cell viability of HeLa cells after 1 and 2 days post-exposure to the polyplexes was measured using the WST-1 proliferation assay (Figures 4.6 and 4.7, respectively).

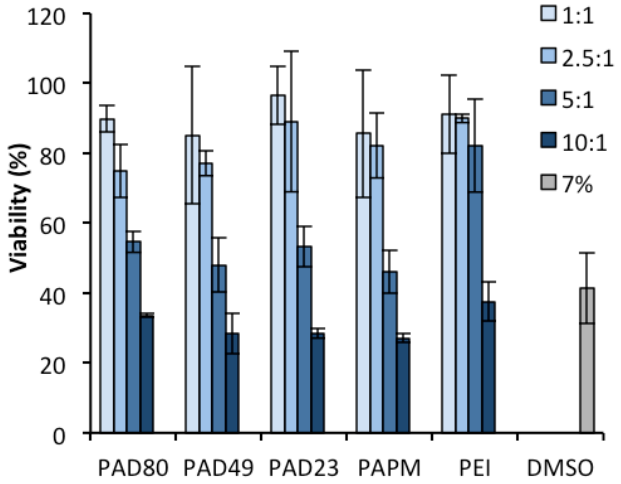

Figure 4.6. HeLa cell viability one day post-exposure to 60bp DNA with PAD copolymers, PAPM, and PEI at 1:1, 2.5:1, 5:1, and 10:1 N/P ratios. HeLa cells were treated with DMSO (7 % (v/v) in FCS-containing DMEM) as a positive control.

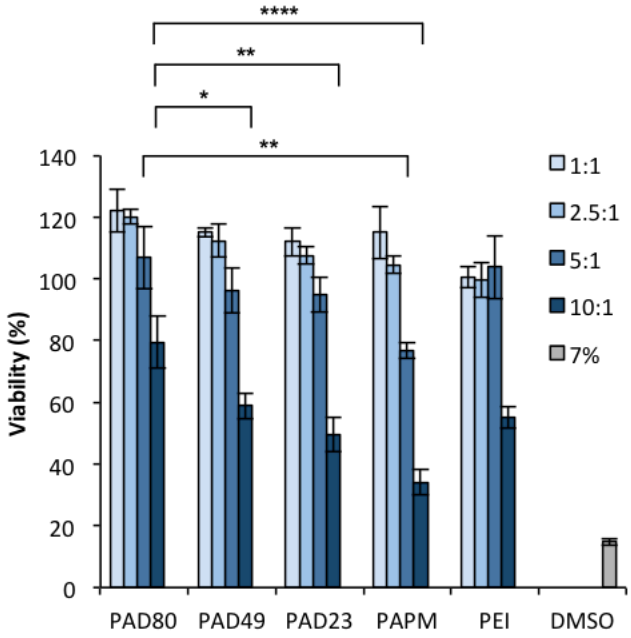

Figure 4.7. HeLa cell viability two days after exposure to polyplexes of 60bp DNA with PAD copolymers, PAPM, and PEI at 1:1, 2.5:1, 5:1, and 10:1 N/P ratios. HeLa cells were treated with DMSO (7 % (v/v) in FCS-containing DMEM) as a positive control. Statistical significance for PAD copolymer samples at 5:1 and 10:1 N/P ratios are shown. * $p \leq 0.05$, ** $p \leq 0.01$, **** $p \leq 0.0001$.

One day after exposure to the polyplexes, viability of HeLa cells appeared to decrease with increasing polycation concentrations for all of the polymers. There is no discernable effect of APM/DMAEA ratios, while PEI shows higher cell viabilities than the PAD copolymers. Interestingly, two days after exposure to polyplexes, viability of HeLa cells shows an effect of PAD composition: HeLa cells treated with PAD_{80} showed higher viabilities than cells treated with PAD_{49}, PAD_{23}, and PAPM. This effect was more pronounced for polymer/DNA ratios of 5:1 and 10:1 N/P.

Similar viability results across the range of compositions of PAD copolymers after one day are not surprising given the relatively slow rate of charge-shifting hydrolysis. Since PAD copolymers maintain enough cationic charge to bind DNA, it is likely that the initial net cationic charge of the polyplexes that cells are exposed to would be similar for all PAD copolymers. Thus, the initial cytotoxicity for the polyplexes, and any excess free polycation, should be similar for the different compositions. This seems to be the challenge in the field of synthetic polymers for transfection as cationic charge is necessary for the condensation and uptake of DNA, however the polymers are also cytotoxic at high concentrations due disruption of the cellular membrane.

At two days post-exposure, viability appeared to be higher for cells exposed to polyplexes made from PAD copolymers with greater charge-shifting ability. In some cases, particularly at lower N/P ratios, cells treated with polyplexes showed viabilities greater than untreated cells (i.e. viability >100%). It is unclear why this was the case, however, the trends observed between polymer composition and concentration (N/P

ratios) remains evident. The results suggest that cells are better able to recover after exposures to these copolymers, which may be due to the degradation of cytotoxic cationic charge. Hydrolysis data showed that after two days, the net charge of PAD_{80}, PAD_{49}, and PAD_{23} were approximately 55, 67, and 84 % net cationic, respectively (Figure 4.2). Thus, it is likely that improved recovery of cell viability may be due to the charge-shifting hydrolysis of the PAD copolymers. This trend matches that observed by other researchers for related charge-shifting polycations.[22,27] Given the poor cell viability observed at the 10:1 N/P ratio for all polycations, subsequent transfection experiments were conducted at more optimal concentrations (1:1, 2.5:1, and 5:1 N/P ratios).

4.4.5. Cellular Uptake

HeLa cells were exposed to polyplexes made from PAD copolymers, PAPM, and PEI with DNA fluorescently labelled with Cy3 (60bp-Cy3). The cells were analyzed by flow cytometry following the 4-hour incubation period with polyplexes. Gating examples of the dot plots obtained are provided in the Supporting Information (Figures 4A.8, 4A.9, 4A.10, 4A.11, 4A.12, and 4A.13), and the results are summarized in Figure 4.8.

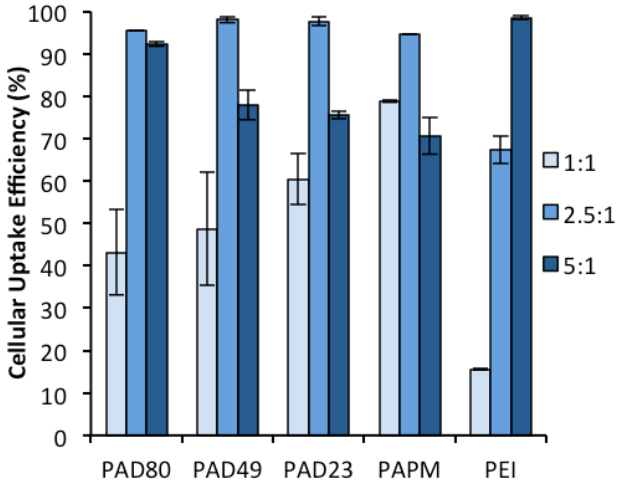

Figure 4.8. Cellular uptake efficiency of 60bp-Cy3 DNA with PAD copolymers, PAPM, and PEI at 1:1, 2.5:1, and 5:1 N/P ratios.

Uptake efficiency of 60bp-Cy3 DNA at the 1:1 N/P ratio is higher for PAPM than the PAD copolymers. The nominal net charge of the polyplex with 2:1 PAD to DNA mol ratio should be neutral, however, as some hydrolysis has occurred, it may actually be slightly negative. This may be why the uptake efficiency of PAPM polyplexes is higher at this low polycation:DNA ratio, as endocytosis of neutral particles would be more likely than of anionic particles.

At the 2.5:1 N/P ratio, uptake efficiency appeared to be very high (>95 %) for all PAD copolymers and PAPM. At 5:1 N/P, uptake efficiency of PAD_{80} polyplexes remained high at 92 %, however uptake efficiency began to decrease for PAD copolymers containing less DMAEA. Similarly, only 70 % of the cells showed fluorescence when treated with PAPM polyplexes at 5:1 N/P. These decreases in cellular uptake efficiency correlate with the cytotoxicity data obtained using the WST-1 assay. HeLa cells treated with PAD copolymer polyplexes richer in APM showed a subpopulation that was thought

to correspond to apoptotic cells. This was confirmed by conducting an Annexin V apoptosis assay at 1:1 and 10:1 N/P ratios that showed a high percentage of apoptotic cells (>80 %) in this subpopulation (Figures 4A.14, 4A.15, and 4A.16). As this subpopulation was more prominent at higher concentrations (10:1 N/P), this is in agreement with the increased cytotoxicity observed at higher polymer concentrations from the WST-1 assay. Thus, the decrease in cellular uptake efficiency of PAPM correlates with the toxicity of the corresponding polyplexes. This could be due to cationic charges of PAPM and PAPM-rich polyplexes that are unable to undergo charge-shifting hydrolysis, causing cell death and thereby reducing the number of cells in the region of healthy, fluorescent cells. Similarly, PAD_{80} polyplexes showed the highest uptake efficiency at the 5:1 N/P, which may be due to PAD_{80} having the greatest charge-shifting ability and hence a greater proportion of healthy, Cy3-positive cells.

Cellular uptake efficiency of PEI polyplexes appeared to be significantly lower than PAD copolymer polyplexes at 1:1 and 2.5:1 N/P ratios (Figure 4.8). At the highest, 5:1 N/P ratio, PEI shows comparable uptake efficiency to PAD copolymers used at the 2.5:1 ratio. These results for PAD copolymers are promising as PEI is currently the gold-standard polycation used in the field due to its high transfection efficiency.

4.5. Conclusions

PAD copolymers of varying composition were synthesized by RAFT polymerization to obtain polymers with controlled molecular weights and dispersities. Model hydrolysis studies of the polymers using ^{1}H NMR spectroscopy provided useful

information on the evolution of the net charge of the polymers at pH 7, suggesting a route for potential intracellular dissociation of complexed DNA for controlled release from PAD_{80} and PAD_{49} polyplexes. HeLa cells transfected with PAD copolymer polyplexes showed very high viability at the 1:1 and 2.5:1 N/P ratios of all of the compositions. However, at higher polymer loadings, HeLa cells transfected with PAD copolymers of higher DMAEA composition showed higher viability than cells treated with non-charge-shifting PAPM. The higher viability associated with PAD copolymers is correlated to the charge-shifting ability of the polymers which likely reduces cytotoxicity, particularly long-term, as cells recovered well 2 days after exposure. Cellular uptake efficiency of PAD copolymer polyplexes was very high (>95 %) at the 2.5:1 N/P ratio, out-performing PEI polyplexes which required double the polycation loading to achieve a similar level of uptake efficiency. Overall, PAD copolymers of higher DMAEA content (PAD_{80} and PAD_{49}) used at the 2.5:1 N/P ratio appear as promising candidates for further cell transfection experiments including gene expression.

In conclusion, the findings in this report suggest that charge-shifting cationic copolymers are a promising class of synthetic polymers suitable for *in vitro* DNA delivery. Future work will involve exploring gene transfection efficiency and mechanism of intracellular release of DNA from polyplexes with these charge-shifting copolymers, both with HeLa and other cell lines.

Associated Content

Supporting Information

The supporting information is available free of charge via the Internet at http://pubs.acs.org. ^{1}H NMR spectra of PAD_{80}, PAD_{49}, PAD_{23}, and PAPM; ^{1}H NMR spectrum of a representative example of hydrolysis showing integration and calculation of percent hydrolysis; First-order kinetic plot of PAD copolymer hydrolysis; Hydrolysis plot of PAD copolymers and PAPM at pH 5; Dot plots from flow cytometry analysis of cellular uptake of 60bp-Cy3 DNA polyplexes; Dot plots from flow cytometry analysis of apoptosis assay post-exposure to PAD_{80}–60bp polyplexes at 1:1 and 10:1 N/P ratios, and untreated cells.

Conflicts of Interest

There are no conflicts of interest to declare.

4.6. Acknowledgements

H.D.H.S and S.R. are grateful for funding support from the Canada Foundation for Innovation and the Natural Sciences and Engineering Research Council of Canada Discovery Grant (RGPIN89661-11). S.R. received funding support from Mitacs through a Globalink Research Award (Project No. 20011323) and an Ontario Graduate Scholarship. S.R. thanks Christin Möser and Martin Sajfutdinow for help with flow cytometry and dynamic light scattering measurements, respectively. Susanne Przybylski is acknowledged for generously providing the sample of PEI. Robel Belay is acknowledged for testing HeLa cell cultures for mycoplasma.

Author Information

Corresponding Author

*Email: stoverh@mcmaster.ca

4.7. References

[1] Agarwal, S.; Zhang, Y.; Maji, S.; Greiner, A. PDMAEMA based gene delivery materials. *Mater. Today* **2012**, *15*, 388−393.

[2] Thomas, M.; Klibanov, A. M. Non-viral gene therapy: polycation-mediated DNA delivery. *Appl Microbiol. Biotechnol*. **2003**, *62*, 27–34.

[3] Pollard, H.; Remy, J. S.; Loussouarn, G.; Demolombe, S.; Behr, J. P.; Escande, D. Polyethylenimine but Not Cationic Lipids Promotes Transgene Delivery to the Nucleus in Mammalian Cells. *J. Biol. Chem*. **1998**, *273*, 7507–7511.

[4] Kabanov, A. V.; Kabanov, V. A. DNA Complexes with Polycations for the Delivery of Genetic Materials into Cells. *Bioconjugate Chem*. **1995**, *6*, 7-20.

[5] Luten, J.; van Nostrum, C. F.; De Smedt, S. C.; Hennink, W. E. Biodegradable polymers as non-viral carriers for plasmid DNA delivery. *J. Controlled Release* **2008**, *126*, 97−110.

[6] van de Wetering, P.; Moret, E. E.; Schuurmans-Nieuwenbroek, N. M. E.; van Steenbergen, M. J.; Hennink, W. E. Structure-Activity Relationships of Water-Soluble Cationic Methacrylate/Methacrylamide Polymers for Nonviral Gene Delivery. *Bioconjugate Chem*. **1999**, *10*, 589−597.

[7] Ong, Z. Y.; Yang, C.; Cheng, W.; Voo, Z. X.; Chin, W.; Hedrick, J. L.; Yang, Y. Y. Biodegradable cationic poly(carbonates): Effect of varying side chain hydrophobicity on key aspects of gene transfection. *Acta Biomaterialia* **2017**, *54*, 201–211.

[8] Eltoukhy, A. A.; Siegwart, D. J.; Alabi, C. A.; Rajan, J. S.; Langer, R.; Anderson, D. G. Effect of molecular weight of amine end-modified poly(β-amino ester)s on gene delivery efficiency and toxicity. *Biomaterials* **2012**, *33*, 3594-3603.

[9] Ahmed, M.; Narain, R. The effect of polymer architecture, composition, and molecular weight on the properties of glycopolymer-based non-viral gene delivery systems. *Biomaterials* **2011**, *32*, 5279-5290.

[10] Godbey, W.T.; Wu, K. K.; Mikos, A. G. Size matters: Molecular weight affects the efficiency of poly(ethylenimine) as a gene delivery vehicle. *J. Biomed. Mater. Res. B* **1998**, *45*, 268-275.

[11] van de Wetering, P.; Cherng, J. Y.; Talsma, H.; Crommelin, D. J. A.; Hennink, W. E. 2-(dimethylamino)ethyl methacrylate based (co)polymers as gene transfer agents. *J. Controlled Release* **1998**, *53*, 145–153.

[12] Synatschke, C.; Schallon, A.; Jérôme, V.; Freitag, R.; Müller, A. H. E. Influence of Polymer Architecture and Molecular Weight of Poly(2-(dimethylamino)ethyl methacrylate) Polycations on Transfection Efficiency and Cell Viability in Gene Delivery. *Biomacromolecules* **2011**, *12*, 4247−4255.

[13] Kadlecova, Z.; Baldi, L.; Hacker, D.; Wurm, F. M.; Klok, H. A. Comparative Study on the *In Vitro* Cytotoxicity of Linear, Dendritic, and Hyperbranched Polylysine Analogues. *Biomacromolecules* **2012**, *13*, 3127−3137.

[14] Srinivasachari, S.; Fichter, K. M.; Reineke, T. M. Polycationic β-Cyclodextrin "Click Clusters": Monodisperse and Versatile Scaffolds for Nucleic Acid Delivery. *J. Am. Chem. Soc.* **2008**, *130*, 4618-4627.

[15] Yin, M. Z.; Ding, K.; Gropeanu, R. A.; Shen, J.; Berger, R.; Weil, T. Müllen, K. Dendritic star polymers for efficient DNA binding and stimulus-dependent DNA release. *Biomacromolecules* **2008**, *9*, 3231–3238.

[16] Rinkenauer, A. C.; Schubert, S.; Traeger, A.; Schubert, U. S. The influence of polymer architecture on in vitro pDNA transfection. *J. Mater. Chem. B* **2015**, *3*, 7477-7493.

[17] Shi, J.; Choi, J. L.; Chou, B.; Johnson, R. N.; Schellinger, J. G.; Pun, S. H. Effect of Polyplex Morphology on Cellular Uptake, Intracellular Trafficking, and Transgene Expression. *ACS Nano* **2013**, *7*(12), 10612–10620.

[18] Lim, Y.-B.; Choi, Y. H.; Park, J.-S. A Self-Destroying Polycationic Polymer: Biodegradable Poly(4-hydroxy-L-proline ester). *J. Am. Chem. Soc*. **1999**, *121*, 5633-5639.

[19] Putnam, D.; Langer, R. Poly(4-hydroxy-L-proline ester): Low-Temperature Polycondensation and Plasmid DNA Complexation. *Macromolecules* **1999**, *32*, 3658-3662.

[20] Liu, X.; Yang, J. W.; Miller, A. D.; Nack, E. A.; Lynn, D. M. Charge-Shifting Cationic Polymers That Promote Self-Assembly and Self-Disassembly with DNA. *Macromolecules* **2005**, *38*, 7907-7914.

[21] Luten, J.; Akeroyd, N.; Funhoff, A.; Lok, M. C.; Talsma, H.; Hennink, W. E. Methacrylamide Polymers with Hydrolysis-Sensitive Cationic Side Groups as Degradable Gene Carriers. *Bioconjugate Chem.* **2006**, *17*, 1077−1084.

[22] Truong, N. P.; Jia, Z.; Burgess, M.; McMillan, N. A. J.; Monteiro, M. J. Self-Catalyzed Degradation of Linear Cationic Poly(2- dimethylaminoethyl acrylate) in Water. *Biomacromolecules* **2011**, *12*, 1876–1882.

[23] Truong, N. P.; Jia, Z.; Burgess, M.; Payne, L.; McMillan, N. A. J.; Monteiro, M. J. Self-Catalyzed Degradable Cationic Polymer for Release of DNA. *Biomacromolecules* **2011**, *12*, 3540–3548.

[24] Truong, N. P.; Gu, W.; Prasadam, I.; Jia, Z.; Crawford, R.; Xiao, Y.; Monteiro, M. J. An influenza virus-inspired polymer system for the timed release of siRNA. *Nat. Comm.* **2013**, 4:1902, DOI: 10.1038/ncomms2905

[25] Novo, L.; Rizzo, L. Y.; Golombek, S. K.; Dakwar, G. R.; Lou, B.; Remaut, K.; Mastrobattista, E.; van Nostrum, C. F.; Jahnen-Dechent, W.; Kiessling, F.; Braeckmans, K.; Lammers, T.; Hennink, W. E. Decationized polyplexes as stable and safe carrier systems for improved biodistribution in systemic gene therapy. *Journal of Controlled Release* **2014**, *195*, 162–175.

[26] Ho, H. T.; Pascual, S.; Montembault, V.; Casse, N.; Fontaine, L. Innovative well-defined primary amine-based polyacrylates for plasmid DNA complexation. *Polym. Chem*., **2014**, *5*, 5542-5545.

[27] Werfel, T. A.; Swain, C.; Nelson, C. E.; Kilchrist, K. V.; Evans, B. C.; Miteva, M.; Duvall, C. L. Hydrolytic charge-reversal of PEGylated polyplexes enhances intracellular un-packaging and activity of siRNA. *J. Biomed. Mater. Res. A.* **2016**, *104A*, 917–927.

[28] Ho, H. T.; Bohec, M. L.; Frémaux, J.; Piogé, S.; Casse, N.; Fontaine, L.; Pascual, S. Tuning the Molar Composition of "Charge-Shifting" Cationic Copolymers Based on 2-(N,N-Dimethylamino)Ethyl Acrylate and 2-(tert-Boc-Amino)Ethyl Acrylate. *Macromol. Rapid Commun*. **2017**, DOI: 10.1002/marc.201600641.

[29] Qiu, N.; Gao, J.; Liu, Q.; Wang, J.; Shen, Y. Enzyme-Responsive Charge-Reversal Polymer-Mediated Effective Gene Therapy for Intraperitoneal Tumors. *Biomacromolecules* **2018**, *19*, 2308−2319.

[30] Cook, A. B.; Peltier, R.; Hartlieb, M.; Whitfield, R.; Moriceau, G.; Burns, J. A.; Haddleton, D. M.; Perrier, S. Cationic and hydrolysable branched polymers by RAFT for complexation and controlled release of dsRNA. *Polym. Chem.* **2018**, *9*, 4025-4035.

[31] Whitfield, R.; Anastasaki, A.; Truong, N. P.; Cook, A. B.; Omedes-Pujol, M.; Rose, V. L.; Nguyen, T. A. H.; Burns, J. A.; Perrier, S.; Davis, T. P.; Haddleton, D. M. Efficient Binding, Protection, and Self-Release of dsRNA in Soil by Linear and Star Cationic Polymers. *ACS Macro Lett.* **2018**, *7*, 8, 909-915.

[32] You, Y.-Z.; Manickam, D. S.; Zhou, Q.-H.; Oupický, D. Reducible poly(2-dimethylaminoethyl methacrylate): Synthesis, cytotoxicity, and gene delivery activity. *Journal of Controlled Release* **2007**, *122*, 217–225.

[33] Lonez, C.; Vandenbranden, M.; Ruysschaert, J.-M. Cationic lipids activate intracellular signaling pathways. Advanced Drug Delivery Reviews **2012**, *64*, 1749–1758.

[34] Cobourn, R. F. Polyamine Effects on Cell Function: Possible Central Role of Plasma Membrane PI(4,5)P2. *J. Cell. Physiol*. **2009**, *221*, 544–551.

[35] Leng, C.; Huang, H.; Zhang, K.; Hung, H.-C.; Xu, Y.; Li, Y.; Jiang, S.; Chen, Z. Effect of Surface Hydration on Antifouling Properties of Mixed Charged Polymers. *Langmuir* **2018**, *34*, 6538−6545.

[36] Chen, S.; Li, L.; Zhao, C.; Zheng, J. Surface hydration: Principles and applications toward low-fouling/nonfouling biomaterials. *Polymer* **2010**, *51*, 5283-5293.

[37] Rinkenauer, A. C.; Schallon, A.; Günther, U.; Wagner, M.; Betthausen, E.; Schubert, U. S.; Schacher, F. H. A Paradigm Change: Efficient Transfection of Human Leukemia Cells by Stimuli-Responsive Multicompartment Micelles. *ACS Nano* **2013**, *7*, 11, 9621-9631.

[38] Ros, S; Burke, N. A. D.; Stöver, H. D. H. Synthesis and Properties of Charge-Shifting Polycations: Poly[3-aminopropylmethacrylamide-co-2-(dimethylamino)ethyl acrylate] *Macromolecules* **2015**, *48*, 8958−8970.

[39] Ros, S.; Kleinberger, R. M.; Burke, N. A. D.; Rossi, N. A. A.; Stöver, H. D. H. Charge-Shifting Polycations with Tunable Rates of Hydrolysis: Effect of Backbone Substituents on Poly[2-(dimethylamino)ethyl acrylates]. *Macromolecules* **2018**, *51*, 5752−5761.

[40] Behr, J. P. The Proton Sponge: a Trick to Enter Cells the Viruses Did Not Exploit *Chimia* **1997**, *51*, 34-36.

[41] Akinc, A.; Thomas, M.; Klibanov, A. M.; Langer, R. Exploring polyethylenimine-mediated DNA transfection and the proton sponge hypothesis. *J. Gene Med.* **2005**; *7*, 657–663.

[42] Dubruel, P.; Christiaens, B.; Rosseneu, M.; Vandekerckhove, J.; Grooten, J.; Goossens, V.; Schacht, E. Buffering Properties of Cationic Polymethacrylates Are Not the Only Key to Successful Gene Delivery. *Biomacromolecules* **2004**, *5*, 379-388.

[43] Benjaminsen, R. V.; Mattebjerg, M. A.; Henriksen, J. R.; Moghimi, S. M.; Andresen, T. L. The Possible "Proton Sponge" Effect of Polyethylenimine (PEI) Does Not Include Change in Lysosomal pH. *Molecular Therapy* **2013**, *21*(1), 149–157.

[44] Gabrielson, N. P.; Pack, D. W. Acetylation of Polyethylenimine Enhances Gene Delivery via Weakened Polymer/DNA Interactions. *Biomacromolecules* **2006**, *7*, 2427-2435.

[45] Werth, S.; Urban-Klein, B.; Dai, L.; Höbel, S.; Grzelinski, M.; Bakowsky, U.; Czubayko, F.; Aigner, A. A low molecular weight fraction of polyethylenimine (PEI) displays increased transfection efficiency of DNA and siRNA in fresh or lyophilized complexes. *Journal of Controlled Release* **2006**, *112*, 257–270.

[46] Pissuwan, D.; Boyer, C.; Gunasekaran, K.; Davis, T. P.; Bulmus, V. In Vitro Cytotoxicity of RAFT Polymers. *Biomacromolecules* **2010**, *11*, 412–420.

[47] Rolph, M. S.; Pitto-Barry, A.; O'Reilly, R. K. The hydrolytic behavior of N,N′-(dimethylamino) ethyl acrylate-functionalized polymeric stars. *Polym. Chem*. **2017**, *8*, 5060−5070.

[48] Higuchi, M.; Senju, R. Kinetic Aspects of Alkaline Hydrolysis of Poly(acrylamide). *Polym. J*. **1972**, *3*, 370−377.

[49] Pezzoli, D.; Giupponi, E.; Mantovani, D.; Candiani, G. Size matters for *in vitro* gene delivery: investigating the relationships among complexation protocol, transfection medium, size and sedimentation. *Scientific Reports* **2017**, *7*:44134, DOI: 10.1038/srep44134.

4.8. Appendix

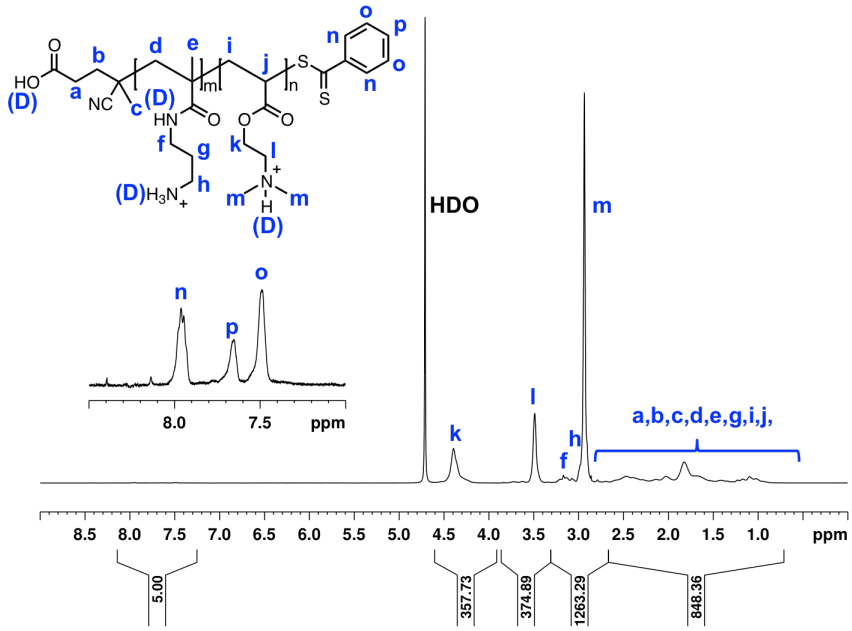

Figure 4A.1. ^{1}H NMR spectrum of PAD_{80} in D_2O recorded with 1024 scans. The inset shows the dithiobenzoate end group used for Mn calculations.

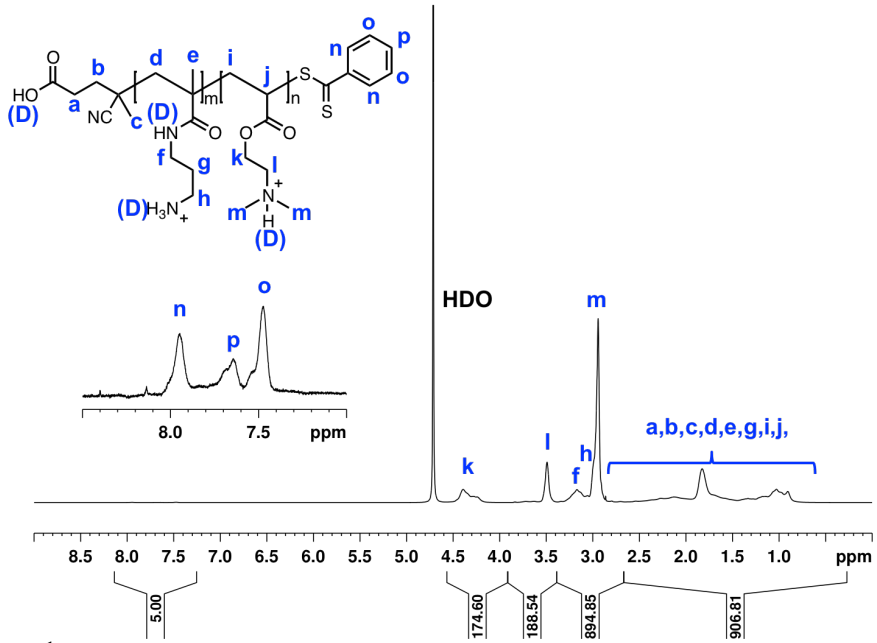

Figure 4A.2. ^{1}H NMR spectrum of PAD_{49} in D_2O recorded with 1024 scans. The inset shows the dithiobenzoate end group used for Mn calculations.

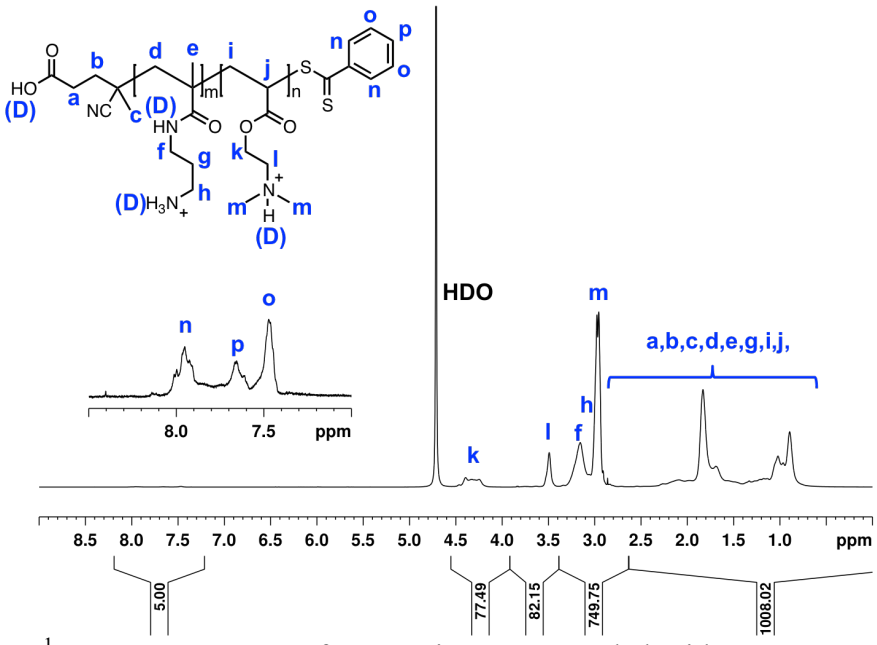

Figure 4A.3. ^{1}H NMR spectrum of PAD_{23} in D_2O recorded with 1024 scans. The inset shows the dithiobenzoate end group used for Mn calculations.

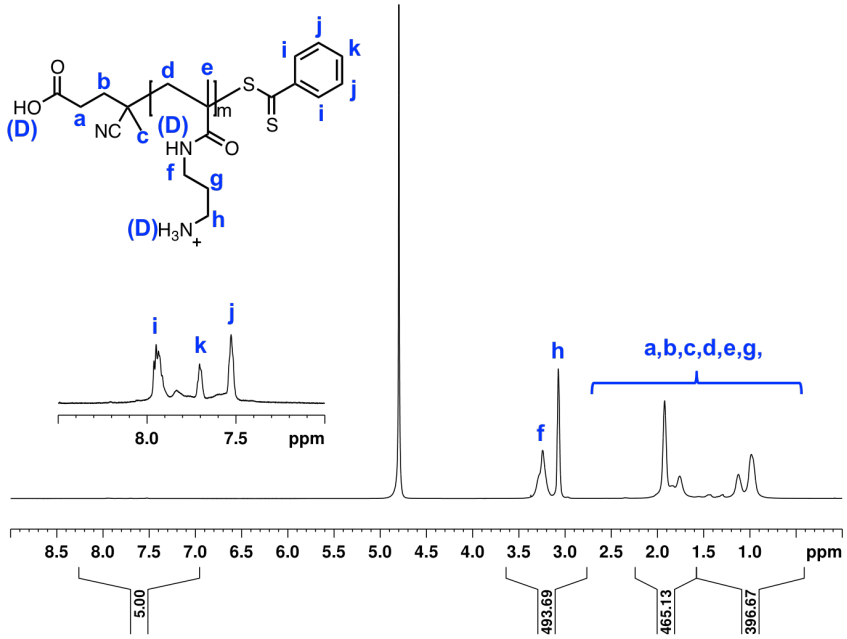

Figure 4A.4. ^{1}H NMR spectrum of PAPM in D_2O recorded with 1024 scans. The inset shows the dithiobenzoate end group used for Mn calculations.

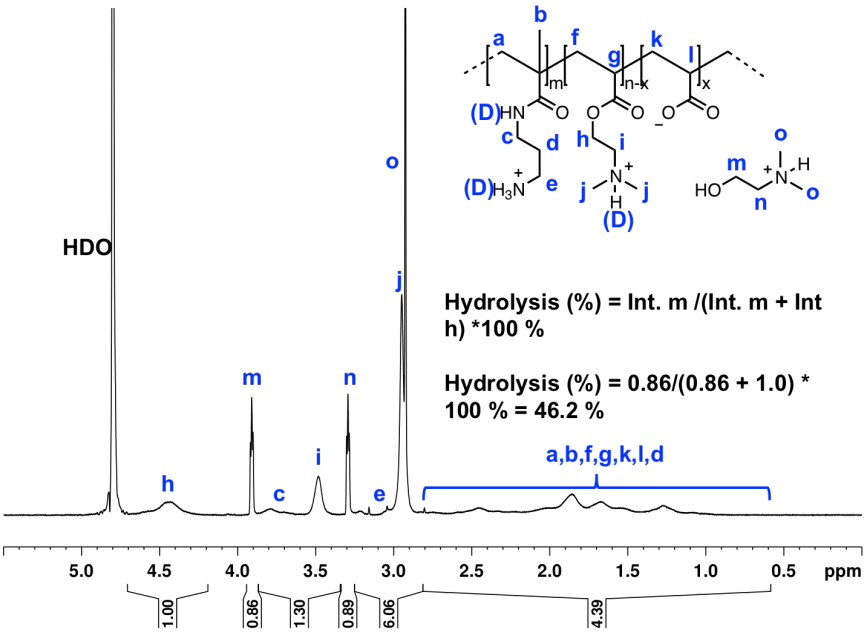

Figure 4A.5. ^{1}H NMR spectrum of PAD_{80} in 100 mM phosphate buffer at pH 7.02 after approximately 11 days at room temperature. A sample calculation for the percent hydrolysis is shown using the methylene CH_2O protons of DMAE small-molecule byproduct (m) and remaining ester protons (h).

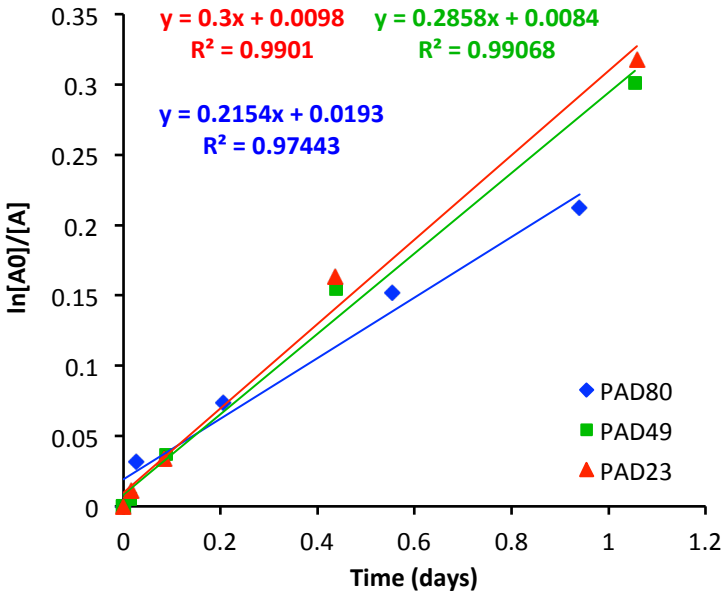

Figure 4A.6. First-order kinetic plot of initial hydrolysis of PAD_{80}, PAD_{49}, and PAD_{23} within the first day. Half-life values obtained were 3.2, 2.4, and 2.3 days for PAD_{80}, PAD_{49}, and PAD_{23}, respectively.

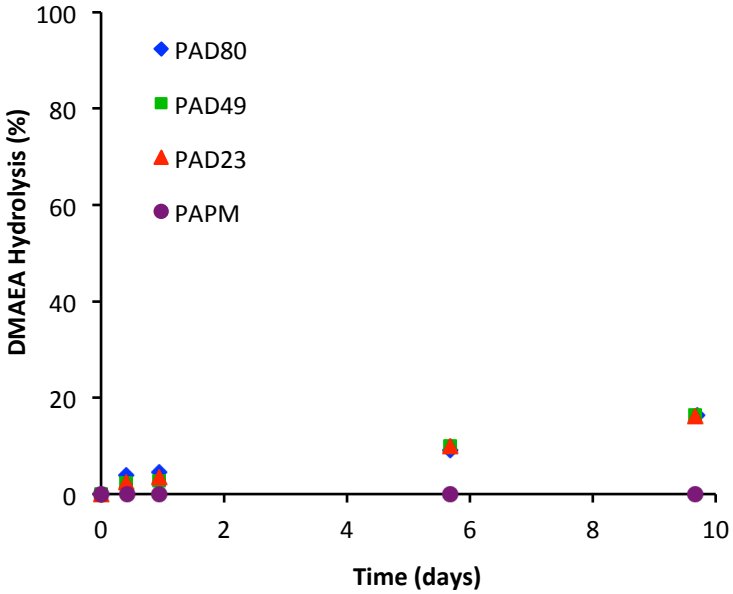

Figure 4A.7. Hydrolysis of PAD_{80}, PAD_{49}, PAD_{23}, and PAPM at pH 5, room temperature (22 °C)

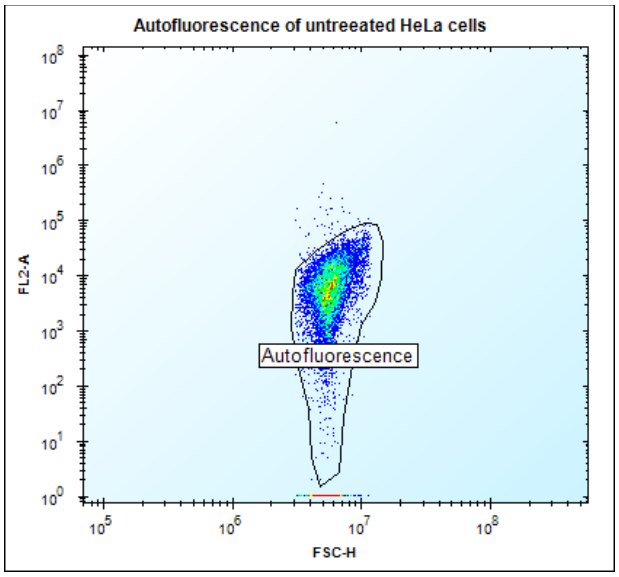

Figure 4A.8. Dot plot of untreated HeLa cells showing auto-fluorescence of the population. Fluorescence intensity (FL2-A) of Cy3 was measured as a function of the forward scattering size of the events (FSC-H).

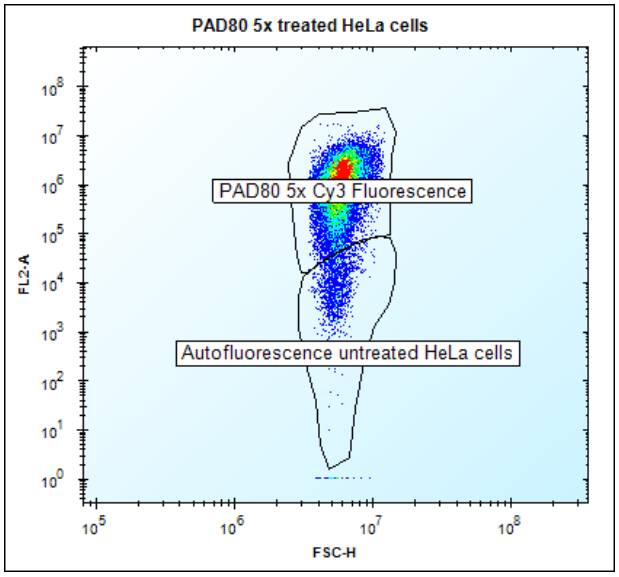

Figure 4A.9. Dot plot of HeLa cells transfected with PAD_{80}–60bp-Cy3 DNA polyplexes at the 5x concentration (2.5:1 N/P ratio). Fluorescence intensity (FL2-A) of Cy3 was measured as a function of the forward scattering size of the events (FSC-H).

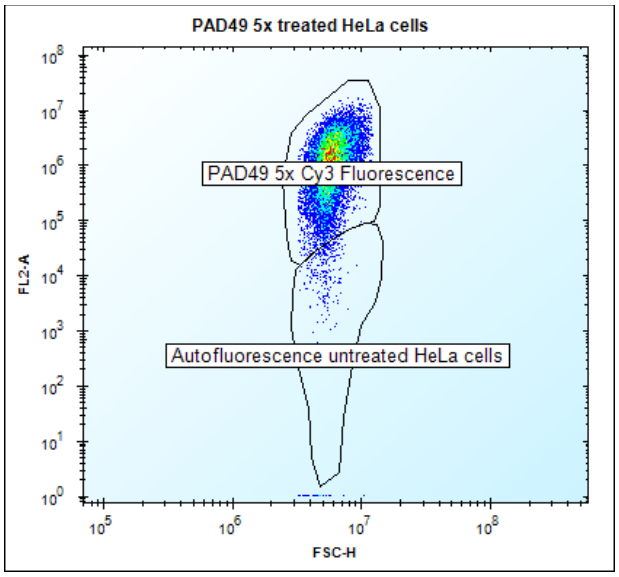

Figure 4A.10. Dot plot of HeLa cells transfected with PAD_{49}–60bp-Cy3 DNA polyplexes at the 5x concentration (2.5:1 N/P). Fluorescence intensity (FL2-A) of Cy3 was measured as a function of the forward scattering size of the events (FSC-H).

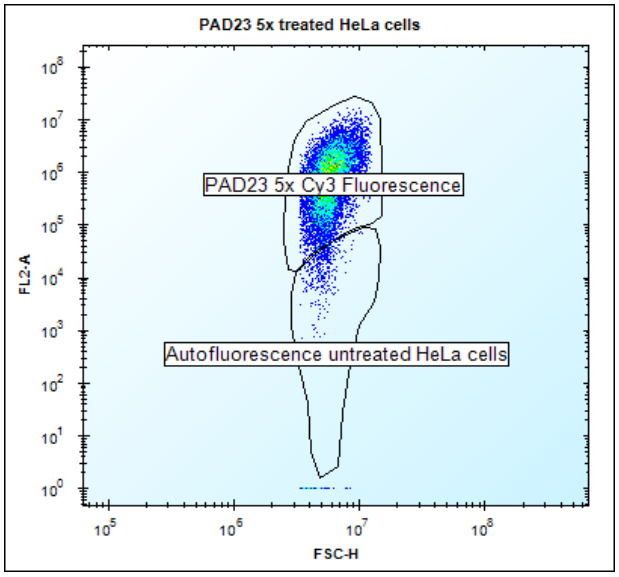

Figure 4A.11. Dot plot of HeLa cells transfected with PAD_{23}–60bp-Cy3 DNA polyplexes at the 5x concentration (2.5:1 N/P). Fluorescence intensity (FL2-A) of Cy3 was measured as a function of the forward scattering size of the events (FSC-H).

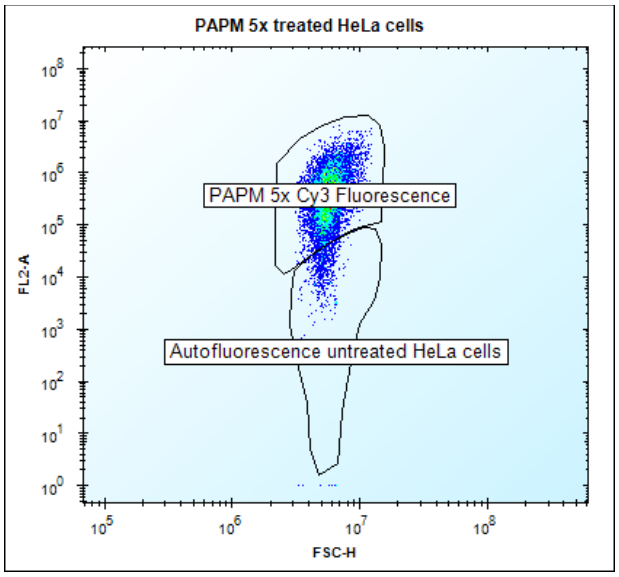

Figure 4A.12. Dot plot of HeLa cells transfected with PAPM–60bp-Cy3 DNA polyplexes at the 5x concentration (2.5:1 N/P). Fluorescence intensity (FL2-A) of Cy3 was measured as a function of the forward scattering size of the events (FSC-H).

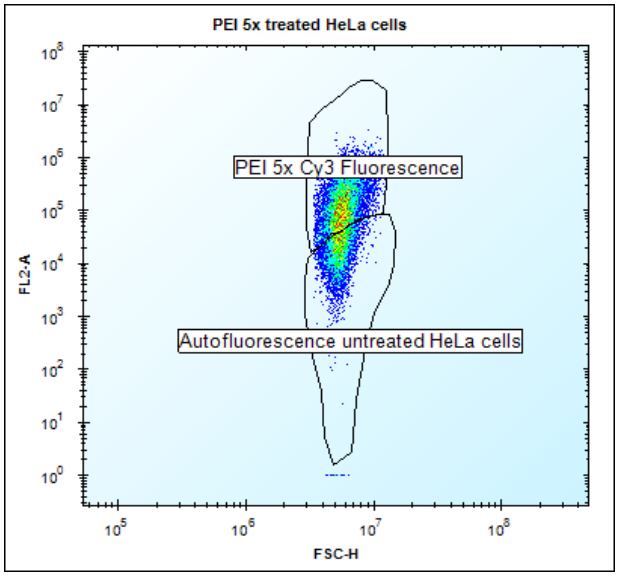

Figure 4A.13. Dot plot of HeLa cells transfected with PEI–60bp-Cy3 DNA polyplexes at the 5x concentration (2.5:1 N/P). Fluorescence intensity (FL2-A) of Cy3 was measured as a function of the forward scattering size of the events (FSC-H).

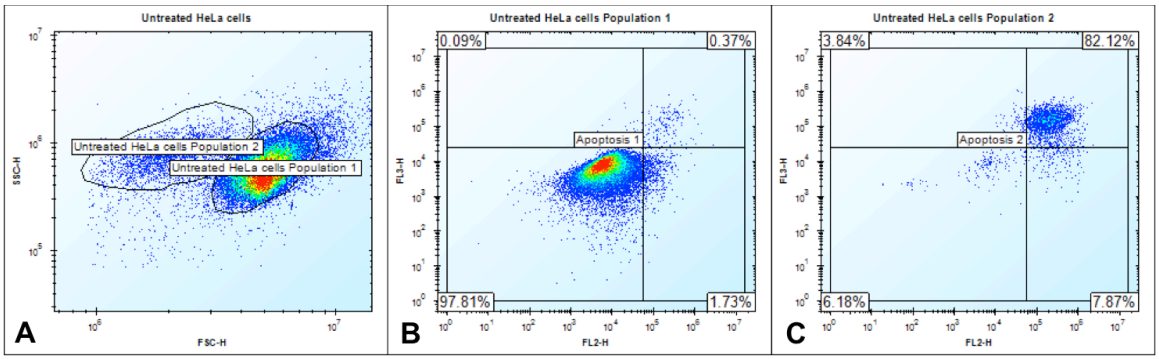

Figure 4A.14. Dot plot of untreated HeLa cells as a function of forward scattering size (FSC) and side scattering granularity (SSC) showing main population 1 and subpopulation 2 (A). Dot plot of main population 1 as a function of fluorescence of PE-Annexin V in the FL2 channel and 7-AAD fluorescence in the FL3 channel (B). Dot plot of subpopulation 2 as a function of fluorescence of PE-Annexin V in the FL2 channel and 7-AAD fluorescence in the FL3 channel (C). The majority of subpopulation 2 (82 %) stains positive for both Annexin V and 7-AAD, which correlates to late-apoptotic cells. Main population 1 consists primarily of non-apoptotic cells that stain negative for PE-Annexin V and 7-AAD (98 %).

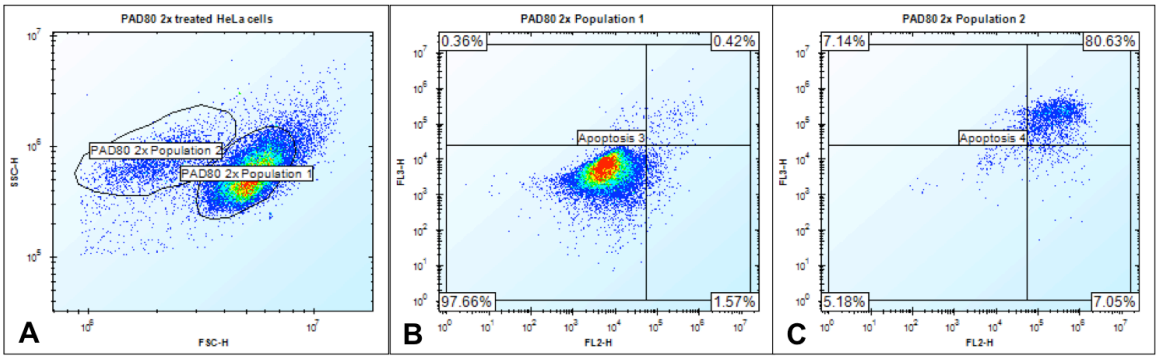

Figure 4A.15. Dot plot of 2x (1:1 N/P) PAD_{80}–60bp treated HeLa cells 24 hours post-exposure as a function of forward scattering size (FSC) and side scattering granularity (SSC) showing main population 1 and subpopulation 2 (A). Dot plot of main population 1 as a function of fluorescence of PE-Annexin V in the FL2 channel and 7-AAD fluorescence in the FL3 channel (B). Dot plot of subpopulation 2 as a function of fluorescence of PE-Annexin V in the FL2 channel and 7-AAD fluorescence in the FL3 channel (C). The majority of subpopulation 2 (81 %) stains positive for both PE-Annexin V and 7-AAD, which correlates to late-apoptotic cells. Main population 1 consists primarily of non-apoptotic cells that stain negative for PE-Annexin V and 7-AAD (98 %).

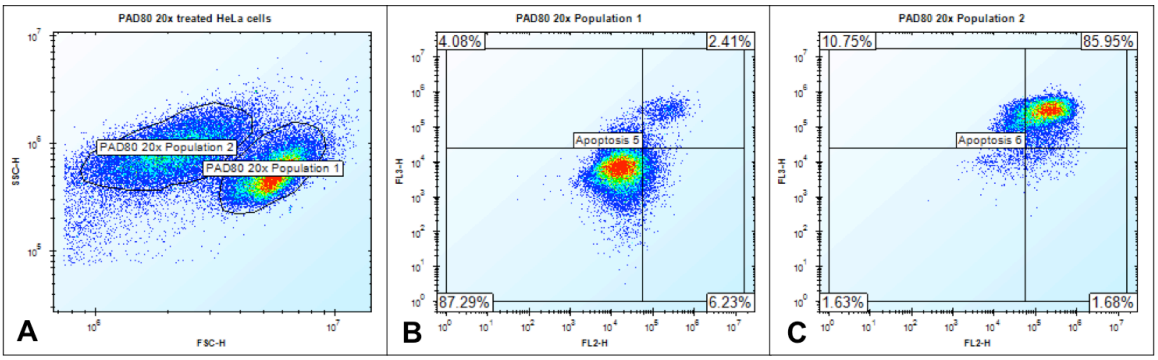

Figure 4A.16. Dot plot of 20x (10:1 N/P) PAD_{80}–60bp treated HeLa cells 24 hours post-exposure as a function of forward scattering size (FSC) and side scattering granularity (SSC) showing main population 1 and subpopulation 2 (A). Dot plot of main population 1 as a function of fluorescence of PE-Annexin V in the FL2 channel and 7-AAD fluorescence in the FL3 channel (B). Dot plot of subpopulation 2 as a function of fluorescence of PE-Annexin V in the FL2 channel and 7-AAD fluorescence in the FL3 channel (C). The majority of subpopulation 2 (86 %) stains positive for both PE-Annexin V and 7-AAD, which correlates to late-apoptotic cells. Main population 1 consists primarily of non-apoptotic cells that stain negative for PE-Annexin V and 7-AAD (87 %).

CHAPTER 5: A Mechanistic Study of the Hydrolysis of Poly[N,N-(Dimethylamino)ethyl Acrylates] as Charge-Shifting Polycations

Samantha Ros[a], Jiexi Wang[a], Nicholas A. D. Burke[a], Harald D. H. Stöver[*,a]

[a] McMaster University, Hamilton, Ontario, Canada, L8S 4L8, Department of Chemistry and Chemical Biology

For table of contents only

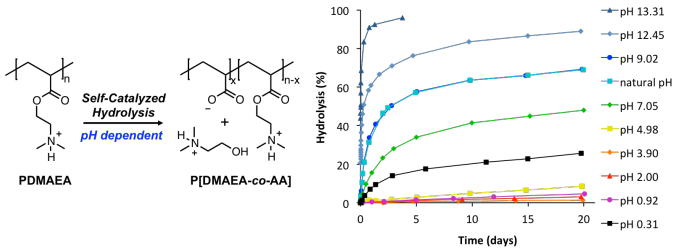

5.1. Abstract

Polycations are used extensively in applications ranging from enhanced oil recovery to biomaterials. Poly[N,N-(dimethylamino)ethyl acrylate] (PDMAEA) has attracted interest for biomaterial applications because of its rapid hydrolysis, however, the mechanism of hydrolysis and the conditions that affect degradation often appear amiss in the field. In this report, a detailed ^{1}H NMR spectroscopy study of the hydrolysis of PDMAEA was carried out between pH 0 and 14. In contrast to a widely held view, the rates of hydrolysis of this polymer were found to be highly pH dependent with half-lives varying from years to minutes as a function of pH. The extent of hydrolysis was also found to be pH dependent, with a distinct plateau at about 50–60 % hydrolysis at pH 7

due to the electrostatic repulsion of anionic carboxylate groups and hydroxide. This was contrasted with the acid-catalyzed mechanism where hydrolysis of PDMAEA at pH 0.3 did not show a plateau in the extent of hydrolysis, reaching 88 % hydrolysis after 8 days at 70 °C. In addition, the effects of neighboring functional groups on DMAEA hydrolysis in copolymers were explored, with anionic, neutral/hydrophilic, and cationic comonomers found to affect the rates of hydrolysis up to 20-fold at pH 7. Finally, two novel analogues of DMAEA with an additional dimethylamino group in different positions of the side-chain were synthesized and polymerized to probe the effect of this added tertiary amine on the hydrolysis of the ester linkages. Poly[1,3-bis(dimethylamino)-2-propyl acrylate] (PBDMAPA) hydrolyzed more than 500 times faster at pH 7 than its linear isomer poly[2-((2-(dimethylamino)ethyl)(methyl)amino)ethyl acrylate] (PDEMEA). These results further highlight the importance of the intramolecular interactions of the dimethylamino substituent of PDMAEA and the effect of proximity and steric hindrance of the amino group as well as neighboring functional groups of comonomers.

5.2. Introduction

Polycations are used extensively in applications including industrial wastewater treatment,[1,2] enhanced oil recovery,[3] and biomedical applications.[4] In particular, polycations with the ability to convert their cationic charge to neutral or anionic groups, called “charge-shifting” polycations, are receiving increasing attention in the biomaterials field.[5-21] Charge-shifting polycations strongly bind to polyanions in their initial cationic state, but then undergo a charge-shifting process that reduces net cationic charge and

leads to dissociation of the polyelectrolyte complex. This property has the potential to be exploited in biomedical applications including DNA delivery,[8-11,13-19,21,27,28] and cell encapsulation.[6] N,N-(Dimethylamino)ethyl acrylate (DMAEA) stands out as one of the most commonly used monomers to develop such charge-shifting materials. The hydrolysis of the DMAEA units in poly[DMAEA] (PDMAEA) to acrylic acid (AA) units was first investigated by McCool and Senogles in 1989.[22] In 2011, Monteiro and co-workers first reported results that suggested that the rate of this charge-shifting hydrolysis of PDMAEA appeared to be independent of solution pH between pH 5 and 10.[23] This work stimulated a number of studies looking to take advantage of the pH independent hydrolysis of PDMAEA.[24-28] In one of these studies, pH-independent hydrolysis was reported to occur over an even wider pH range (pH 1-10).[27] This reported pH-independent hydrolysis stands in contrast to the typical behavior of esters,[29,30,31] including closely related small-molecule DMAE esters.[5] In addition, we have observed pH-dependent hydrolysis for some DMAEA-containing polymers.[6,7] Thus, it seemed worthwhile to examine the hydrolysis of DMAE esters in polymeric systems in greater detail.

Researchers have hypothesized that the hydrolysis of DMAEA may be self-catalyzed, e.g. involving intramolecular interactions of the dimethylamino substituent with the ester carbonyl in both base- and acid-catalyzed mechanisms (Figure 5.1).[5] The hydrolysis of DMAEA analogues, including versions with a methylated quaternary ammonium,[2,23] longer alkyl spacer,[5] and an α-hydroxymethyl substituent,[7] appear to be remarkably sensitive to the nature and position of the neighboring functional groups,

including hydrogen-bonding groups. To the best of our knowledge, the effect of an additional dimethylamino substituent on the rate of hydrolysis had not yet been explored. In addition, the effect of functional groups located on neighboring monomer groups on the hydrolysis of DMAEA needs to be understood. Clarifying the mechanism of DMAEA hydrolysis in polymeric systems, as well as the factors that affect the rate and extent of this hydrolysis, becomes increasingly important as research advances with such degradable polyacrylates in biomaterial applications, especially in DNA delivery for gene therapy.

In this study, we report on three aspects of the hydrolysis of PDMAEA-type polymers. The first and major focus is on describing in detail the effect of pH on the rate and extent of ester hydrolysis in PDMAEA homopolymers. Second, we describe the effects of neutral/hydrophilic (2-hydroxyethyl acrylate (HEA)) and charged comonomers (acrylic acid (AA) and 3-aminopropylmethacrylamide (APM)), on the rate and extent of hydrolysis. Finally, 1,3-bis(dimethylamino)propyl acrylate (BDMAPA) and 2-((2-(dimethylamino)ethyl)(methyl)amino)ethyl acrylate (DEMEA) were synthesized as novel analogues of DMAEA with an additional tertiary amino group and the hydrolysis of the corresponding polymers was studied (Figure 5.2).

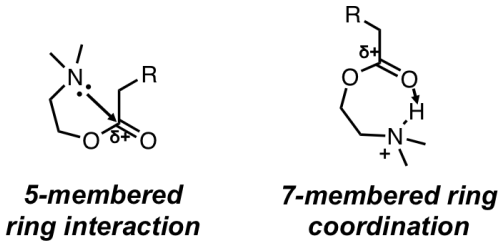

Figure 5.1. Proposed interactions of the dimethylamino substituent with the ester of PDMAEA under basic and acidic conditions *via* 5- or 7-membered rings, respectively.

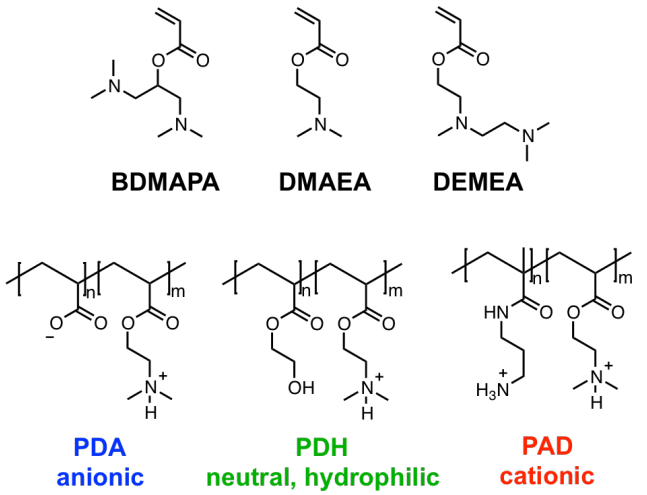

Figure 5.2. BDMAPA and DEMEA as analogues of DMAEA to probe effect of the dimethylamino group on the hydrolysis of PDMAEA. Effect of anionic, neutral/hydrophilic, and cationic comonomers on the hydrolysis of DMAEA units using AA, HEA, and APM, respectively.

5.3. Experimental

5.3.1. Materials

All materials were used as received unless otherwise stated. N,N-(Dimethylamino)ethyl acrylate (98 %), 1,3-bis(dimethylamino)-2-propanol (97 %), 2-{[2-(dimethylamino)ethyl]methylamino} ethanol (98 %), 2-hydroxyethyl acrylate (96 %), acrylic acid (99 %), acryloyl chloride (>97 %), methacryloyl chloride (97 %), triethylamine (≥99 %), 4-cyano-4-(phenylcarbonothioylthio)pentanoic acid (CTP, >98 %), 4,4-azobis(4-cyanovaleric acid) (V501, >97 %), 2,2-dimethoxy-2-phenylacetophenone (DMPA, 99 %), 2,2'-azobis(2-methylpropionamidine) dihydrochloride (Vazo-56, 97 %), sodium hydroxide pellets (≥97 %), 37 % deuterium chloride solution (99 %D), D_2O (>99 %), and N,N-dimethylformamide (99.9 %) were

purchased from Sigma-Aldrich. Acrylic acid was purified by vacuum distillation prior to use. Azobis(isobutyronitrile) (AIBN) (>99 %) was purchased from Dupont and used as received. $CDCl_3$ (99.9% D), C_6D_6 (99.9 % D), D_2O (99.9 % D), and DMSO-*d6* (99.9 % D) were purchased from Cambridge Isotope Laboratories Inc. Dialysis tubing (3.5 kDa) was purchased from Spectrum Laboratories. Benzene (ACS reagent grade) was purchased from Fisher Scientific. 1,4-Dioxane, dimethylsulfoxide (DMSO), and 12 M HCl aq. solution was purchased from Caledon Laboratory Chemicals.

5.3.2. Polymerization of DMAEA

DMAEA was passed neat through a plug of basic alumina prior to use. DMAEA (5 g, 34.9 mmol) and AIBN (57 mg, 0.349 mmol) were dissolved in 50 mL of 1,4-dioxane in a 100 mL round bottom flask equipped with a magnetic stir-bar. The reaction vessel was sealed with a septum and the polymerization mixture was purged with N_2 gas for 1 hour with stirring at room temperature (22 °C). The reaction vessel was then heated in an oil bath at 70 °C for 17 h, and then quenched in an ice-water bath and exposed to air. ^{1}H NMR analysis of the polymerization mixture in $CDCl_3$ showed >90 % conversion. The polymerization mixture was precipitated into 40-fold excess of 1,4-dioxane containing 1 mol eq. of anhydrous HCl, resulting in precipitation of solid white PDMAEA as the hydrochloride salt. The mixture was centrifuged at 3500 rpm for 5 min and the supernatant was discarded. The polymer isolated by centrifugation and then dissolved in 40 mL distilled water and the pH was adjusted to pH 3–4, followed by dialysis with cellulose acetate tubing (3.5 kDa molecular weight cutoff (MWCO)) against

distilled water at pH 3–4. The polymer solution was dialyzed for 2 days with several water bath changes (pH 3–4) and then freeze-dried, resulting in an off-white, glassy solid. The ^{1}H NMR spectrum of PDMAEA in the hydrochloride salt form in D_2O (pH 3-4) was recorded on a Bruker AV600 (Figure 5A.1) and confirms both the homopolymer structure and the absence of residual monomer.

5.3.3. Reversible-Addition Chain-Transfer (RAFT) Polymerization of DMAEA

DMAEA was passed neat through a plug of basic alumina prior to use. DMAEA (1.8 g, 12.6 mmol) was dissolved into 2:1 water:1,4-dioxane at 30 % w/v with 1 mol eq. of HCl added that was cooled in an ice-water bath during the addition. The pH of the solution was adjusted to pH 3.52, followed by the addition of the CTP (13.5 mg, 0.048 mmol) and V501 (2.7 mg, 0.0097 mmol). The reaction vessel was equipped with a magnetic stir bar, sealed with a septum, and purged with N_2 for 45 min at room temperature. The reaction mixture was kept under positive N_2 pressure and placed into a 70 °C oil bath for 2 hours, followed by quenching into an ice-water bath and exposure to air. The polymer was purified by dialysis using cellulose acetate tubing with a MWCO of 3.5 kDa against distilled water adjusted to pH 3-4 over 2 days, with twice daily water bath changes (pH 3-4). The polymer solution was freeze-dried, resulting in PDMAEA in the hydrochloride salt as a pink solid. Herein, PDMAEA obtained by RAFT polymerization will be referred to as PDMAEA-30k. ^{1}H NMR spectrum of PDMAEA-30k was recorded in D_2O (pH 3-4) on a Bruker AVN500 with 512 scans for end group analysis of the dithiobenzoate group (Figure 5A.2).

5.3.4. Synthesis of 1,3-bis(dimethylamino)-2-propyl acrylate (BDMAPA)

1,3-Bis(dimethylamino)propanol (5 g, 34.9 mmol) and triethylamine (TEA) (5.30 g, 52.4 mmol) were dissolved in 100 mL dichloromethane (DCM) in a round bottom flask equipped with a magnetic stir-bar and maintained at 0 °C with an external ice bath. Acryloyl chloride (4.74 g, 52.4 mmol) was added dropwise over 10 min to the stirred reaction mixture, which turned orange/red. After addition was complete, the reaction was left to stir for another 2 h at 0 °C, followed by an additional 2 h at room temperature. The reaction mixture was washed 4 times, each with 40 mL saturated sodium bicarbonate and 40 mL saturated brine solution. The organic layer was dried with anhydrous sodium sulfate, filtered, and concentrated *in vacuo* to give an orange oil containing some precipitate. ^{1}H NMR analysis showed that the solution and precipitate both consisted of the pure monomer. The yield obtained was 87 %. ^{1}H NMR ($CDCl_3$, 600 MHz) δ 6.37 (^{1}H, dd), 6.11 (1H, dd), 5.78 (1H, dd), 5.17 (1H, tt), 2.50 (2H, dd), 2.46 (2H, dd), 2.24 (12H, s); ^{13}C NMR ($CDCl_3$, 600 MHz) δ 165.9, 130.8, 128.9, 70.2, 61.3, 46.2. (Figure 5A.3). HRMS (ESI/TOF) m/z: $[M+H]^+$ Calcd for $C_{10}H_{20}N_2O_2$ 201.1598; Found 201.1597.

5.3.5. Polymerization of BDMAPA

BDMAPA (0.5 g, 2.50 mmol) and 1 mol% DMPA (6.4 mg, 2.5 μmol) were dissolved in 2.5 mL benzene in a 4 mL vial sealed with a septum. The reaction mixture was purged with N_2 for 20 min. The reaction vessel was placed in an ice-water bath and

irradiated with four F8T5-BL 350 nm lamps for approximately 8 h to achieve >70 % conversion as determined by ^{1}H NMR. The polymer was isolated by precipitation into approximately 40 mL hexanes followed by centrifugation. The viscous liquid was re-dissolved in DMSO followed by precipitation into hexanes. This cycle was repeated 4-5 times until residual monomer and other small molecules were removed as seen by ^{1}H NMR. The ^{1}H NMR spectrum of PBDMAPA in D_2O (pH 3–4) was recorded on a Bruker AV600 (Figure 5A.4).

5.3.6. Synthesis of 2-((2-(dimethylamino)ethyl)(methyl)amino)ethyl acrylate (DEMEA)

2-((2-(Dimethylamino)ethyl)(methylamino)ethanol (DEME) (2.0 g, 13.7 mmol) and TEA (1.67 g, 16.4 mmol) were added to 40 mL DCM in a 100 mL round bottom flask equipped with a stir bar, maintained at 0 °C. Acryloyl chloride (1.49 g, 13.7 mmol) was added drop-wise to the stirring reaction mixture over 5 min, resulting in a yellow solution. The reaction mixture was stirred at 0 °C for another 2 h, followed by overnight stirring at room temperature. The reaction mixture was washed 4 times, each with saturated sodium bicarbonate and brine. The organic layer was dried with anhydrous sodium sulfate, filtered, and concentrated *in vacuo*, resulting in DEMEA as an orange liquid in 85 % yield. ^{1}H NMR ($CDCl_3$, 600 MHz) δ 6.34 (1H, dd), 6.07 (1H, dd), 5.75 (1H, dd), 4.19 (2H, t), 2.65 (2H, t), 2.48 (2H, t), 2.36 (2H, t), 2.26 (3H, s), 2.17 (6H, s); ^{13}C NMR ($CDCl_3$, 600 MHz) δ 166.2, 130.8, 128.5, 62.4, 57.3, 56.2, 55.8, 45.8, 42.9. (Figure 5A.5). HRMS (ESI/TOF) m/z: $[M+H]^+$ Calcd for $C_{10}H_{20}N_2O_2$ 201.1598; Found 201.1597.

5.3.7. Polymerization of PDEMEA

DEMEA (0.5 g, 2.5 mmol) and 1 mol% Vazo-56 was dissolved in 2.5 mL distilled water at pH 3–4 in a 4 mL vial sealed with a septum. The reaction mixture was purged with N_2 for 20 min. The reaction vessel was heated to 55 °C for 28 h to achieve 67 % conversion as determined by ^{1}H NMR. The polymer was purified by dialysis using cellulose acetate tubing with a MWCO of 3.5 kDa against distilled water at pH 3–4 over 2 days with several water bath changes (pH 3–4). The polymer solution was then freeze-dried, resulting in an off-white solid. ^{1}H NMR spectrum of PDEMEA as the hydrochloride salt in D_2O (pH 3–4) was recorded on a Bruker AV700 (Figure 5A.6).

5.3.8. Copolymerization of DMAEA and 2-Hydroxyethyl Acrylate (HEA)

The drift in DMAEA and HEA copolymerizations was assessed to confirm that a random copolymer sequence was formed. DMAEA/HEA copolymerizations (10 wt.% total monomer loading in DMSO-*d6*, 1 mol% AIBN) with initial monomer feeds of 15:85, 38:62, 60:40, 78:22, and 91:9 mol ratios, respectively, were followed using a Bruker AVN500 MHz spectrometer. Samples were heated at 55 °C in a water bath and analyzed by NMR at various time intervals. Incremental relative monomer consumptions of each monomer were calculated for low conversion steps (5–10 %) by integrating the vinyl signals of DMAEA (6.31 ppm) and HEA (6.37 ppm) with respect to the combined dimethylamino singlet of DMAEA in both the monomer and polymer (ca. 2.2 ppm). Reactivity ratios were estimated by fitting the instantaneous copolymer composition

equation to the data obtained by the least squares method as previously reported[6] (Figure 5A.7).

Preparative copolymerizations of DMAEA and HEA with initial monomer mol feed ratios of 83:17, 50:50, 21:79, and 0:100, respectively, were carried out at a concentration of 1 g total monomer in 20 mL of 1,4-dioxane with 1 mol% of AIBN. The reaction mixtures were heated at 70 °C for 3 h followed by quenching in an ice-water bath and exposure to air. The homopolymerization of HEA was heated for 16 h at 70 °C. ^{1}H NMR analysis of the polymerizations showed total monomer conversions of approximately 25, 50, 82, and 97 % conversion for P[DMAEA-*co*-HEA] (PDH) 83:17, 50:50, 21:79, 0:100, respectively. Each polymerization solution was added to approximately 80 mL of hexanes, followed by centrifugation. The supernatant was removed, and the remaining yellow oils were dissolved in 10 mL distilled water and adjusted to pH 3–4 with 1 M HCl. The polymer solutions were dialyzed using cellulose acetate tubing (3.5 kDa MWCO) against distilled water at pH 3–4. Dialysis water baths were replaced twice daily for 2 days, and then the polymer solutions were freeze-dried. The PDH copolymers were analyzed by ^{1}H NMR spectroscopy (Figures 5A.8, 5A.9, and 5A.10), showing relative mol compositions of 77:23, 46:54, and 19:81 DMAEA:HEA, called PDH_{77}, PDH_{46}, and PDH_{19}, respectively. Herein PDH_0 will be referred to as PHEA. The ^{1}H NMR spectrum of PHEA in D_2O is shown is Figure 5A.11.

5.3.9. Copolymerization of DMAEA with Acrylic Acid (AA)

The drift in DMAEA and AA monomer feed ratios were assessed experimentally due to their anticipated different reactivities. DMAEA/AA copolymerizations of 10 wt.%

total monomer loading in DMSO-*d6* with 1 mol% AIBN with initial monomer feeds of 77:23, 48:51, and 25:75 mol ratios, respectively, were conducted using a 500 MHz Bruker Avance spectrometer. The samples were heated to 55 °C and ^{1}H NMR spectra were recorded in approximately 5–10 min intervals. Incremental relative monomer consumptions of each monomer were calculated for low conversion steps (5–10 %) by integrating the vinyl signals of DMAEA and AA with respect to the combined dimethylamino singlet of DMAEA in both the monomer and polymer (ca. 2.2 ppm). The drift in monomer consumption is shown in Figure 5A.12, and reactivity ratios were estimated by fitting the instantaneous copolymer composition equation to the data obtained by the least squares method as previously reported[6] (Figure 5A.13).

A preparative scale copolymerization of DMAEA and AA (1 g total monomer loading) with a 49:51 initial monomer feed ratio, respectively, was conducted in DMSO as described above. The reaction mixture was heated to 55 °C for 3.7 h for low conversion (~42 %) to limit drift in monomer feed and copolymer composition. The polymer was precipitated into approximately 80 mL of hexanes, followed by centrifugation. The solid was dissolved in 10 mL distilled water and the pH was adjusted to pH 3–4 with 1 M HCl. The solution was transferred into cellulose acetate tubing (3.5 kDa MWCO) for dialysis against distilled water at pH 3–4. Dialysis baths were replaced twice daily for 4 days, and then the polymer solution was freeze-dried. The polymer was analyzed by ^{1}H NMR spectroscopy (Figure 5A.14) showing relative mol composition of 58:42 of DMAEA and AA, respectively, called PDA_{58}.

5.3.10. Gel Permeation Chromatography

Gel permeation chromatography (GPC) was conducted using a Waters GPC consisting of a 717plus autosampler, 515 HPLC pump, 2414 refractive index detector, Ultrahydrogel (120, 250, and 500) columns (30 cm × 7.8 mm (inner diameter); 6 μm particles) using poly[ethylene glycol] standards ranging from 106 Da to 881 kDa (Waters Inc.) for a 15-point, third-order polynomial calibration. The mobile phase was a 1 M acetic acid–sodium acetate buffer at pH 4.8.

5.3.11. Hydrolysis of PDMAEA

The hydrolysis of PDMAEA (0.5 wt.%) was conducted in D_2O solutions ranging from pH 0.31 to 13.31. The pH values were recorded with a Corning pH meter 440 and VWR SympHony pH electrode calibrated with pH 4.00, pH 7.00, and pH 10.00 buffers. Initial polymer solution pH values were measured after PDMAEA was dissolved in the corresponding acid, base, or buffer solution. Where needed, 1 M DCl or 1 M NaOD were added to the corresponding solution to adjust the pH. The solution used, and the corresponding pH values, are listed as follows: 1 M DCl (pH 0.31), 100 mM DCl (pH 0.92), 100 mM phosphate (pH 2.00 and 7.05), 100 mM acetate (pH 3.90 and 4.98), 100 mM borate (pH 9.02), 100 mM NaOD (12.45), 1 M NaOD (pH 13.31). The hydrolysis of PDMAEA-30k was conducted at pH 7.00 in 100 mM phosphate buffered solution. As the hydrolysis solutions were prepared in D_2O, the pD of the solutions can be approximated by adding 0.4 from the recorded pH value.[32] The solutions were transferred to 5 mm NMR tubes, maintained at room temperature (22 °C) and ^{1}H NMR spectra were recorded

at various time intervals on a Bruker AV600. Percent hydrolysis of DMAEA was calculated by comparing the integrations of the CH_2O– methylene signal of the ester in the polymer (ca. 4.5 ppm) and the alcohol of dimethylaminoethanol (DMAE) small-molecule byproduct (ca. 3.9 ppm), as shown in Figure 5A.15. Pseudo-first order kinetic graphs were plotted using the data points within the initial 20 % hydrolysis, with the exception of the hydrolysis experiment at pH 13.31, where the data points within the initial 50 % hydrolysis were analyzed. Initial rates of hydrolysis ($k_{initial}$) were obtained from the slopes of the linear trend lines of the pseudo-first order kinetic plots (Figures 5A.16, 5A.17, and 5A.18).

5.3.12. Hydrolysis of PBDMAPA and PDEMEA

Hydrolysis of PBDMAPA and PDEMEA at 0.5 wt% was conducted at pH 5, 7, and 9, using 100 mM acetate, phosphate, and borate buffers, respectively. Initial pH values of the polymer solutions were measured as described above. The samples were maintained at room temperature (22 °C), and ^{1}H NMR spectra were recorded at various time intervals. For PBDMAPA, percent hydrolysis was calculated by comparing the ratio of the methine CH–O proton of the ester in the polymer (ca. 5.4 ppm) to that of the small molecule alcohol by-product 1,3-bis(dimethylamino)-2-propanol (ca. 4.4 ppm), as shown in Figure 5A.19. For PDEMEA, percent hydrolysis was calculated by comparing the methylene CH_2–O signal of the ester in the polymer (ca. 4.2 ppm) to that of the small molecule alcohol 2-{[2-(dimethylamino)ethyl]methylamino} ethanol (ca. 3.8 ppm), as shown in Figure 5A.20.

5.3.13. Hydrolysis DMAEA Copolymers

The hydrolysis of DMAEA copolymers at 0.5 wt% was conducted in 100 mM phosphate buffer at pH 7, room temperature (22 °C). Initial pH values of the polymer solutions were measured as described above. ^{1}H NMR spectra were recorded at various time intervals. Percent hydrolysis of DMAEA copolymers was calculated as described for PDMAEA with the exception of PDH copolymers where the methylene CH_2O– of HEA units overlaps partially with DMAEA units. Thus, percent hydrolysis was calculated using the dimethylamino- singlet of the DMAE in the polymer and small molecule (ca. 2.9 ppm) as an internal standard for 6 protons, as shown in Figure 5A.21 for a representative example. Hydrolysis of PDMAEA calculated through this method gives similar results.

5.4. Results and Discussion

5.4.1. Polymerizations

The polymerization of DMAEA was conducted in aqueous conditions at pH 3–4 to prevent premature hydrolysis. Purification of PDMAEA by dialysis was also conducted at pH 3–4 followed by isolation of the polymer by freeze-drying, resulting in the polymer in the hydrochloride salt form where the polymer is stable as confirmed by ^{1}H NMR where the integrations of the pendant side-chains correlate with the integrations of the polymer backbone (Figure 5A.1). A sample of PDMAEA with a higher MW and

narrower MW distribution was prepared by RAFT polymerization to study the possible effect of molecular weight (MW) on hydrolysis. CTP and V501 were selected as the RAFT agent and initiator, respectively, and allowed for a controlled polymerization as indicated by the low dispersity obtained ($Đ$ = 1.25). End group analysis of the dithiobenzoate group by ^{1}H NMR (Figure 5A.2) showed a degree of polymerization (DP) of about 254, corresponding to a MW (Mn) of approximately 36,400 g/mol, which was in close agreement with 31,200 g/mol as the Mn obtained by GPC analysis.

The polymerization of BDMAPA was particularly challenging as initial attempts to polymerize the monomer in similar conditions stated above for DMAEA was not successful due to significant hydrolysis, especially with the elevated temperatures required for thermal initiated radical initiators such as Vazo-56 and AIBN. Polymerization of BDMAPA was then attempted in organic solvents such as 1,4-dioxane, DMSO, acetonitrile, and toluene, however only low MW polymers (~2000 g/mol) were obtained (Figure 5A.22). It was suspected that chain-transfer to the BDMAPA group (monomer or polymer-bound) might be occurring by abstraction of the tertiary hydrogen atom. This would result in a more stable tertiary radical over the propagating secondary radical of the acrylate polymer. Thus, DMPA photo-initiated polymerization at 0 °C in benzene was attempted to minimize chain-transfer and ester degradation. These conditions provided polymers of reasonable MWs with Mn around 9000 g/mol with ester units intact.

Interestingly, the polymerization of DEMEA, which is a constitutional isomer of BDMAPA, did not suffer the same instability issues. Thus, polymerization was conducted

in conditions similar to those used for DMAEA and resulted in a polymer MW (Mn) of 15200 g/mol, similar to that seen for PDMAEA. As DEMEA does not contain tertiary hydrogen atoms available for hydrogen abstraction, this gave some support to the suggestion that chain-transfer was responsible for the low MW polymers formed during polymerization of BDMAPA.

DMAEA and AA were anticipated to have differing reactivity especially in aqueous conditions due to the pH sensitivity of AA that affects the reactivity of the monomer.[33] Thus, copolymerization was conducted in organic solvent and reactivity ratios were determined by following relative monomer consumption within small conversion steps throughout copolymerization. At high DMAEA compositions, there was very little drift observed (~4 %) in remaining relative DMAEA monomer feed after about 60 % conversion. With increasing mol feeds of AA, drift in monomer consumption was more evident, particularly at higher conversion beyond ~40 %, with about 10 % drift in DMAEA feed after 60–70% conversion. The data obtained was used to estimate reactivity ratios by the Least Squares method, giving r_1 and r_2 values of 1.29 and 0.49 for DMAEA and AA, respectively, indicating a slight preference for incorporation of DMAEA in copolymerizations. Joint confidence regions at 95 % confidence level for the reactivity ratios obtained for DMAEA/AA are provided in the Supporting Information (Figure 5A.23). Thus, preparative copolymerization of DMAEA and AA was conducted and limited to low conversion (~40 %) to prevent significant drift in composition. Copolymerization of DMAEA and AA with an initial feed ratio of 49:51 resulted in a

copolymer with 58:42 mol composition, respectively, which is in agreement with the reactivity ratios obtained.

Little compositional drift was expected to occur during copolymerization of DMAEA with HEA since they are both acrylates. This was confirmed as similar reactivity ratios were obtained for DMAEA and HEA, 1.13 and 0.94, respectively, and as copolymer compositions were not very different to the initial monomer feed ratios. Joint confidence regions at 95 % confidence level for the reactivity ratios obtained for DMAEA/HEA are provided in the Supporting Information (Figure 5A.24).

A summary of polymer properties including composition, conversion, MW, and dispersity is included in Table 1.

Table 5.1. Summary of polymer properties.

Polymer name	DMAEA Monomer Feed (mol%)[a]	DMAEA Copolymer Composition (mol%)[a]	Conv. (%)[a]	Mn[b] (kg/mol)	$Đ^b$
PDMAEA	100	100	91	15.3	2.12
PDMAEA-30k	100	100	95	31.2	1.25
PBDMAPA	-	-	77	9.1	1.49
PDEMEA	-	-	67	15.2	2.11
PDA_{58}	49	58	42	33.5	1.81
PDH_{77}	83	77	25	7.3	1.79
PDH_{46}	50	46	50	7.3	1.56
PDH_{19}	21	19	82	9.3	3.35
PHEA	-	-	97	1.5	1.46

[a] Data obtained from ^{1}H NMR analysis. [b] Data obtained from GPC analysis with 1 M acetic acid-acetate at pH 4.8 as the mobile phase using PEG standards for MW calibration.

5.4.2. Hydrolysis of PDMAEA – Effect of pH

The hydrolysis of simple esters like ethyl acetate (EtAc) has a strong dependence on pH, and exhibits a V-shaped log k_{obs} *vs*. pH plot where acid- and base-catalyzed processes dominate on the low and high pH sides of the minimum, respectively (Figure 5A.25).[29,30,31] N,N-Dimethylaminoalkyl esters, such as DMAEA and DMAE isobutyrate (DMAEIB), also show pH-dependent hydrolysis but their log k_{obs} *vs*. pH plots are slightly more complex as protonation of the amino group, which occurs near the pKa (~8.4), enhances hydroxide-catalyzed hydrolysis but slows acid-catalyzed hydrolysis (cf. EtAc) as shown in Figure 5A.25.[5] Protonation of the dimethylamino group may make the DMAE unit a better leaving group, lead to increased hydroxide concentration near the ester, or enable H-bonding between the ammonium ion and ester group, as shown in Figure 5.1.[5] But, protonation of the amino group could lead to electrostatic repulsion of protons that would retard hydrolysis at low pH when it is acid-catalyzed.

The hydrolysis of PDMAEA was studied at various pH ranging from 13.31 to 0.31 at room temperature (22 °C), and the results are summarized in Figure 5.3. The initial pH value of each polymer solution was recorded after dissolution of the polymer in the buffer, and after any (minimal) pH adjustment back to target values.

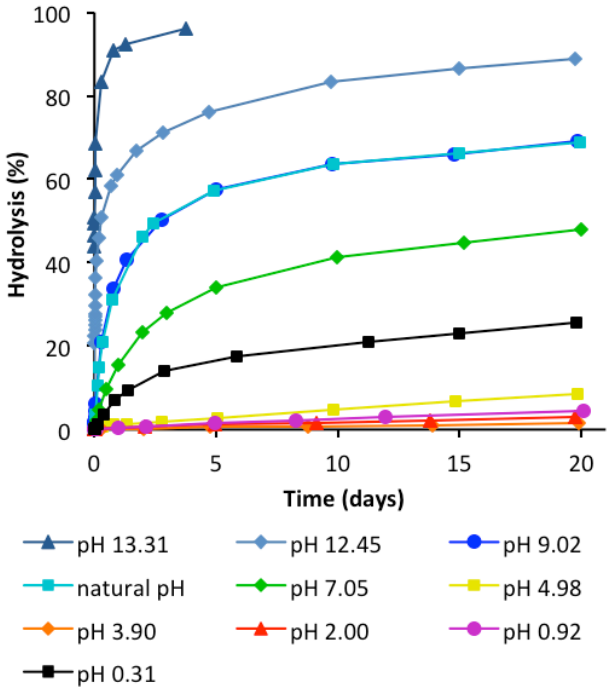

Figure 5.3. Hydrolysis of PDMAEA at pH 13.31 to 0.31 at room temperature (22 °C). Natural pH refers to a 0.5 wt% solution of PDMAEA (free-base form) in unbuffered D_2O.

The initial rates of hydrolysis were calculated from data at ≤20% hydrolysis for most of the curves shown in Figure 5.3. In the case of hydrolyses at pH 13.31 and 12.45, which were very rapid, the initial rate constants were obtained from data up to 50 % hydrolysis. The data showed linear pseudo-first order kinetics (Figures 5A.16-5A.18), and the obtained initial rate constants ($k_{initial}$) plotted as a function of pH are shown in Figure 5.4.

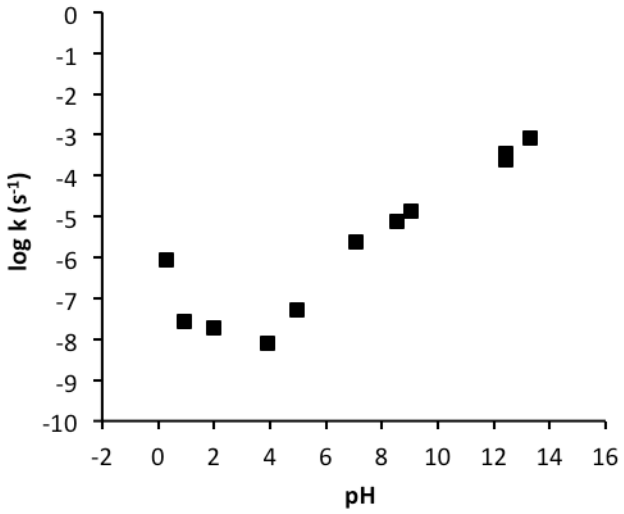

Figure 5.4. Log k *vs*. pH plot for initial pseudo first order rates ($k_{initial}$) of PDMAEA hydrolysis.

The data in Figures 5.3 and 5.4 clearly show that the hydrolysis of PDMAEA is pH dependent with the initial rate falling by five orders of magnitude between pH 13.3 and pH 3.9. This corresponds to hydrolysis half-lives of about 14 min and 2.7 years, respectively. The rate of hydrolysis increased with increasing pH at pH >4, in agreement with a hydroxide-mediated mechanism of ester hydrolysis under these conditions. The rate of hydrolysis appeared to reach a minimum around pH 3–4 and then increased again as pH was lowered further, which is consistent with an acid-catalyzed mechanism of ester hydrolysis at pH <3. The half-life obtained at pH 0.31 was approximately 9 days, which is on a similar timescale to the half-life of about 3.5 days at pH 7.05.

The initial rates of hydrolysis obtained for PDMAEA in this study are similar to rates reported by Hennink and co-workers[5] for the hydrolysis of the small-molecule analogue DMAEIB across the range of pH, both showing a minimum rate of hydrolysis

around pH 4 in addition to a slight shoulder in rates around pH 8 likely corresponding to the pKa of the ammonium (Figure 5A.25). At first glance, the similarity is not surprising because the repeat unit of PDMAEA is nearly identical to DMAEIB, however, polymeric esters are often much more resistant to hydrolysis than similar small-molecule esters. For instance, PDMAEMA is several orders of magnitude more stable to hydrolysis than the monomer.[5] That this effect is not seen with the polyacrylate is thought to be due to reduced steric hindrance, and greater hydrophilicity along the polymer backbone, cf. the polymethacrylate.

Figures 3 and 4 clearly show that the hydrolysis of PDMAEA is pH dependent as expected for such ester groups. The reports of pH-independent hydrolysis,[23,27] were probably the result of inadequate pH control during dissolution and hydrolysis, in particular using solutions with too little buffer capacity to deal with the pH changes caused by dissolution of PDMAEA. A 1% solution of the free-base form of PDMAEA in neat, buffer-free D_2O has pH 8.5–9 not 7. A similar pH (i.e., 8.5-9) would have been obtained when 30-40 mg of PDMAEA (210-280 μmol amine) was dissolved in 0.75 mL of a pH 5.5 acetate buffer in D_2O (150 mM; 13.5 μmol acetic acid) because the solution has a 15-20-fold excess of amine wrt acid.[23,27] The likely reason for reports of "pH independent" rates of hydrolysis is that each of the solutions had a similar pH, and one that was often quite different than the initial pH of the solvent or buffer system.

The hydrolysis of PDMAEA in the free-base form in neat, commercial D_2O was repeated in this study as described by others. The pH in the resulting solutions is sometimes described as "natural pH", and was measured by us to be 8.54 initially, drifting

up to 8.74 after about 5 days (~57 % hydrolysis). As seen in Figure 5.3, the hydrolysis at this natural pH in an un-buffered system overlays very closely with the 100 mM borate-buffered system at pH 9.02. The drift from initial pH in this borate-buffered hydrolysis experiment did not exceed 0.1 pH units. Thus, it is useful to have sufficient buffering capacity to deal with potential changes in pH as the result of hydrolysis.

5.4.3. Hydrolysis of PDMAEA – Extent of Hydrolysis

The initial rates of hydrolysis of PDMAEA observed here are very similar to those reported for the small-molecule analogue N,N-(dimethylamino)ethyl isobutyrate.[5] However, it was noticed in this study, as well as earlier ones, that PDMAEA hydrolysis slows dramatically as it approaches approximately 50–60 % hydrolysis at pH 7. This degree of hydrolysis corresponds to a polymer chain with approximately zero net charge at pH 7 (i.e., equal numbers of carboxylate and ammonium ions). This slowing near 50 % hydrolysis has been hypothesized to be due, in part, to the growing electrostatic repulsion of hydroxide anions by the carboxylates formed after DMAE ester hydrolysis.[5,7,22,25] In contrast, at low pH where hydrolysis is acid-catalyzed, hydrolysis would not be expected to plateau because the polymer is cationic throughout polymerization and water is the principal nucleophile (Figure 5.5). Protonation of the esters in the acid catalyzed mechanism is likely more difficult than for simple neutral esters (small-molecule or polymeric) because of repulsion from the ammonium ions. The hydrolyses of PDMAEA at pH 7 and pH 0.31 were conducted at 70 °C as accelerated experiments to study the extent of hydrolysis, and the results are shown in Figure 5.6.

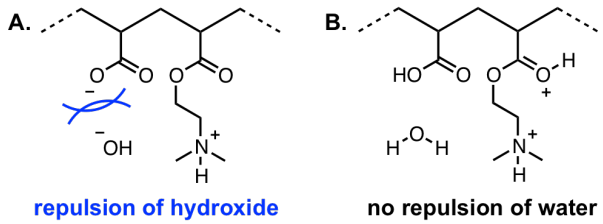

Figure 5.5. (**A**) Anionic repulsion of hydroxide anions may limit the extent of DMAEA hydrolysis at pH 7 under base-catalyzed mechanism. (**B**) Acid-catalyzed mechanism of hydrolysis at pH 0.3 involves neutral water as the nucleophile and decrease of proton–DMAEA electrostatic repulsion with progressive hydrolysis.

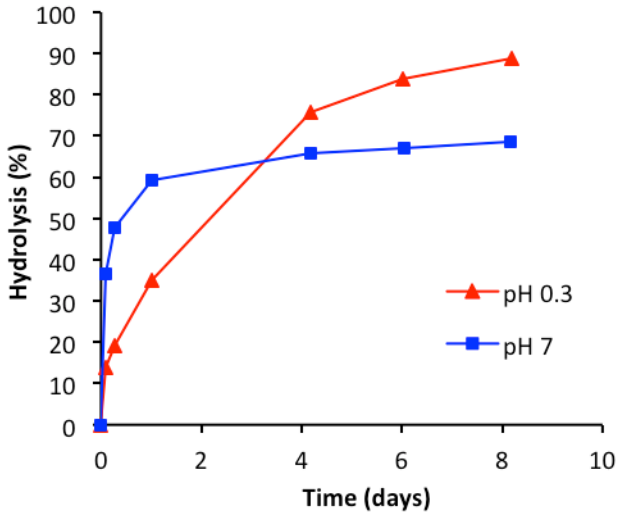

Figure 5.6. Hydrolysis of PDMAEA at pH 0.3 and pH 7 at 70 °C.

The hydrolysis of PDMAEA at pH 7 was rapid initially but then slowed and reached a plateau near 60 %, similar to experiments at room temperature, however it took just a day due to the higher temperature. At pH 0.3, the initial rate of hydrolysis was slower than at pH 7 as expected from the rates obtained at room temperature. However, it did not plateau near 60 %, as seen at pH 7, and crossed the pH 7 curve reaching 88 % hydrolysis after 8 days. The main nucleophile at low pH is water, a neutral species, so the charge on the polymer and electrostatic repulsion are not important. At high pH, the hydrolysis rates

for polyacrylamides are called "auto-retarded" as the carboxylate anions formed initially repel the approach of more hydroxide.[34,35] These results are consistent with the plateau in hydrolysis observed here for PDMAEA under more basic conditions being caused by repulsion of hydroxide anions by carboxylate units of the polymer. As the acid-catalyzed hydrolysis of PDMAEA neared completion, this suggests that the extent of hydrolysis for PDMAEA and related charge-shifting polymers can be controlled by pH, and the hydrolysis of such acrylic polymers may proceed quantitatively under strongly acidic conditions.

It should be noted that the ionic strengths of the solutions varied somewhat over the pH range. The ionic strength of the solution has the potential to play an important role in both the rate and extent of PDMAEA hydrolysis as it can affect electrostatic interactions or polymer conformation. However, a previous study found little effect upon addition of up to 500 mM sodium chloride on the hydrolysis of APM-DMAEA copolymer with 88% DMAEA in a phosphate buffer (50 mM, pH 7) at 37 °C.[6]

5.4.4. Hydrolysis of PDMAEA – Effect of MW

The PDMAEA-30k was synthesized by RAFT polymerization to study the possible effect of MW and broad dispersity on hydrolysis. GPC traces for PDMAEA synthesized from conventional free radical (PDMAEA-15k) and RAFT polymerization are shown in Figure 5A.26 and the results of hydrolysis studies at pH 7 are shown in Figure 5A.27. Polymer MW and dispersity were not anticipated to have a significant effect as other studies have shown little effect on PDMAEA hydrolysis for MWs ranging

from about 3,000 to 10,000 g/mol.[23,27] In the current study, the hydrolysis of PDMAEA-30k showed the same initial rate of hydrolysis as PDMAEA-15k of lower MW and broader dispersity. After about 1 day, the hydrolysis of PDMAEA-30k appeared to follow the same trend as PDMAEA-15k, though slightly slower. The hydrophobic dithiobenzoate end group of PDMAEA-30k may cause a slight reduction to the hydrophilicity on average in the vicinity of the ester groups, leading to a decrease in the rate of hydrolysis. On the whole, the results suggest that MWs of up to ca. 30,000 g/mol do not significantly affect the rate of hydrolysis of PDMAEA, which is in agreement with previous studies.[23,27]

5.4.5. Hydrolysis of PBDMAPA and PDEMEA: Effect of Dimethylamino Substituent

PBDMAPA and PDEMEA are analogues of PDMAEA with an additional tertiary amine in the side-chain. In PBDMAPA, the additional amine is in a symmetrical branched structure with the same proximity to the ester group, whereas the side-chain of PDEMEA is linear with the additional amine positioned further from the ester (Figure 5.2). The polymers of these constitutional isomers were studied to extend our probe of the effect of pendant dimethylamino groups on the reactivity of the ester. The hydrolyses of PBDMAPA, PDMAEA, and PDEMEA, were conducted at pH 7, room temperature, and the results are shown in Figure 5.7.

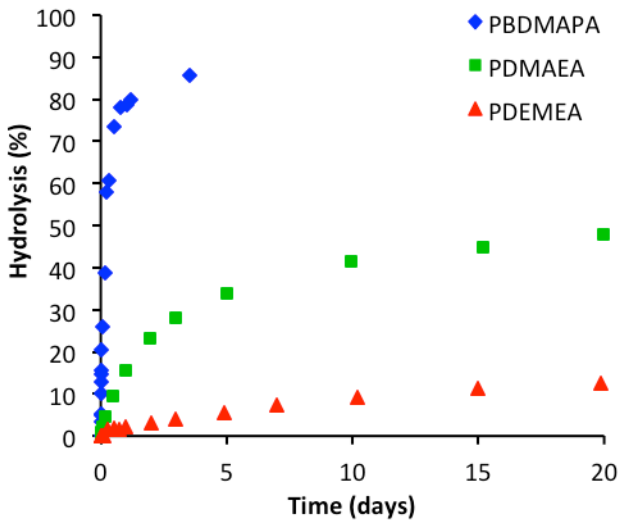

Figure 5.7. Hydrolysis of PBDMAPA, PDMAEA, and PDEMEA at pH 7, 22 °C.

The hydrolysis of PBDMAPA was much faster than for PDMAEA, approaching complete hydrolysis within several days. In contrast, the hydrolysis of PDEMEA is much slower than that of PDMAEA, reaching only about 16 % hydrolysis after 25 days. The initial rates of hydrolysis of PBDMAPA and PDEMEA obtained within the first 20 % hydrolysis showed reasonably linear pseudo-first order kinetics (Figure 5A.28 and 5A.29). The initial rate of hydrolysis of PBDMAPA was more than 500 times faster than PDEMEA and more than 20 times faster than PDMAEA. The stark difference in the rate of hydrolysis of the constitutional isomers was surprising. The branched structure of the side-chain of BDMAPA units may allow both dimethylamino groups to interact with the ester, or it is possible that interaction with neighboring or more remote ester groups becomes more likely. The proximity of both amino groups to the backbone may result in a more polar environment around the ester groups. In contrast, the linear structure of the DEMEA side-chain makes the inner amino group more sterically hindered while

interaction of the terminal amino group with the ester would require the formation of an 8- or 10–membered ring. These results suggest that the hydrolysis of DMAE esters is strongly influenced by the intra-molecular interaction of the dimethylamino group with the ester. This may in future be tested further by probing the reactivity of more sterically hindered dialkylaminoethyl acrylates.

Another possible reason for the slow hydrolysis of PDEMEA was revealed in the ^{1}H NMR spectrum of the polymer in D_2O at pH 3-4 (Figure 5A.6). The chemical shift of the inner methyl group is significantly lower (ca. 2.5 ppm) than that for the terminal methyl groups (ca. 3.0 ppm), suggesting that the terminal amine is preferentially protonated. This amine may be in a more hydrophilic environment as it is further from the polymer backbone making it easier to protonate than the inner amine. This is in contrast to PBDMAPA, where the equivalent amino groups will spend an equal amount of time protonated. This is reflected in the ^{1}H NMR spectrum of PBDMAPA (Figure 5A.4) as the signal for the methyl groups appears at ca. 3.0 ppm as a broad signal, which indicates protonation of the amine groups that is in rapid exchange with each other. For PDEMEA, having the ammonium cation at the terminal position suggests that there may be a correlation between the potential inductive effects of the ammonium cation and the reactivity of the ester, which may be another possible explanation for its decreased reactivity towards hydrolysis relative to PBDMAPA. This effect of the ammonium cation is in agreement with the comparison of DMAE esters relative to simple esters like EtAc (Figure 5A.25). Future work may involve probing the effects of methylated, quaternized ammonium derivatives of the PDMAEA, PDEMEA, and PBDMAPA, to study the

potential electron-withdrawing effects of the cation through induction in the absence of the acid and base interactions of the tertiary ammonium and amine with the ester.

5.4.6. Effect of Comonomer on DMAEA Hydrolysis

Copolymers of DMAEA with acrylic acid (AA) and 2-hydroxyethylacrylate (HEA) were synthesized and their hydrolysis behavior was compared to that of a DMAEA/3-aminopropylmethacrylamide (APM) copolymer that was reported earlier. This allowed us to probe the effect of anionic, neutral/hydrophilic, and cationic comonomers, respectively, on the hydrolysis of DMAEA. The hydrolysis of P[DMAEA-*co*-AA] (PDA), P[DMAEA-*co*-HEA] (PDH), and P[DMAEA-*co*-APM] (PAD) with DMAEA contents of 58, 46, and 49 mol%, respectively, was studied at pH 7 and room temperature (22 °C) (Figure 5.8). PAD_{49} had been synthesized and its hydrolysis reported, in a previous study.[36]

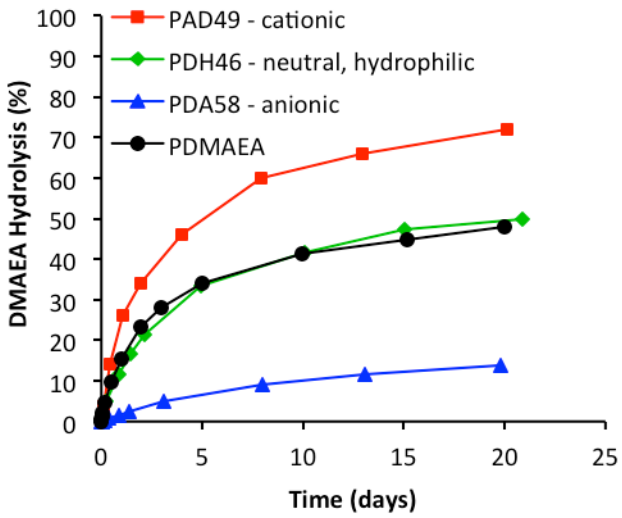

Figure 5.8. Hydrolysis over time of PDH_{46}, PAD_{49}, PDA_{58}, and PDMAEA at pH 7, room temperature (22 °C). Data for PAD_{49} from ref.[36]

The hydrolysis of DMAEA within PDA_{58} was distinctly slower than in PDMAEA and the other copolymers, reaching only 14 % percent hydrolysis after 20 days. This was not surprising because at that point the copolymer had a composition of 50:50 DMAEA/AA, the same composition at which hydrolysis of the homopolymer PDMAEA reached a plateau. As discussed above, the origin of the limiting extent of hydrolysis of PDMAEA at pH 7 is further confirmed here by the slow hydrolysis of PDA_{58}, emphasizing the effect of neighboring anionic groups on hydroxide-mediated ester hydrolysis. The net-charge of the polymer would also be close to neutral, which may result in a more hydrophobic, collapsed polymer conformation that would prevent hydroxide from attacking remaining DMAE esters.[6,7] In addition to the electrostatic repulsion of hydroxide anions, the anionic carboxylates of AA units might ion-pair with the protonated dimethylammonium cation of DMAEA units, which may also disrupt the intra-molecular activation pathways of DMAE esters and slow hydrolysis.

Dilution of the DMAEA with about 50% of neutral, hydrophilic HEA had little effect as the PDH_{46} hydrolysis curve overlays very closely with the PDMAEA curve (Figure 5A.30). This was somewhat surprising as it was anticipated that HEA comonomers would decrease the charge density on the polymer chain and reduce the impact of the negative charges formed during hydrolysis. PDH_{77} behaved similarly to PDH_{46}, but PDH_{19}, which has 81% HEA, allowed a greater extent of DMAEA hydrolysis after 21 days (61% *vs*. ~50% for PDMAEA, PDH_{46} and PDH_{77}). It was also interesting that there was little formation of ethylene glycol (<1%; Figure 5A.31) that would result

from the hydrolysis of 2-hydroxyethyl esters of HEA units. This suggests that the DMAE group does not promote the hydrolysis of neighboring esters. As a control, the homopolymer of HEA (PHEA) was studied at pH 7 in the presence and absence of triethylamine (~ 1 eq. relative to HEA units). PHEA did not show significant signs of hydrolysis after 20 days in either case (Figure 5A.31), suggesting that tertiary amines (ammonium ions) that are not attached to the polymer do not catalyze ester hydrolysis under these conditions. Thus, the hydrolysis of DMAEA was not significantly affected by the presence of a neutral, hydrophilic comonomer. In addition, the presence of DMAEA does not appear to affect the stability of neighboring acrylate esters, suggesting that its hydrolysis may be promoted through intra-side-group interactions. This may also include increased reactivity of DMAE esters though inductive effects when in the positively charged ammonium form, potentially rendering the corresponding alcohol a better leaving group relative to ethylene glycol for HEA esters.

Interestingly, the hydrolysis of DMAEA within PAD_{49} showed a faster rate of hydrolysis relative to PDMAEA, likely because the polymer remains cationic throughout hydrolysis of the DMAEA groups, unlike PDH and PDA copolymers, which may attract hydroxide anions and facilitate further DMAE ester hydrolysis. The increased rate of DMAEA hydrolysis in PAD_{49} might also be due to the neighboring amide groups of APM, which are more hydrophilic than esters and further may hydrogen-bond with the DMAEA ester group. Reactivity ratios of 0.37 and 0.89 for DMAEA and APM, respectively,[6] suggest that DMAEA units are likely to be next to APM units and thus may experience amide hydrogen-bonding interactions with the ester. Another possibility,

attack of the primary amine on the ester to form an amide and release DMAE, was examined in our previous study,[6] but there was no evidence that this was an important pathway. The hydrolysis of PAD_{49} also examined at pH 5 where attack by a primary amine would be even less likely (Figure 5.9).

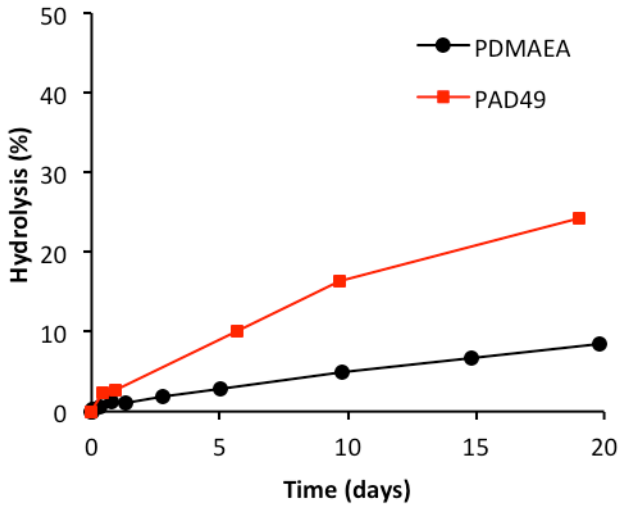

Figure 5.9. Hydrolysis of PAD_{49} and PDMAEA at pH 5, room temperature (22 °C).

The hydrolysis of PAD_{49} and PDMAEA were slower at pH 5 than pH 7 as expected, however the hydrolysis of DMAEA within PAD_{49} remained significantly faster than in the homopolymer PDMAEA. These results suggest that the accelerated rate of DMAEA hydrolysis is not due to reaction with the primary amine, but instead is due to the higher cationic charge-density in the later stages of hydrolysis, increased backbone hydrophilicity, and/or H-bonding between the amide and ester groups. Future experiments to probe the accelerated rate of DMAEA hydrolysis within PAD copolymers will include copolymerization with the methacrylate version of APM to test the effect of the neighboring amide, as well as the tertiary amine and quaternary ammonium versions.

5.5. Conclusions

The hydrolysis of PDMAEA was studied in carefully pH-controlled experiments from pH 0 to 14, and was shown be highly pH dependent with half-lives ranging from years to minutes. The initial rates of PDMAEA hydrolysis closely matched rates observed for small-molecule analogue N,N-(dimethylamino)ethyl isobutyrate, however the extent of hydrolysis appeared to also depend on pH and ionization state of AA units that form on the polymer. This effect was further probed by studying the effect of comonomers on the hydrolysis of DMAEA. At pH 7, AA units decreased the rate of DMAEA hydrolysis, likely due to repulsion of hydroxide anions as well as possible electrostatic interaction of AA units with cationic dimethylammonium cations of DMAEA. The latter would disrupt the activation pathways of DMAE esters. Neutral and hydrophilic HEA as the comonomer did not affect DMAEA hydrolysis, whereas cationic APM accelerated the hydrolysis, which may be due to the higher net-cationic charge of the polymer that attracts hydroxide anions for further hydrolysis of DMAE esters. The effect of the dimethylamino group of DMAEA was probed with novel analogues, BDMAPA and DEMEA, which contain an additional amino group in the pendent side chain. The hydrolysis of PBDMAPA was much faster than PDMAEA likely due to the increased interaction of the additional amino group to the ester, whereas hydrolysis of PDEMEA was much slower, likely due to the increased steric hindrance of the inner amino group.

The results of this report demonstrate the importance of pH and neighboring functional groups on the rate and extent of PDMAEA hydrolysis. The mechanism of

PDMAEA hydrolysis provides useful insight towards the application of such charge-shifting polycations, as well as fundamental information to design degradable polymers.

Supporting Information

NMR spectra of PDMAEA, PDMAEA-30k, BDMAPA, PBDMAPA, DEMEA, PDEMEA, PDH_{77}, PDH_{46}, PDH_{19}, PHEA, and PDA_{58}; DMAEA and AA monomer feeds throughout copolymerization; Instantaneous copolymer composition plot of DMAEA/AA and DMAEA/HEA; Representative ^{1}H NMR spectrum of PDMAEA hydrolysis with sample calculations; Pseudo-first order kinetic plots of initial PDMAEA hydrolysis; Representative ^{1}H NMR spectra of PBDMAPA, PDEMEA, and PDH hydrolysis with sample calculations; GPC traces of PBDMAPA following polymerization in 1,4-dioxane and benzene; Log K_{obs} *vs*. pH plot for EtAc, DMAEIB, and PDMAEA; GPC traces of PDMAEA-15k and PDMAEA-30k; Hydrolysis plots of PDMAEA-15k and PDMAEA-30k at pH 7; Pseudo-first order kinetic plots of PBDMAPA and PDEMEA; Hydrolysis plots of PDH_{77}, PDH_{46}, PDH_{19}, and PHEA relative to PDMAEA at pH 7; ^{1}H NMR spectrum of PHEA with triethylamine after 20 days at pH 7.

Author Information

Corresponding Author

*E-mail: stoverh@mcmaster.ca, Ph.: 1-905-525-9140 ext. 24983.

Notes:

The authors declare no competing financial interest.

5.6. Acknowledgements

The authors are grateful for funding support from the Canada Foundation for Innovation and the Natural Sciences and Engineering Research Council of Canada Discovery Grant (RGPIN89661-11). S. R. was funded through an Ontario Graduate Scholarship.

5.7. References

[1] Bolto, B.; Gregory, J. Organic Polyelectrolytes in Water Treatment. *Water Res*. **2007**, *41*, 2301-2324.

[2] Saveyn, H.; Hendrickx, P. M. S.; Dentel, S. K.; Martins, J. C.; Van der Meeren, P. Quantification of hydrolytic charge loss of DMAEA-Q-based polyelectrolytes by proton NMR spectroscopy and implications for colloid titration. *Water Res*. **2008**, *42*, 2718 – 2728.

[3] Wever, D. A. Z.; Picchioni, F.; Broekhuis, A. A. Polymers for enhanced oil recovery: A paradigm for structure–property relationship in aqueous solution. *Prog. Polym. Sci.* **2011**, *36*, 1558-1628.

[4] Peyratout, C. S.; Dähne, L. Tailor-Made Polyelectrolyte Microcapsules: From Multilayers to Smart Containers. *Angew. Chem. Int. Ed*. **2004**, *43*, 3762–3783.

[5] van de Wetering, P.; Zuidam, N. J.; van Steenbergen, M. J.; van der Houwen, O. A. G. J.; Underberg, W. J. M.; Hennink, W. E. A Mechanistic Study of the Hydrolytic Stability of Poly(2-(dimethylamino)ethyl methacrylate). *Macromolecules* **1998**, *31*, 8063−8068.

[6] Ros, S.; Burke, N. A. D.; Stöver, H. D. H. Synthesis and Properties of Charge-Shifting Polycations: Poly[3-aminopropylmethacrylamide-*co*-2-(dimethylamino)ethyl acrylate]. *Macromolecules* **2015**, *48*, 8958−8970.

[7] Ros, S.; Kleinberger, R. M.; Burke, N. A. D.; Rossi, N. A. A.; Stöver, H. D. H. Charge-Shifting Polycations with Tunable Rates of Hydrolysis: Effect of Backbone Substituents on Poly[2-(Dimethylamino)ethyl acrylates]. *Macromolecules* **2018**, *51*, 5752−5761.

[8] Luten, J.; van Nostrum, C. F.; De Smedt, S. C.; Hennink, W. E. Biodegradable polymers as non-viral carriers for plasmid DNA delivery. *J. Controlled Release* **2008**, *126*, 97–110.

[9] Luten, J.; Akeroyd, N.; Funhoff, A.; Lok, M. C.; Talsma, H.; Hennink, W. E. Methacrylamide Polymers with Hydrolysis-Sensitive Cationic Side Groups as Degradable Gene Carriers. *Bioconjugate Chem*. **2006**, *17*, 1077−1084.

[10] Lynn, D. M.; Langer, R. Degradable Poly(β-amino esters): Synthesis, Characterization, and Self-Assembly with Plasmid DNA. *J. Am. Chem. Soc*. **2000**, *122*, 10761-10768.

[11] Sinclair, A.; Bai, T.; Carr, L. R.; Ella-Menye, J. R.; Zhang, L.; Jiang, S. Engineering Buffering and Hydrolytic or Photolabile Charge Shifting in a Polycarboxybetaine Ester Gene Delivery Platform. *Biomacromolecules* **2013**, *14*, 1587-1593

[12] Vazquez, E.; Dewitt, D. M.; Hammond, P. T.; Lynn, D. M. Construction of Hydrolytically-Degradable Thin Films via Layer-by-Layer Deposition of Degradable Polyelectrolytes. *J. Am. Chem. Soc*. **2002**, *124*, 13992-13993.

[13] Flessner, R. M.; Jewell, C. M.; Anderson, D. G.; Lynn, D. M. Degradable Polyelectrolyte Multilayers that Promote the Release of siRNA. *Langmuir* **2011**, *27*, 7868–7876.

[14] Sun, B.; Lynn, D. M. Release of DNA from polyelectrolyte multilayers fabricated using 'charge-shifting' cationic polymers: Tunable temporal control and sequential, multi-agent release. *J. Controlled Release* **2010**, *148*, 91-100.

[15] Truong, N. P.; Jia, Z.; Burgess, M.; Payne, L.; McMillan, N. A. J.; Monteiro, M. J. Self-Catalyzed Degradable Cationic Polymer for Release of DNA. *Biomacromolecules*, **2011**, *12*, 3540-3548.

[16] Truong, N. P.; Gu, W.; Prasadam, I.; Jia, Z.; Crawford, R.; Xiao, Y.; Monteiro, M. J. An influenza virus-inspired polymer system for the timed release of siRNA. *Nat. Commun.* **2013**, *4*:1902. doi: 10.1038/ncomms2905

[17] You, Y.Z.; Manickam, D. S.; Zhou, Q. H.; Oupický, D. Reducible poly(2-dimethylaminoethyl methacrylate): Synthesis, cytotoxicity, and gene delivery activity. *J. Controlled Release* **2007**, *122*, 217-225.

[18] Ho, H. T.; Pascual, S. P.; Montembault, V.; Casse, N.; Fontaine, L. Innovative well-defined primary amine-based polyacrylates for plasmid DNA complexation. *Polym. Chem.* **2014**, *5*, 5542-5545.

[19] Ho, H. T.; Le Bohec, M.; Frémaux, J.; Piogé, S.; Casse, N.; Fontaine, L.; Pascual, S. Tuning the Molar Composition of "Charge- Shifting" Cationic Copolymers Based on 2-(N,N-Dimethylamino)- Ethyl Acrylate and 2-(tert-Boc-Amino)Ethyl Acrylate. *Macromol. Rapid Commun.* **2017**, DOI: 10.1002/marc.201600641

[20] Hu, X.; Feeney, M. J.; McIntosh, E.; Mullahoo, J.; Jia, F.; Xu, Q.; Thomas III, S. W. Triggered Release of Encapsulated Cargo from Photoresponsive Polyelectrolyte Nanocomplexes. *ACS Appl. Mater. Interfaces* **2016**, *8*, 23517−23522.

[21] Qiu, N.; Gao, J.; Liu, Q.; Wang, J.; Shen, Y. Enzyme-Responsive Charge-Reversal Polymer-Mediated Effective Gene Therapy for Intraperitoneal Tumors. *Biomacromolecules* **2018**, *19*, 2308−2319.

[22] McCool, M. B.; Senogles, E.The Self-Catalyzed Hydrolysis of Poly(N,N-dimethylaminoethyl acrylate). *Eur. Polym. J.* **1989**, *25*, 857–860.

[23] Truong, N. P.; Jia, Z.; Burges, M.; McMillan, N. A. J.; Monteiro, M. J. Self-Catalyzed Degradation of Linear Cationic Poly(2-dimethylaminoethyl acrylate) in Water. *Biomacromolecules* **2011**, *12*, 1876–1882.

[24] Cotanda, P.; Wright, D. B.; Tyler, M.; O'Reilly, R. K. A Comparative Study of the Stimuli-Responsive Properties of DMAEA and DMAEMA Containing Polymers. *J. Polym. Sci., Part A: Polym. Chem.* **2013**, *51*, 3333–3338.

[25] Rolph, M. S.; Pitto-Barry, A; O'Reilly, R. K. The hydrolytic behavior of N,N'-(dimethylamino) ethyl acrylate-functionalized polymeric stars. *Polym. Chem*. **2017**, *8*, 5060-5070.

[26] Zhao, W.; Fonsny, P.; FitzGerald, P.; Warr, G. G.; Perrier, S. Unexpected behavior of polydimethylsiloxane/ poly(2-(dimethylamino)ethyl acrylate) (charged) amphiphilic block copolymers in aqueous solution. *Polym. Chem*., **2013**, *4*, 2140–2150.

[27] Whitfield, R.; Anastasaki, A.; Truong, N. P.; Cook, A. B.; Omedes-Pujol, M.; Rose, V. L.; Nguyen, T. A. H.; Burns, J. A.; Perrier, S.; Davis, T. P.; Haddleton, D. M. Efficient Binding, Protection, and Self-Release of dsRNA in Soil by Linear and Star Cationic Polymers. *ACS Macro Lett*. **2018**, *7*, 909−915.

[28] Cook, A. B.; Peltier, R.; Hartlieb, M.; Whitfield, R.; Moriceau, G.; Burns, J. A.; Haddleton, D. M.; Perrier, S. Cationic and hydrolysable branched polymers by RAFT for complexation and controlled release of dsRNA. *Polym. Chem*., **2018**, *9*, 4025–4035.

[29] Hilal, S. H. Estimation of Hydrolysis Rate Constants of Carboxylic Acid Ester and Phosphate Ester Compounds in Aqueous Systems from Molecular Structure by SPARC.

U.S. Environmental Protection Agency, Washington, DC, EPA/600/R-06/105 (NTIS PB2007-100142), **2006**.

[30] Drossman, H.; Johnson, H.; Mill, T. Structure Activity Relationships for Environmental Processes 1: Hydrolysis of Esters and Carbamates. *Chemosphere* **1988**. *17***,** 1509-1530.

[31] Taft, R. W. Linear Free Energy Relationships from Rates of Esterification and Hydrolysis of Aliphatic and Ortho-Substituted Benzoate Esters. *J. Am. Chem. Soc.* **1952**, *74*, 2729-2732.

[32] Krezel, A.; Bal, W. A formula for correlating pKa values determined in D_2O and H_2O. *Journal of Inorganic Biochemistry* **2004**, *98*, 161–166.

[33] Dubey, A.; Burke, N. A. D.; Stover, H. D. H. Preparation and Characterization of Narrow Compositional Distribution Polyampholytes as Potential Biomaterials: Copolymers of N-(3-Aminopropyl)methacrylamide Hydrochloride (APM) and Methacrylic Acid (MAA). *J. Polym. Sci., Part A: Polym. Chem.* **2015**, *53*, 353–365.

[34] Kheradmand, H.; François, J.; Plazanet V. Hydrolysis of polyacrylamide and acrylic acid-acrylamide copolymers at neutral pH and high temperature. *Polymer* **1988**, *29*, 860-870.

[35] Truong, N. D.; Galin, J. C.; François, J. Microstructure of acrylamide-acrylic acid copolymers: 1. As obtained by alkaline hydrolysis. *Polymer* **1986**, *27*, 459-466.

[36] Ros, S.; Freitag, J. S.; Smith, D. M.; Stöver, H. D. H. Charge-Shifting Polycations based on N,N-(Dimethylamino)ethyl Acrylate for Improving Cytocompatibility During DNA Delivery. *ACS Omega* **2020**, *accepted*.

5.8. Appendix

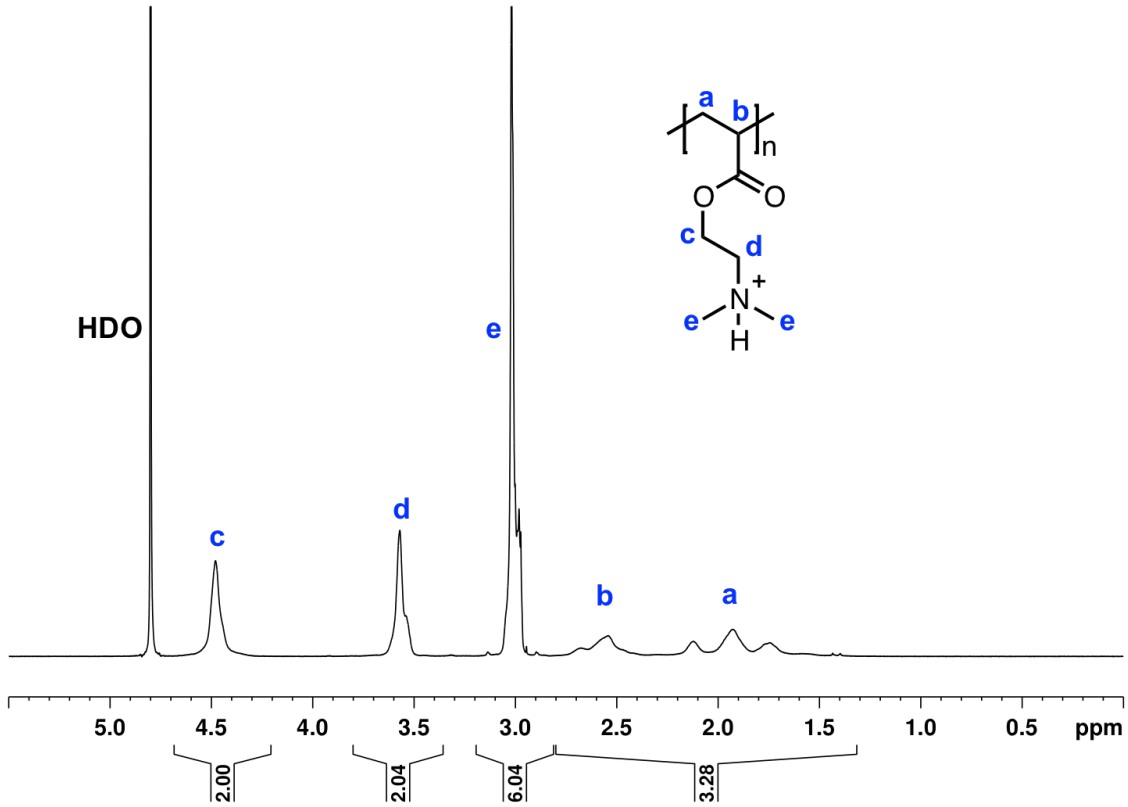

Figure 5A.1. ^{1}H NMR spectrum of PDMAEA in D_2O (pH 3-4) recorded at 600 MHz.

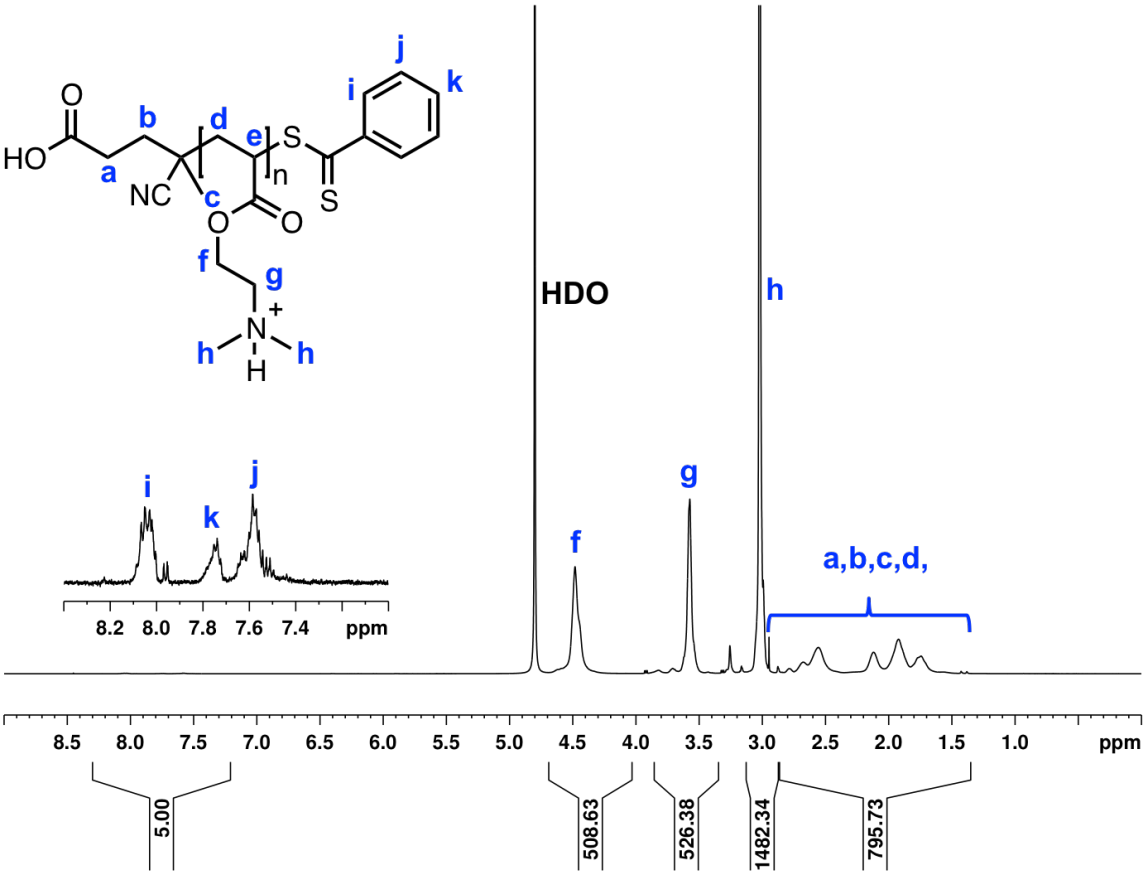

Figure 5A.2. ^{1}H NMR spectrum of PDMAEA by RAFT polymerization in D_2O (pH 3-4) recorded at 500 MHz with 512 scans. End group analysis of dithiobenzoate group showed DP of approximately 254.

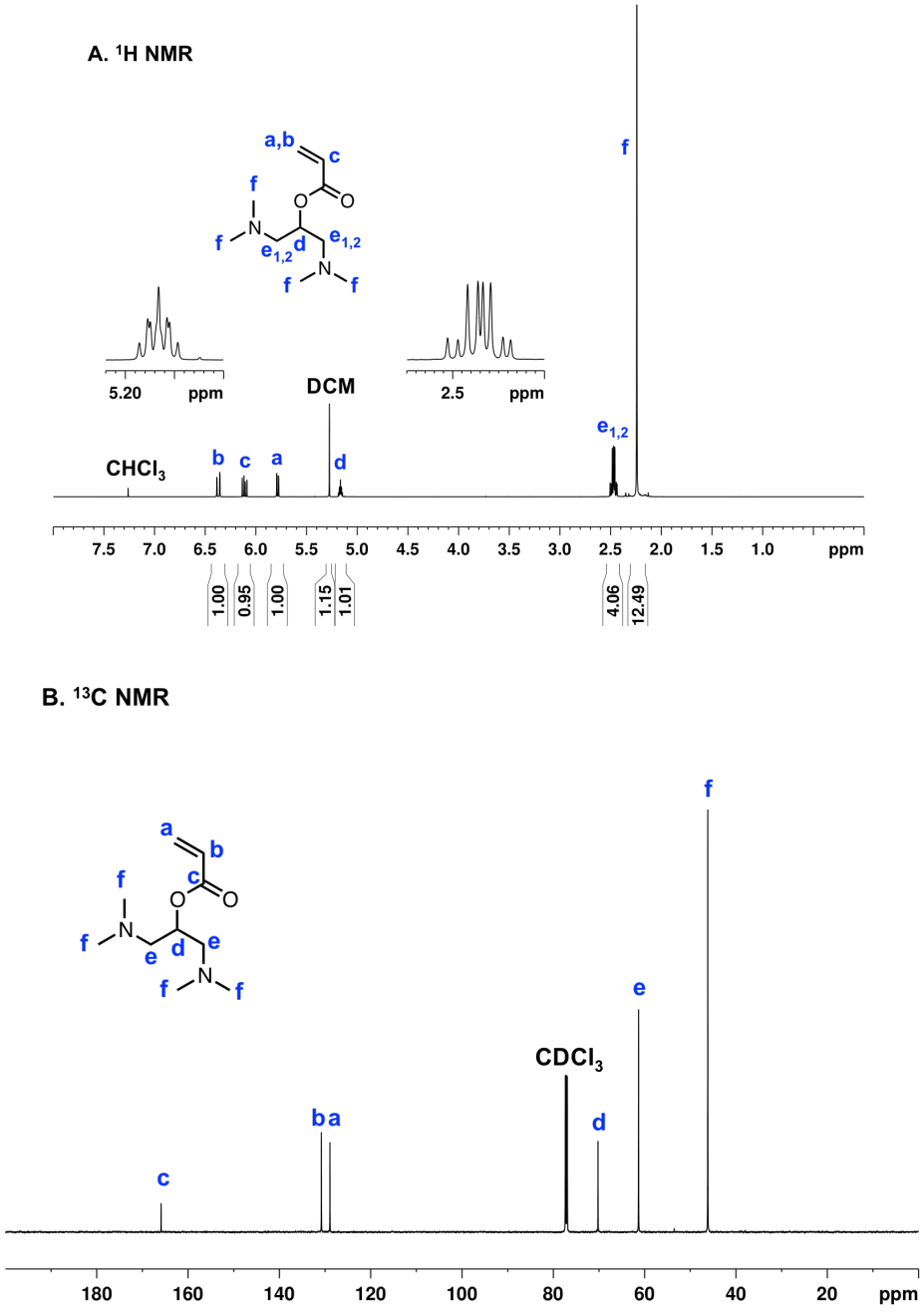

Figure 5A.3. ^{1}H (**A**) and ^{13}C (**B**) NMR spectra of BDMAPA in $CDCl_3$ recorded at 600 MHz. The protons at position **e** are diastereotopic, which leads to two distinct signals, each a doublet of doublets.

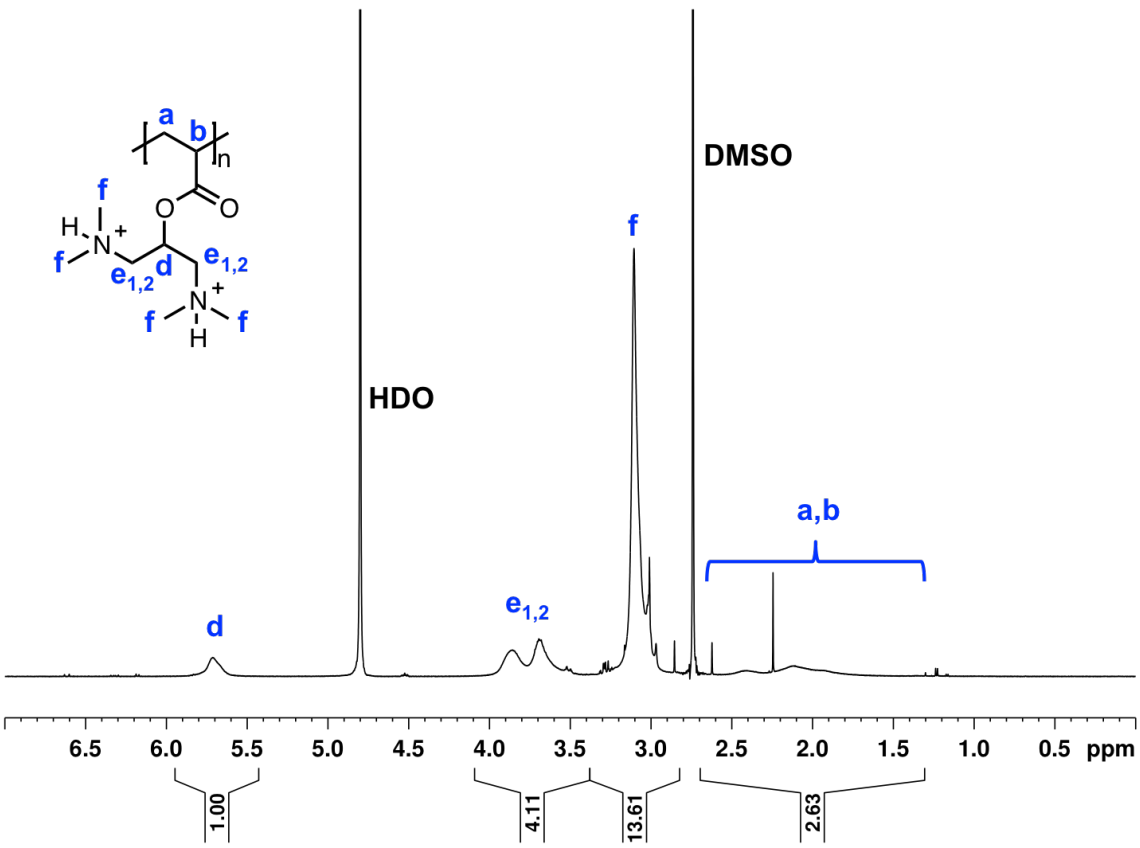

Figure 5A.4. ^{1}H NMR spectrum of PBDMAPA in D_2O (pH 3-4) recorded at 600 MHz.

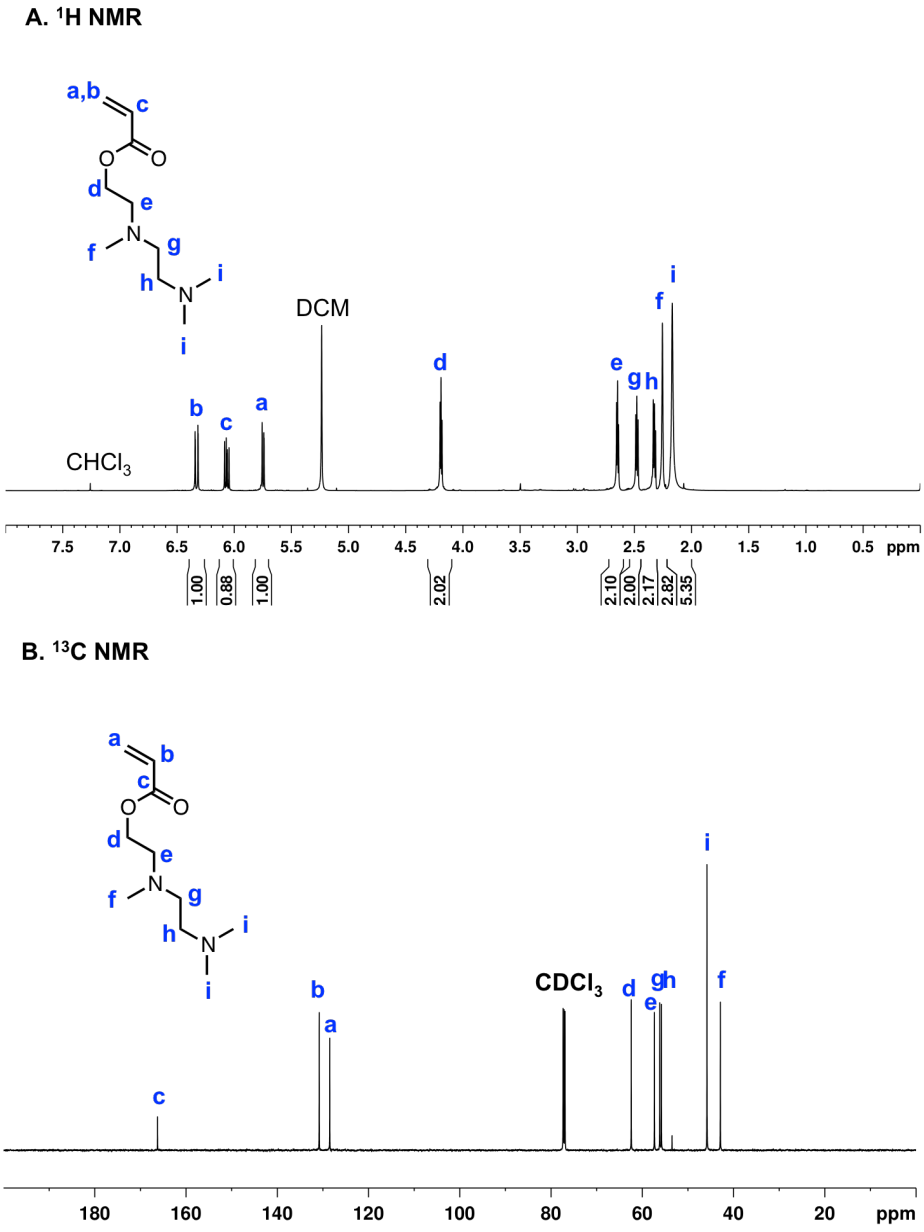

Figure 5A.5. ^{1}H (**A**) and ^{13}C (**B**) NMR spectra of DEMEA in $CDCl_3$ recorded at 600 MHz.

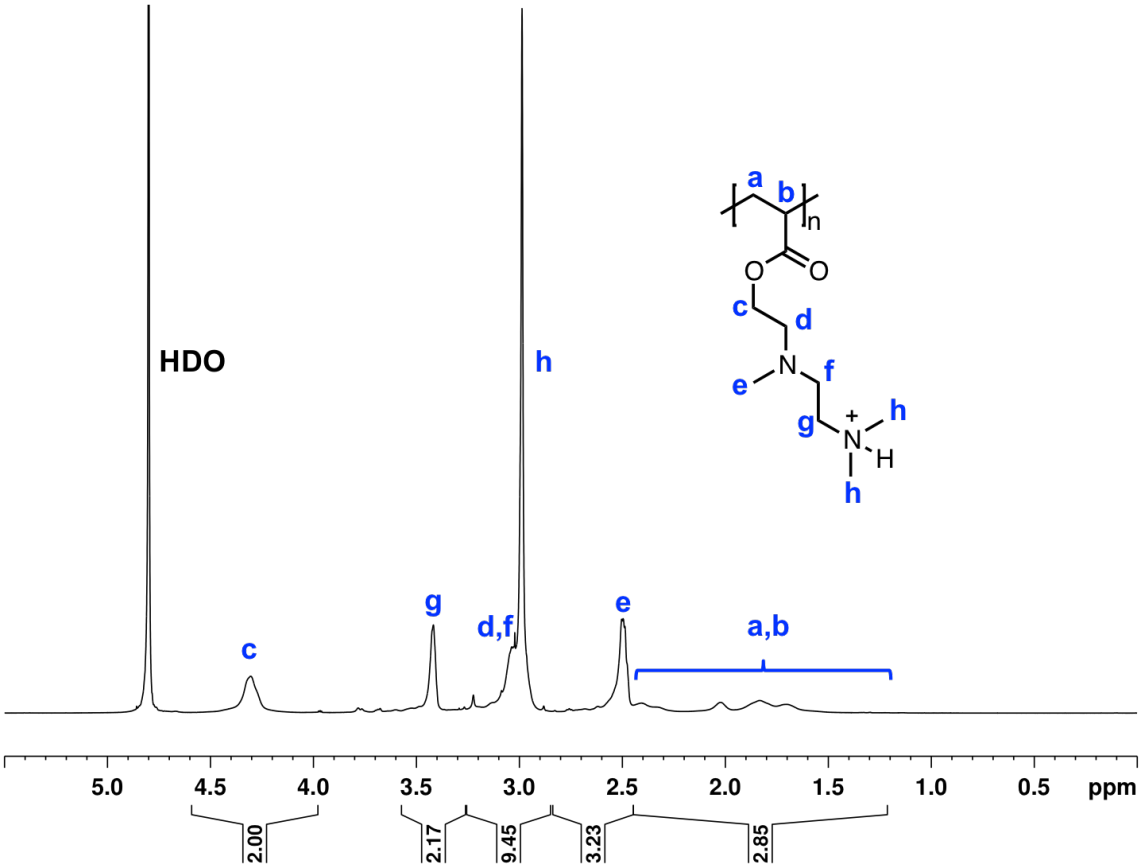

Figure 5A.6. ^{1}H NMR spectrum of PDEMEA in D_2O (pH 3-4) recorded at 700 MHz.

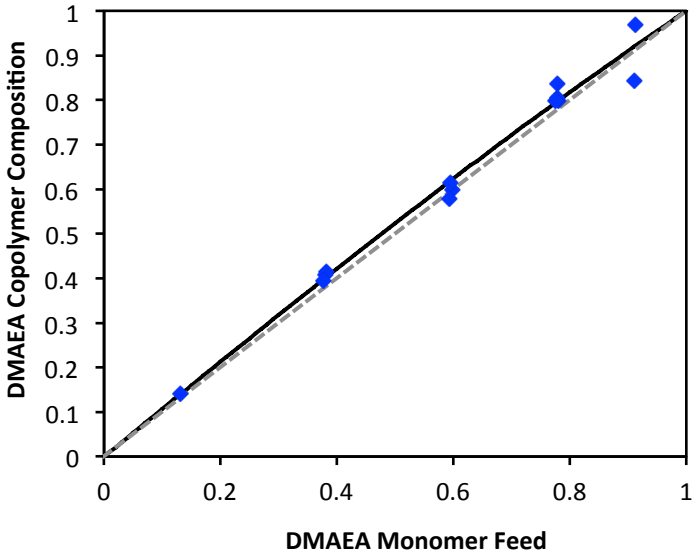

Figure 5A.7. Instantaneous copolymer composition plot showing experimental data points (blue diamonds) from various DMAEA/HEA feed ratios. The solid black line shows the best fit of the copolymer equation to the experimental data obtained using the least squares method with the Solver tool in Microsoft Excel. Reactivity ratios were estimated to be $r_1 = 1.13$ (DMAEA) and $r_2 = 0.94$ (HEA).

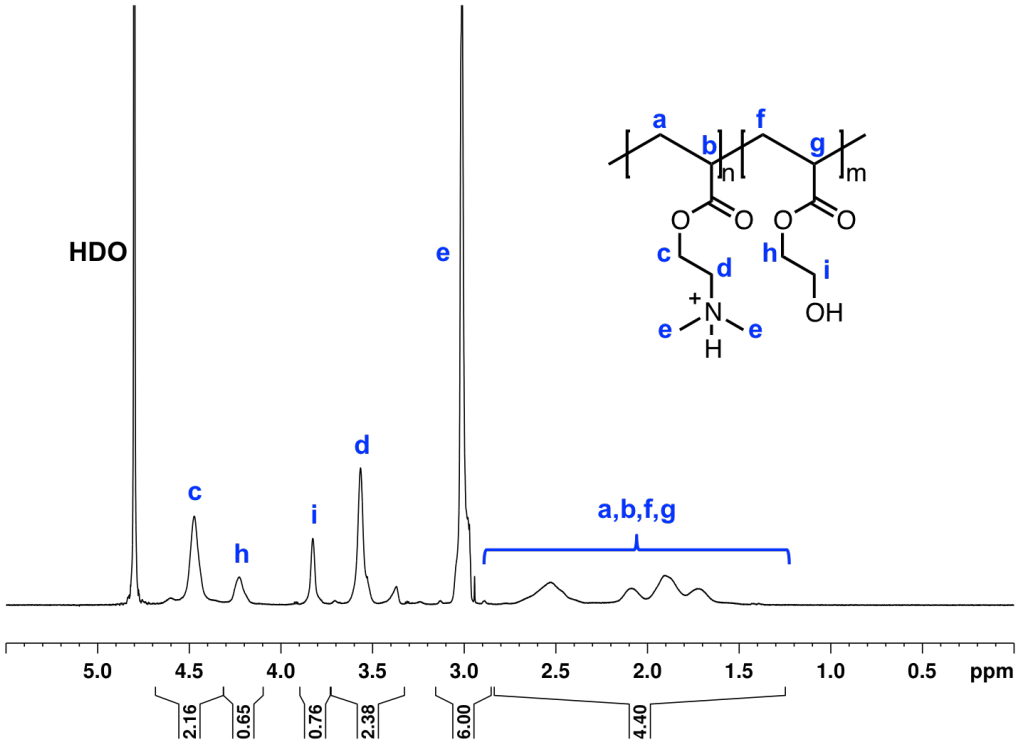

Figure 5A.8. ^{1}H NMR spectrum of PDH_{77} in D_2O (pH 3-4) recorded at 600 MHz.

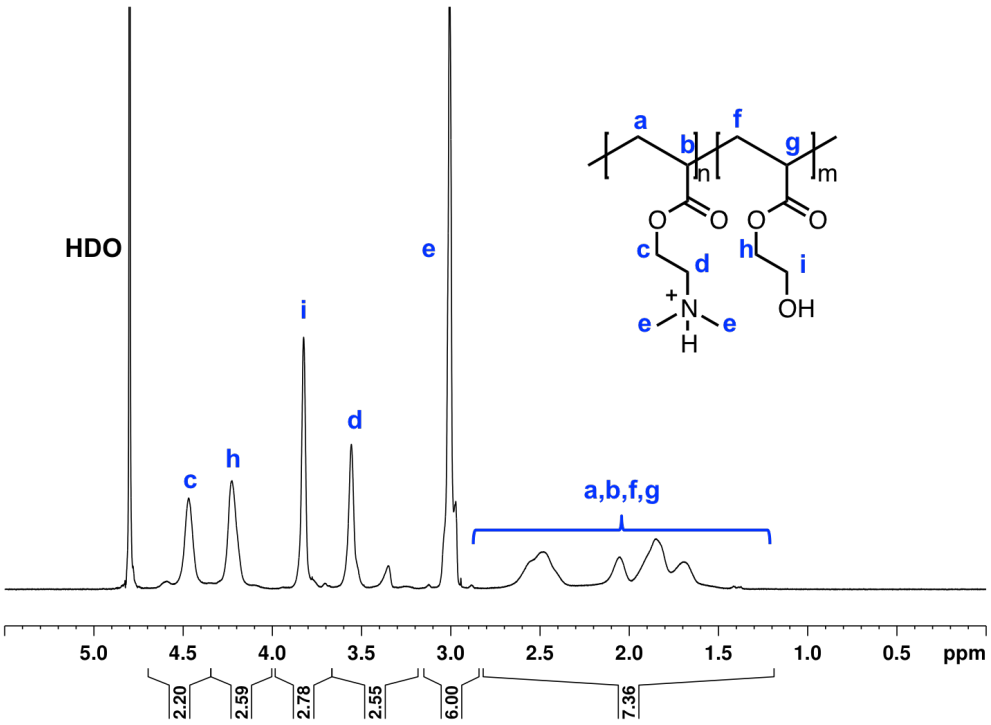

Figure 5A.9. ^{1}H NMR spectrum of PDH_{46} in D_2O (pH 3-4) recorded at 600 MHz.

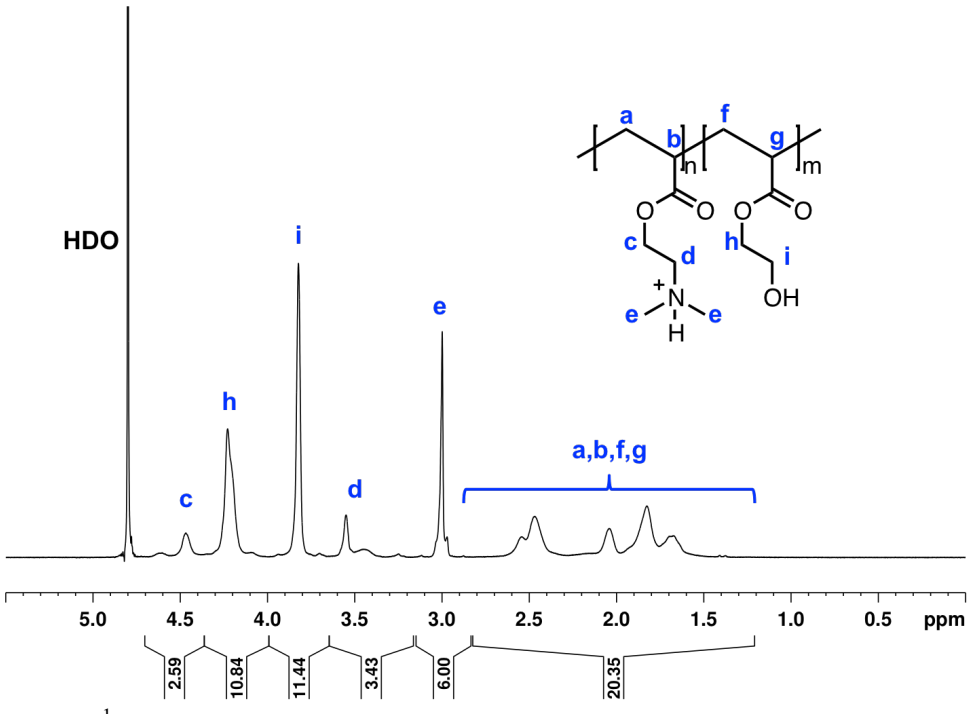

Figure 5A.10. ^{1}H NMR spectrum of PDH_{19} in D_2O (pH 3-4) recorded at 600 MHz.

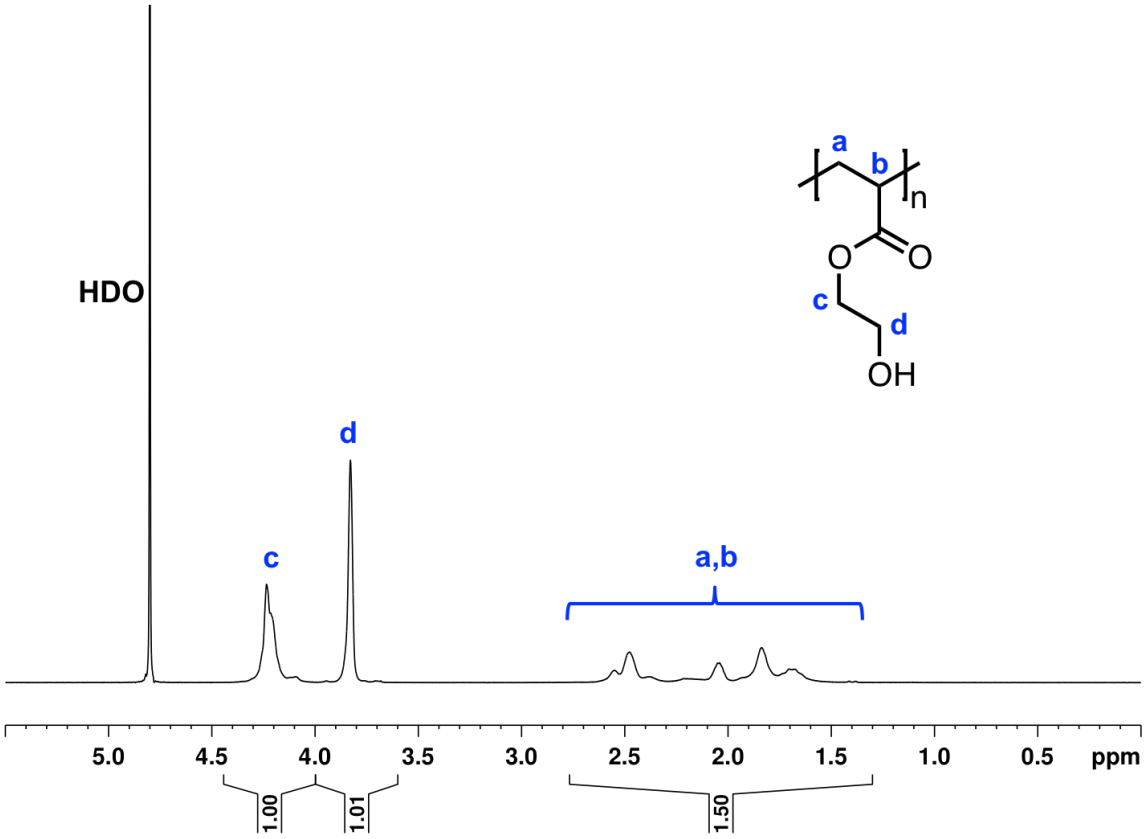

Figure 5A.11. ^{1}H NMR spectrum of PHEA in D_2O (pH 3-4) recorded at 600 MHz.

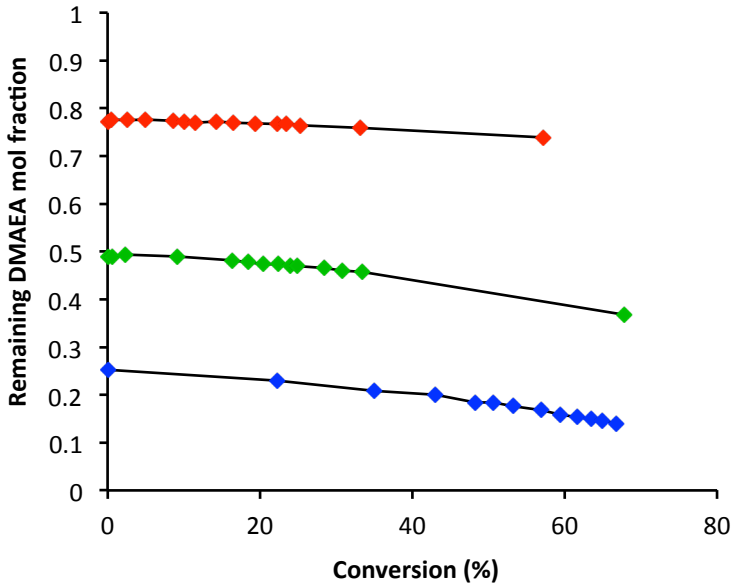

Figure 5A.12. Remaining mol fraction of DMAEA relative to AA throughout copolymerizations at 55 °C in DMSO-*d6* as a function of total monomer conversion.

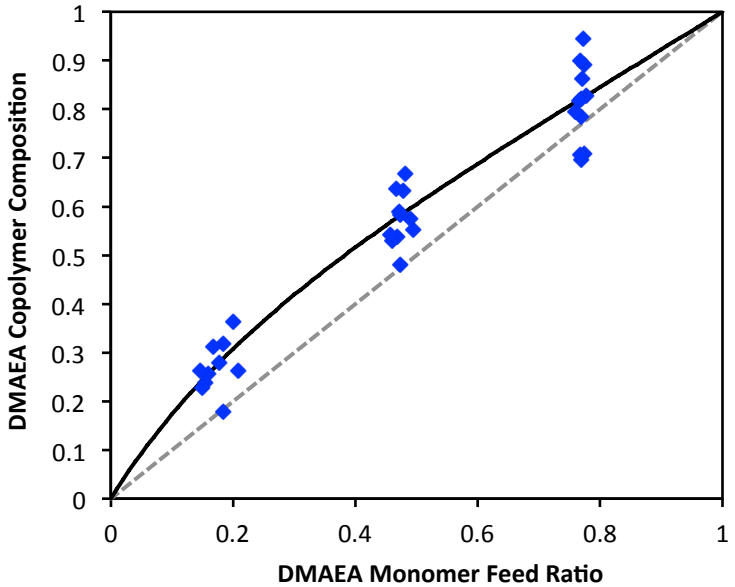

Figure 5A.13. Instantaneous copolymer composition plot showing experimental data points (blue diamonds) from various DMAEA/AA feed ratios. The solid black line shows the best fit of the copolymer equation to the experimental data obtained using the least squares method with the Solver tool in Microsoft Excel. Reactivity ratios were estimated to be $r_1 = 1.29$ (DMAEA) and $r_2 = 0.49$ (AA).

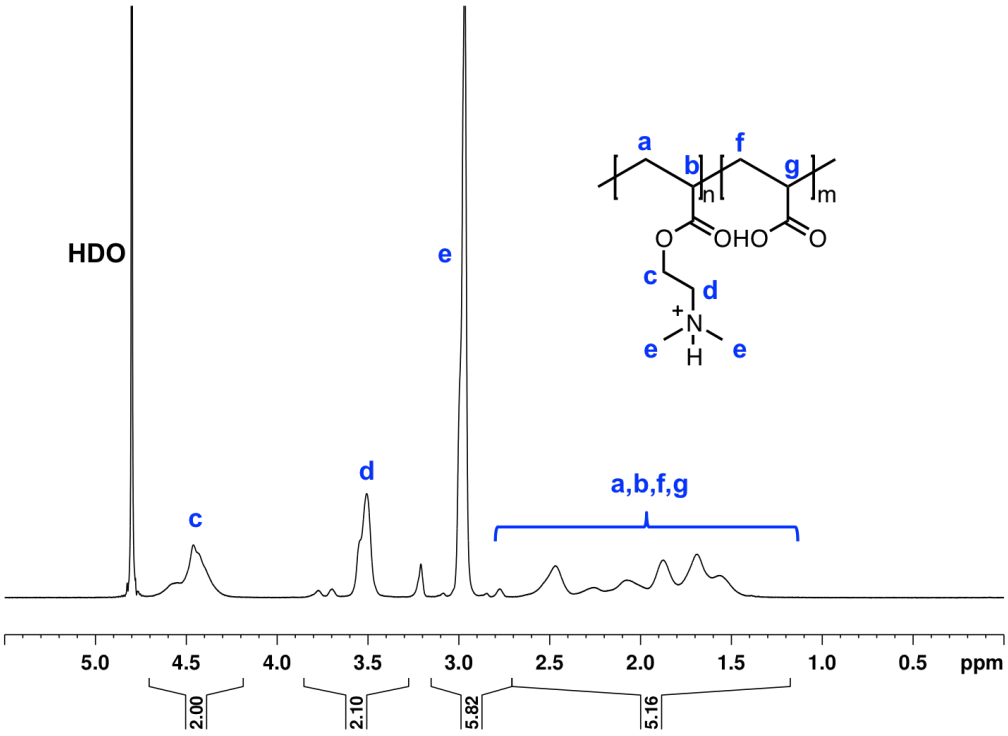

Figure 5A.14. ^{1}H NMR spectrum of PDA_{58} in D_2O (pH 3-4) recorded at 600 MHz.

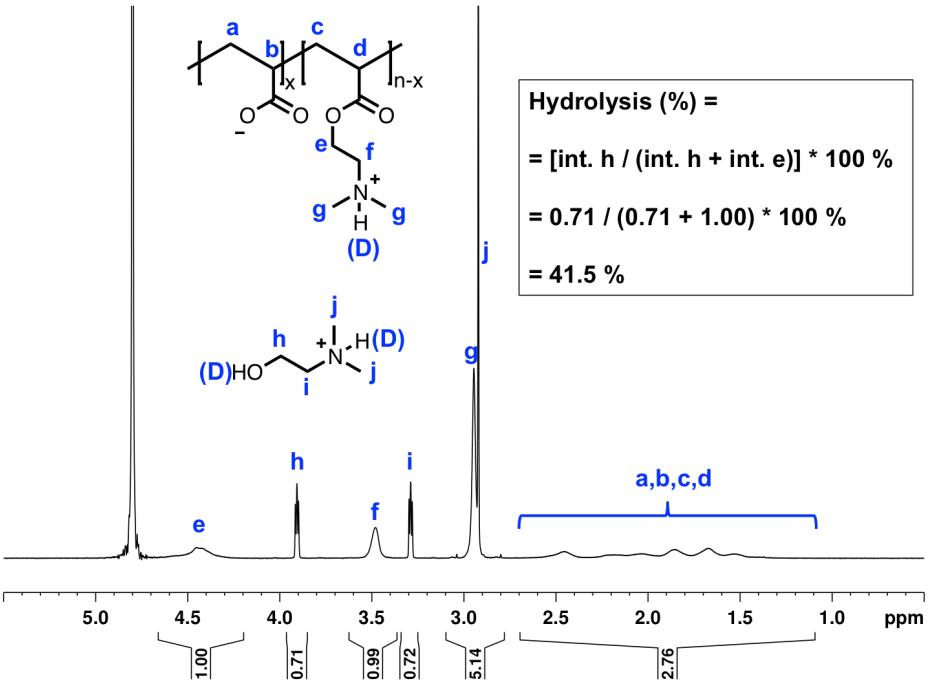

Figure 5A.15. A representative ^{1}H NMR spectrum of PDMAEA hydrolysis at pH 7 with a sample calculation showing percent hydrolysis.

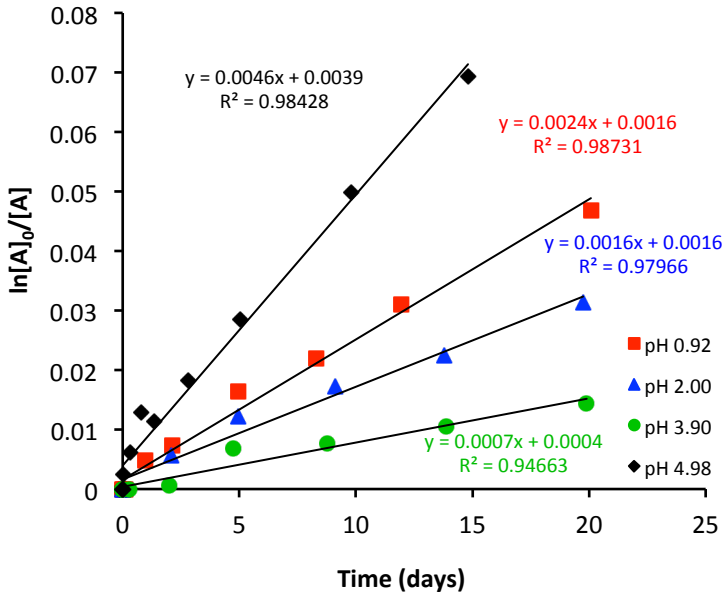

Figure 5A.16. Pseudo-first order kinetic plot of the initial rates of PDMAEA hydrolysis at pH 0.92, 2.00, 3.90, and 4.98 at 22 °C. The y-axis shows the natural log of the ratio of initial ester concentration ($[A]_0$) to the concentration of ester at time t ([A]).

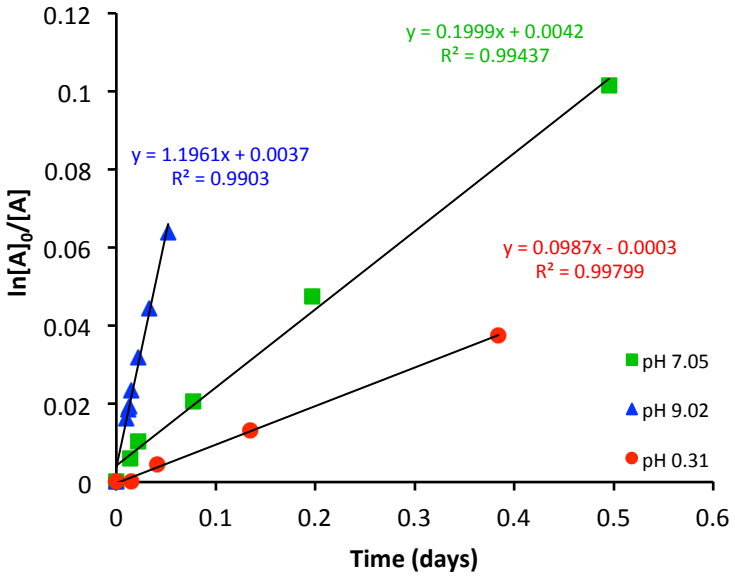

Figure 5A.17. Pseudo-first order kinetic plots of PDMAEA hydrolysis at pH 7.05, 9.02 and 0.31 at 22 °C. The y-axis shows the natural log of the ratio of initial ester concentration ($[A]_0$) to the concentration of ester after hydrolysis with time ([A]).

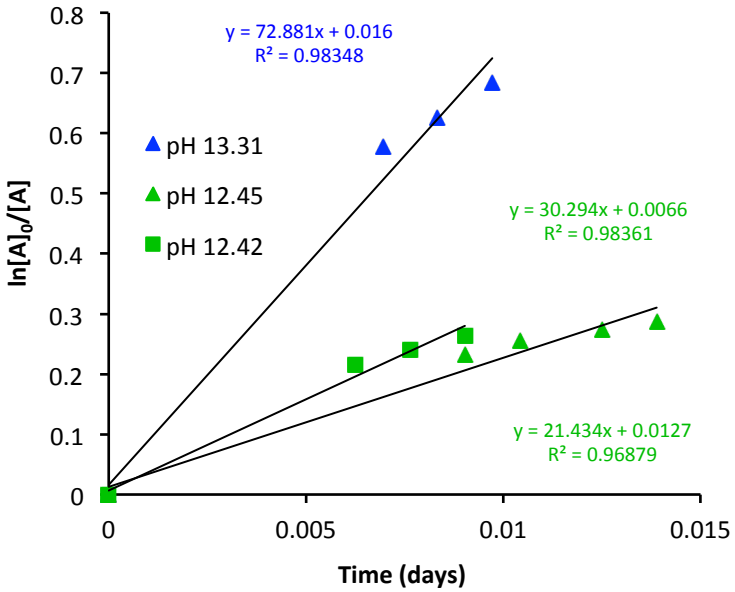

Figure 5A.18. Pseudo-first order kinetic plots of PDMAEA hydrolysis at pH 13.31, 12.45 and 12.42 at 22 °C. The y-axis shows the natural log of the ratio of initial ester concentration ($[A]_0$) to the concentration of ester after hydrolysis with time ([A]).

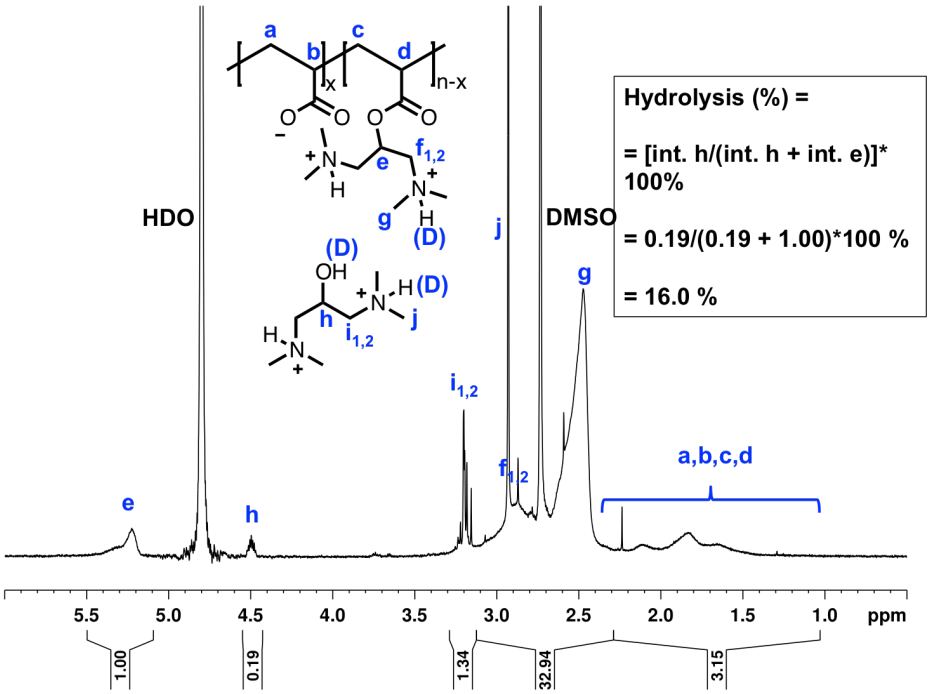

Figure 5A.19. A representative ^{1}H NMR spectrum of PBDMAPA hydrolysis at pH 7 with a sample calculation showing percent hydrolysis.

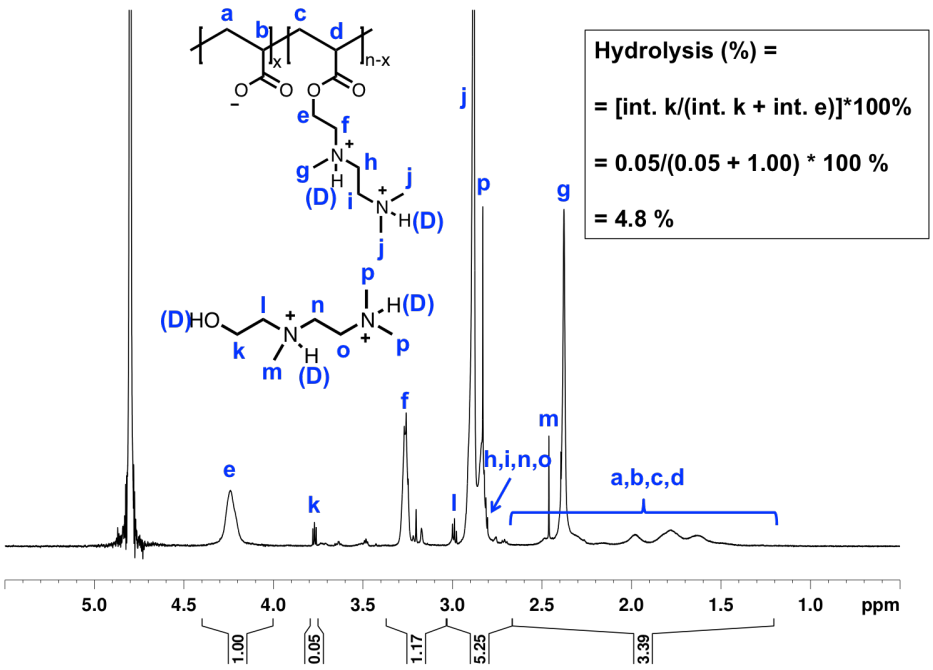

Figure 5A.20. A representative ^{1}H NMR spectrum of PDEMEA hydrolysis at pH 7 with a sample calculation showing percent hydrolysis.

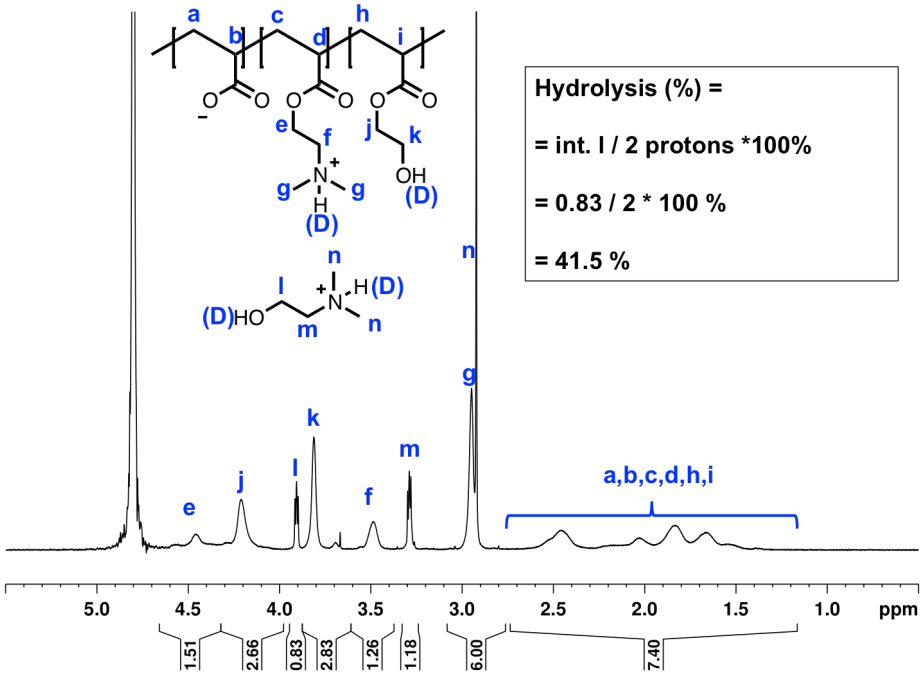

Figure 5A.21. A representative ^{1}H NMR spectrum of PDH_{50} hydrolysis at pH 7 with a sample calculation showing percent hydrolysis. The HEA esters remain largely intact as

there is little change in peaks j and k and only a tiny ethylene glycol peak (<1 %) (sharp singlet at 3.65 ppm).

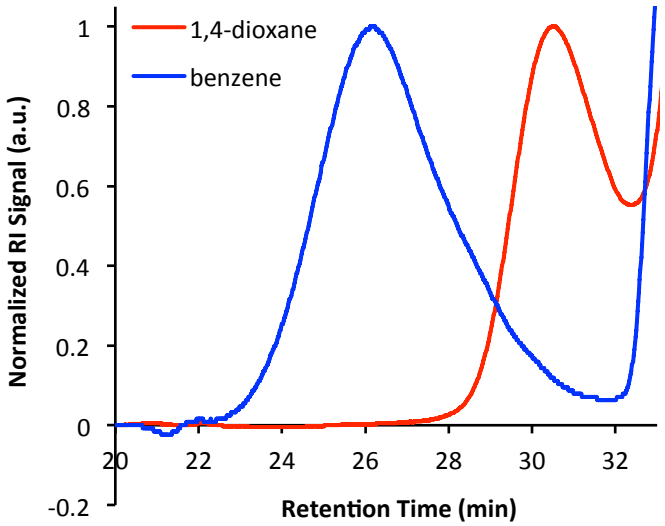

Figure 5A.22. GPC traces of PBDMAPA prepared by conventional free radical polymerization in 1,4-dioxane and by photopolymerization at 0 °C in benzene. The polymers have Mn values of approximately 2800 g/mol (Mp = 2900 g/mol) and 9100 g/mol, respectively. Mn for the PBDMAPA polymerized in 1,4-dioxane is given as an estimate as the peak overlaps with the solvent peak after ~ 32 min. GPC traces similar to the one obtained for PBDMAPA made in 1,4-dioxane were seen for polymerization in acetonitrile, DMSO, and toluene.

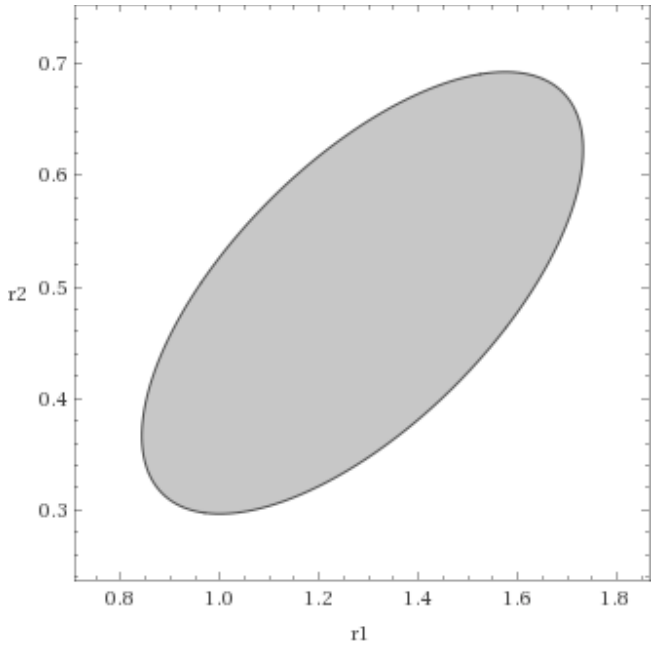

Figure 5A.23. Joint confidence region at 95 % confidence level for reactivity ratios obtained for DMAEA/AA using a method described by Kitanidis et al.[1]

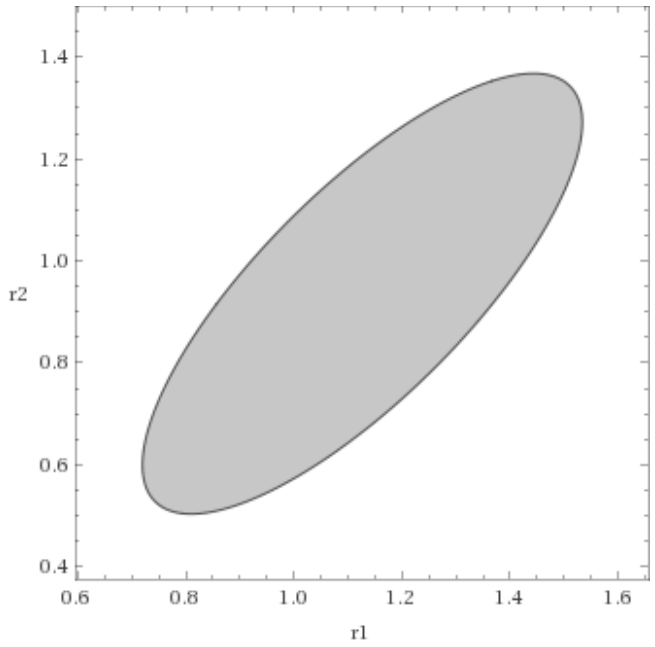

Figure 5A.24. Joint confidence region at 95 % confidence level for reactivity ratios obtained for DMAEA/HEA using a method described by Kitanidis et al.[1]

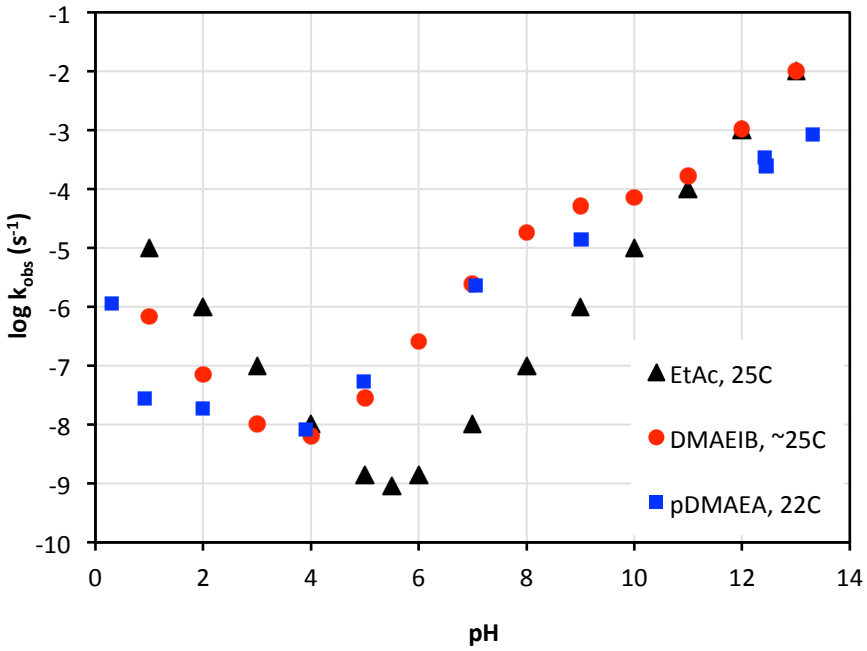

Figure 5A.25. Log k_{obs} *vs.* pH for hydrolysis of ethyl acetate,[2,3,4] N,N-dimethylaminoethyl isobutyrate (DMAEIB),[5] and PDMAEA at ~22-25 °C. van de Wetering et al found that the k_{obs} for DMAEIB hydrolysis decreased ~2.5-fold with a 10 °C decrease in T, so their k values determined at 37 °C were divided by 2.5 to generate the ~25 °C-curve shown in this figure.

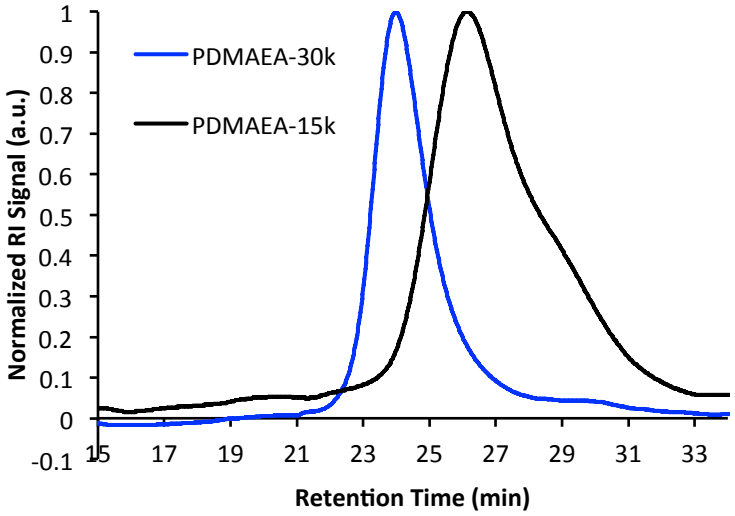

Figure 5A.26. GPC traces of PDMAEA prepared by conventional free radical polymerization and PDMAEA-30k prepared by RAFT polymerization.

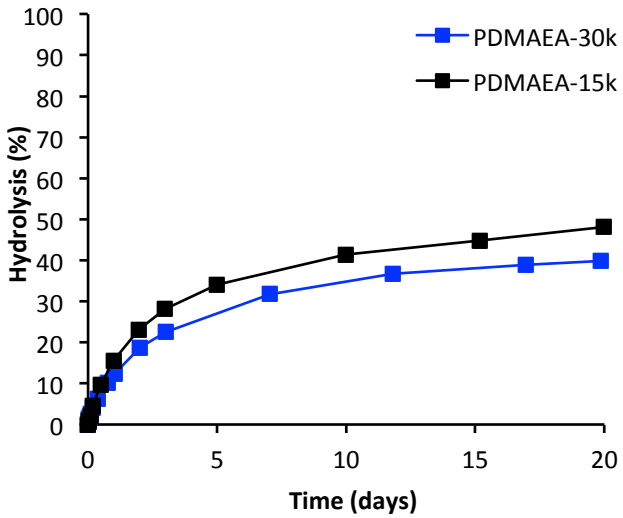

Figure 5A.27. Hydrolysis of PDMAEA-15k by conventional free radical polymerization and PDMAEA-30k by RAFT polymerization at pH 7, room temperature (22 °C).

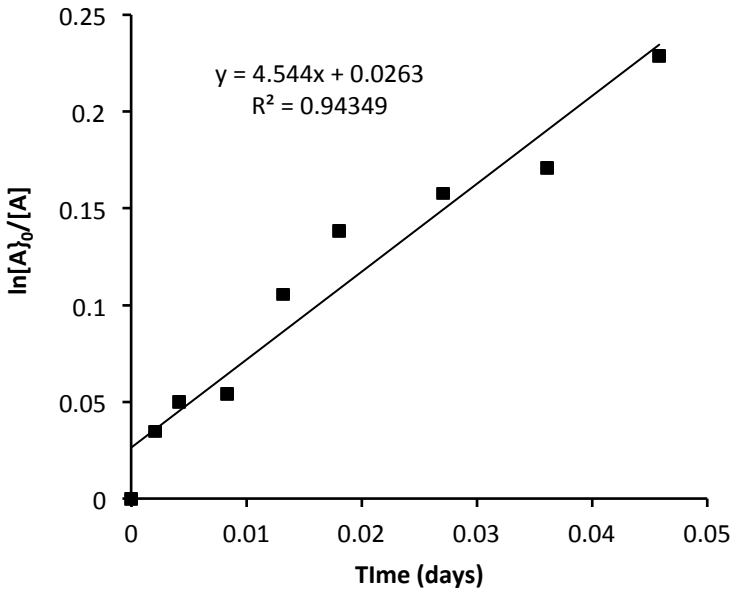

Figure 5A.28. Pseudo-first order kinetic plot of PBDMAPA hydrolysis at pH 7 at 22 °C. The y-axis shows the natural log of the ratio of initial ester concentration ($[A]_0$) to the concentration of ester after hydrolysis with time ([A]).

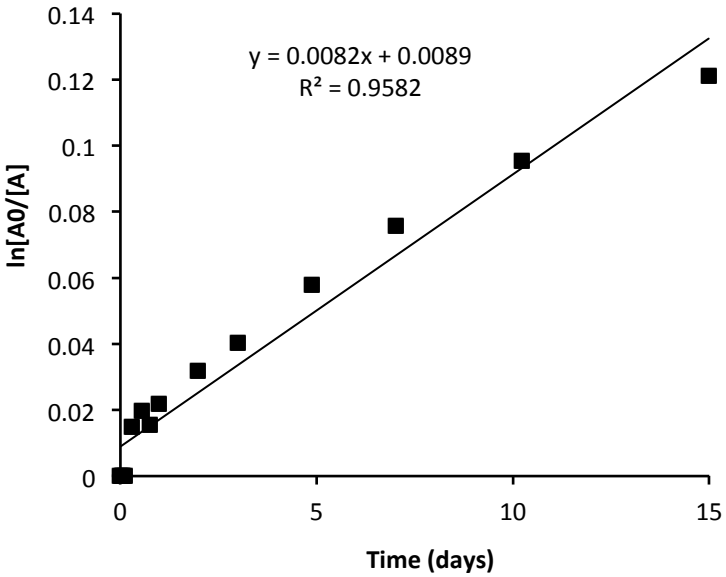

Figure 5A.29. Pseudo-first order kinetic plot of PDEMEA hydrolysis at pH 7 at 22 °C. The y-axis shows the natural log of the ratio of initial ester concentration ($[A]_0$) to the concentration of ester after hydrolysis with time ([A]).

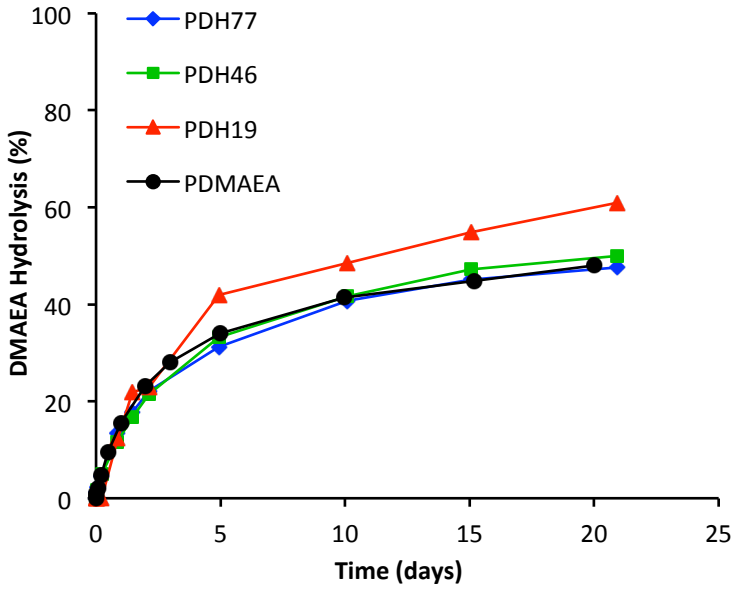

Figure 5A.30. Hydrolysis of DMAEA within PDH copolymers and PDMAEA at pH 7. PHEA showed less than 1 % ester hydrolysis after about 20 days at pH 7 as monitored by appearance of small-molecule ethylene glycol.

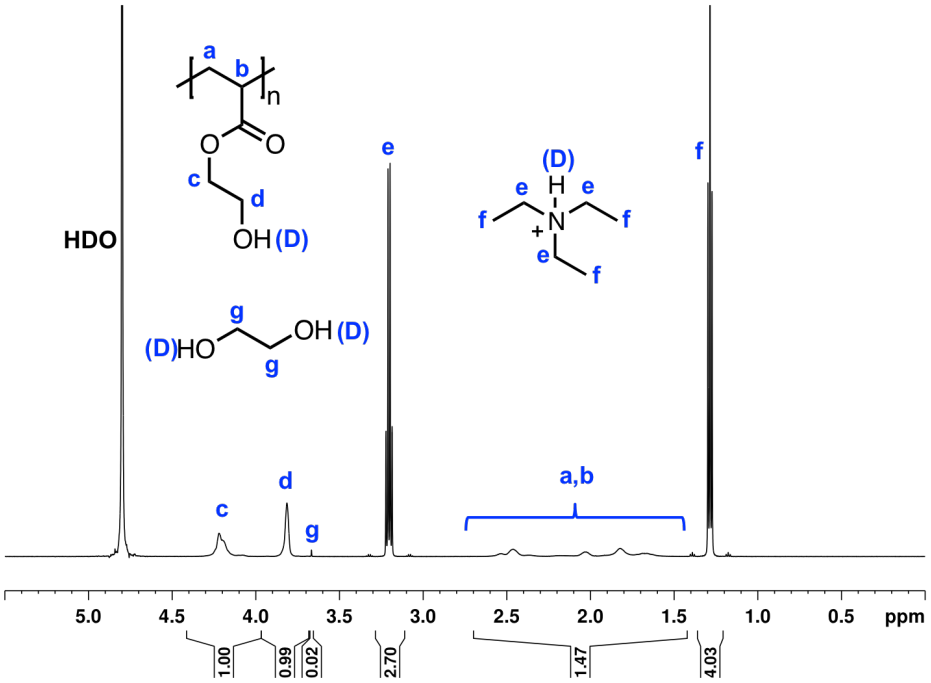

Figure 5A.31. [1]H NMR spectrum of PHEA with ~ 1 mol eq. of triethylamine (TEA) added to model the tertiary amino group of DMAEA that is not covalently bound to the ester. After 20 days in 100 mM phosphate buffer pH 7.03 at room temperature, less than 1 % of ethylene glycol (g) was measured.

References

[1] Smith, L. H.; McCarty, P. L., Kitanidis, P. K. Spreadsheet Method for Evaluation of Biochemical Reaction Rate Coefficients and Their Uncertainties by Weighted Nonlinear Least-Squares Analysis of the Integrated Monod Equation. *Applied and Environmental Microbiology* **1998**, *64(6)*, 2044–2050.

[2] Hilal, S. H. Estimation of Hydrolysis Rate Constants of Carboxylic Acid Ester and Phosphate Ester Compounds in Aqueous Systems from Molecular Structure by SPARC. U.S. Environmental Protection Agency, Washington, DC, EPA/600/R-06/105 (NTIS PB2007-100142), **2006**.

[3] Drossman, H.; Johnson, H.; Mill, T. Structure Activity Relationships for Environmental Processes 1: Hydrolysis of Esters and Carbamates. *Chemosphere* **1988**. *17*, 1509-1530.

[4] Taft, R. W. Linear Free Energy Relationships from Rates of Esterification and Hydrolysis of Aliphatic and Ortho-Substituted Benzoate Esters. *J. Am. Chem. Soc.* **1952**, *74*, 2729-2732.

[5] van de Wetering, P.; Zuidam, N. J.; van Steenbergen, M. J.; van der Houwen, O. A. G. J.; Underberg, W. J. M.; Hennink, W. E. A Mechanistic Study of the Hydrolytic Stability of Poly(2-(dimethylamino)ethyl methacrylate). *Macromolecules* **1998**, *31*, 8063−8068.

CHAPTER 6: Summary and Future Work

6.1. Chapter 2

Charge-shifting polycations based on copolymers of 2-(dimethylamino)ethyl acrylate (DMAEA) and 3-aminopropylmethacrylamide (APM), called PAD, were synthesized as building blocks for polyelectrolyte complexes with alginate. Hydrolysis of DMAEA within PAD copolymers showed kinetics that was dependent on pH, temperature, and copolymer composition. PAD copolymers of 8 and 30 kDa with varying compositions were synthesized by RAFT polymerization and used as coating materials with calcium alginate beads. PAD copolymers with MW of 30 kDa were shown to form capsule membranes over the lower MW copolymers that diffused throughout the alginate core. Hydrolysis of the coatings was demonstrated as the reduction in net cationic charge led to the dissociation of the polyelectrolyte complex with anionic alginate beads and PMSM polymer particles. Covalent crosslinking of PAD copolymers as polyelectrolyte complexes was demonstrated with THPC. The results of this chapter demonstrate that PAD copolymers may be used to efficiently form polyelectrolyte complexes, capable of covalent crosslinking, followed by hydrolysis to reduce net cationic charge of the material.

Future work may involve exploring other crosslinking mechanisms and the cyto- and bio-compatibility of alginate–PAD capsules.

6.2. Chapter 3

The reactivity of polymers based on DMAEA was investigated with a novel analogue that introduced hydroxymethyl groups as part of the polymer backbone. The synthesis of 2-(Dimethylamino)ethyl 2-(hydroxymethyl)acrylate (DHMA) and the (co)polymerization of stable, alcohol-protected versions of DHMA was described. The hydrolysis of PDHMA was found to be very rapid in comparison to PDMAEA and PDMAEMA, which may be due to intra-molecular hydrogen-bonding interaction of the alcohol with the ester carbonyl *via* a 6-membered ring conformation in addition to increased hydrophilicity. The incorporation of the hydroxymethyl groups into the polymer backbone was used to tune the rate of hydrolysis by changing copolymer composition of DHMA and DMAEA. The work in this chapter highlight that the reactivity of acrylic esters is highly sensitive to neighboring groups though various hydrogen bonding, steric, hydrophilic, and hydrophobic interactions, which can be used to design degradable polymers.

Future work may explore copolymers of DHMA with comonomers such as DMAEMA and acrylic acid to further probe the mechanism of hydrolysis and properties of the polymers. Other derivatives of hydroxymethyl acrylates with varying pendant side chains may also be explored to probe reactivity of the ester with other functional groups in addition to potential applications involving controlled release of conjugated drugs.

6.3. Chapter 4

PAD copolymers with low to high compositions of DMAEA were synthesized by RAFT polymerization as described in Chapter 2 to study the effect of charge-shifting hydrolysis of the polycations as DNA delivery vehicles. The hydrolysis of PAD copolymers was conducted to model the intracellular environments of the cytoplasm at pH 7 and the endo-lysosomal vesicles at pH 5. Hydrolysis was found to be significantly slower at pH 5 than at pH 7, which suggests that DNA can be protected in polyplexes while in the endosome, and then potentially be released from the polyplexes after endosomal escape where charge-shifting hydrolysis can continue in the cytoplasm. HeLa cells exposed to PAD–DNA polyplexes were shown to have very high uptake efficiencies that exceeded PEI as the gold standard polycation for transfection. In addition, cells exposed to PAD copolymers with greater charge-shifting ability were shown to have improved viabilities 2 days after exposure relative to standard polycations. The results in this chapter provide fundamental hydrolysis kinetics not fully acknowledged in the literature for related charge-shifting polycations that may be useful in interpreting the intracellular fate of polycations. Further, it was demonstrated that charge-shifting polycations with initial high cationic charge density could efficiently condense and deliver DNA into cells and subsequently improve cytocompatibility after hydrolysis.

Future work may explore the gene knockdown efficiency with transfection of siRNA, in addition to studies that probe the intracellular fate of the polycation. Charge-shifting polycations with faster rates of hydrolysis may also be explored to tune DNA release and cytocompatibility.

6.4. Chapter 5

PDMAEA was studied to probe the mechanism of hydrolysis as a function of pH and neighboring functional groups on the pendant side chain and of comonomers. The hydrolysis of PDMAEA was studied between pH 14 – 0, and showed clear pH dependence with half-lives based on initial rates ranging from years to minutes. These results are in stark contrast to numerous reports in the literature that claim pH independent hydrolysis. This disparity was addressed in this chapter, and was likely due to poor pH control with too little or no buffer present for the conflicting studies. The extent of hydrolysis was found to depend on the mechanism, as hydroxide mediated hydrolysis reaches a limiting extent of ~50-60 % due to the repulsion of the incoming nucleophile. The acid-catalyzed mechanism of hydrolysis was found exceed the limiting extent to reach ~90 % as there was no repulsion of the neutral nucleophile water. The hydrolysis of PDMAEA was further probed with novel analogues with an additional amine group in the pendent side chain, which showed a strong influence of the dimethylamino group of DMAEA and the interactions with the ester that result in its unique reactivity. It was further demonstrated that charge of comonomers strongly affected the rate of DMAEA hydrolysis at pH 7, as anionic groups repel hydroxide ions, preventing further hydrolysis, whereas cationic groups may attract hydroxide ions and promote hydrolysis. In addition, collapsed and swollen polymer conformations of the anionic and cationic copolymers, respectively, may affect the accessibility of the esters towards hydrolysis. The results of this chapter provide clear evidence of pH dependent

hydrolysis of DMAEA polymers, in addition to highlighting the sensitivity of polyacrylate ester reactivity with neighboring groups.

Future work may explore the effect of comonomers with other charges such as permanent quaternary ammonium cations and sulfonate anions, as well as the effect of (meth)acrylate and (meth)acrylamide comonomers on hydrolysis. The effect of other dialkylamines and trialkylammonium cations in the pendent side chain may also be explored.